ERDC/CHL TR-12-10

Coastal and Hydraulics Laboratory

US Army Corps
of Engineers®
Engineer Research and
Development Center

Sedimentation Solutions for Military Ocean Terminal Sunny Point (MOTSU), North Carolina

Jeremy A. Sharp, Jennifer N. Tate, and William H. McAnally

July 2012

ERDC/CHL TR-12-10
July 2012

Sedimentation Solutions for Military Ocean Terminal Sunny Point (MOTSU), North Carolina

Jeremy A. Sharp, Jennifer N. Tate, and William H. McAnally

Coastal and Hydraulics Laboratory
US Army Engineer Research and Development Center
3909 Halls Ferry Road
Vicksburg, MS 39180-6199

Final report

Prepared for US Army Engineer District–Wilmington
Wilmington, NC 28403

Under Project 155479, "MOTSU Channel Dredging"

Abstract

The US Army's Military Ocean Terminal Sunny Point (MOTSU) went into service in 1955, and serves as a military munitions terminal. The facility is located in Brunswick County, North Carolina, approximately 10 miles up-stream of the mouth of the Cape Fear River. Shoaling issues have been a problem since the opening of the port. The objective of this work is three fold: reduce long term dredging costs, achieve operational readiness goals, and maintain or enhance environmental quality at MOTSU at the request of US Army Engineer District–Wilmington (USAED-SAW). The objective was achieved through numerical modeling, literature review, and sediment forecasting. This report documents the results of the numerical modeling study only.

Two advantageous approaches for shoaling mitigation are recommended for further analysis, and those solutions could be combined to achieve an optimum dredging-reduction scheme. It is concluded that by integrating multiple solutions it is possible to create a cost-effective long-term shoal-ing-mitigation plan.

Table of Contents

List of Figures and Tables

Figures

Tables

Preface

The model investigation documented in this report was authorized and funded by US Army Engineer District–Wilmington under Project 155479, "MOTSU Channel Dredging," dated 27 July 2010. The technical review was performed by Dr. Gaurav Savant, (Contractor, Dynamic Solutions, LLC).

This work was performed at the US Army Engineer Research and Development Center, Coastal and Hydraulics Laboratory (ERDC-CHL), Vicksburg, MS. The study was conducted by Mr. Jeremy Sharp, Ms. Jennifer Tate, and Dr. William McAnally (Contractor, Dynamic Solutions, LLC). The research was performed under the general direction of Dr. William D. Martin, Director; and Mr. Jose Sanchez, Deputy Director, ERDC-CHL. Direct supervision was provided by Mr. Bruce A. Ebersole, Chief, Flood and Storm Protection Division (CEERD-HF), and Dr. Robert McAdory, Chief, Estuarine Engineering Branch (CEERD-HF-E).

COL Kevin J. Wilson was the Commander and Executive Director of ERDC, and Dr. Jeffery P. Holland was the Director.

Executive Summary

The US Army's Military Ocean Terminal Sunny Point (MOTSU), located approximately 10 miles upstream of the mouth of the Cape Fear River in Brunswick County, NC, is a mission-critical military munitions terminal. Shoaling has been a problem for the port since it opened in 1955. At the request of US Army Engineer District–Wilmington (USAED-SAW), ERDC-CHL performed a study to mitigate MOTSU shoaling issues in order to reduce long-term dredging costs, sustain operational readiness, and maintain or enhance environmental quality. The study was accomplished through numerical modeling, literature review, and sediment forecasting (details not included in this report).

Numerical modeling was based on a TABS-MDS model used in a previous fairway study as modified to evaluate eight alternate port configurations. TABS-MDS is a three-dimensional hydrodynamic, salinity, and sediment model that accounts for tidal flows, freshwater river flows, and winds. The existing conditions and the recommended fairway design were derived from previous model runs. Using the existing-conditions model as the Base, the model mesh was refined to increase resolution around the port, improve representation of the area behind the wharfs, and update bathymetry from bank to bank. This reconfigured model was validated prior to simulating the eight alternate port configurations. Shoaling change analyses as well as changes to velocity patterns were performed to determine which of the plans is most effective for shoaling reduction.

The literature review was performed to examine historical alternatives to reduce dredging at MOTSU in light of current knowledge. Multiple studies have been conducted at MOTSU for the determination of a mitigating solution to reduce the required dredging. Summarizing and highlighting the historical recommendations helps to avoid repeating past mistakes and provides a point of departure for developing new solutions. Studies reviewed include but are not limited to those done by Trawle, Banchetti, and Berger (1980) and the Committee on Tidal Hydraulics (1971 and 1995). The literature was evaluated to help guide and possibly amend future work plans. Also, a summary of scour jet systems is included at the request of the sponsor for consideration as a possible supplemental application to

enhance the effectiveness of the most beneficial shoaling-mitigation options.

Based on the outcome of the analyses included in this study, a list of findings and recommendations is provided here. Recommendations of the most beneficial alternatives are based both on engineering judgment and numerical analyses excluding cost considerations. In order of expected benefits, they are:

1. Construction of an island-type structure that would increase current velocity and shear stresses in the channel to facilitate the flushing of excessive sedimentation. The island could be configured as a containment structure where dredged materials could be deposited.
2. Dredging to active nautical depth, which would reduce the required amount of dredging needed.
3. Realignment of the MOTSU channel just south of the center wharf. This plan would have some negative shoaling impacts in the area of the MOTSU channel realignment but a positive impact on the navigation channel, and could serve as an intermediate solution as part of a larger integrated solution.
4. At a minimum, nautical-depth dredging could be immediately implemented, but this approach would require acceptance by and education for the pilots.

These four candidate approaches for shoaling mitigation—two realignment and two dredging plans—each require specific analyses that are beyond the scope of this modeling work. The options are recommended based on their net positive impacts for MOTSU and the navigation channel as determined through modeling. The authors further recommend how the four proposed solutions may be integrated to achieve an effective, affordable dredging-reduction program.

It is concluded that the execution of all four prospective solutions should significantly reduce shoaling and that the facility should see improvements in operational readiness. It is recommended that one or more of these solutions be implemented to mitigate the shoaling problem. Regardless of the chosen solution, continued effort should be made to reduce shoaling issues at MOTSU.

Unit Conversion Factors

Multiply	By	To Obtain
acres	4,046.873	square meters
acre-feet	1,233.5	cubic meters
cubic feet	0.02831685	cubic meters
cubic inches	1.6387064 E-05	cubic meters
cubic yards	0.7645549	cubic meters
degrees (angle)	0.01745329	radians
degrees Fahrenheit	(F-32)/1.8	degrees Celsius
fathoms	1.8288	meters
feet	0.3048	meters
foot-pounds force	1.355818	joules
inches	0.0254	meters
inch-pounds (force)	0.1129848	newton meters
knots	0.5144444	meters per second
microns	1.0 E-06	meters
miles (nautical)	1,852	meters
miles (US statute)	1,609.347	meters
slugs	14.59390	kilograms
square feet	0.09290304	square meters
square yards	0.8361274	square meters
yards	0.9144	meters

1 Introduction

1.1 Background

The US Army's Military Ocean Terminal Sunny Point (MOTSU) went into service in 1955 and serves as a mission-critical military munitions terminal. The facility is located in Brunswick County, NC, approximately 10 miles upstream of the mouth of the Cape Fear River. Shoaling has been a problem since the opening of the port. Prior to completion of the original excavation dredging it became evident that maintenance dredging would be required (USACE 1976). The location on the West Bank of the Cape Fear River Estuary (Figure 1-1) is less than ideal, being the site of a naturally occurring shoal (MTMC 1984) that accumulates 2 million cubic yards of material per year (MTMC 1986). Here the river widens and is also the site of the turbidity maximum, which oscillates upstream and downstream dependent on fresh water inflow and the tide.

The Cape Fear Estuary is situated in the southeast corner of North Carolina, with a watershed covering 9,140 square miles (Giese, Wilder, and Parker 1985). Two main lower tributaries merge with the Cape Fear River—the Black River and the Northeast Cape Fear River, which converge 22 miles upstream from the mouth (Figure 1-2). At the confluence, the system widens and is characterized by a deep navigation channel (maintained at 42 ft) and shallow flats. The system was first altered for navigation by the state downstream of Wilmington in 1822 (USACE 1976). Because dredging has created an artificially deep channel, the tidal range has increased, with tidally influenced water up to Lock and Dam 1, 65 miles upstream of the mouth (McAdory 2000). The current mean tidal range at Wilmington is 4.28 ft[1], as compared with reports from the turn of the past century indicating a mean tidal range of 2.7 ft (USACE 1976). The Cape Fear Estuary is a partially to well mixed system (Wilder 1967; USACE 1976; Carpenter and Yonts 1979).

[1] NOAA Tides and Currents (April 2010).

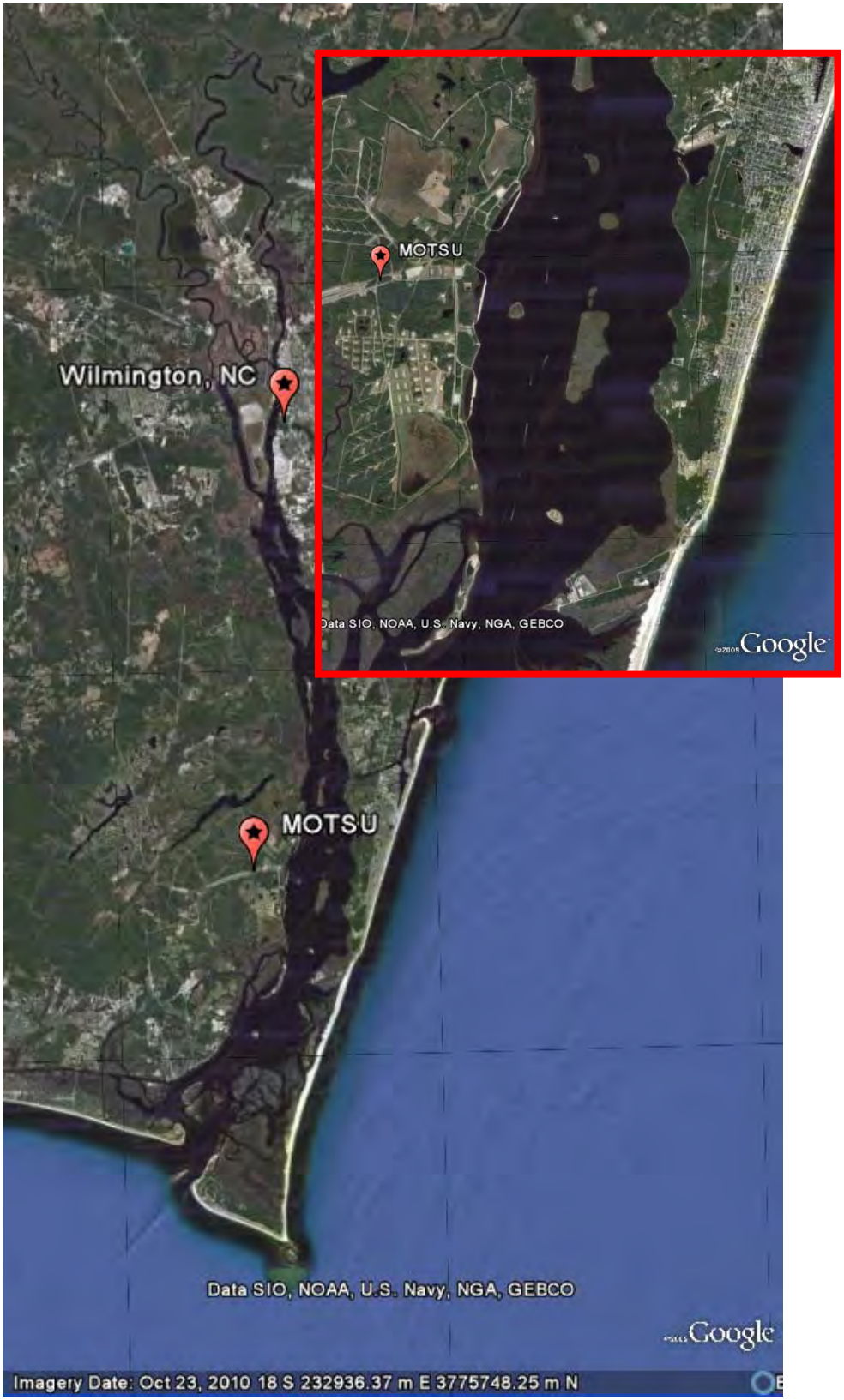

Figure 1-1. Location of MOTSU on the Lower Cape Fear River.

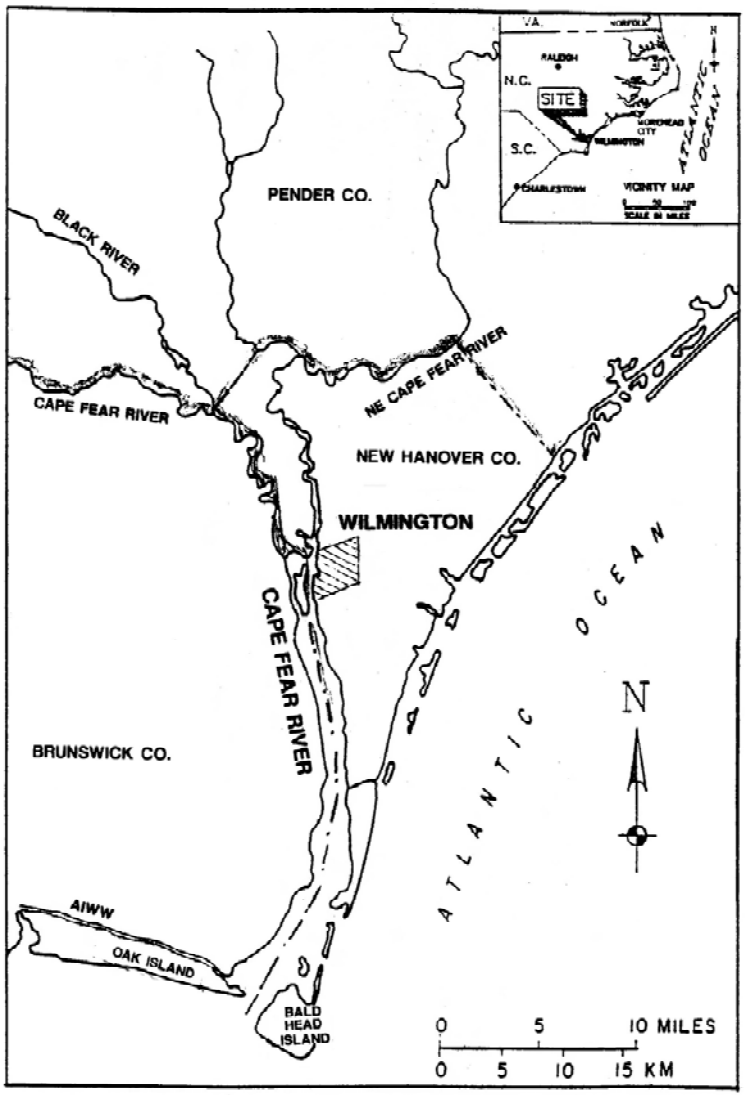

Figure 1-2. River network feeding freshwater flow for the Cape Fear River.

Peak historical stream flows from the three main rivers—the Cape Fear, Black, and Northeast Cape Fear rivers—are 57,700 cfs 3 March 1979 at Lock and Dam #1, 28,500 cfs 18 September 1999 near Tomahawk, and 30,700 cfs 18 September 1999 near Chinquapin, respectively (USGS 2010). It is reported that flow averages in the Cape Fear River range from 11,000 – 18,000 cfs, with a low flow of 1,000 cfs and a high flow of 40,000 cfs (Giese, Wilder, and Parker 1985).

Limiting factors at all ports around the world have arisen in past years, increasing the cost of dredging (USACE 1995) and therefore decreasing the appeal of dredging as a means of siltation control. Every issue typically faced by a port is further compounded at MOTSU by its location. Disposal

of material must be properly executed to comply with environmental restrictions, ultimately causing a reduction in the number of economical disposal sites. The doubling of fuel costs in the past few years has increased operational costs of a dredge, further hindering dredging appeal. As container vessels are built larger with deeper drafts, MOTSU must be able to accommodate them or risk losing the support capabilities required in sustaining the nation's overseas military operations. All of these issues are causing dredging to be less attractive than it once was, forcing port operators to evaluate and consider alternative measures.

Sedimentation patterns at the port are caused by lateral flows that were identified in a radioactive sediment trace test (Carpenter 1979). These flows were also shown in a STUDH model study that indicated a large portion of the shoaled material was passing over the shallows between the north and center entrance channel and depositing in the port (Trawle 1982). For the first couple of decades of service, the idea of keeping sediment out by using dikes or movable silt-barriers was prevalent. However, this was shown in both a physical and numerical model study, completed in the mid 1980s, to only increase the sediment-trapping efficiency of the Port and in turn increast the need for dredging. During this time it was being shown and understood that the problem at MOTSU is mud, or the finer grain material floculating. Mud is defined by Mehta (2002) as:

> Sediment-water mixture of grains that are predominantly less that 63 microns in size, exhibits a rheological behavior that is poroelastic or viscoelastic when the mixture is particle-supported, and is highly viscous and non-Newtonian when it is in a fluid-like state.

The fluid-like state (i.e., fluid mud) causes the rapidly occurring thick shoals that occur at MOTSU, reportedly as much as 6 ft in a single event. It is believed that "episodic shoaling events, related to high river discharges, contribute to the large sediment volumes by depositing 0.5 to 1.0 million cubic yards of sediment in a matter of weeks" (MTMC 1984). Examples of the large amount of shoaling include many in the literature, such as the observation in February 1982 when the facility shoaled approximately 770,000 cubic yards in 2 weeks and resulted in 5 to 6 foot reduction of draft in three of the berths (MTMC 1986). Maintaining facility readiness

requires the dredging of material in areas of rapid shoaling and the removal of material for the maintenance of project conditions (MTMC 1984).

The reasons for incredibly high shoaling rates are due to two contributing factors as outlined by MTMC 1984. First, as stated previously, the location of the facility is detrimental to maintaining navigation depth since it is in the location of the turbidity maximum. Second the configuration of the port with its artificial deep depths along with the naturally widened section of the river yields a location that facilitates deposition. The combination of these two previously known issues results in a situation where current dredging operations do not allow for consistent maintenance of the facility.

1.2 Objective

At the request of US Army Engineer District–Wilmington (USAED-SAW), ERDC-CHL performed a study to mitigate MOTSU shoaling issues in order to reduce long-term dredging costs, sustain operational readiness, and maintain or enhance environmental quality.

1.3 Approach

This study was accomplished through numerical modeling, literature review, and sediment forecasting (details not included in this report).

The tasks described here directly continue previous undocumented work by Dr. Kevin Barry at ERDC-CHL in which a “fairway” design was recommended to increase shear stress and thereby flush a portion of the sediment out of the port. The following tasks address questions raised by Wilmington District.

The existing TABS-MDS[2] model, used in the fairway study, is modified to evaluate ten different port configurations. This is a 3-dimensional hydrodynamic, salinity, and sediment model that includes tidal flows, freshwater river flows, and winds. Previous model runs comprise the existing conditions and the recommended fairway design. Using the existing conditions model as the base, the model mesh is refined to include increased resolution around the port as well as a better representation of the

[2] For a description, see http://chl.erdc.usace.army.mil/tabs.

area behind the wharfs. ERDC simulated eight additional port configurations defined below and discussed in Chapters 6 and 7.

1. Retain existing channels, except realign northern entrance channel (Figure 1-3)
   a. northern entrance channel depth at existing depth of northern wharf (-34 ft) [opened simply to change flow] (Figure 1-4)
   b. northern entrance channel and North wharf channels deepened to -38 ft design depth [ships would turn at center wharf and be backed to North wharf – or – ships coming from State Port would enter at north entrance] (Figure 1-5).
2. Smooth existing alignment to include realigning channel between South and Center wharf (Figure 1-6).
3. Realign northern entrance channel (1a) and smooth existing alignment (2) (Figure 1-7).
4. Realign and deepen northern entrance channel (1b) and include turning basin in Wilmington Harbor channel (-38 ft) (Figure 1-8).
5. Realign and deepen northern entrance channel (1b), include turning basin in Wilmington Harbor channel and smooth existing alignment (2) This may also include filling existing basins to achieve near constant channel width (Figure 1-9).
6. Marsh island placement with turning basin (Figure 1-10).
7. Training structure alternative 1, wall configuration (Figure 1-11), discussed in Chapter 7.

Figure 1-3. Existing condition.

Figure 1-4. Plan 1a.

Figure 1-5. Plan 1b.

Figure 1-6. Plan 2.

Figure 1-7. Plan 3.

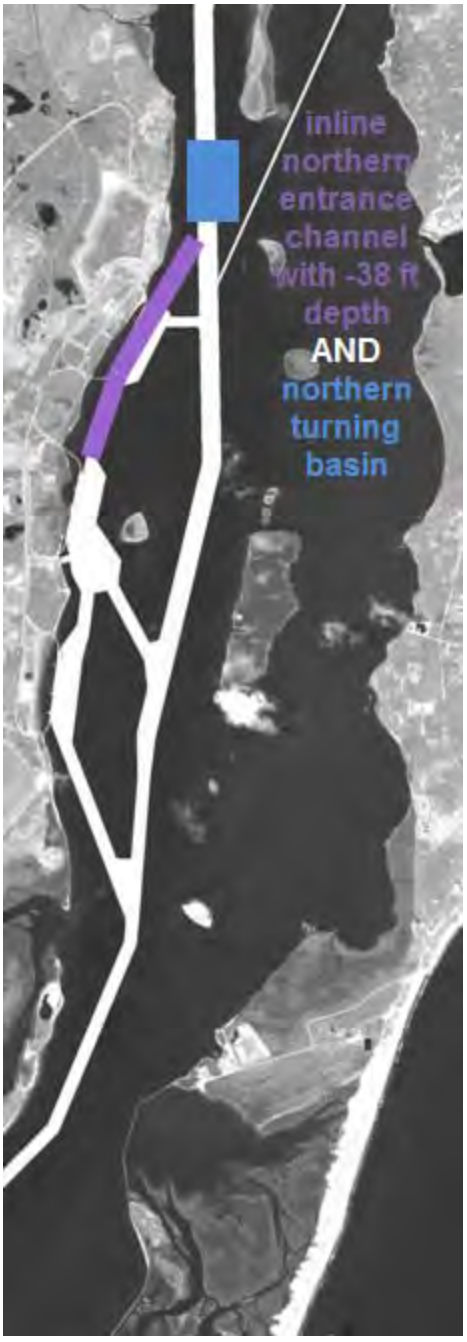

Figure 1-8. Plan 4.

Figure 1-9. Plan 5.

Figure 1-10. Plan 6.

Figure 1-11. Plan 7 (wall).

2 Engineering Investigation

When ports and channels experience sediment deposition that will lead to unacceptable loss of water depth, solutions are needed to maintain navigability. Solutions may include both dredging and non-dredging alternatives that eliminate or reduce sediment deposition. Solutions recently considered for MOTSU have included channel realignment, scour jets, and adopting the passive or active nautical depth, all of which have proven in some capacity to be beneficial either onsite or at other locations around the world. PIANC (2008) has produced a report documenting these solutions and many more, which are briefly described here.

2.1 Solution concepts

A variety of engineered solutions are available to reduce deposition problems. Solutions tend to be unique to each site. Successful design depends on port layout, waterway configuration, flow conditions, and sediment type and supply. However, all solutions can be placed in a few simple categories. Krone (1987) specified three categories: methods that keep sediment out, methods that keep sediment moving, and methods that remove sediment after it has deposited.

To these three, PIANC (2008) added a fourth category: keeping sediment navigable. This category uses the concept of *nautical depth*, which defines the channel bottom in terms of a density or viscosity value instead of a specifically defined acoustic signal. This approach allows a specified amount of sediment to remain within the channel as long as it is of low enough density to permit safe and effective navigation.

The following lists some solutions from each of these categories.

2.1.1 Methods that keep sediment out

Keeping excess sediment out of the port or channel that might otherwise enter and deposit can be accomplished by:

- Stabilizing sediment sources.
- Diverting sediment-laden flows.
- Trapping sediment before it enters.

- Blocking sediment entry.

Examples include diverting freshwater flow out of Charleston Harbor, SC, which reduced port and channel sedimentation by more than 70 percent (Teeter 1989); and a sediment trap and tide gate combination in Savannah Harbor, GA, that reduced port and waterway dredging by more than 50 percent (Committee on Tidal Hydraulics 1995). The inland Port of Toronto (Torontoport 2003) employs a sediment trap to keep its entrance channel open.

2.1.2 Methods that keep the sediment moving

If very fine, slow-settling sediment can be kept suspended while the flow passes through the port, or if the flow maintains high enough tractive force (usually expressed as shear stress, or drag force per unit area) to keep coarser particles moving, sediment can pass through without depositing. Methods to keep sediment moving include:

- Structural elements that train natural flows.
- Devices that increase tractive forces on the bed.
- Designs and equipment that increase sediment mobility.
- Designs that reduce cohesive sediment flocculation.

Structural elements include transverse training (spur) dikes that are used in many locations to train flow and prevent local deposition of sediment and longitudinal dikes to train and separate flows (CTH 1995). The Current Deflecting Wall, a curved training structure, is employed in the Port of Hamburg to reduce side channel/basin sedimentation (PIANC 2008).

Devices to increase bed tractive forces, including submerged wings (Jenkins 1987) and water jet manifolds, or scour jets (Bailard 1987), were tested in the Navy berths of Mare Island Strait, CA, and found to be effective in reducing sediment deposition locally. Recent research on underwater scour jets has produced updated technologies (SedCon 2010). Cohesive sediment flocculation can be reduced by designs that reduce turbulence, such as solid wharf walls instead of piling supported wharfs.

2.1.3 Methods that remove deposited sediment

Sediment can be removed after it deposits. Methods include:

- Traditional dredging and disposal.
- Agitation of deposits so that the sediment becomes mobile again.

Removing sediment includes traditional dredging disposal in water or in confined disposal facilities, but also includes sediment agitation methods of intentional overflow, dragging, and propwash erosion. Agitation dredging is subject to regulation, as is traditional dredging, and can be perceived as contributing to water quality problems.

2.1.4 Methods that keep sediment navigable

Sediment can be kept navigable such that navigation is not impeded in systems that have high concentrations of fine material (i.e., fluid mud). Such fine sediments form a high-concentration suspension that may show up on acoustic surveys as a false bottom, but when dredged consists only of muddy water. The phenomenon occurs because acoustic fathometers show reflections at density gradients, or lutoclines, which may occur anywhere in the water column when sediment concentrations are high. Dual-frequency fathometers, once thought to resolve the layers of fluid mud from the actual channel bottom, actually provide two wrong answers about where the bottom lies (McAnally et al. 2007). If left undisturbed, fluid mud will eventually consolidate into a firm bed that needs to be removed.

The fluid mud problem has been resolved in dozens of ports around the world by adopting the nautical depth concept—defining the channel bottom in terms of density and/or viscosity criteria instead of signals returned by acoustic fathometers (PIANC 2008). Nautical depth is usually defined using density ranging from 1.15 to 1.24 t/m^3 (Vantorre 1984).

Methods that keep sediment navigable include:

- passive nautical depth that defines depth based on density and/or viscosity of the water-sediment suspension
- active nautical depth in which sediment is conditioned so that it remains navigable under the nautical depth definition.

2.2 Specific solutions

2.2.1 Agitation

Removing deposited sediment by agitation includes using standard dredging equipment with intentional overflow or discharge into nearby waters, dragging, and propwash erosion. It is usually intended to suspend sediment so currents can carry it away. Anchorage Harbor, AK, was dredged with a combination of agitation and dredge-and-haul in 2000 when normal dredge-and-haul could not achieve desired results soon enough (Hilton 2000). Dragging a rake behind a vessel to suspend sediment so that it can be carried away by currents has been practiced for centuries in China (Luo 1986), and propeller wash is used in the same way in some ports, either intentionally or incidental to normal port operations (Richardson 1984).

Propeller wash resuspension of deposited fine sediment can be achieved by a vessel (such as a tow) running its propeller at a high rate in areas of the port to disrupt and resuspend the deposited sediment. Once resuspended, some of the sediment will flow or diffuse out of the port, but some or even most will redeposit in the port. This method requires no design time, installation, or specialized training. Agitation can be scheduled to avoid conflict with other port operations or access. Prop agitation is widely used in tidal areas, where the agitation can be timed to coincide with seaward flowing currents to move the resuspended sediment away from the port, but can be employed in inland ports, also, if the sediment is sufficiently fine grained and either currents or slope is present to move the resuspended sediment away from the port.

A special case of agitation dredging involves use of specialized vessel-mounted equipment to fluidize bed sediment such that it flows down slope or with ambient currents (Hales 1995; PIANC 2008).

Agitation dredging is prohibited in some locations because it increases turbidity, at least locally. If the sediment contains organic materials in an anaerobic state, resuspension will increase the biological oxygen demand and depress dissolved oxygen (Johnson 1976). Another aspect to this question is reaeration. Qaisi, et al. (1997) note that as much as 30% reaeration in high-traffic waterways is due to barge traffic, so it might be expected that agitation dredging by propwash may either increase or decrease dissolved oxygen (DO) depending on local conditions. DO impacts will be

minimized if the practice is employed at least once per month. A pilot study can be performed in which deposits are agitated and DO measurements taken to document the degree and duration of impact.

2.2.2 Pneumatic barrier

A pneumatic barrier, or bubble curtain, pumps compressed air through a submerged manifold. Bubbles rising from the manifold create a current that flows in toward the manifold at the bottom, upward toward the surface, and outward at the surface. As sediment particles approach the rising current they are carried upward away from the bed and toward the surface, then away from the bubbler. The two most common configurations of pneumatic barriers are in a line across the mouth of a basin or in clusters throughout the basin. In the line arrangement, the pneumatic barrier acts as a curtain across the mouth of the port to reduce the amount of depositing sediment in two ways. The rising current of air entrains water, creating an upward flow near the bubble curtain, an inward flow near the bottom, and an outward flow at the surface. This flow pattern carries suspended fine particles upward, and a portion is transported away from the barrier. The rising air bubbles act as a physical barrier limiting the passage of particles to the other side of the curtain, thus reducing the amount of sediment entering the protected area. Increased bottom currents near the curtain will also prevent close-by deposition of fine sediments. Although the pneumatic barrier does not prevent all sediment from passing through it and depositing, it is a potential tool in the reduction of sedimentation (e.g., Gray's Harbor College 1973).

Pneumatic systems are typically composed of three parts: an onshore air compressor, supply line, and a diffuser system. It is advised that a steel pipe be used as the first reach of the supply line to dissipate heat generated by compression of air. The air exiting the compressor is extremely hot and should be cooled before entering the water to prevent artificial warming.

The cluster arrangement consists of several bubblers throughout an area. This configuration does not attempt to prevent the entrance of sediment into the port. Its objective is to prevent the deposition of sediment. The layout of the clusters depends on the size of the port and the depth of the water. This method will not completely prevent the deposition of sediment, but has shown reduction in sediment accumulation (e.g., Chapman and Douglas 2003).

Installation of either pneumatic barrier arrangement will require port downtime. Operation of the line pneumatic barrier could be continuous, but depending on experience with the system, also could be activated only during tow passages in the waterway. Regular, periodic maintenance will be required of the compressor and the manifold.

2.2.3 Silt screen

A silt screen, or silt curtain, is a physical barrier that is opened only to allow the passage of vessels. It provides positive control of sediment influx. Silt screens are typically used to contain sediment plumes during dredging and disposal, but can be used to exclude sediment from a port if practical given local traffic or current condition. As it is a solid membrane, no sediment will pass through it into the port while in use; however, if there are gaps in the curtain, particularly at the bed, some sediment will get past. The primary drawback of the sediment curtain solution is that it will require special training and a work boat to open it for vessel passage, therefore possibly disrupting the daily activities of the port.

2.2.4 Sediment trap

A sediment trap is designed to slow currents so that all or part of the sediment load is deposited within the trap. Since ports are often dredged deeper and wider than the natural channels in which they occur, ports serve as unintentional sediment traps. In general, sediment traps do not reduce the amount of required dredging (they may actually increase it); however, they may reduce the unit cost of dredging by avoiding conflicts with navigation during dredging operations or the frequency of dredging operations. If a trap locates sediment accumulation outside the port area, the port will experience longer periods of full design depth even as sediment accumulates in the trap.

A sediment trap and tide gate combination in Savannah Harbor, GA, reduced port and waterway dredging by more than 50% (Committee on Tidal Hydraulics 1995). In the Savannah case, locating the sediment trap out of the port area reduced interference between dredging equipment and vessel traffic, placed the dredging closer to the disposal area, and reduced the unit cost. However, the project was alleged to cause salinity increases upstream, and was taken out of service (Committee on Tidal Hydraulics 1995).

Sediment traps can be environmentally beneficial compared with conventional dredging, for example, if fine sediments are allowed to consolidate so that low turbidity, low water volume methods such as clamshell dredging can be employed.

A sediment trap can either be dredged at intervals or regularly pumped out. Eductor-type pumps have been used for sediment removal in a number of locations, usually in sand environments (e.g., Richardson and McNair 1981; McClellan and Hopman 2000). In a mud environment they will tend to be made inoperative unless run regularly since consolidated mud will not flow toward the pump. Deposition in a trap can be moved to a piece of fixed dredging equipment by a fluidizing pipe—a perforated pipe through which water is pumped to fluidize the bed and cause it to flow down a trench. Fluidizing pipes have been used in sand bed locations, but work in mud beds if operated before the mud consolidates (Van Dorn 1975; PIANC 2008).

2.2.5 Training structures

Training structures are used worldwide to keep sediment moving and prevent deposition. Numerous examples are described by Parchure and Teeter (2002). They include transverse training (spur) dikes that are used in many locations to train flow and prevent local deposition of sediment, as in the Red River, LA (Pinkard 1995), and in specialized training structures such as the Current Deflector Wall, a curved training structure that reduced sedimentation in Hamburg Harbor's Kohlfleet basin by 40% (Smith et al. 2001). Unlike some solutions, studies by multiple agencies have shown that training dikes can be constructed so as to confer positive habitat benefits (US Army Corps of Engineers 2003; Byars et al. 2000; Lower Mississippi River Conservation Committee 2003; Kuhnle et al. 2003; Stauffer 1991; and Shields et al. 1995).

Transverse dikes have been found to be most effective when submerged during high-flow events (Parchure and Teeter 2002). Corps of Engineers guidelines (Biedenharn et al. 1997) and generally accepted principles for training structures call for a dike top elevation between low-water level and bankful stage long enough to constrict the channel cross section to convey the sediment load, and dike spacing about 3 to 5 times the dike length.

Dikes may be constructed of riprap (stone), piles, and/or geotubes (geotextile fabric tubes filled with dredged material). If constructed of riprap, the dikes may be made solely of stone, earth, or rubble fill covered with a riprap blanket. Geotubes covered with riprap have been used in training structures and dredged material containment dikes.

Dikes may present a hazard to vessels, or they may prevent current conditions that adversely affect navigability. Dike placement can and must be designed with safe commercial and recreational traffic in mind.

2.2.6 Dredging

Dredging in ports has been accomplished by means of contract dredging in which bids are solicited and a contract awarded to private dredging companies or by use of in-house dredge plant. Costs of dredge mobilization and demobilization are relatively constant for both small-volume jobs and large-volume jobs, so the cost per cubic yard dredged material goes up for small contracts. Disposal of dredged material is often challenging and can substantially increase the total cost.

2.2.7 Nautical depth metric

In order for a channel to meet the criteria of safety and effectiveness, a vessel must not incur damage when navigating at full draft, and maneuverability must not be adversely affected. The nautical depth metric uses a density value (usually about 1,200 kg/m^3) or a viscosity value to define the bottom instead of an acoustic signal return that indicates a sudden change in density. Acoustic instruments may falsely indicate a firm bottom due to bubbles in the water column, a sediment suspension lutocline, or even a saline gradient (Parker and Kirby 1982; Teeter 1992; Alexander et al. 1997). Multiple attempts to use software processing and multi-frequency fathometers have proved to be inadequate for reliably defining the sediment bed except in areas where a consolidated bed exists without fluid mud.

PIANC (2008) documents the dozens of ports worldwide that have successfully adopted the nautical depth approach. The port of Rotterdam, Netherlands, has employed passive nautical depth since the late 1970s, using density as a measure. Initially the port used nuclear densitometers, but has since switched to other, less-difficult techniques. Since adoption of the

practice, the port has not been closed due to dredging needs (PIANC 2008), which was a common occurrence prior to adopting nautical depth.

Objections to adopting the nautical depth metric in the United States include fears of damaging cooling water intakes, grounding, and environmental damage. However, the experience of dozens of major ports worldwide employing the same vessels as the United States and employing even stricter controls has shown that such concerns are groundless and can be resolved through education. MOTSU, with a single owner/tenant, is a good candidate location to demonstrate the effectiveness of the nautical depth approach in the United States It is also a candidate for active nautical depth.

2.2.8 Active nautical depth

Active nautical depth is a term for the systematic manipulation of fluid mud by reoxygenating it while avoiding excessive re-entrainment so that the local nautical depth metric is maintained for safe navigation. Locations with high volumes of fluid mud that quickly return after removal are viable sites for applying active nautical depth methods. The adoption of active nautical depth eliminated the need for removal of fluid mud at the Port of Emden, Germany, by establishing and maintaining a fluid mud equilibrium condition (Wurpts 2005). This condition falls within the nautical depth definition specific for the facility. The fluid mud is kept in place, creating an adverse density gradient so new material is prevented from entering the facility. In situ treatment is accomplished at Emden through the use of a hopper dredge with its suction head integrated with an underwater pump. Material is lifted off the bottom and placed in the hopper where it is re-oxygenated and placed back on the bed. Re-oxygenation stimulates bacteria whose secretions coats flocs and grains, reducing flocculation tendencies and allowing for the continued suspension of the fluid mud. Wurpts (2005) reports conditioning durations of 4 months at the Port of Emden. Details of the treatment process are described in Wurpts (2005) and PIANC (2008).

3 Field Data Collection

In this work, a field data collection effort was conducted over approximately 3 months in 2008. These data aided the understanding of the system as well as the numerical model setup. In addition to the data collection effort, investigators are also using past findings. There are three key characteristics that have proven to be detrimental to the functionality of the MOTSU facility. First, the overall layout of the port and the hydrodynamic behavior is such that it optimizes the sediment-trapping efficiency of MOTSU. Second, the port is situated, hydraulically, in the worst location, where the turbidity maximum due to the tide range and the river inflows cause maximum sediment concentrations to fall. Third, the fine-grain flocculated sediment found in and around MOTSU has a high accumulation rate and is not easily removed. These hydraulic distinctions are well documented in the field data.

3.1 Historic field data

The presence or absence of flow, which ultimately dictates shear stress, is critical for the formation or, conversely, the flushing of sediment from critical locations. It has also been shown that a reduction in the flow through the MOTSU channels greatly increases the deposition in the channel (Trawle 1982). Flow is predominately upstream in the facility, as indicated by field data, 87.5% of the time. Furthermore, there is no strong upstream flow predominance in the river channel at or below 26 ft (USACE 1976). The maximum tidal currents in the navigation channel outside MOTSU are 2.2 fps during flood and 2.7 fps during ebb tide (Palermo 1990), while locations in the port are at or near stagnant conditions. Areas that did shoal rapidly were shown in the physical model (1979) to be stagnant or low-current locations. The northern basin has the highest rate of siltation whereas the center basin has the lowest (USACE 1976). With it being impractical to move the port, the only alternative is to reduce the deposition by decreasing the trapping efficiency through increasing/altering the currents through the port or applying one of the methods discussed in Chapter 2.

It has been shown from past efforts that the underlying issue at MOTSU is one of fluid mud (USACE 1998, USACE 1983, USACE 1976, Wilder 1967 etc.) The primary composition of sediment in the watershed is clay and silt

coming from clay-rich plains that are the original source of the fine sediment at MOTSU. Division of the watershed is as described: "The Cape Fear River Drainage basin has an area of 9,140 square miles, of which about 3,500 square miles are in the eastern Piedmont providence" (USACE 1976) and contain 40–60 % of clay size particles, with kaolinite being the most abundant. The remaining watershed is the coastal plain, with clay content of 25–35%. The composition of the plain represents a huge source for fluid mud.

Further insight into the fluid mud issue at MOTSU is provided by an evaluation of the sediments mass per volume rate. "Suspended sediment concentrations ranging from 10 – 250 mg/l (at surface) and 30 – 900 mg/l (3 ft off bottom) were measured within the waters of MOTSU and the adjacent Cape Fear River navigation channel during sampling extending from 1978 to 1979 (USACE 1983)" (MTMC 1984). It has also been shown that the sediment concentrations in the MOTSU basin are higher than those in the adjacent river (USACE 1976), explaining the broad range of suspended sediment concentrations. Furthermore, dredge material from the site is classified as fat clay (Palermo 1990), a material of high plasticity that is both highly cohesive and compressible. Core samples taken indicate that the in situ material is 86% silt and clay (finer than 0.074 mm) and 14% sand with a D50 of 0.04 mm (Jones, Edmunds and Associates, Inc. 1979). The presence of high suspended sediment concentration along with a high percentage of clay indicates the occurrence of fluid mud.

Field studies have also examined the near-bed density characteristics. The Jones, Edmuds and Associates, Inc. (1979) field investigation evaluated the in situ density with a nuclear density probe and determined a density at the sediment surface of 1.01 to 1.2 or more at 35 ft depth (navigation depth at time of investigation). A Towed Density Follower (TDF) designed to seek neutral buoyancy at a density of 1.56 g/cm^3 was deployed in February 1998 and was found to closely follow the bottom surface contour of a 28 mHz depth sounder (USACE 1998). Previously it had been understood that there was a divergence in a dual-frequency instrument (USACE 1992). This was found to be 7 to 10 ft deeper than the depth inferred from a higher frequency instrument (200 mHz) where the difference between the TDF and high-frequency instrument was attributed to a fluid mud layer (USACE 1998). In the entrance channel to the Cape Fear River a towed sled attached with a nuclear transmission density gage and a dual-frequency recorder indicated the sled floated at depths between the appar-

ent surfaces indentified by the upper (200 mHz) and lower (28 mHz) frequency sensors with approximately 1–2 ft of fluid mud (USACE 1992). The difference between the two studies suggests, as has been indicated by other reports, that thicker layers of fluid mud are found in the port than in the river, but that they extend over the whole system.

3.2 2008 field data

The most recent data collection in the MOTSU area occurred from February to May 2008. At this time, ERDC-CHL personnel collected a wide range of velocity and sediment data.

3.2.1 Velocity data

Acoustic Doppler Current Profiler (ADCP) data were collected at three transects in the vicinity of MOTSU. The ADCP transects are shown in Figure 3-1 and labeled as Range 1, Range 2, and Range 3. Data were collected hourly across these ranges to compute total discharge over a 13 hour period. Conductivity, temperature, and depth (CTD) sensors were placed at five locations around MOTSU for the entire sampling period. Salinity measurements for the surface and bottom were collected over approximately 6 months with the CTD sensors. Figure 3-2 shows the location of four of these sites. The fifth site is located in the shallows to the east of the MOTSU area. Of the salinity data collection sites, all sites collected surface data for the entire collection period, but the bottom collection for sites 2 and 3 were lost after a few days.

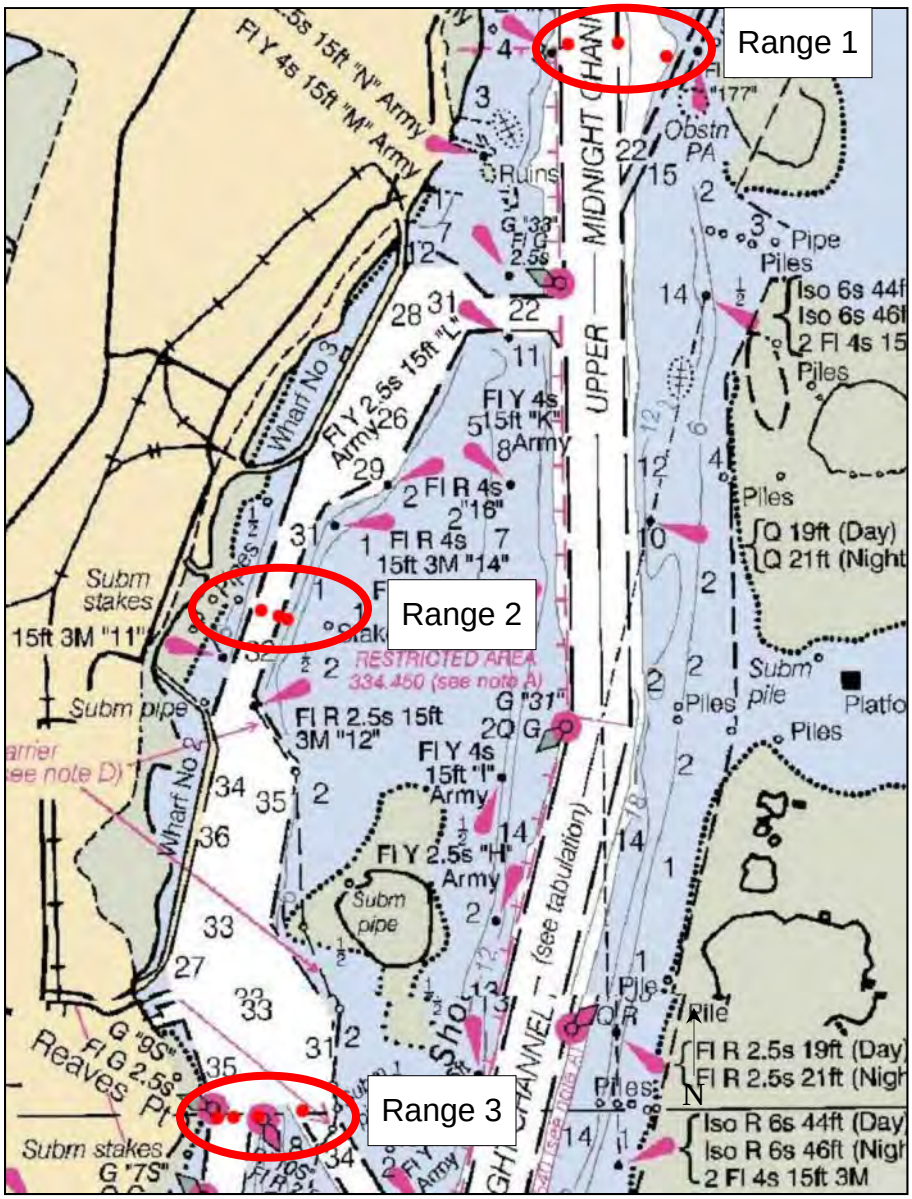

Figure 3-1. ADCP transect locations from 2008 data collection.

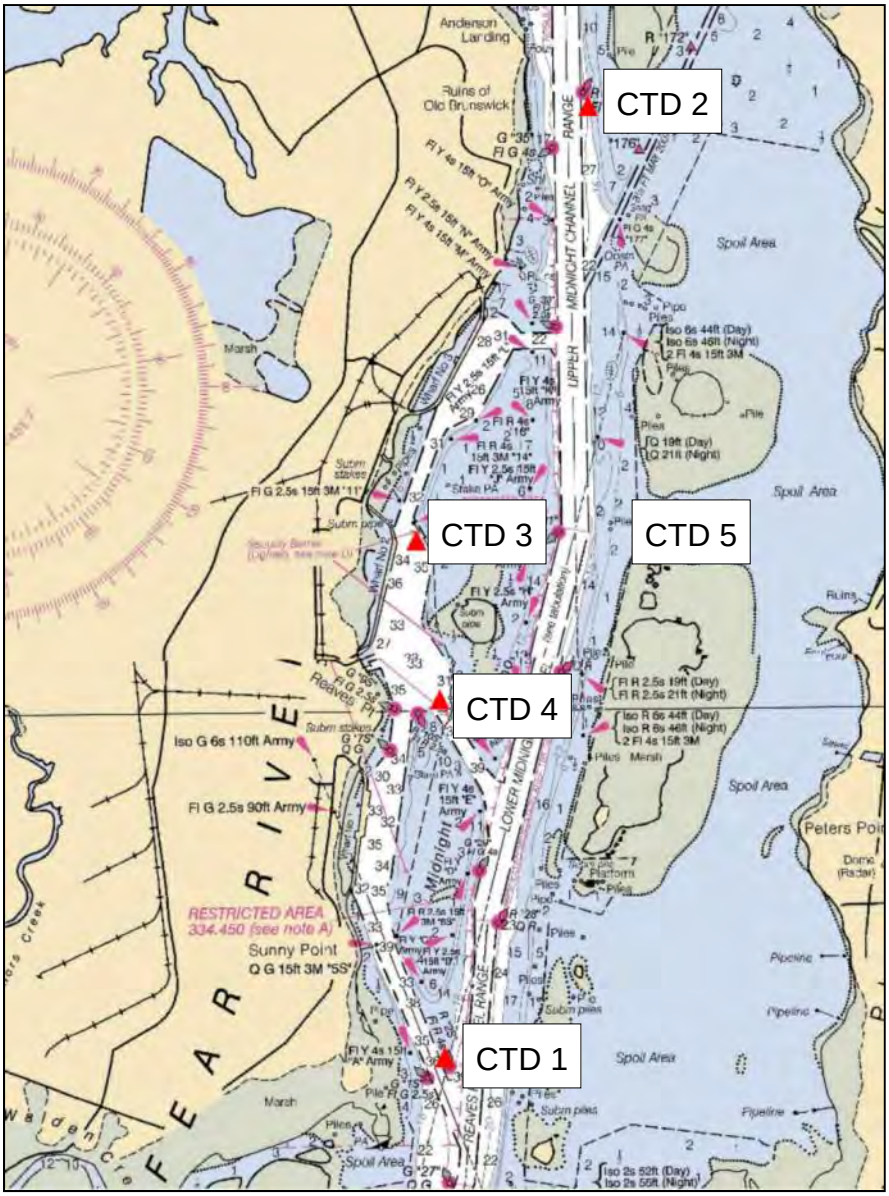

Figure 3-2. CTD station locations for salinity data collection.

3.2.2 Sediment data

Also collected during this effort were Total Suspended Material (TSM) samples at two stations shown in Figure 3-3. The concentration stations recorded TSM at five vertical locations over 72 hours, with optical backscatter (OBS) as well as collecting pump samples every 2 hours at two depths over a 48 hour sample time. Station 1 also collected concentration with a downward-looking ADCP. Suspended sediment concentrations were also collected during the 13 hour ADCP velocity surveys. These data were collected at three depths. The locations of the data collection are given in Figure 3-4 and the suspended sediment concentrations with time are

shown in Figure 3-5. The higher concentrations are found at the bottom for each sample time and the lower values are for the surface.

Thirty-five bed samples were collected throughout the area and analyzed for bulk density, organic content, moisture content, and grain size distribution. These data are important for setting the sediment bed parameters for the sediment modeling effort detailed in Chapter 4. The location of these samples is given in Figure 3-6. Five samples from the four locations shown in Figure 3-7 were analyzed with the SEDFlume. This device allows for the surface of a bed core to be continuously exposed to varying flow rates in order to determine erosion properties of the bed with depth. A second subset of the bed samples are shown in Figure 3-8, and their accompanying grain size distribution results from the Coulter Laser sampler are shown in Figure 3-9. These results indicate that sites along the edge of the MOTSU channel consist of higher percentages of large grains (approximately 200 microns) while the sites in the channel center are largely finer grains, on the order of 20 microns.

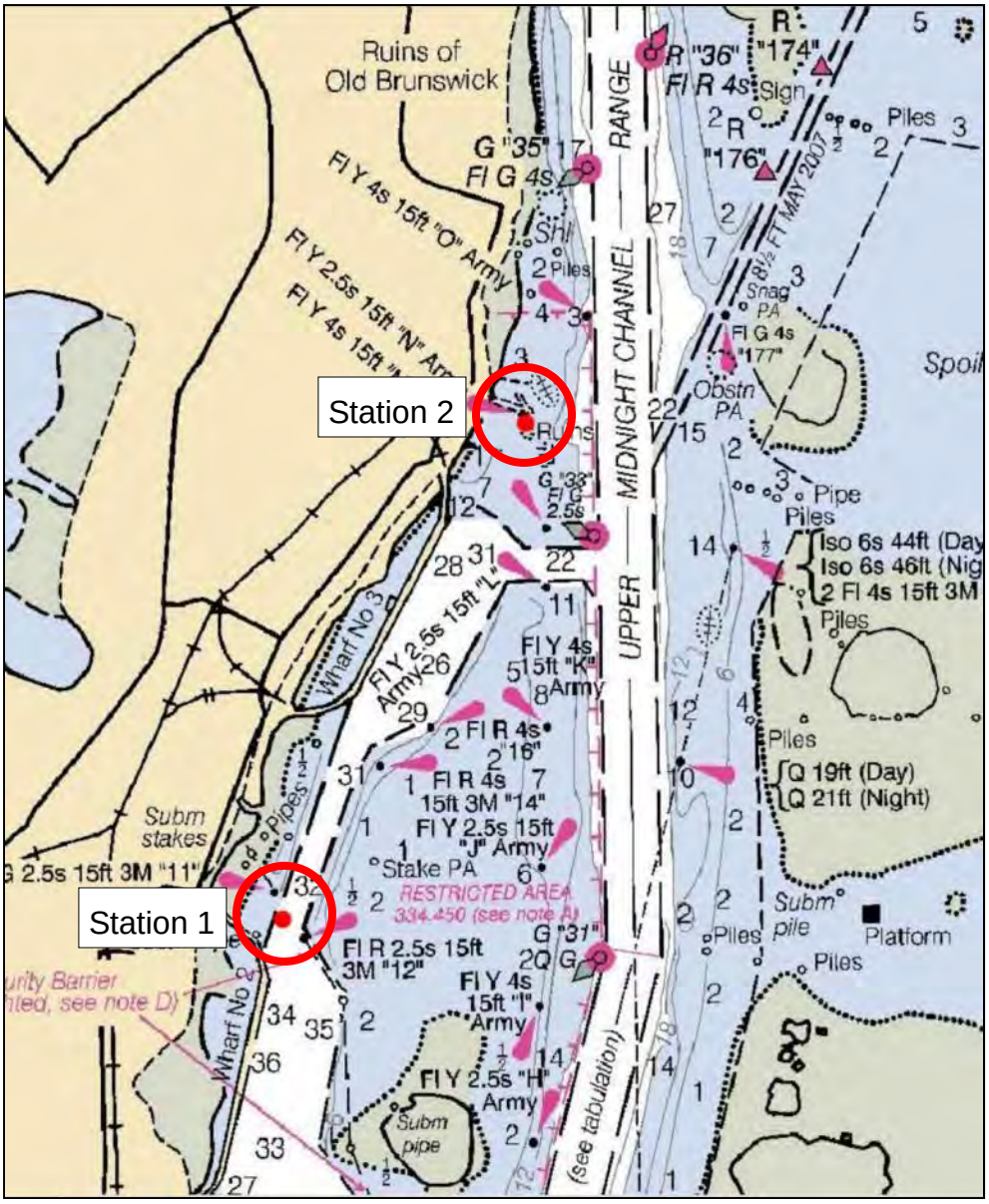

Figure 3-3. Concentration stations from 2008 data collection.

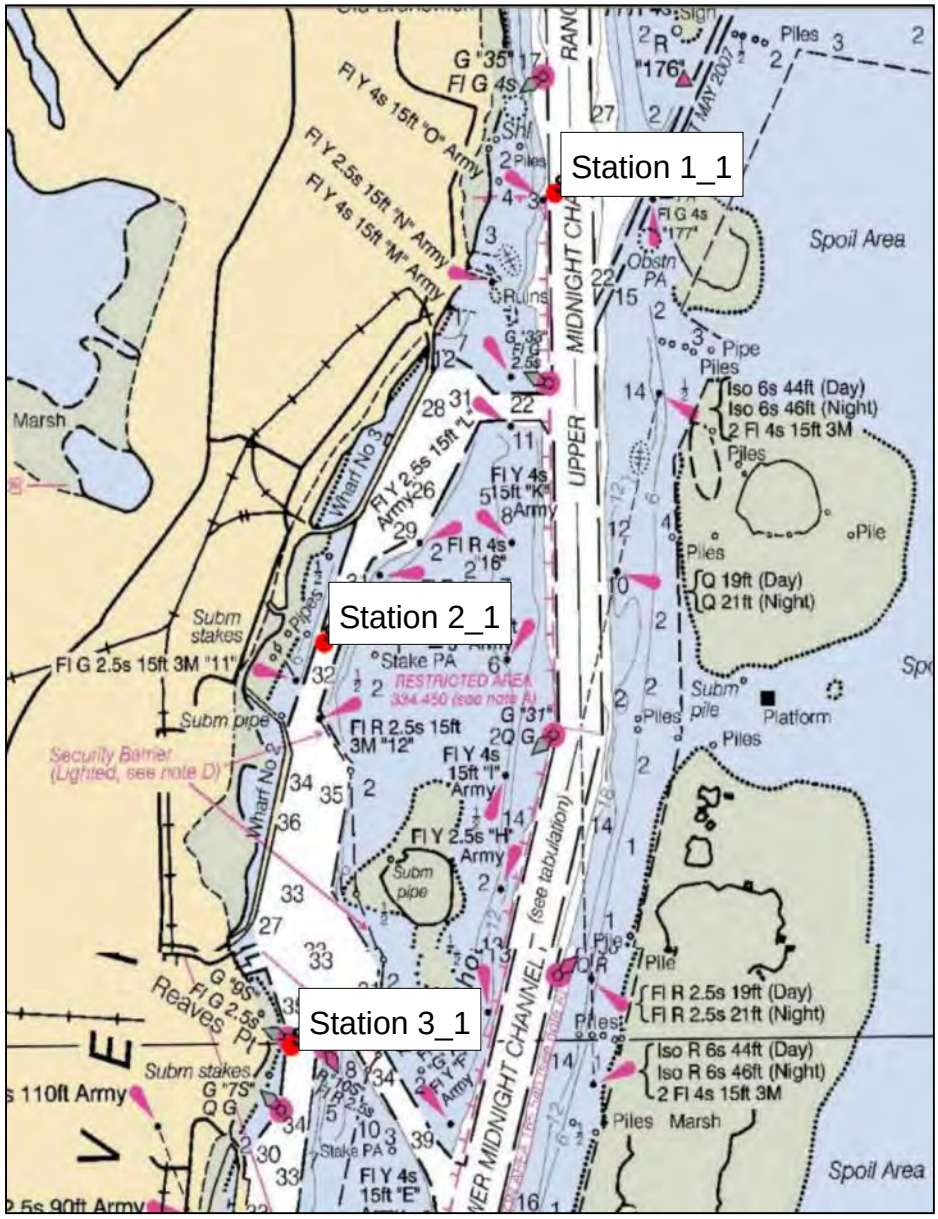

Figure 3-4. Survey station locations for concentration.

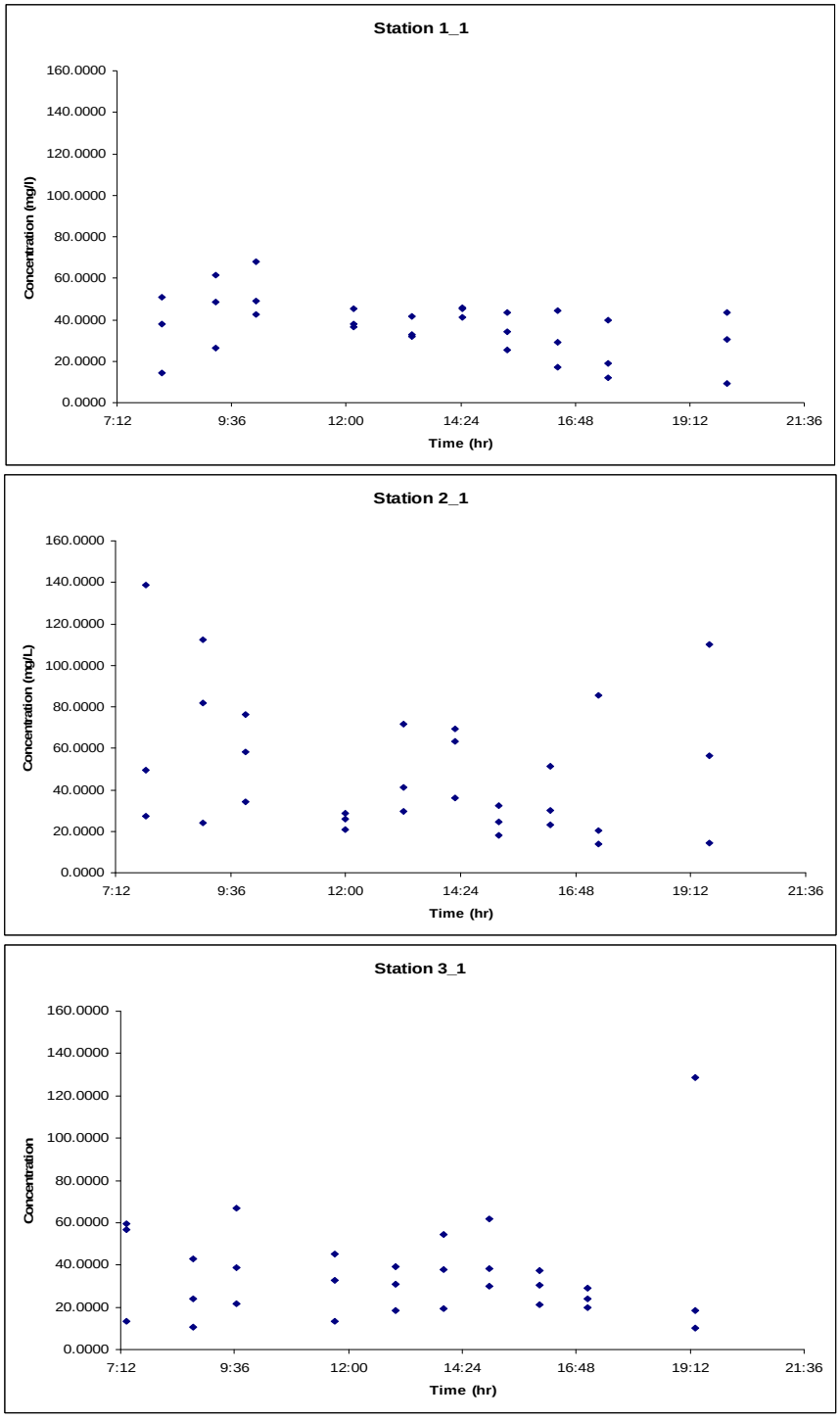

Figure 3-5. Suspended sediment concentrations (mg/l).

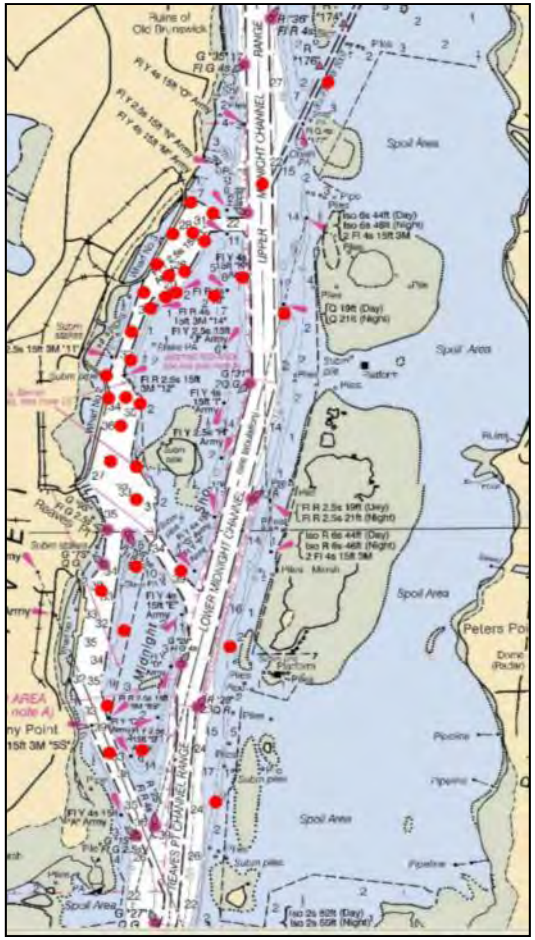

Figure 3-6. Bed samples from 2008 field data collection.

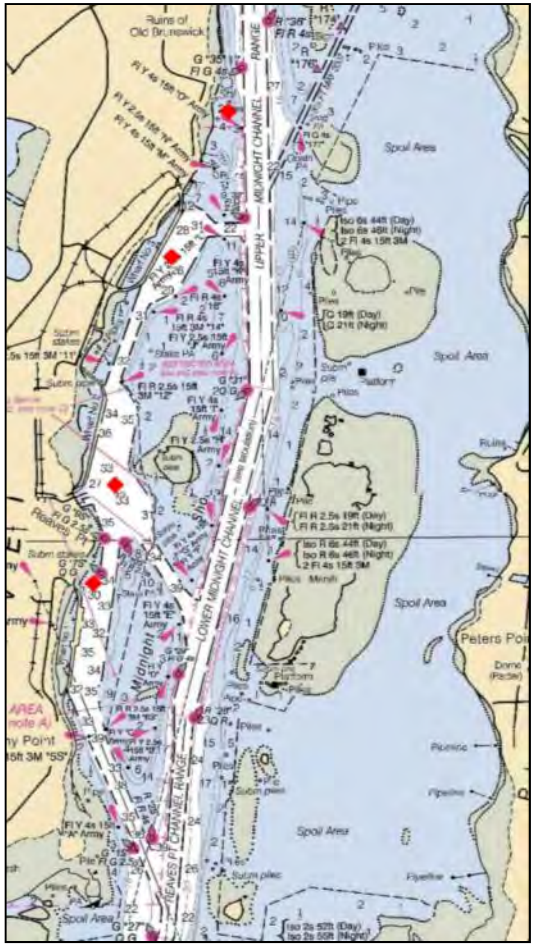

Figure 3-7. SEDFlume core locations (red diamonds).

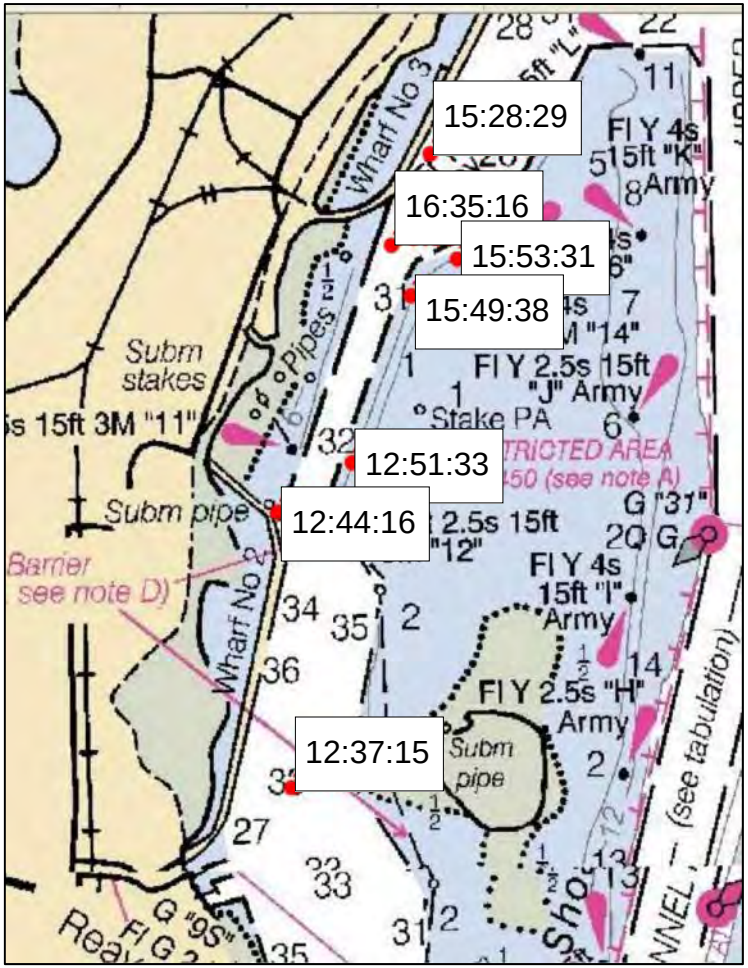

Figure 3-8. Grain size analysis subset.

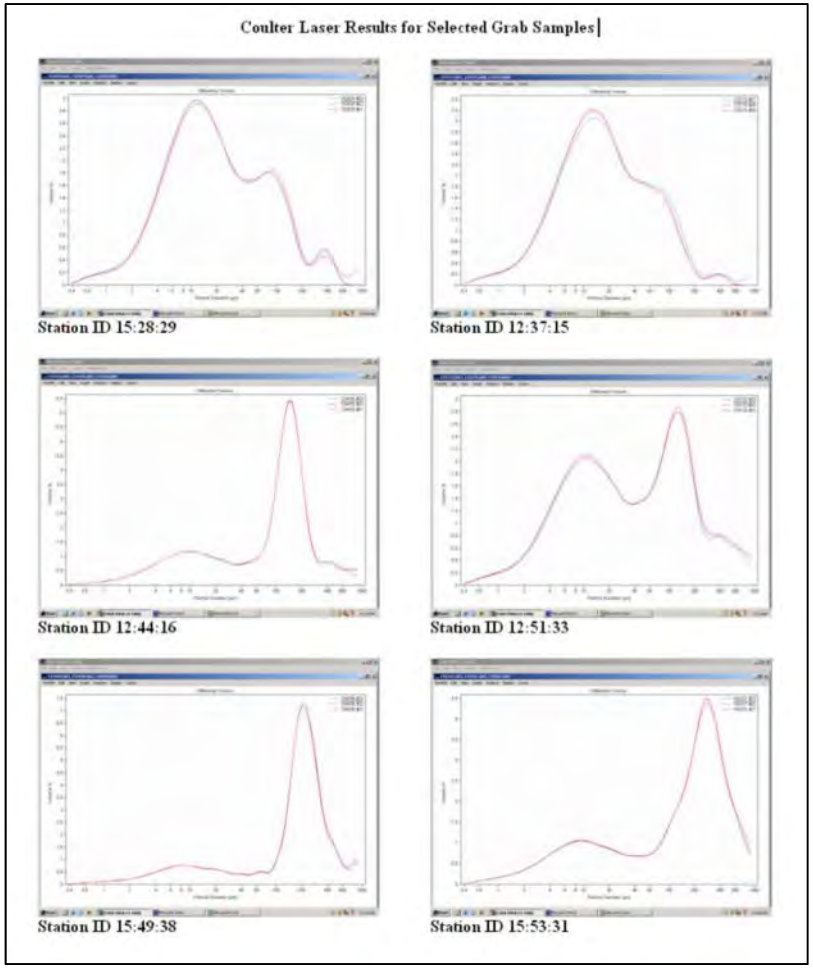

Figure 3-9. Grain size distribution results for subset.

4 Model Development

A numerical model was developed to analyze the alternate plans for changes to the MOTSU area and to test plans for reducing the dredging frequency and/or volume. The model incorporates the natural driving forces of the system—winds, tides, salinity, freshwater inflows, and friction effects. Model validation is conducted with the available field data collected during the January – June 2008 simulation period to ensure an accurate representation of the system. Once validated, the model was used to determine how changes to the facility affect the hydrodynamics and, more specifically, the sediment transport and shoaling patterns within the port.

4.1 Hydrodynamic/sediment numerical model

The TABS-MDS model is used for the design alternatives tested under this study. TABS-MDS is a two-dimensional/three-dimensional finite element code that simulates hydrodynamics, salinity, and sediment transport. The code solves the basic physics of hydrodynamics and salinity transport through the use of the laws of mass and momentum conservation. A similar version of this code was used in a previous study of the Cape Fear River (McAdory 2000). The current work builds from that study. The mesh resolution was increased for the new work and a new model validation was performed. Once the hydrodynamics were modeled, the sediment model were run using the results of the previous hydrodynamic and salinity simulations to drive the sediment transport. Therefore, the hydrodynamics and sediment were solved in an uncoupled fashion for this project, making the assumption that the bed changes due to sediment transport will not impact the hydrodynamics within the system. The TABS-MDS model has been used successfully on many estuarine systems, including Galveston Bay, the Lake Pontchartrain – Lake Borgne area, New York Harbor, and San Francisco Bay.

4.2 Mesh development

The mesh used in McAdory (2000) was a starting point in mesh development for the current modeling effort. The mesh domain encompasses a total of 3,634 square miles. It extends 40 miles into the Atlantic Ocean southward from the river's mouth and a maximum of 94 miles east to west. The Cape Fear River is included from the mouth at the Atlantic

Ocean to the head of tides approximately 41 miles (linearly) upstream. Also included is the lower Black River and Northeast Cape Fear River, Figure 4-1 shows the full model domain. The extensive advances in computational capabilities since the previous study have allowed for significant increases in grid resolution, especially in the study area. Shown in Figure 4-2 is a comparison of the previous mesh resolution and the current increased resolution. The number of elements increased from 5,461 to 10,523 and the number of nodes increased from 18,036 to 31,663. This amounts to an approximately 90% increase in mesh resolution because it was added primarily in the study area. (Higher resolution is not required in all areas.) The refined mesh allows for more detailed results in the area of interest as well as improved visualization and analysis ability. The datums for this model are NAVD 88 for the vertical and State Plane NAD 83, North Carolina, for the horizontal. US standard units are used for the hydrodynamic modeling and metric units are used for the sediment model.

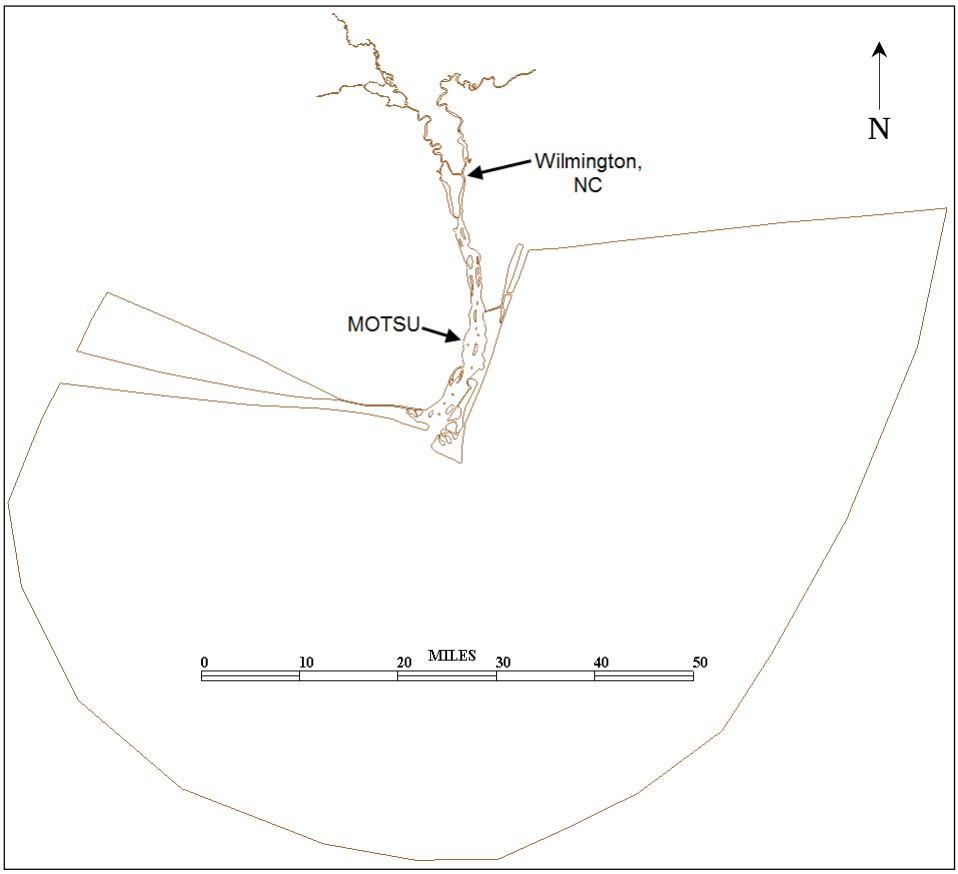

Figure 4-1. Numerical model domain.

Figure 4-2. Mesh resolution comparison (original on left, current on right).

The bathymetry data used in the current modeling effort came from three sources:

- survey data provided by Wilmington District
- survey data obtained using NOAA digital nautical charts
- bathymetry data from the 2000 study model mesh.

Wilmington District provided three sets of survey data: bathymetry data in the navigation channel, bathymetry data of the shallows to the east of the navigation channel, and bathymetry data for the landward side of the three wharfs at MOTSU. These data were the most recent and/or deemed the most accurate for their respective area. Figure 4-3 shows the recent data provided by the sponsor. Data from the NOAA nautical charts (chart numbers 11534, 11536, and 11537) were used to fill in the vast majority of the remaining areas of the mesh, but a few areas remained undefined. For the undefined areas, no new bathymetry data were available, so the best available data are the elevations from the 2000 mesh.

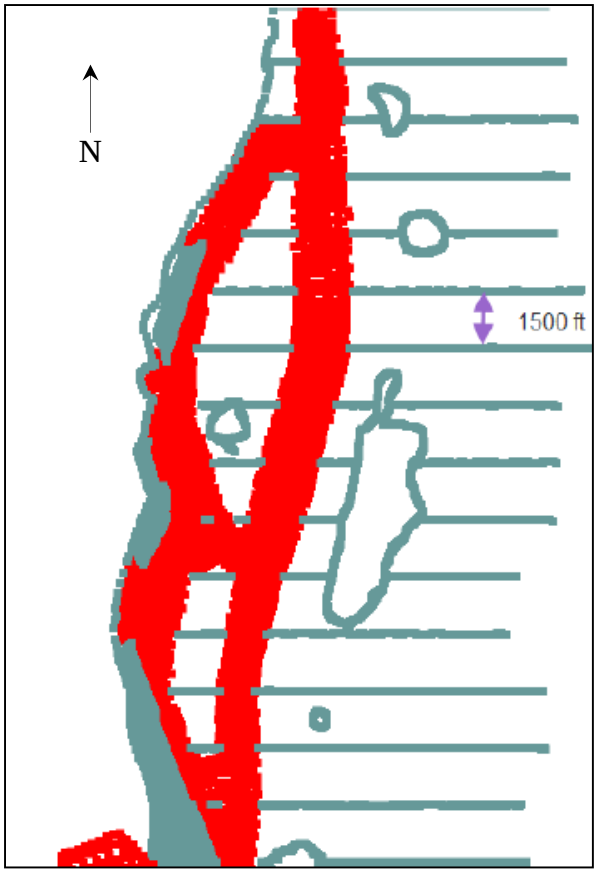

Figure 4-3. Bathymetry data locations provided by Wilmington District.

The coverage of the NOAA data is shown in Figure 4-4. The vertical datum for the NOAA charts was converted from Mean Lower Low Water (MLLW) to NAVD88. Due to the large area encompassed by the mesh, a constant shift from MLLW to NAVD88 was not appropriate. Two shifts from MLLW to NAVD88 were obtained at two separate NOAA gages (Southport and Wilmington, shown in Figure 4-4). The shift at Southport was reported as -2.78 ft (subtract 2.78 ft from the MLLW elevation to convert to NAVD88) and the shift at Wilmington was reported as -2.41 ft (subtract 2.41 ft from the MLLW elevation to convert to NAVD88).

To obtain the most accurate shift from MLLW to NAVD88, a linear interpolation was applied (by latitude inside the estuary) between Wilmington, NC, and Southport, NC. The Southport shift (-2.78 ft) was applied to all points with latitudes south of the Southport gage (33.915°) and in the ocean areas. The Wilmington, NC, shift (-2.41 ft) was applied to all points north of the Wilmington gage (34.23°) inside the estuary. A linear interpolation was used for all points with latitudes between 33.915° and 34.23° inside the estuary.

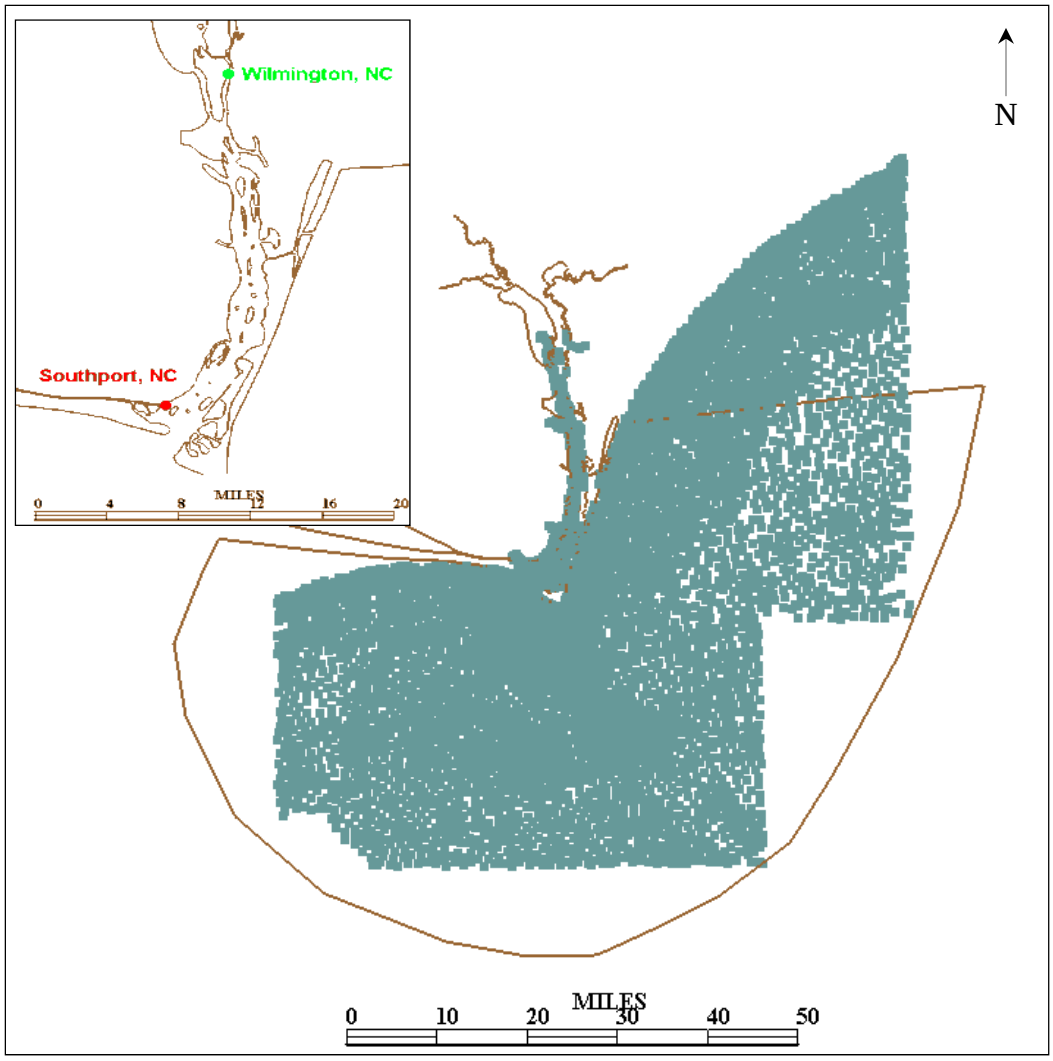

Figure 4-4. NOAA bathymetry data coverage.

For the undefined areas, the bathymetry was obtained from the 2000 study mesh. The elevations in this grid were converted from Mean Low Water to NAVD88 and used to represent the remainder of the mesh not covered with the more recent data. Due to the dating of this 2000 data, its accuracy is unknown but all of these areas are a significant distance from the study area. This makes uncertainties in these elevations relatively unimportant when compared to their effect on the behavior of the hydrodynamics of the study area.

The resulting mesh bathymetry is shown in Figure 4-5. These bathymetry data were utilized to ensure that the most recent data was used in the study area at MOTSU and older data sets are utilized farther away.

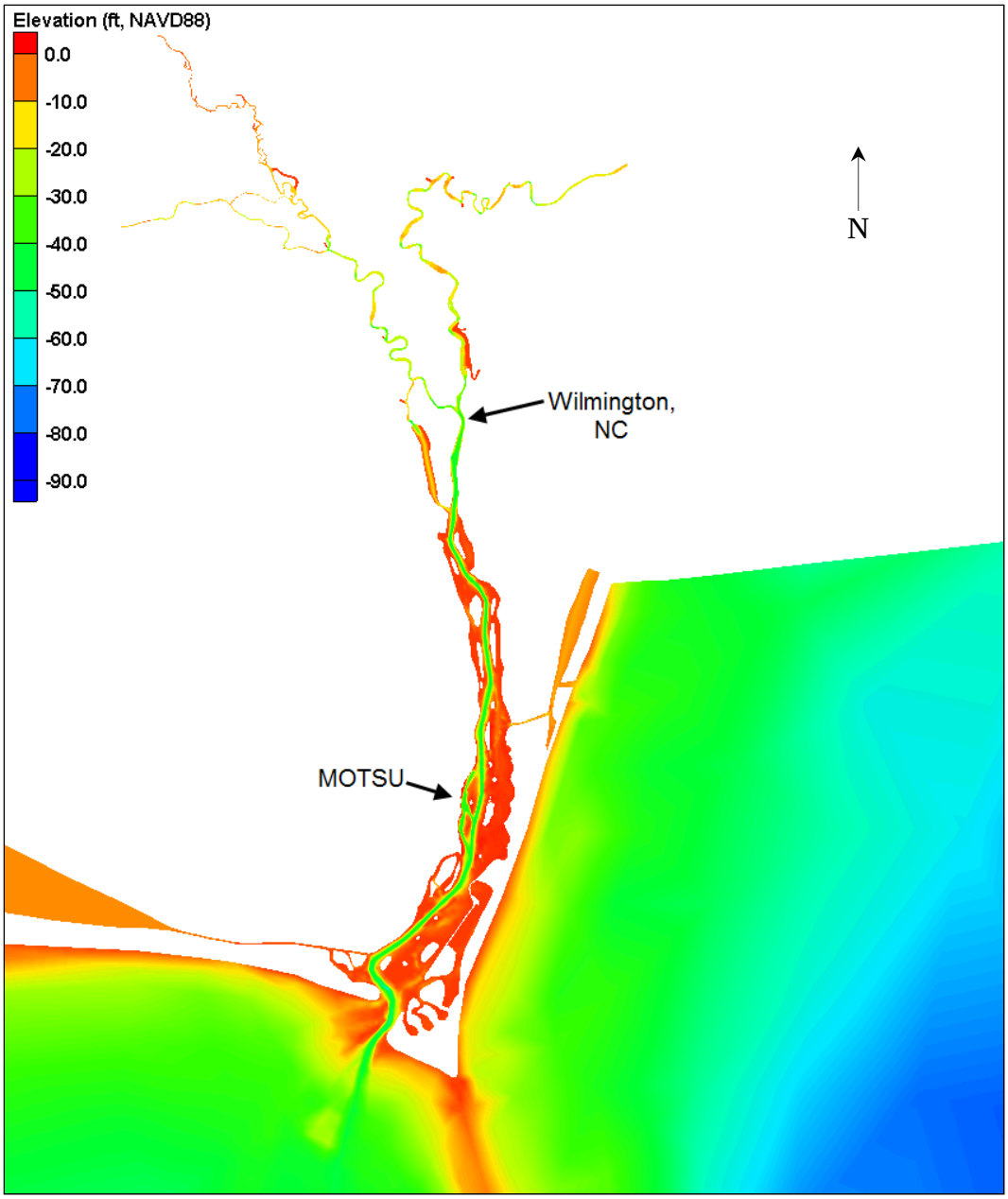

Figure 4-5. Mesh bathymetry.

Spatial material designations were maintained from the previous study (McAdory 2000) to ensure the same bed roughness parameters. The bed roughness was applied using Manning's formulation with variable roughness and a depth algorithm such that at 1 ft depth the vegetation can affect the roughness. The depth-adjusted roughness parameter, when necessary if depth becomes equal to or less than 1 ft, is equal to the ratio of the initial roughness parameter to the depth raised to the $1/6^{th}$ power ($n^* = n/h^{0.167}$, US standard units). The initial roughness parameters are given in Table 4-1, and the spatial designations are shown in Figure 4-6. These Manning's

roughness values were maintained from the previous studies of this area and are supported by the model-to-field comparisons.

Table 4-1. Manning's roughness parameters.

Material	1	2	3	4	5	6	7	8
Manning's Roughness	0.02	0.028	0.03	0.035	0.036	0.037	0.0375	0.04

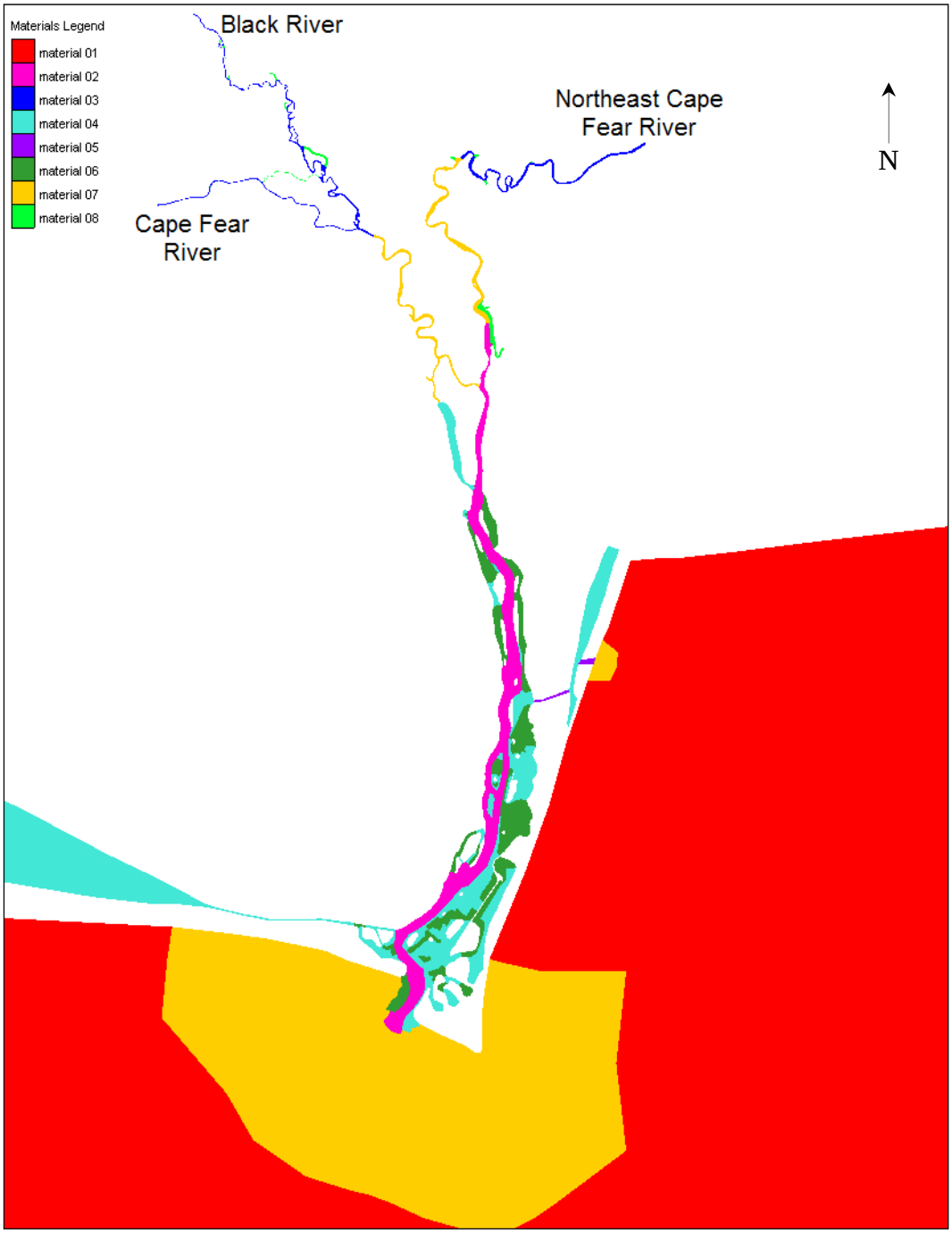

Figure 4-6. Spatial material designations for bed roughness.

The material designations also define the number of vertical layers for the three-dimensional computations. TABS-MDS uses quadratic elements, so each element will have a mid-side node. This allows for more resolution, and vertical computations include an additional node for each layer along with the two corner nodes. Figure 4-7 shows this spatial definition.

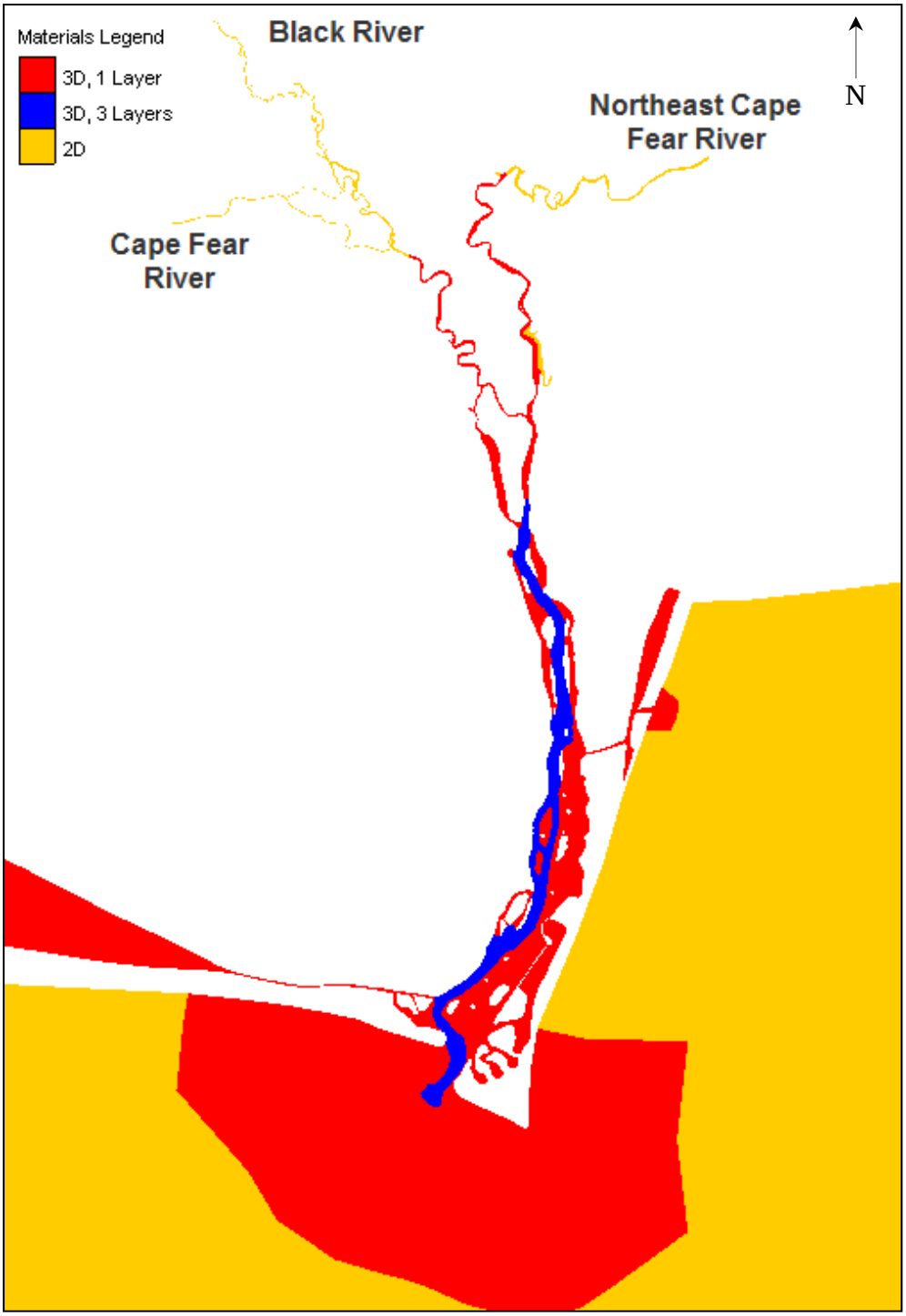

Figure 4-7. Spatial material designations for computation type.

Areas in red will be computed as three-dimensional with one vertical layer. Areas in blue will be computed as three-dimensional with three vertical layers equally spaced based on the depth. Areas in yellow will be computed as two-dimensional, depth averaged.

4.3 Boundary conditions

4.3.1 Hydrodynamic boundary conditions

The hydrodynamic numerical model is driven by the ocean tide, winds, and freshwater river inflows. These boundary conditions, along with the bed roughness parameters, define how the flows propagate within the system. The model is set up to simulate January 1 – June 30, 2008. This period includes the time when field data were collected in the area for water surface elevation, salinity, discharge, and sediment concentrations, and it will be used for the model validation. The tide condition in this area semi-diurnal such that it has an approximately 12 hour signal with two highs and lows per day. The average tide range for this period is approximately 4 ft. Figure 4-8 shows the tide signal used for this modeling effort, applied uniformly around the ocean boundary. The vertical datum for this elevation is NAVD88.

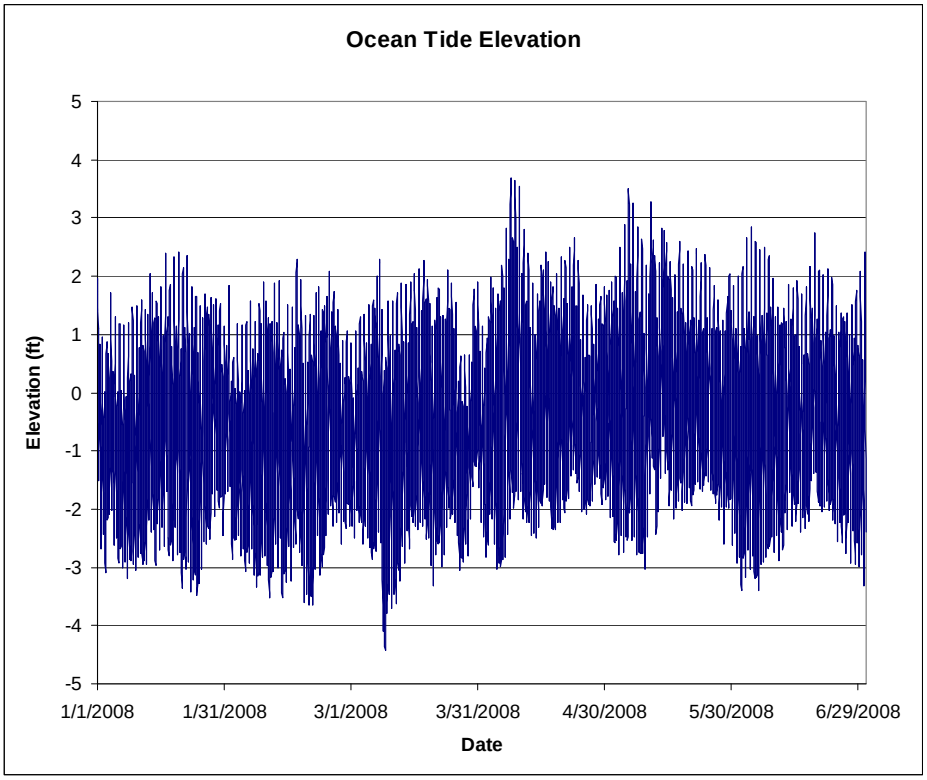

Figure 4-8. Ocean tidal boundary condition.

Three freshwater inflow locations are included in this modeling study: the Cape Fear River, the Black River, and the Northeast Cape Fear River. The combined discharge at each of these upstream locations is the driving fresh water source for the model. The Cape Fear River provides the largest discharges, with the peak being 18,000 cfs during this 6 month simulation period (Figure 4-9). The Northeast Cape Fear River and the Black River contribute similar flows to the system—generally less than 3,000 cfs (Figure 4-10 and Figure 4-11, respectively).

Wind data are also applied over the model domain to help drive currents representative of the natural environment. These winds are provided to the model with a speed at 10 meters above the ground and a direction based on the standard Cartesian system (counterclockwise from east). The wind speed is shown in Figure 4-12 and the direction in Figure 4-13. Both the speed and direction are constant over the entire model domain.

The initial salinity is set such that the ocean salinity is 30 ppt and the initial values decrease up the estuary to zero at the river boundaries. Figure 4-14 shows the initial salinity field. The boundary condition at the ocean was set at 36 ppt throughout the simulation.

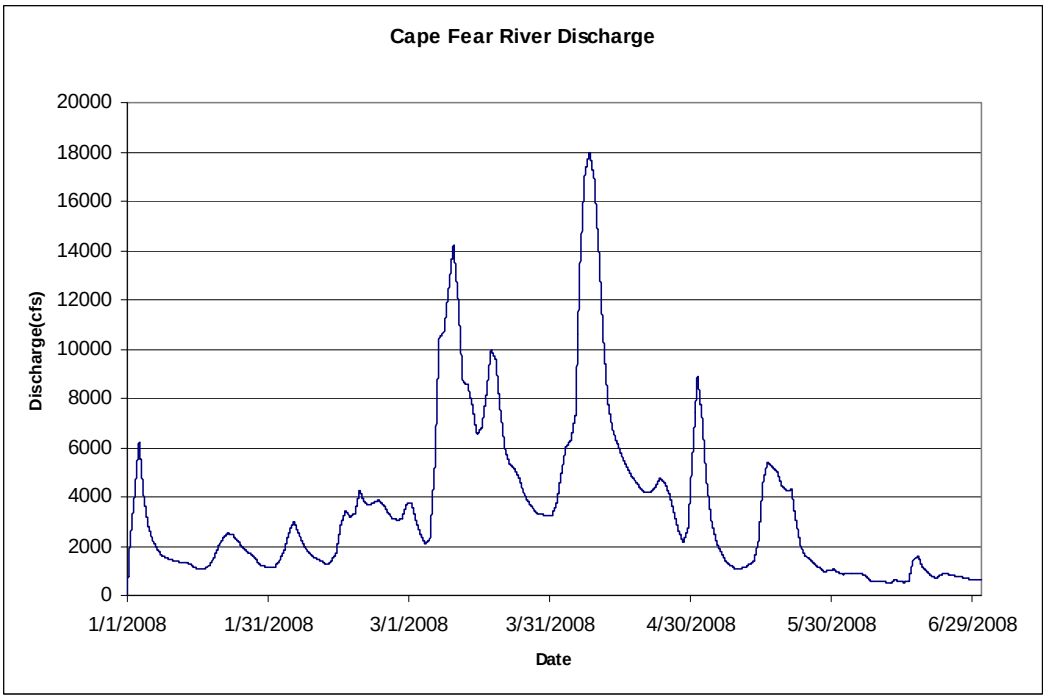

Figure 4-9. Cape Fear River discharge.

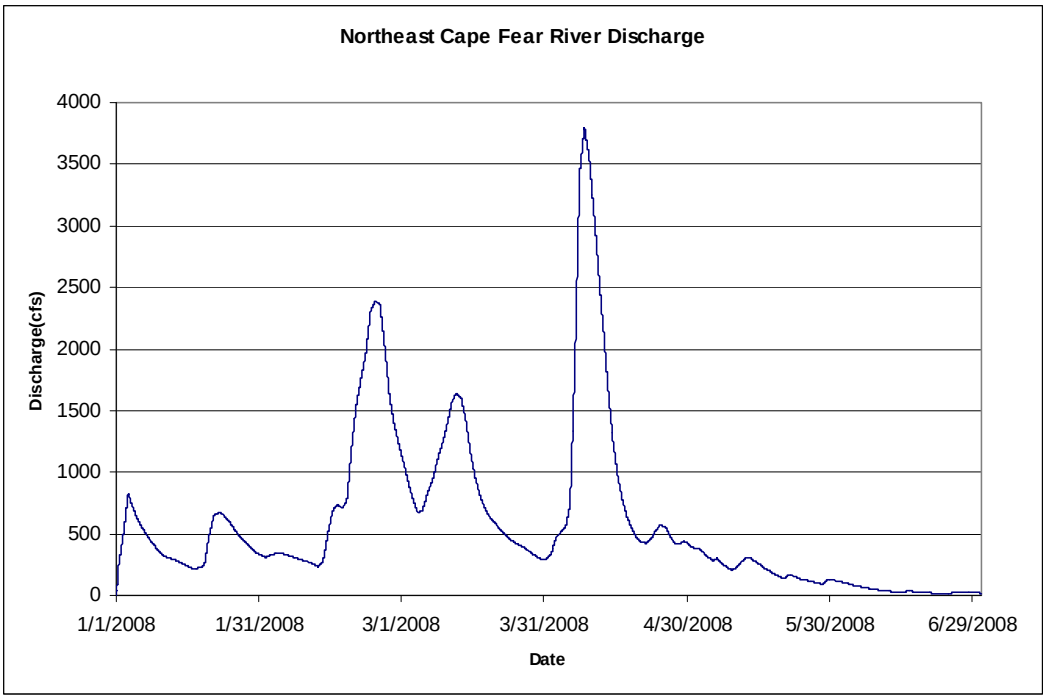

Figure 4-10. Northeast Cape Fear River discharge.

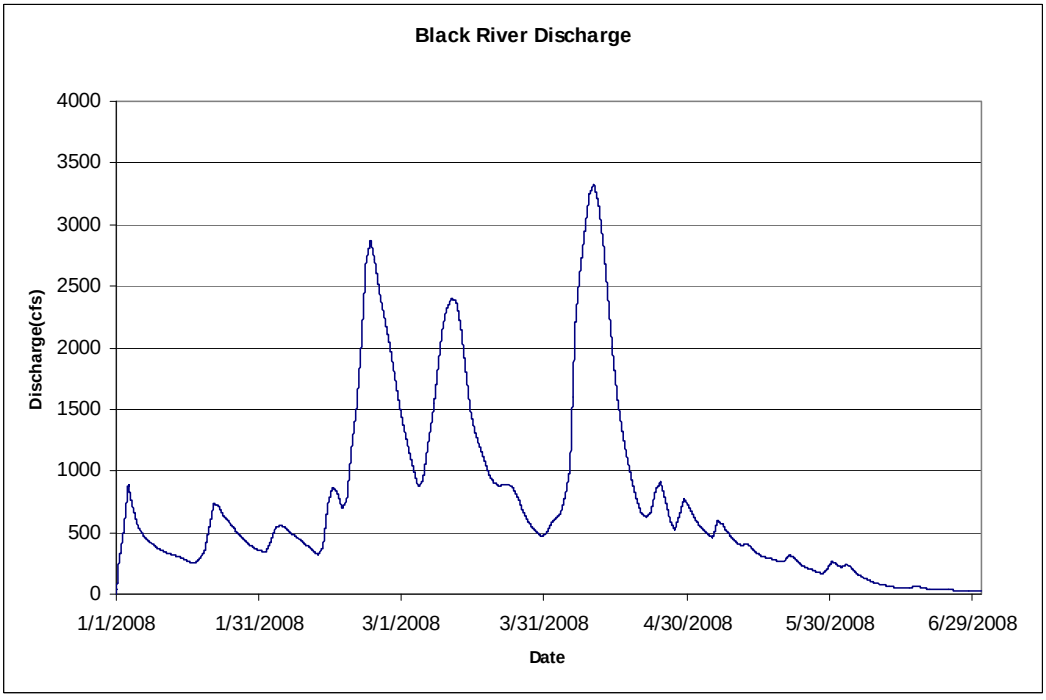

Figure 4-11. Black River discharge.

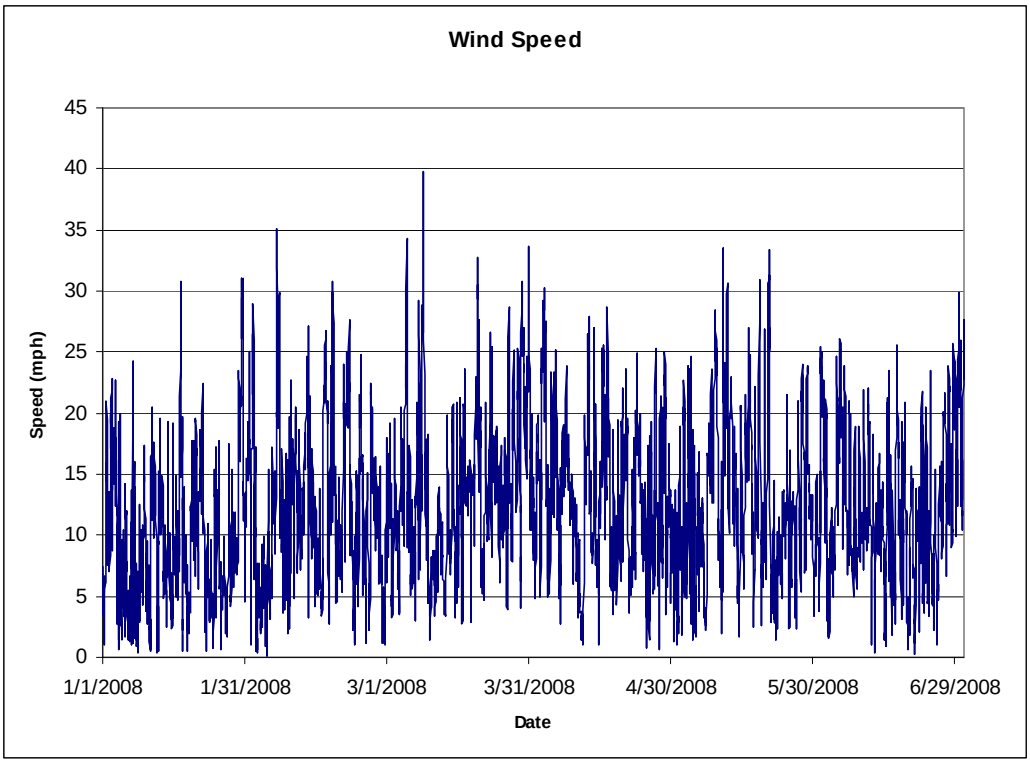

Figure 4-12. Wind speed in mph at 10 m elevation.

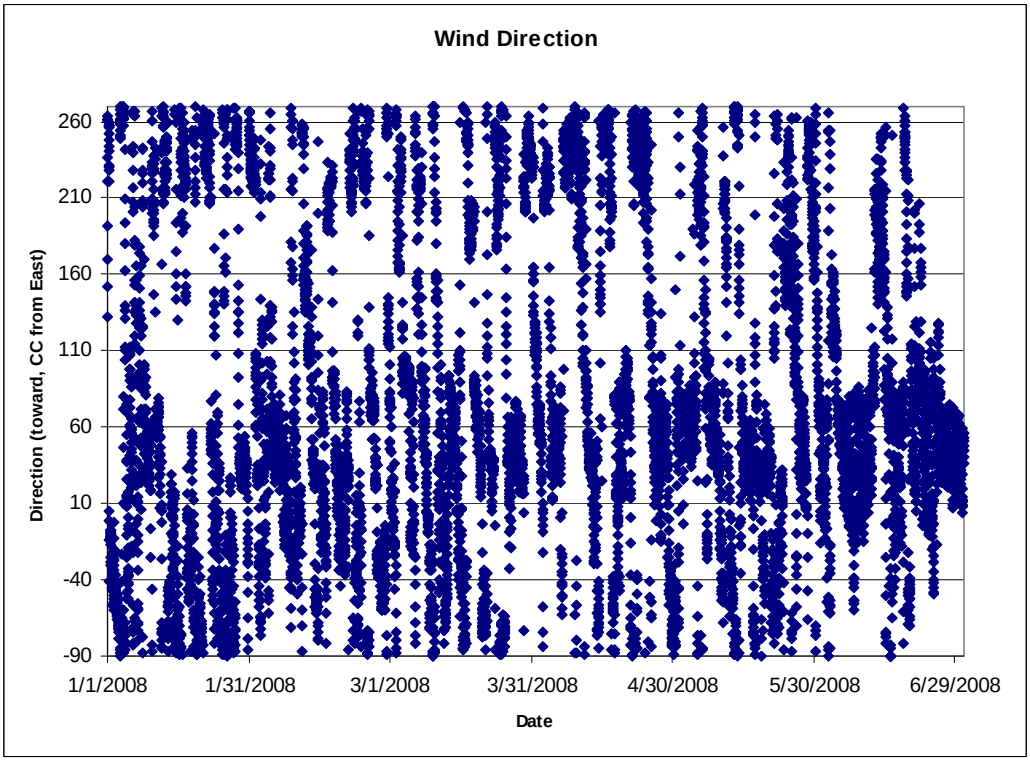

Figure 4-13. Direction toward which wind is blowing, measured counterclockwise from east.

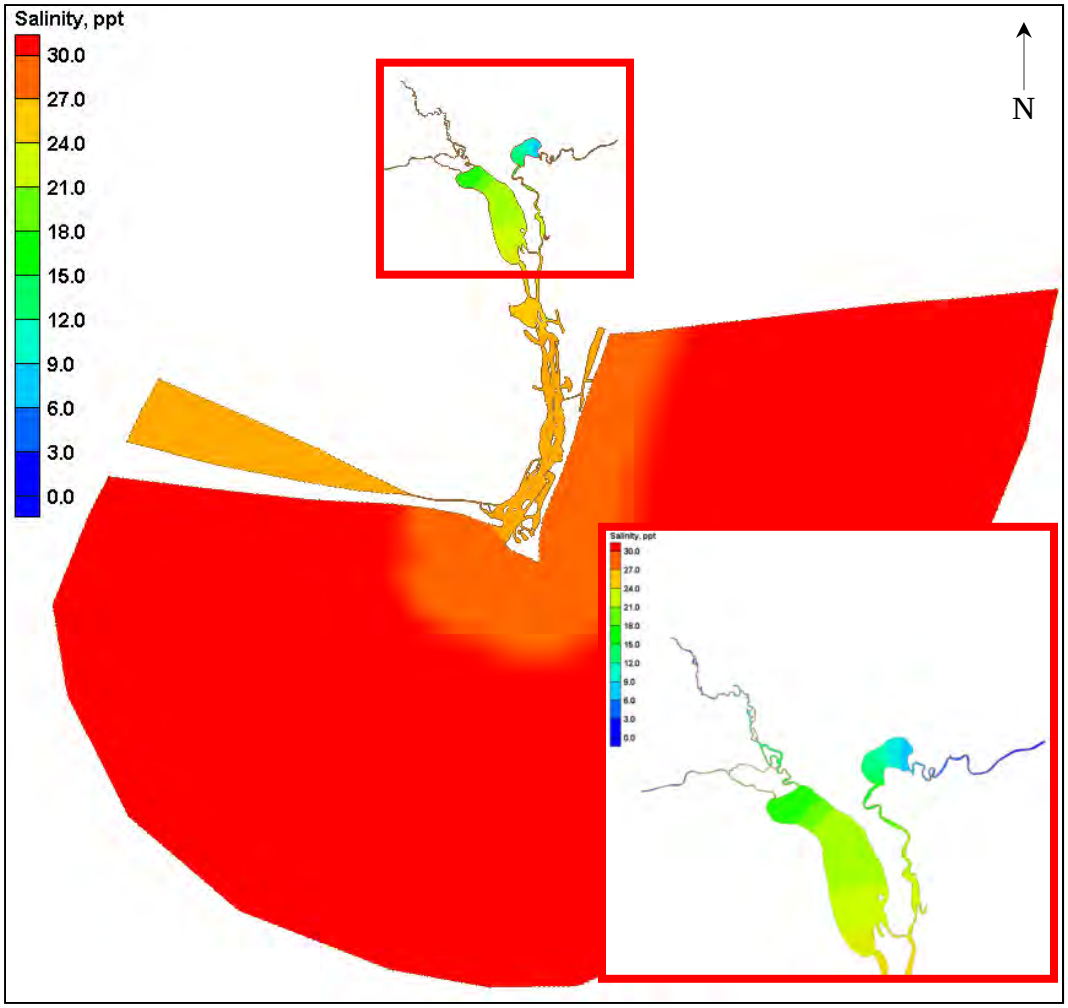

Figure 4-14. Initial salinity concentrations.

4.3.2 Sediment boundary conditions

The sediment model uses the results from the hydrodynamic simulations to drive the sediment transport simulations. Additional information is added to the boundary condition file for the sediment simulations. The sediment model must be run in metric units, so all unit-specific parameters are first converted to metric units. The sediment grain properties are based on the results of the 2010 US Geological Survey (USGS) field data analysis, and inflow loads are obtained from field data and USGS sediment load rating curves.

For this model, four grain classes are simulated based on the grain-size distribution found in the field. Table 4-2 below gives the grain-specific parameters for each grain class. The first grain is actually a clay constituent that has some additional grain parameters, whereas the other three are

silt/sand classes. Clay beds settle and consolidate under their own weight, so consolidation parameters are also provided based on bed core samples taken from the field. This model includes three bed layers, with initial thicknesses of 0.355 m for the upper layer, 0.025 m for the middle layer, and 0.025 m for the bottom layer. Additional bed properties are defined for each layer and grain class as shown in Table 4-2. Fluid mud, known to exist in the study area, is not included in the model computations. This assumption implies that once the fines are settled they remain in the bed, thus losing the ability to mobilize and transport in a characteristic manner associated with fluid mud.

Sediment is available for transport from the bed as well as from the river inflows. Because no sediment load data are available for the specific portion of the Cape Fear River being modeled, discharge and load data were derived from a USGS rating curve for the Haw River, which is located somewhat upstream within the same watershed. The discharge data used for the three inflow rivers in the hydrodynamic model were then used with the rating curve to generate estimated sediment loads at the model boundaries. The sediment load was not applied individually by grain class but rather as a combined load at each river based on its discharge. Figure 4-15 shows the Haw River rating curve, and Figure 4-16 shows the sediment concentrations for each of the river inflows during the 6 month model simulation period. The rating curve does present a level of uncertainty because of the overall lack of data and possible small variations in the curve fit. It is important to note, however, in an estuarine environment all of the material available for movement within the system may not be accounted for in the initial bed characteristics or river loads. Due to the tidal action of the currents, material settles and resuspends on a daily basis and has many opportunities to move about in the system in addition to non-gaged runoff.

Table 4-2. Sediment-specific parameters

Grain Parameter	Grain 1	Grain 2	Grain 3	Grain 4
Critical Shear Stress for Erosion (τ_{ce}, N/m^2)	$0.000026 * Conc^{1.58}$	0.067	0.188	0.527
Critical Shear Stress for Deposition (N/m^2)	0.021	0.024	0.067	0.188
Erosion Rate Constant	$\tau_{ce} * 200 * e^{(-14.5*\tau_{ce}{}^{0.122})}$	--	--	--
Excess Shear Stress Exponent	0.85	--	--	--
Maximum Allowable Silt Fraction	0.995	--	--	--
Hiding Factor (Hf)	0.7			
Minimum Concentration Threshold for Settling (Tmin, kg/m^3)	0.11			
Maximum Concentration Threshold for Settling (Tmax, kg/m^3)	1.0	3.0	5.0	8.0
Settling Exponent (Se)	1.33	1.1	0.9	0.8
Fall Velocity	$If\ Tmin \geq Conc;\ Vs * (Tmin/Tmax)^{Se}$ $If\ Tmax \geq Conc > Tmin;\ Vs * (Conc/Tmax^{Se})$ $If\ Conc > Tmax;\ Vs$			
Nominal/Hindered Bed Settling Velocity (Vs, m/s)	0.00072	0.00106	0.0014	0.003
Consolidation Exponent (Ce)	5.28	5.28	5.28	5.28
Consolidation Coefficient (Cc)	0.00085	0.00078	0.00078	0.00062
Bed Layer Settling Velocity (m/s)	$Vs * (1 - Cc * Conc)^{Ce}$			
Fall Velocity Concentration Threshold (kg/m^3)	1.0	3.0	5.0	8.0
Settling Exponent	1.33	1.1	0.9	0.8
Bed Layer Mass Concentration (kg/m^3) – 3 layers	136.0	55.0	45.0	1200.0
	90.0	59.0	52.0	1250.0
	105.0	69.0	61.0	1200.0

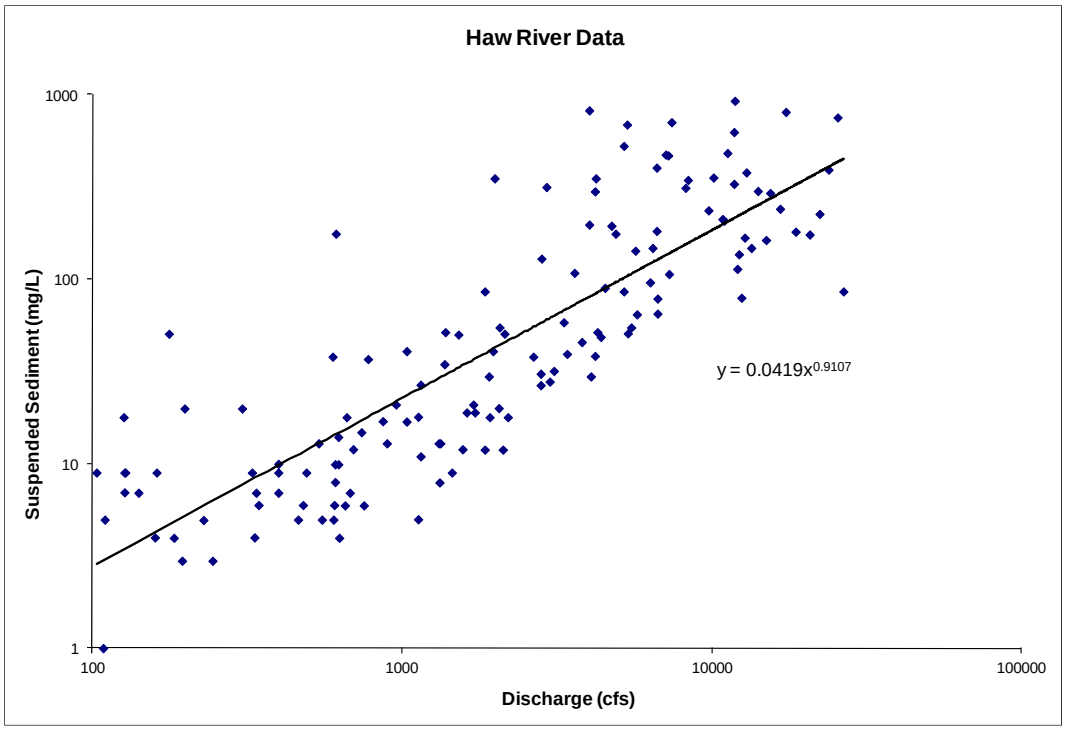

Figure 4-15. Haw River sediment load rating curve (100 mg/L = 1 ppt).

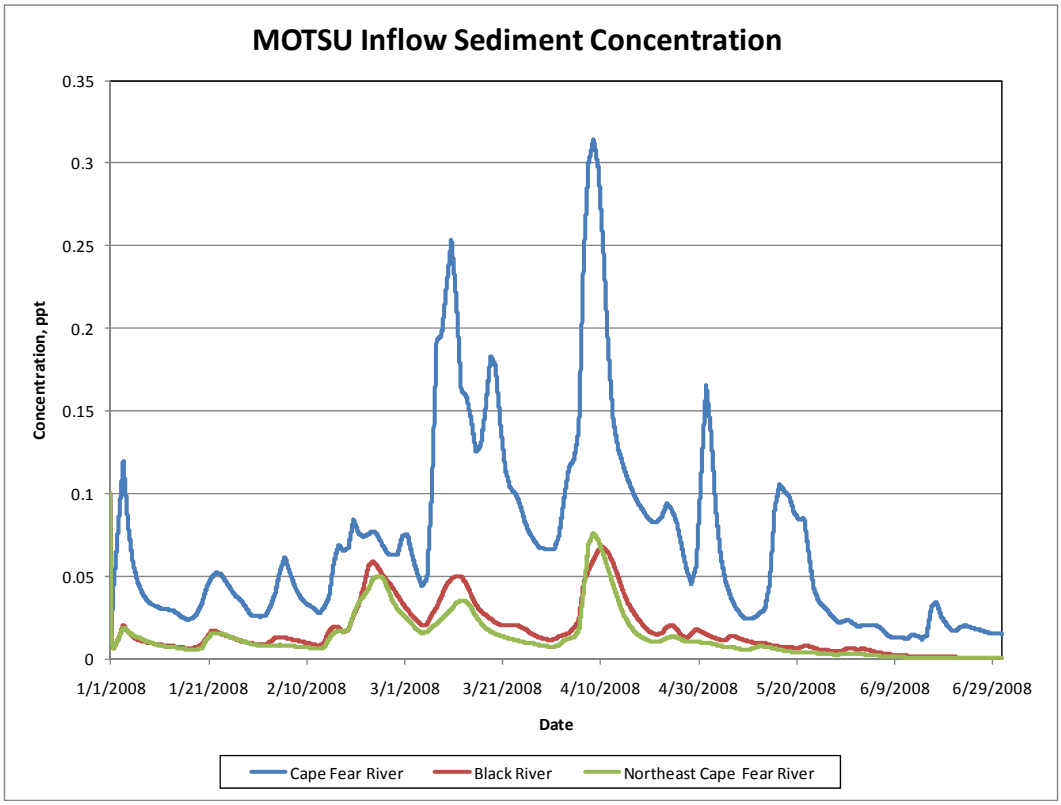

Figure 4-16. Sediment loads for model boundary conditions.

5 Model Validation

The hydrodynamic and sediment model must be compared to several different types of field data to ensure that the model accurately represents the field. Discharge, water surface, salinity, and shoaling data were all used to determine how well this model replicates the system.

The field data for discharge were collected on 8 February 2008. ADCP data were taken hourly at three transects along the MOTSU area over this single day. Range 1 is the northernmost range, and it is located just north of the northern wharf along the main navigation channel in the Cape Fear River. Range two is southward from Range 1, and is located about midway between the northern and center wharfs. Range 3 is the southernmost range, and is located just south of the center wharf turning basin and extends into the central entrance channel. Figure 5-1 shows the location of the three ADCP ranges for discharge collection.

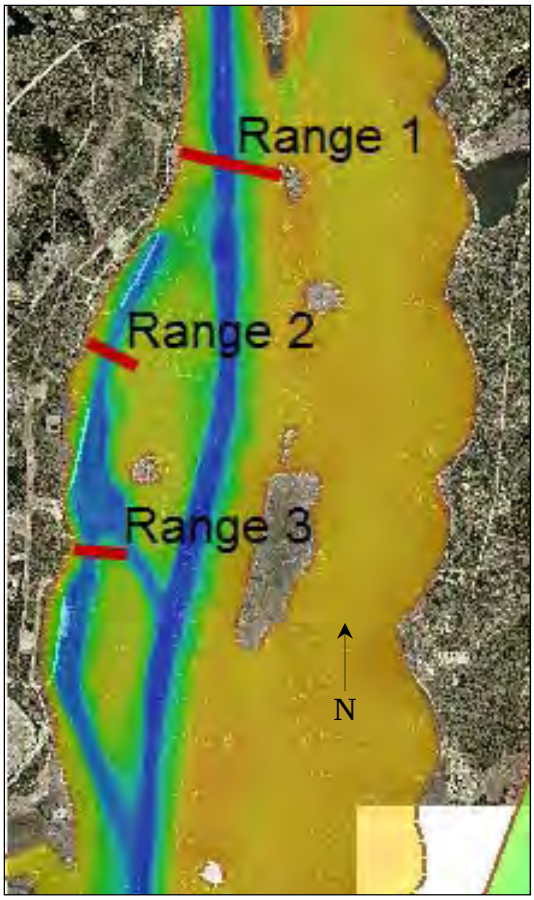

Figure 5-1. Discharge range locations for field data comparison.

The model comparison to the measured field discharge values at the three ranges is shown in Figure 5-2 through Figure 5-4. The field data are shown as the black symbols, and the model results are shown as the solid red line.

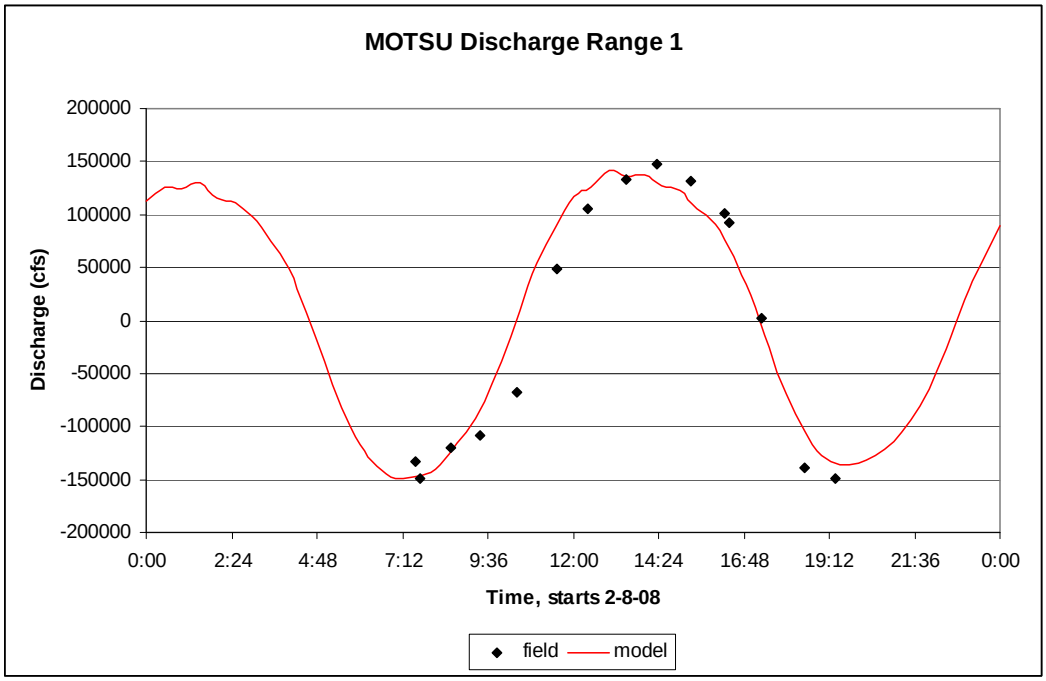

Figure 5-2. Discharge comparison for Range 1 (northernmost).

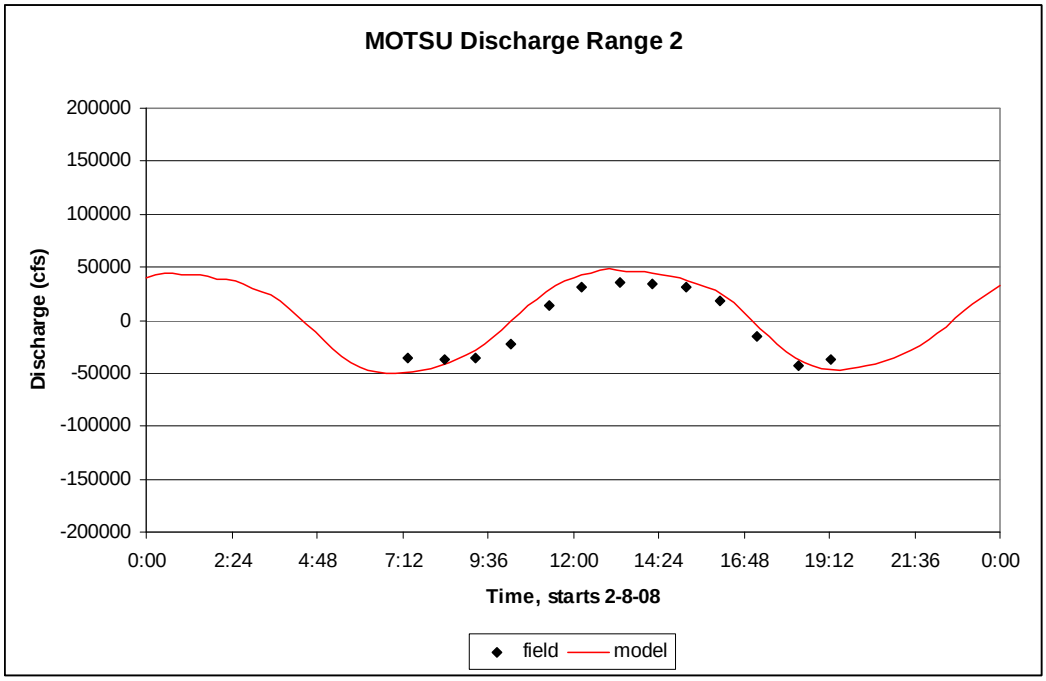

Figure 5-3. Discharge comparison for Range 2 (central).

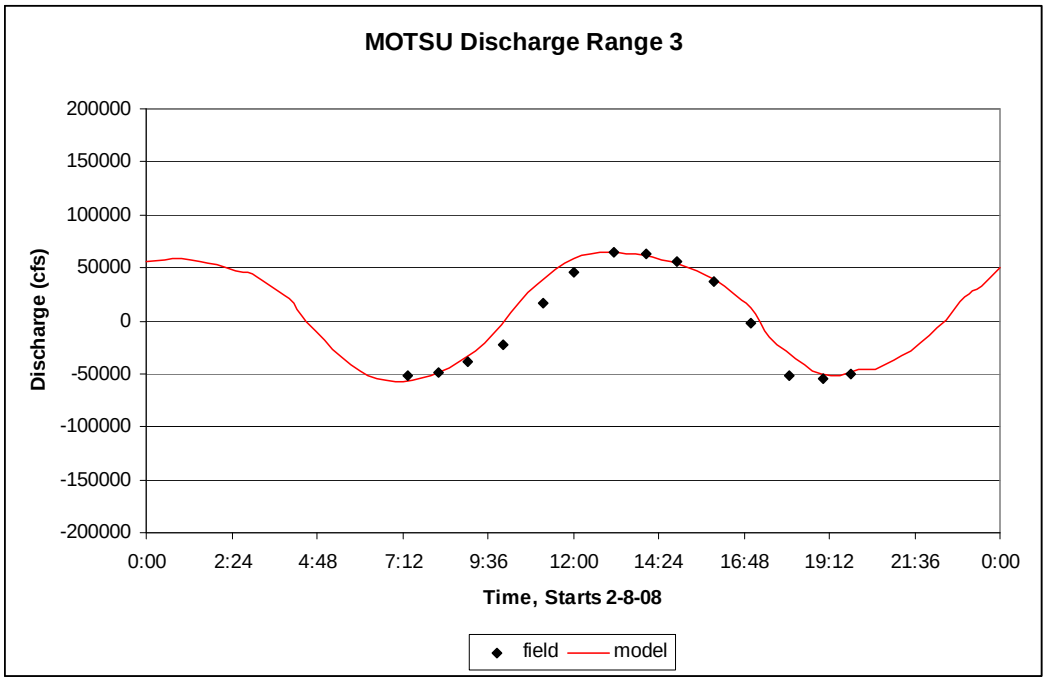

Figure 5-4. Discharge comparison for Range 3 (southernmost).

Positive values are ebb-directed, with flows directed toward the ocean; negative values are flood-directed, with flows directed inland toward Wilmington. The model does a good job matching the highs and lows of the discharge over this 1 day interval. There does appear to be a phase lag from peak flood to peak ebb flow as indicated by the shift of the model results as compared with the field data. However, the time of peak flood and ebb is matched well by the model.

Salinity data were collected at the surface and bottom at the five locations shown in Figure 5-5 over a three-month period from February to May 2008. At some sample sites, data were not acquired over the entire sample period, leaving large gaps in the data set, so only a subset of the ten sampling locations is used for model comparison. Figure 5-6 through Figure 5-12 show the salinity comparison, with the field being the solid blue line and the model being the red dashed line. These figures indicate that the model does not continuously reproduce the exact salinity magnitudes, but the pattern of change is depicted well. At times the model computes salinity values lower than the field. This may be due to inexact representation of the shallows, which can modify the tidal prism and therefore the distance that the salinity wedge travels upstream. It is known that the higher salt concentrations lie near the bottom due to the increased density of high-saline water. This surface-to-bottom variation in salinity is seen in both

the field data and the model data, indicating that the model is representing this three-dimensional effect correctly. Fine sediment processes are closely tied to salinity values since particles will flocculate at salinity values around 2 ppt and higher. However, in the MOTSU vicinity, the salinity values are higher than 2 ppt, so these differences in the model salinity should not adversely affect the model results for sedimentation.

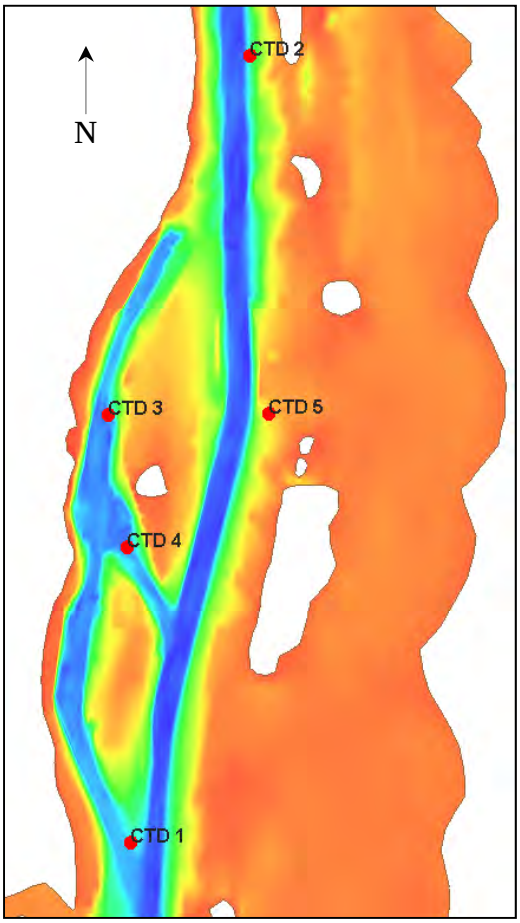

Figure 5-5. Salinity field data comparison locations.

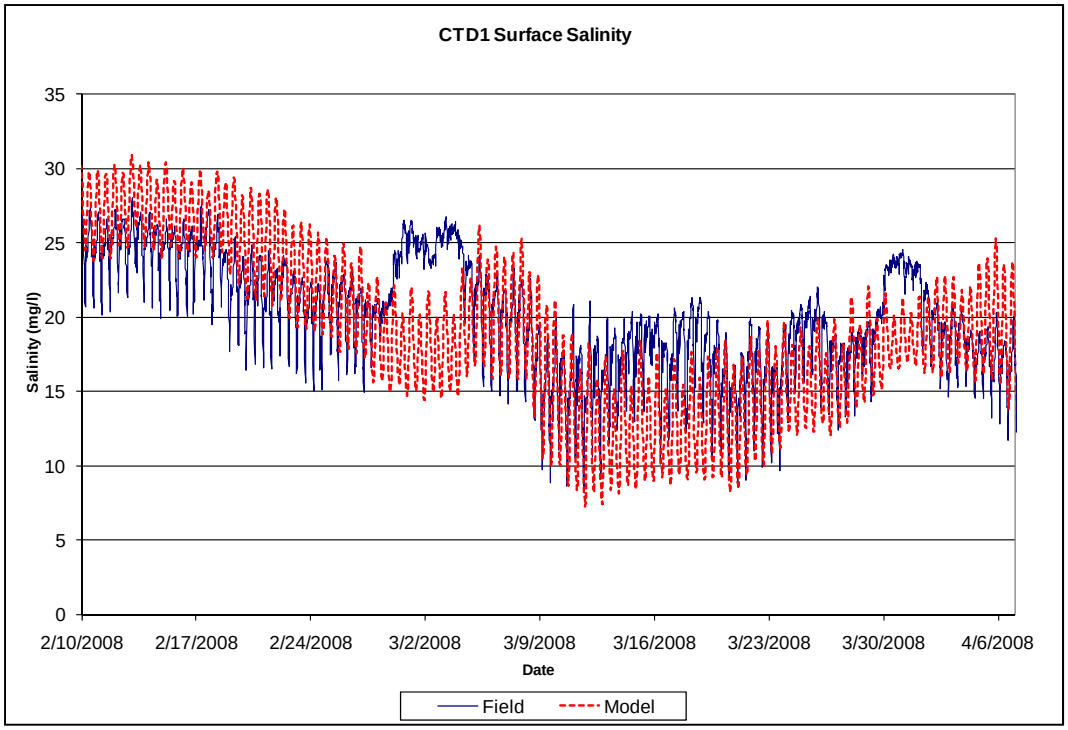

Figure 5-6. Surface salinity comparison for location 1.

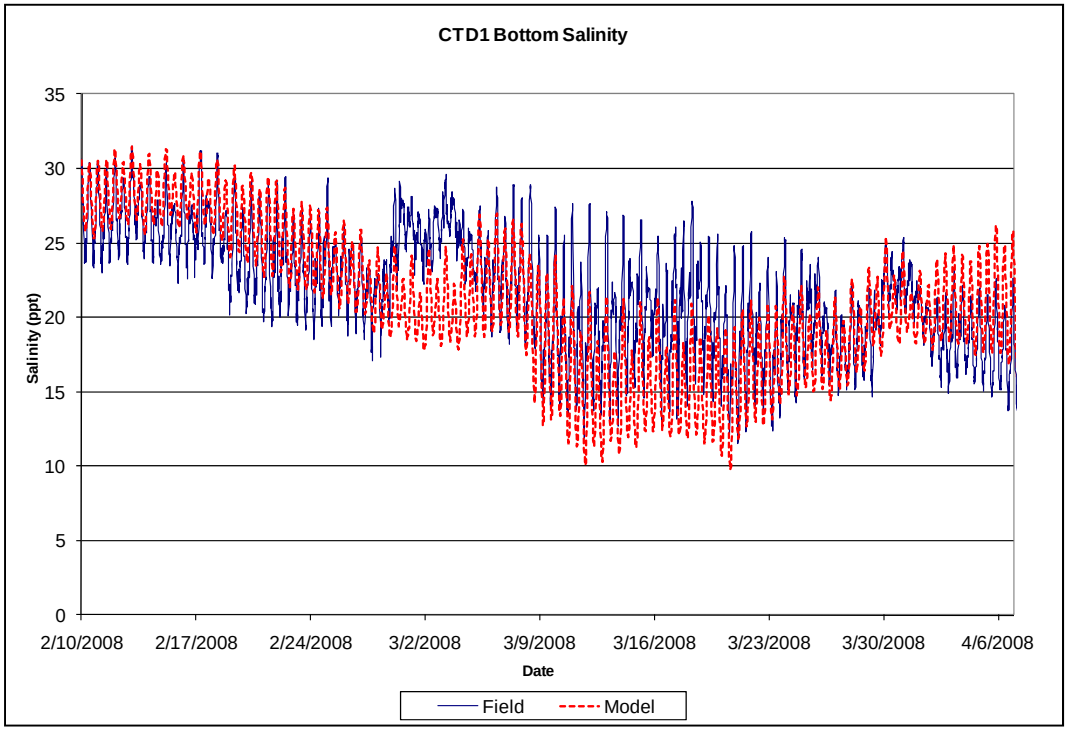

Figure 5-7. Bottom salinity comparison for location 1.

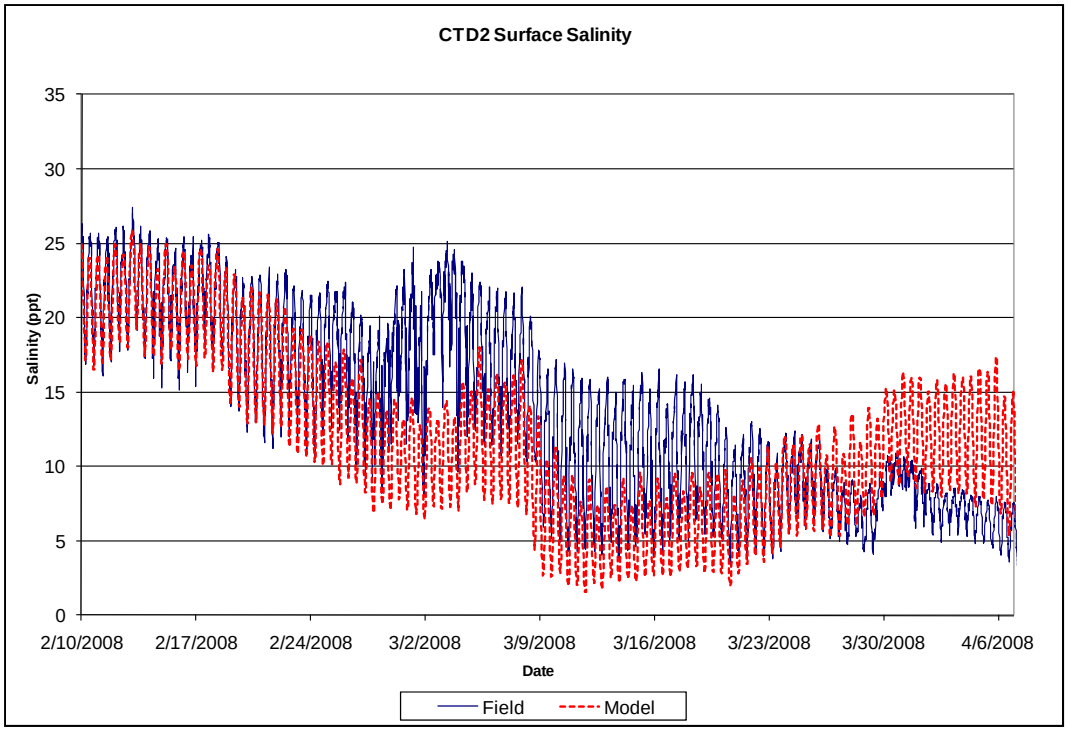

Figure 5-8. Surface salinity comparison for location 2.

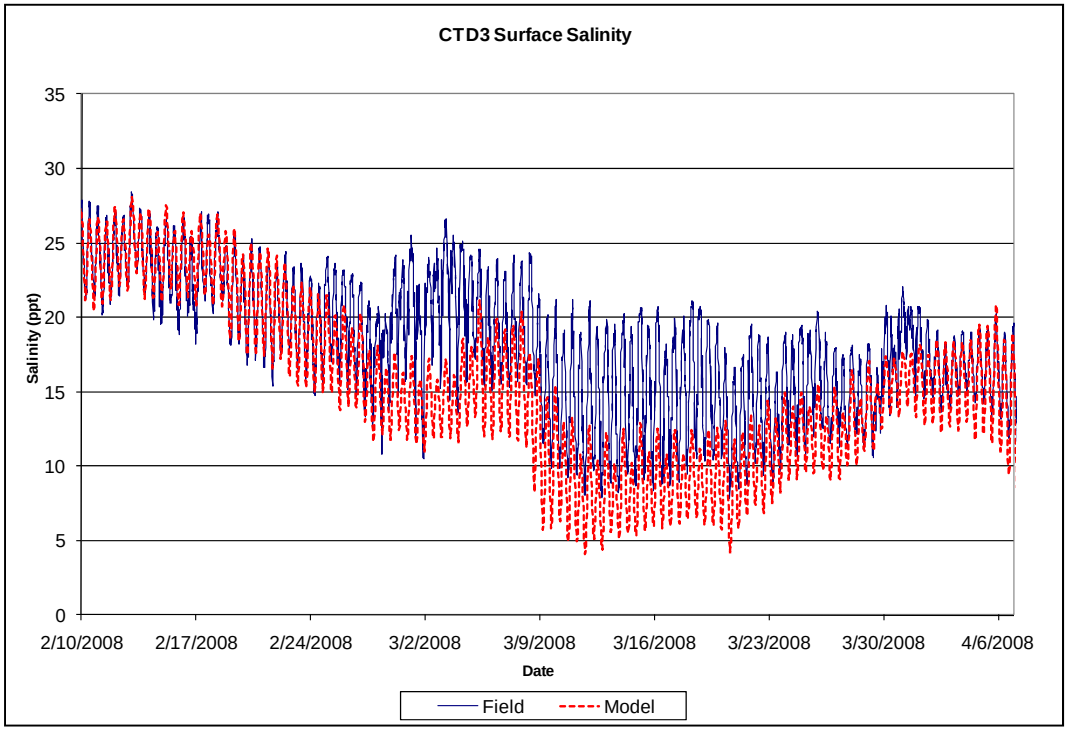

Figure 5-9. Surface salinity comparison for location 3.

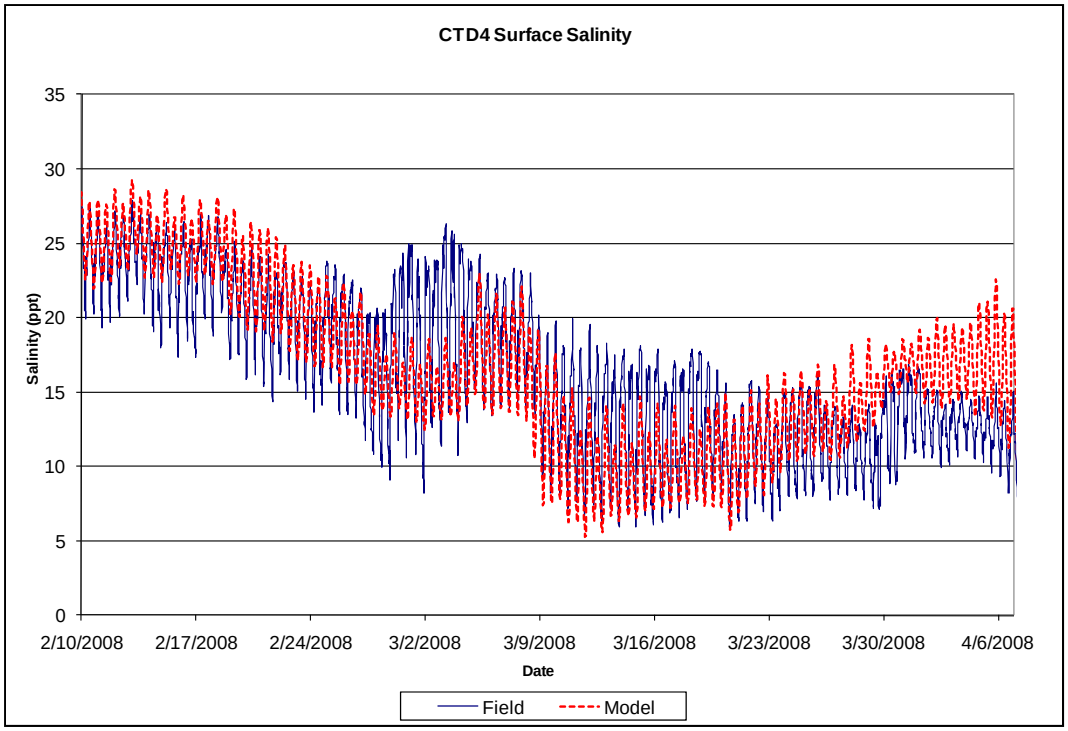

Figure 5-10. Surface salinity comparison for location 4.

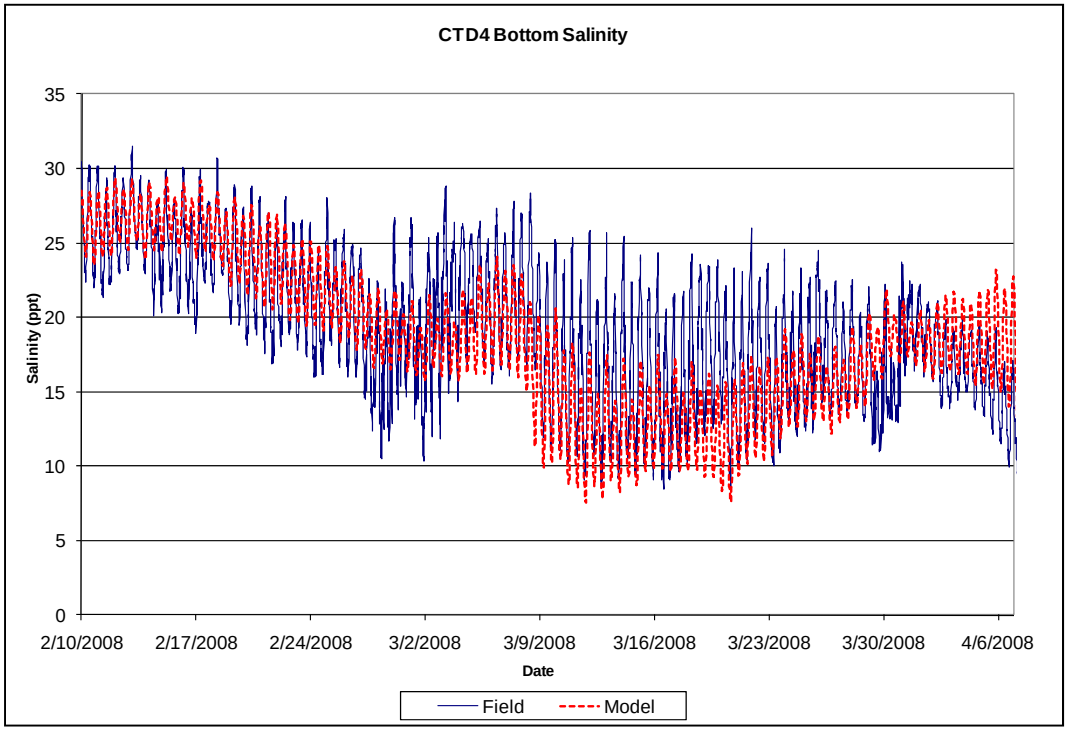

Figure 5-11. Bottom salinity comparison for location 4.

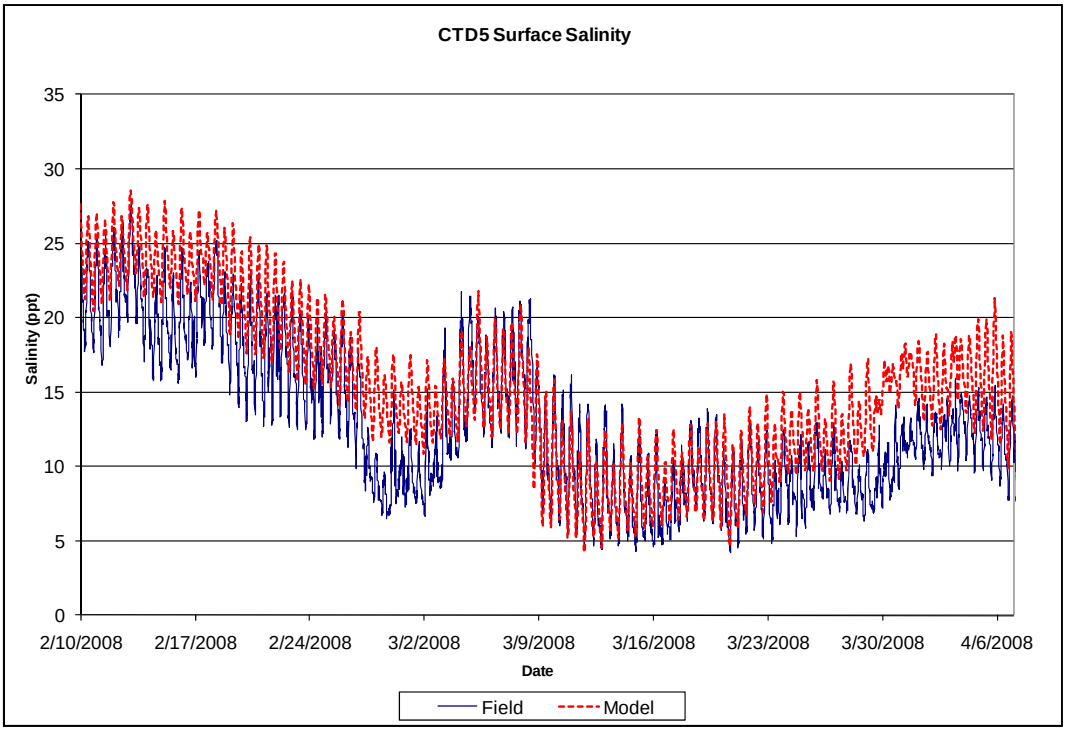

Figure 5-12. Surface salinity comparison for location 5.

The sediment model was validated using the shoaling data pattern in the MOTSU area. Periodic surveys were used to determine these patterns, and the model parameters were set to best match the sediment properties from the field data collection and these shoaling patterns. Two surveys were taken in the area of interest during January and June 2008. The difference between these field surveys can be compared to the shoaling shown in the model to determine how the model represents the field. Figure 5-13 shows this shoaling comparison. The high shoaling seen at the northern wharf is reproduced in the model as is the shoaling in the central turning basin. However, the high shoaling volume in the southwest corner of this turning basin is underpredicted by the model.

Overall, the magnitude of the shoaling is not being replicated by the model, which is common for sediment modeling. Increasing the sediment loads entering the system or weighting the bed change results are ways to better account for all of the sediment in the domain based on the model-to-field sediment comparisons. A simulation was performed with sediment inflow loads are increased by a factor of 15 to ensure that the model will reproduce the shoaling patterns even if the total load is underpredicted by the model prior to applying a weighting factor. If an increased load changes the shoaling patterns within the system, then accepting the results for

base-versus-plan comparisons when the computed bed change is much less will not yield reliable percentage change results when using the model to test alternate plans. This increased-load simulation is a way to ensure that the model qualitatively reproduces the field knowing that the current magnitudes of the bed change computed by the model are not accounting for the total change observed in the field. The result of the increased-sediment-load simulation is provided in Figure 5-14. This simulation produces shoaling patterns consistent with the MOTSU survey data for the same time period. This test verifies that the results for base/plan comparisons and percentage changes are consistent with the original Haw River sediment load conditions, so the information will be used for all plan simulations.

In general, sediment modeling has much greater uncertainty than the modeling of water alone, and this was true of the sediment modeling for MOTSU. The sources of uncertainty are the quantity and character of sediment delivered to the MOTSU site, i.e., the upstream boundary condition adopted for the sediment modeling. As noted in section 4.3.2, the sediment modeling relies on a sediment load rating curve derived from the Haw River, which is well upstream of the Cape Fear River watershed. This was the only information available for establishing the sediment flux boundary condition, and it is not clear how well this curve represents actual sediment delivery in the lower river, just upstream from MOTSU. After initial simulations, the sediment load input was increased by a factor of 15. This change produced shoaling rates that more accurately conformed with the field data throughout the MOTSU navigation channel system, including areas of relatively higher shoaling that were predicted reasonably well. This suggests that the amount of sediment delivered to the MOTSU site are probably understated in the present modeling.

For the Cape Fear River discharge range that was typical of the six-month validation period, averaging 2,000 cfs to peaks in the 14,000 – 15,000 cfs range (Figure 4-9), there was substantial variability in the sediment load data from the Haw River used to derive the sediment rating curve (Figure 4-15). This variability is another source of modeling uncertainty. At any particular discharge rate in this range, there was approximately an order of magnitude (factor of 10) variability in sediment load. This amount of variability is comparable to the increase in sediment load that yielded improved shoaling predictions in the MOTSU channel.

The MOTSU area experiences times of fluid mud, i.e., material that is mixed with enough water that it flows under its own density gradient. The model used for this study does not include an explicit fluid mud component, so the sediment transport moving as fluid mud may not be distributed in the model as it is in the field. This is a limitation of the model. Furthermore, it is likely that fluid mud is getting trapped in the southwest corner of the center turning basin, where the model shows less shoaling relative to the other areas, due to the geometry of this basin and the high tendency for eddy formation. Settling and collecting of fluid mud is common in areas of this type, with eddy flow due to the so-called "tea-cup effect." When stirring a tea cup, the circular flow allows material to collect in the center and fall to the bottom because there is a low-velocity area at the center of the area of circulation that allows material to fall out of suspension.

Refinements to the model are possible that could improve its predictive capability and reduce uncertainty in predictions and assessment of the various alternate plans. A field data collection program of velocity and sediment measurements for the entire river cross section, at a location just upstream from MOTSU, would be needed to improve the sediment boundary conditions. Sampling should be done perhaps once a month for 6 months, with another sample at spring peak discharge, to facilitate development of a sediment rating curve that more accurately and more confidently represents conditions in the lower river. The monitoring plan should repeat the bathymetric survey at the beginning and end of the six-month period in the MOTSU channel complex, and add similar surveying in the navigation channel, so that model calibration and validation can be done in light of sediment shoaling in both channels. Additional sediment modeling could include refinement, recalibration and revalidation, and the alternate plans could then be evaluated with the refined model to examine the impacts of different input sediment amounts and characteristics on plan performance and characteristics.

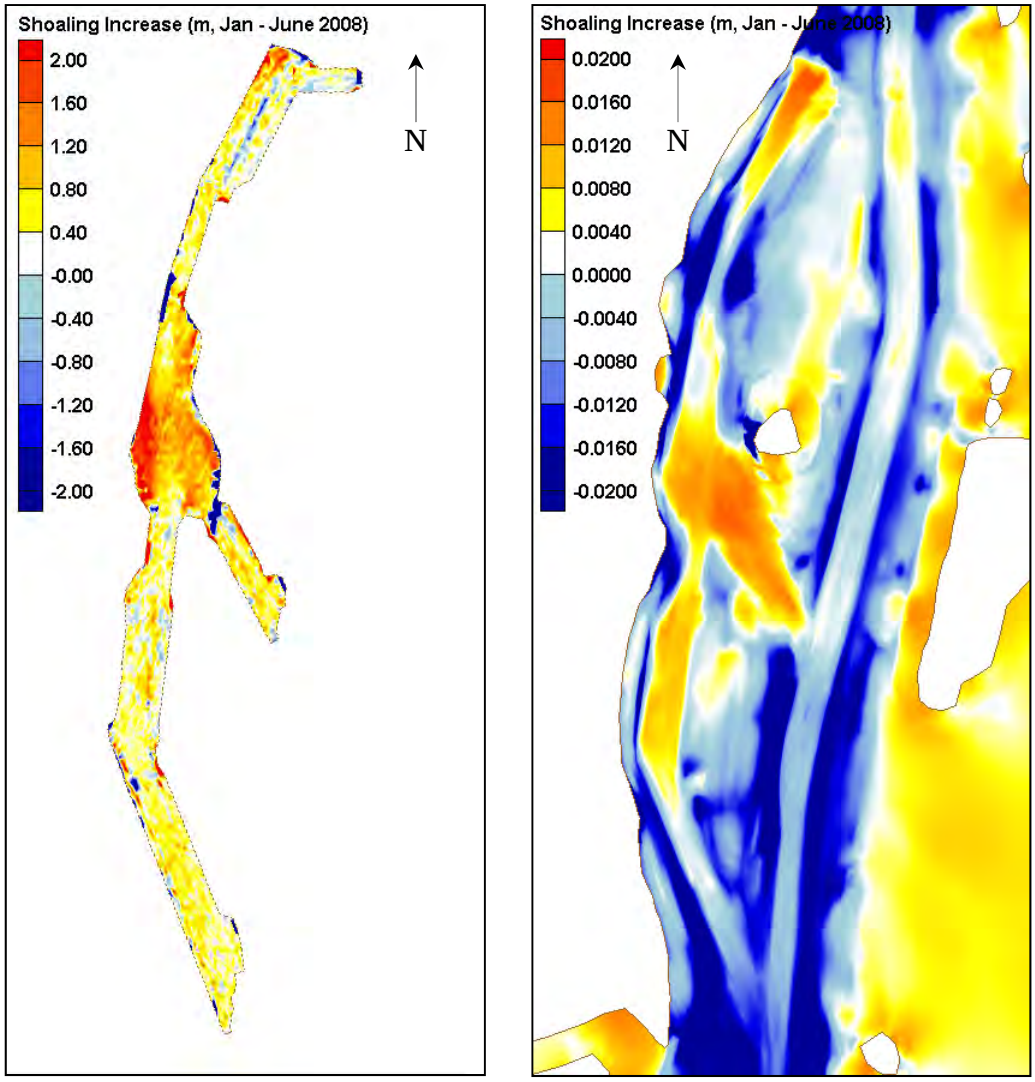

Figure 5-13. Six-month shoaling pattern comparison, field (left) and model (right).

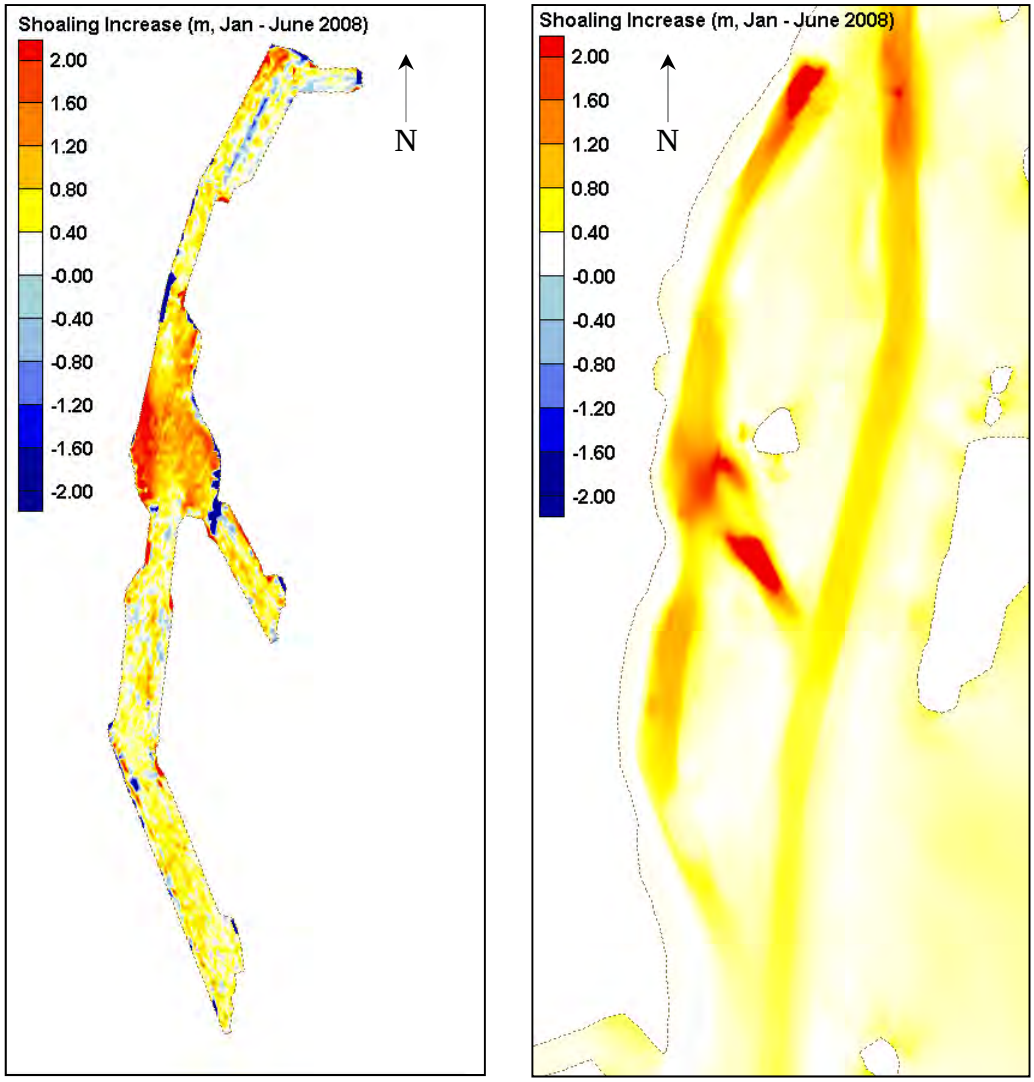

Figure 5-14. Six month shoaling pattern comparison with increased sediment load, field (left) and model (right).

6 Simulation of Alternate Plans

6.1 Model scenarios

Eight plan alternatives to reduce shoaling have been simulated with the TABS-MDS numerical model. The images below show the MOTSU area initial bathymetry for the base (Figure 6-1) and each plan condition. These plans are defined as:

1. Retain existing channels, except realign northern entrance channel in line with the flow
   a. northern entrance channel depth at existing depth of northern wharf, -34 ft MLLW (Figure 6-2).
   b. northern entrance channel and northern wharf channels deepened to -38 ft MLLW design depth (Figure 6-3).
2. Smooth the existing alignment to include realigning the channel between the south and center wharfs (Figure 6-4).
3. Realign the northern entrance channel (1a) and smooth the existing alignment of the channel between the south and center wharfs (2) (Figure 6-5).
4. Realign and deepen the northern entrance channel (1b) and include the turning basin in the Wilmington Harbor channel with a -38 ft MLLW depth (Figure 6-6).
5. Realign and deepen the northern entrance channel (1b), include the turning basin in the Wilmington Harbor channel and smooth the existing alignment (2) (Figure 6-7).
6. Marsh island placement with the turning basin in the Wilmington Harbor channel - island sized such that the MOTSU channel and the Wilmington Harbor Channel are streamlined and connect on the north and south of MOTSU as defined in plan 5 (Figure 6-8).

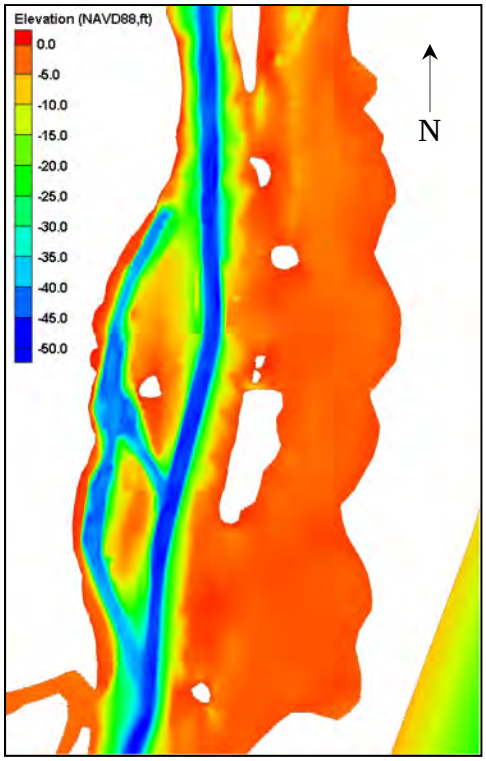

Figure 6-1. Base configuration bathymetry.

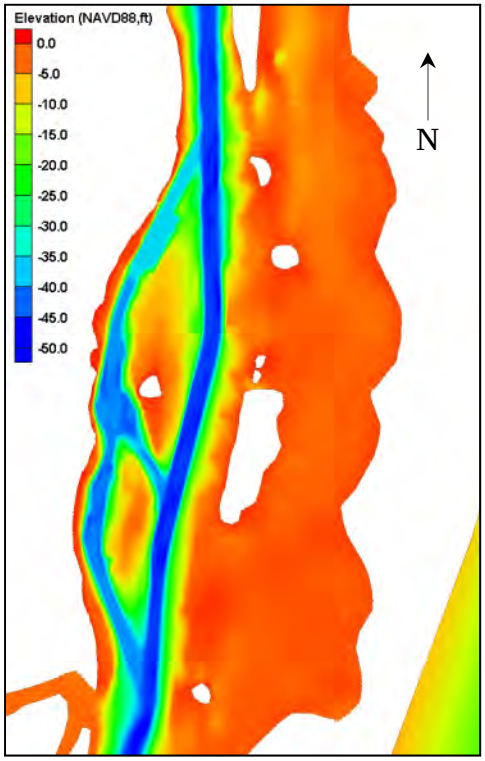

Figure 6-2. Plan 1a configuration bathymetry.

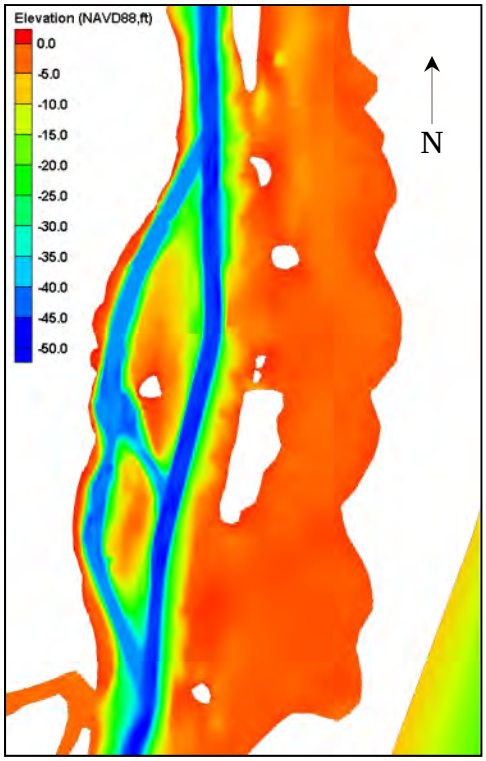

Figure 6-3. Plan 1b configuration bathymetry.

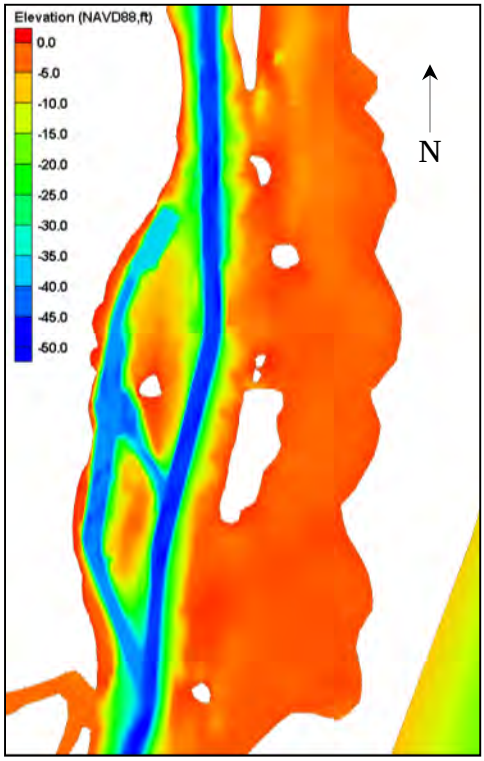

Figure 6-4. Plan 2 configuration bathymetry.

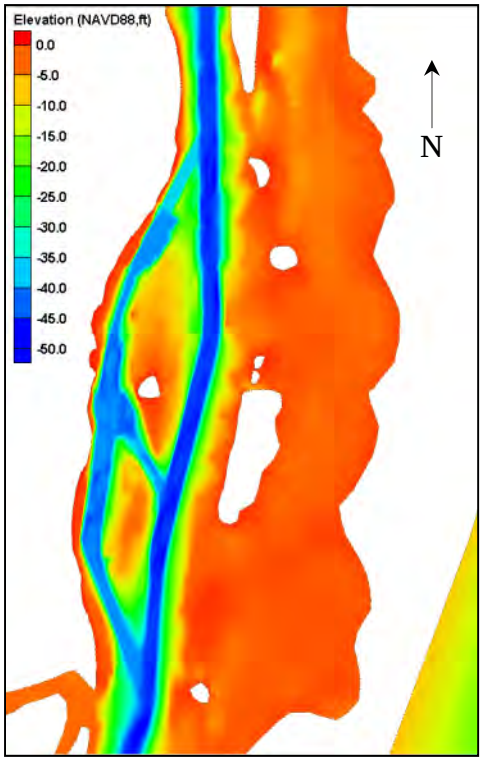

Figure 6-5. Plan 3 configuration bathymetry.

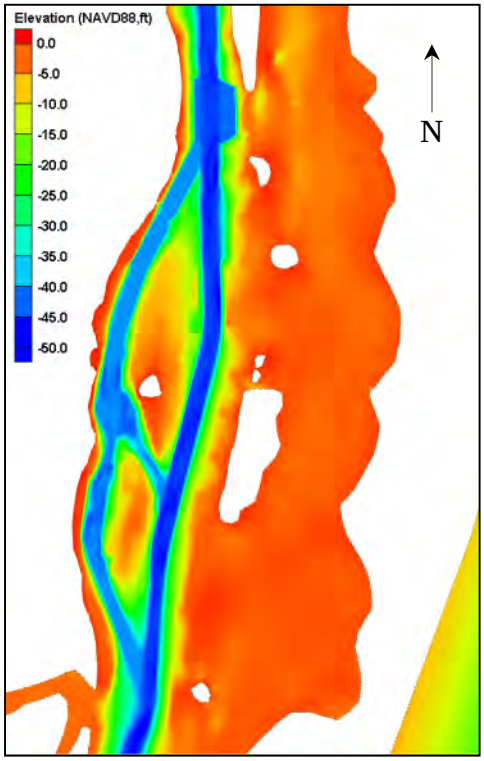

Figure 6-6. Plan 4 configuration bathymetry.

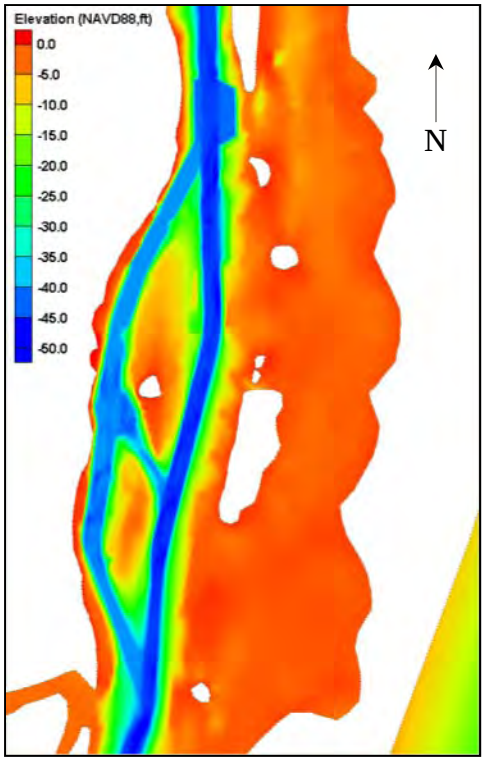

Figure 6-7. Plan 5 configuration bathymetry.

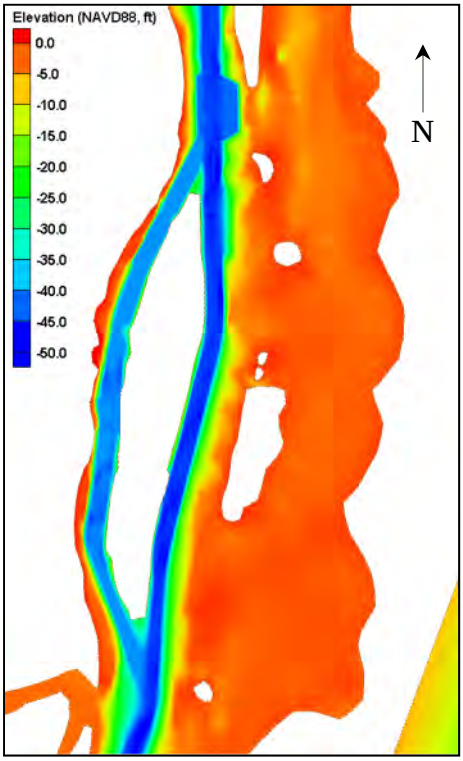

Figure 6-8. Plan 6 configuration bathymetry.

6.2 Hydrodynamic results

Surface and bottom velocity magnitudes, with flood and ebb defined, are shown at eight locations within the study area. These points are located according to Figure 6-9 below. The velocity results over a two-day period are shown in the time series plots for the surface and bottom, at all eight locations, and for the base and all plans. These two days were selected randomly during a time far enough into the simulation when initial conditions would no longer influence the results. Flood-directed flow, or flow traveling northward, is positive; ebb-directed flow, or flow traveling toward the Atlantic Ocean, is negative. These results are provided in Figure 6-10 through Figure 6-25. Additionally, the maximum flood and ebb velocity and average flood and ebb velocity over the 6 month simulation period (January – June 2008) is computed at each location for each plan condition. This information is shown on the column plots in Figure 6-26 through Figure 6-33. These velocity analyses will show how the surface and bottom velocity magnitudes change with each alternative. Higher velocities typically indicate higher bed shear stress and therefore a larger likelihood that material will be eroded from the bed or, at least, hindered more from settling to the bed. Although the sediment results will give a better indication of the shoaling behavior, the velocity results are a first step toward understanding the processes within the system.

As expected, the velocity variations among the plans are greatest in the MOTSU area because that is the location of most of the changes. These results show that Plan 6 produces the largest change from Base at most locations within the MOTSU channels and at Point 7 in the navigation channel. The variation in velocity in the navigation channel at Points 6 and 8 are small regardless of the plan condition. To reduce the shoaling in MOTSU, higher bottom velocities (and therefore higher shear stresses) are necessary at Points 1, 2, 3, and 4. This trend is observed in the model results for all locations, although the change at Point 2 is quite small.

Figure 6-34 through Figure 6-41 are percent exceedance plots for all plans at the eight analysis points for the bottom velocity magnitude over the entire six-month simulation period. These are generated from a cumulative distribution function (CDF). These functions give the percentage of time that each velocity magnitude is computed by the model. The minimum velocity is plotted at a percentage of 100, indicating that the velocity is equal to or greater than this value 100% of the time. The velocity at 50% is the velocity that is computed less than half the time and greater

than half the time. The maximum value is given approximately zero percent since this value is only computed by the model for a very small percentage of the simulation time. The results of this analysis support the previous findings that Plan 6 generates higher velocities at the points in the MOTSU area. The velocity does not vary greatly among the plans in the navigation channel (Points 6, 7, and 8). The slope of the curve is also important. Larger (i.e., steeper) negative slopes indicate that the higher velocities are experienced over a shorter percentage of time than if the slope were less steep, or flatter. This percentage of time that a higher velocity is produced will translate to more time of higher bed shear stresses and, therefore, sediment movement.

Residual velocity images for the surface and bottom velocities in the MOTSU area are shown in Figure 6-42 and Figure 6-43 for the Base condition. These residuals show the predominant flow direction and average magnitude over 168 days, or 336 tidal cycles. This is essentially a six-month velocity residual for the area. The bottom velocity residuals are flood-directed in the navigation channels due to the dense salinity flows along the bottom, while the surface velocity residuals are ebb-directed due to the river inflows adding to the tidal influence along the surface. This pattern indicates that material in the channels will move upstream as it falls to the bed, becoming trapped at the northern wharf due to the geometry of the entrance channel. Modifying this trapping behavior will greatly impact the shoaling in this area. The plan alternatives do not change this pattern, but by opening up the channel at the northern wharf, the material moving upstream will continue to do so and not become trapped at this location.

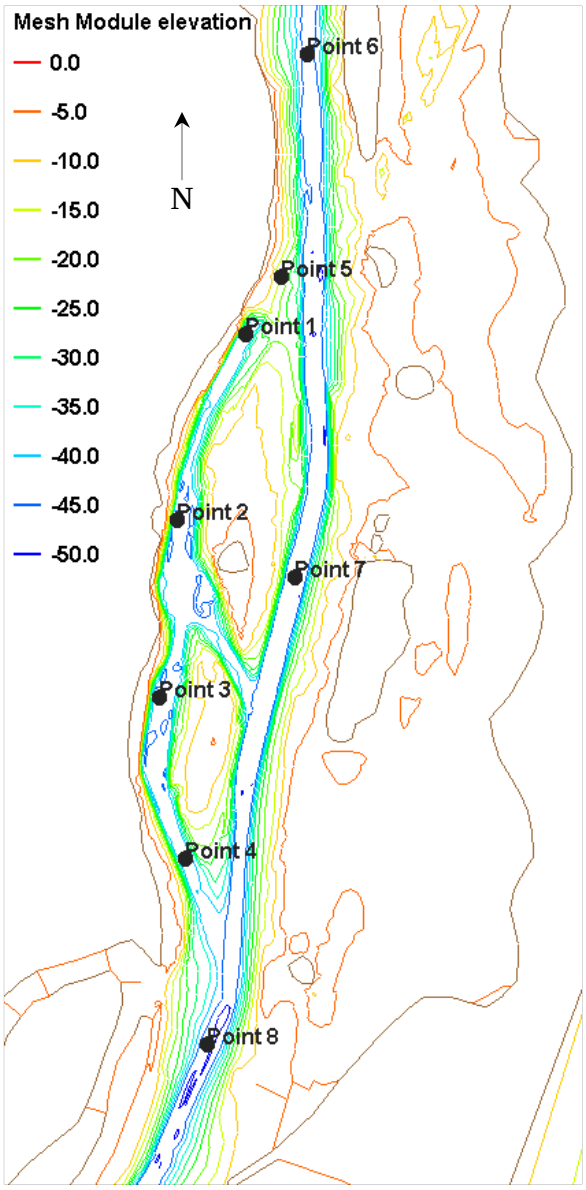

Figure 6-9. Time history analysis locations shown on contours, in feet.

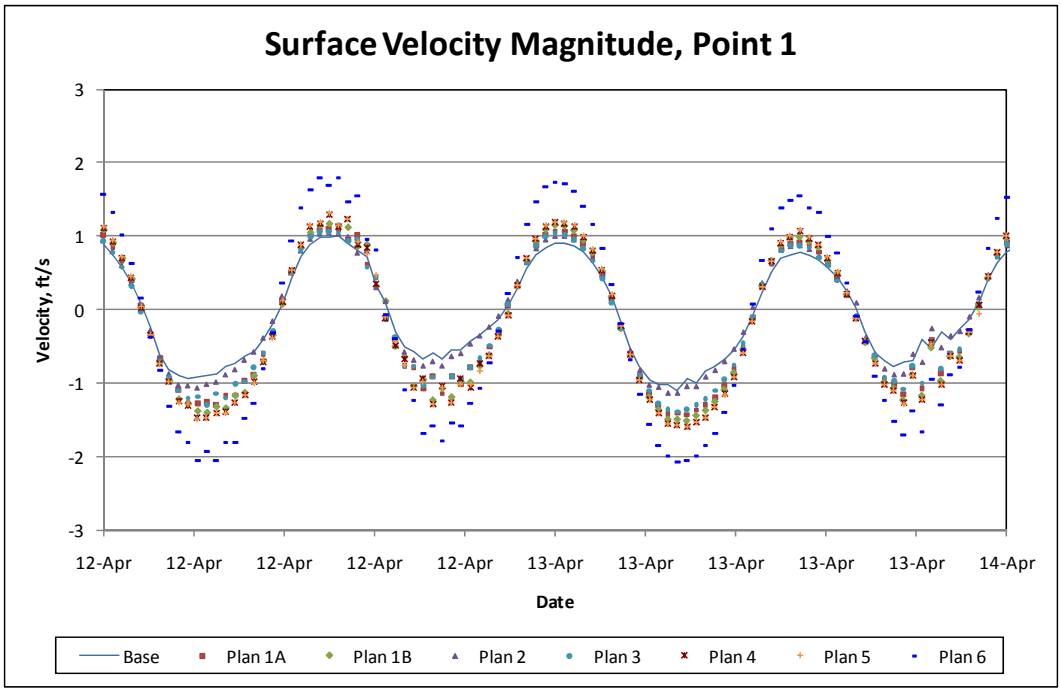

Figure 6-10. Surface velocity for Point 1.

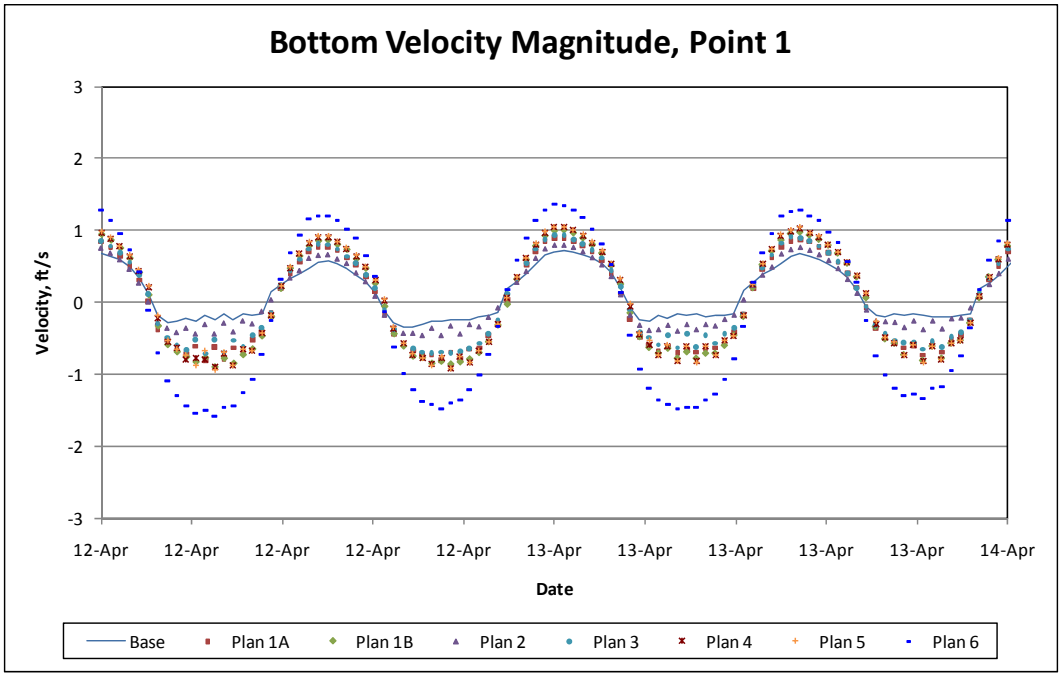

Figure 6-11. Bottom velocity for Point 1.

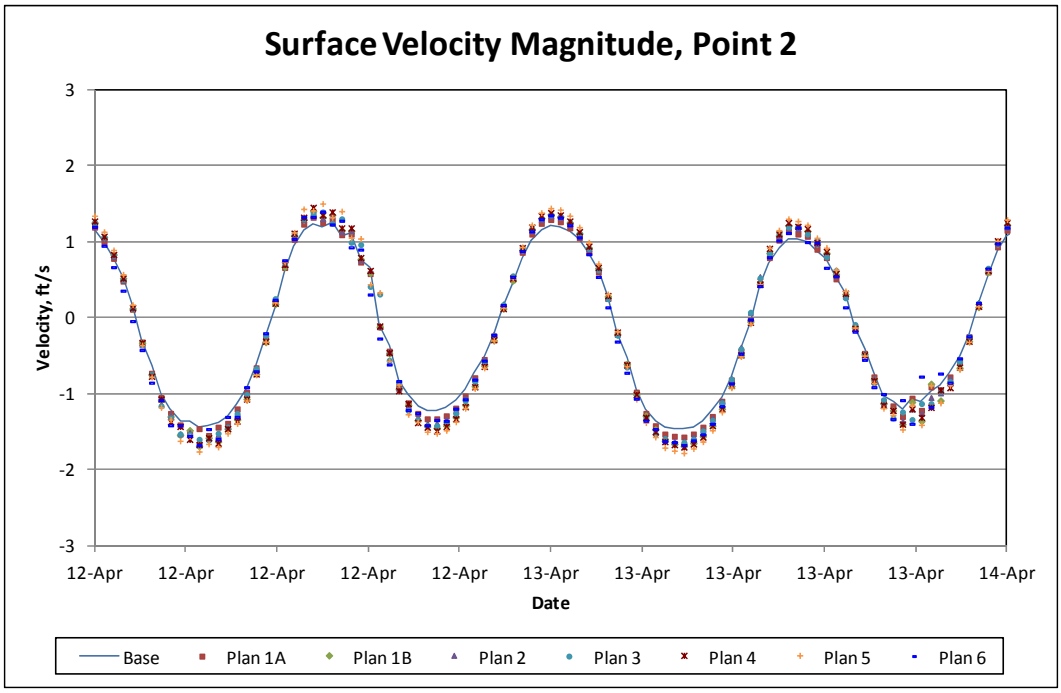

Figure 6-12. Surface velocity for Point 2.

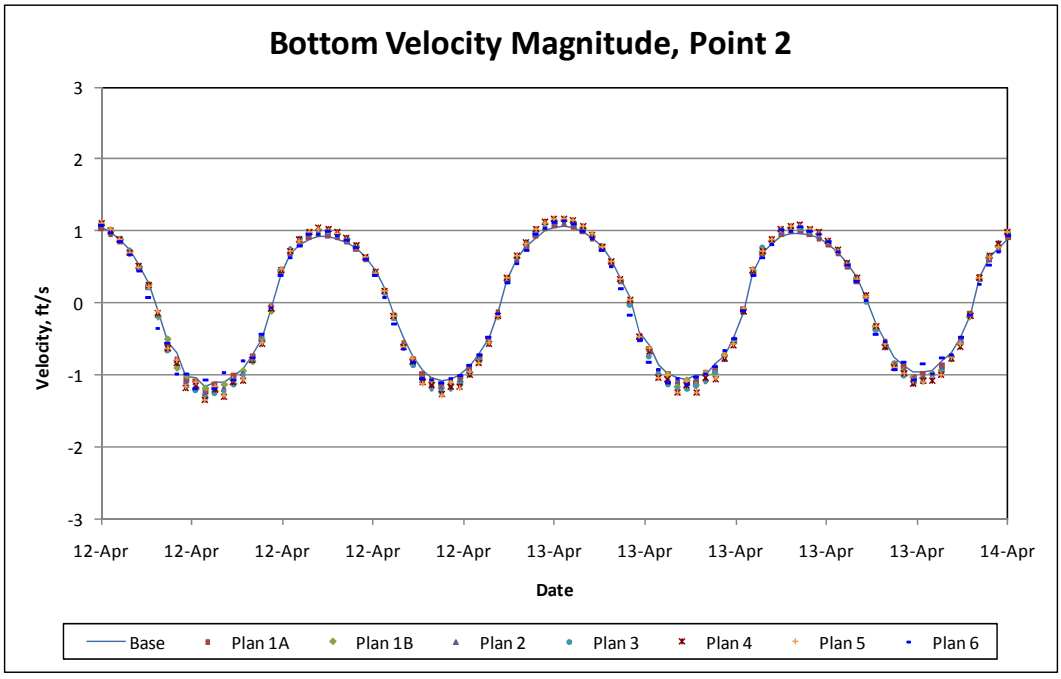

Figure 6-13. Bottom velocity for Point 2.

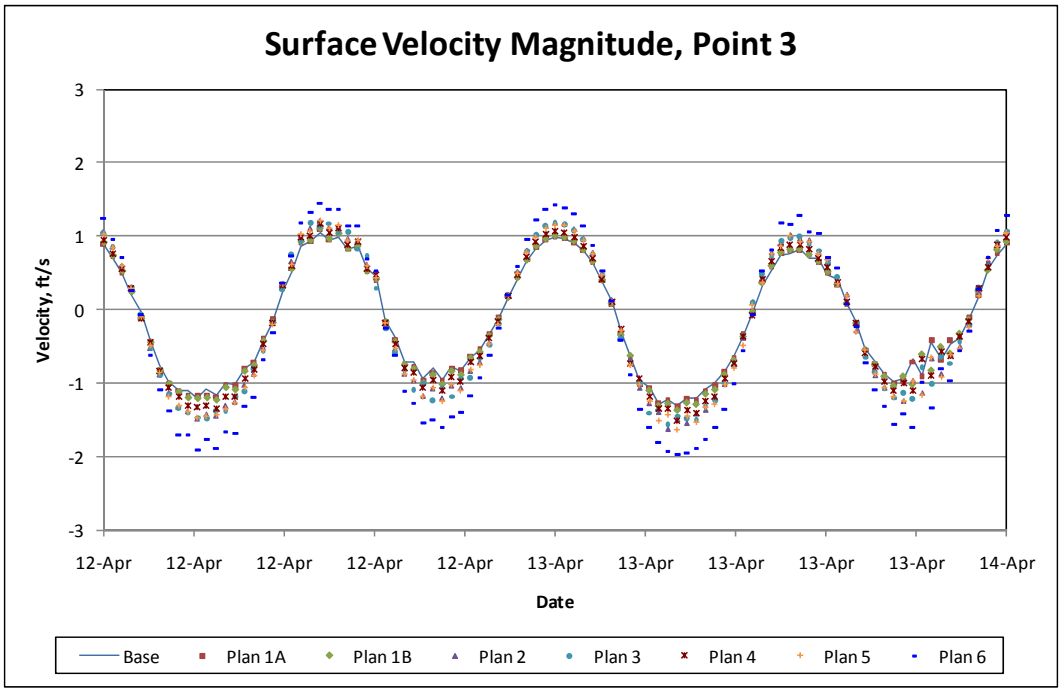

Figure 6-14. Surface velocity at Point 3.

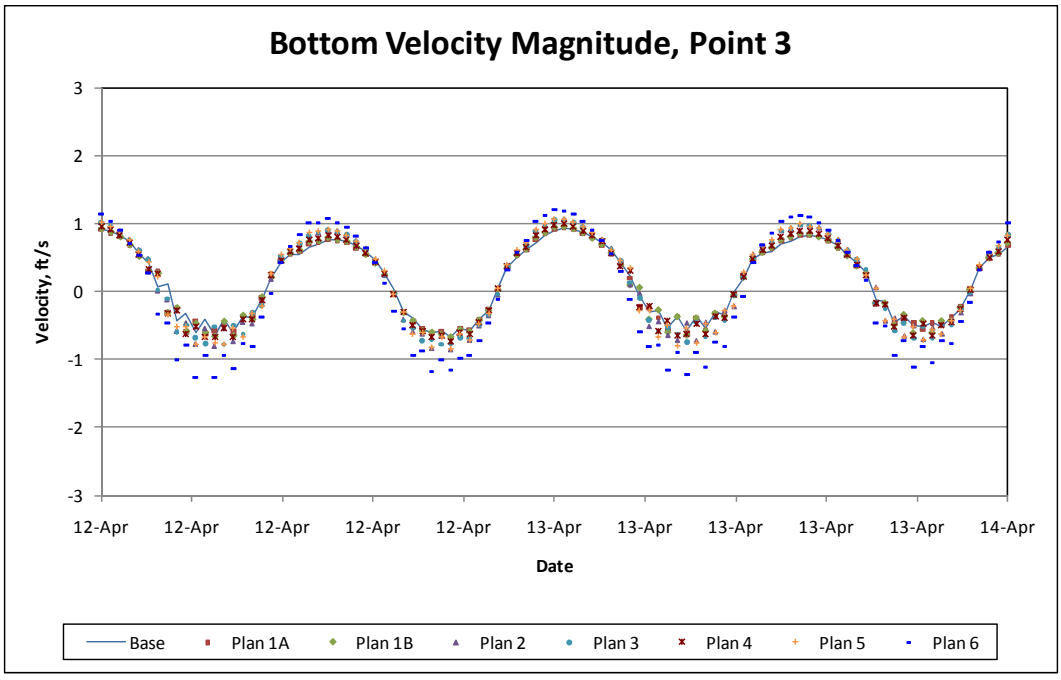

Figure 6-15. Bottom velocity at Point 3.

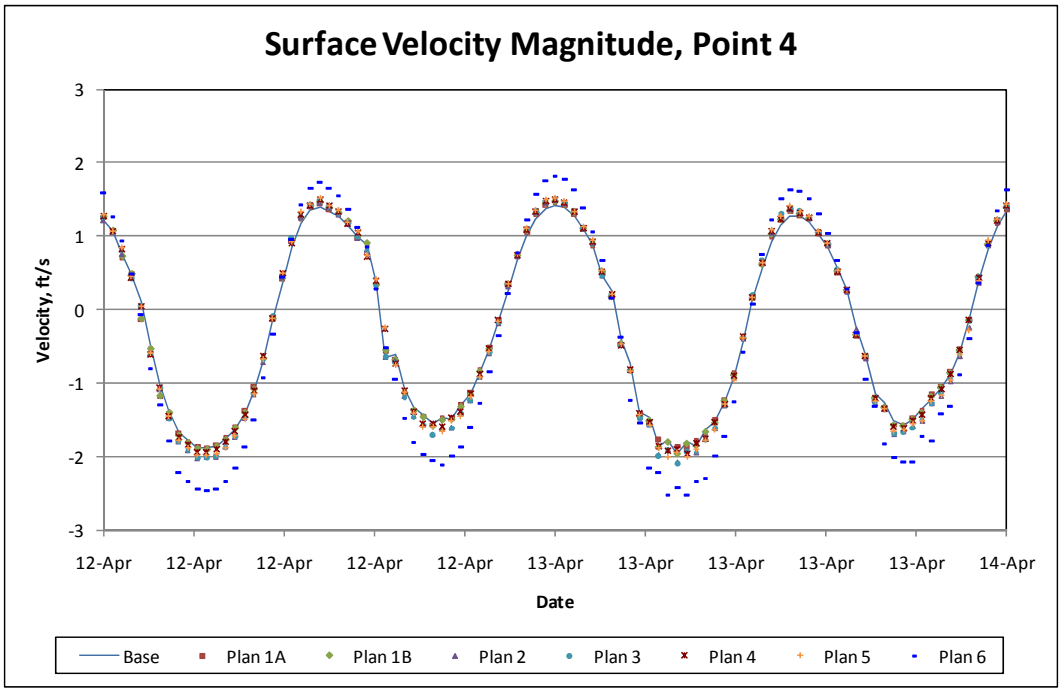

Figure 6-16. Surface velocity at Point 4.

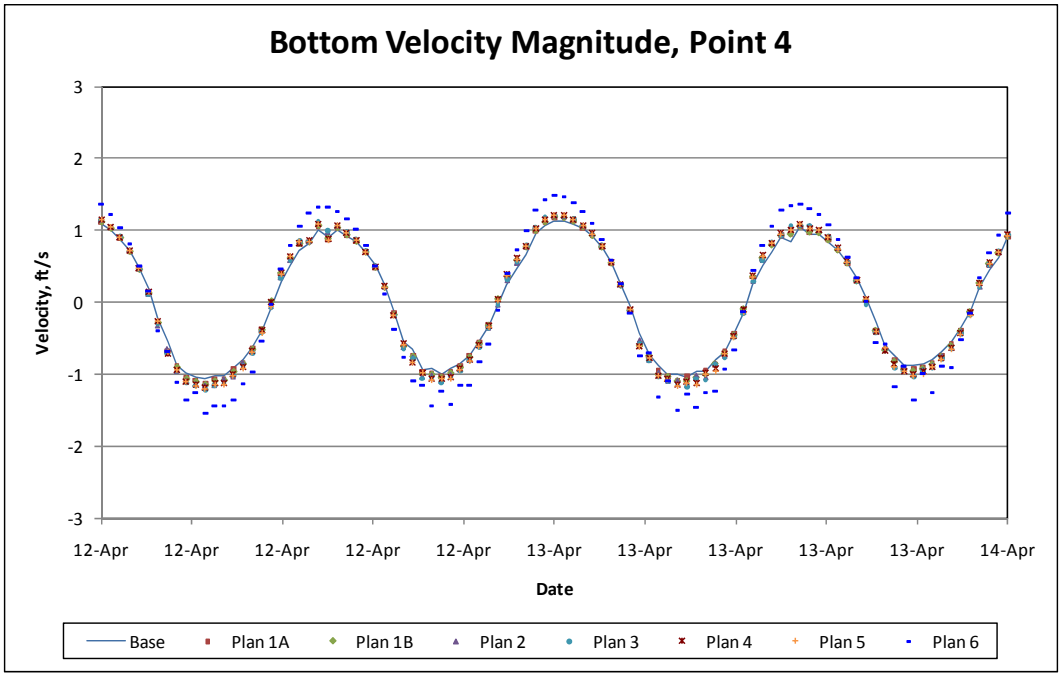

Figure 6-17. Bottom velocity at Point 4.

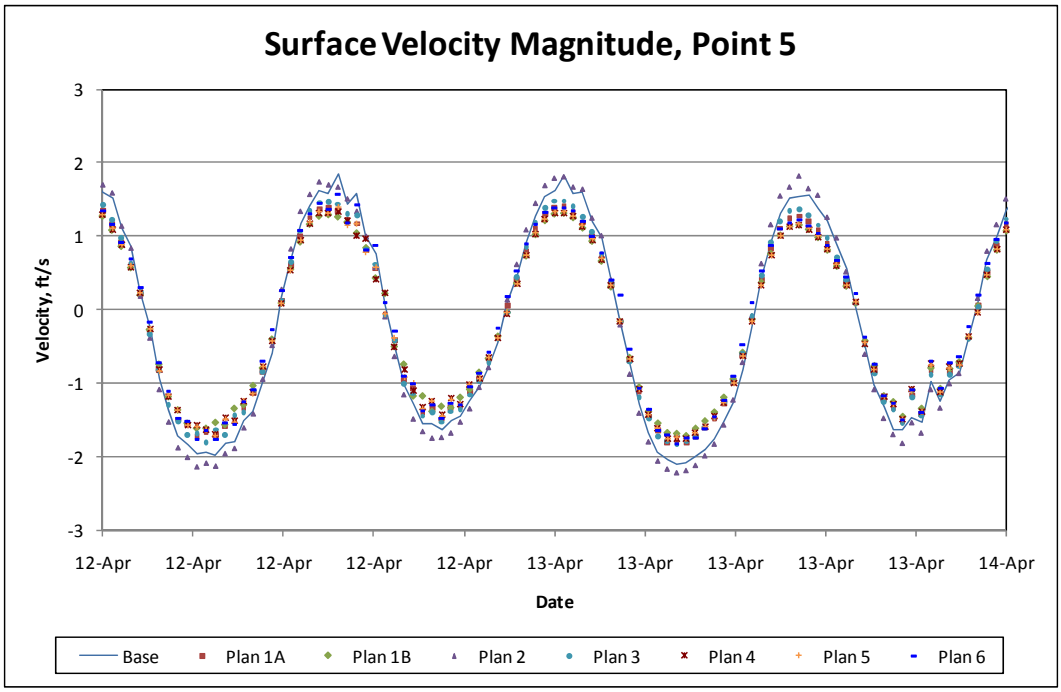

Figure 6-18. Surface velocity at Point 5.

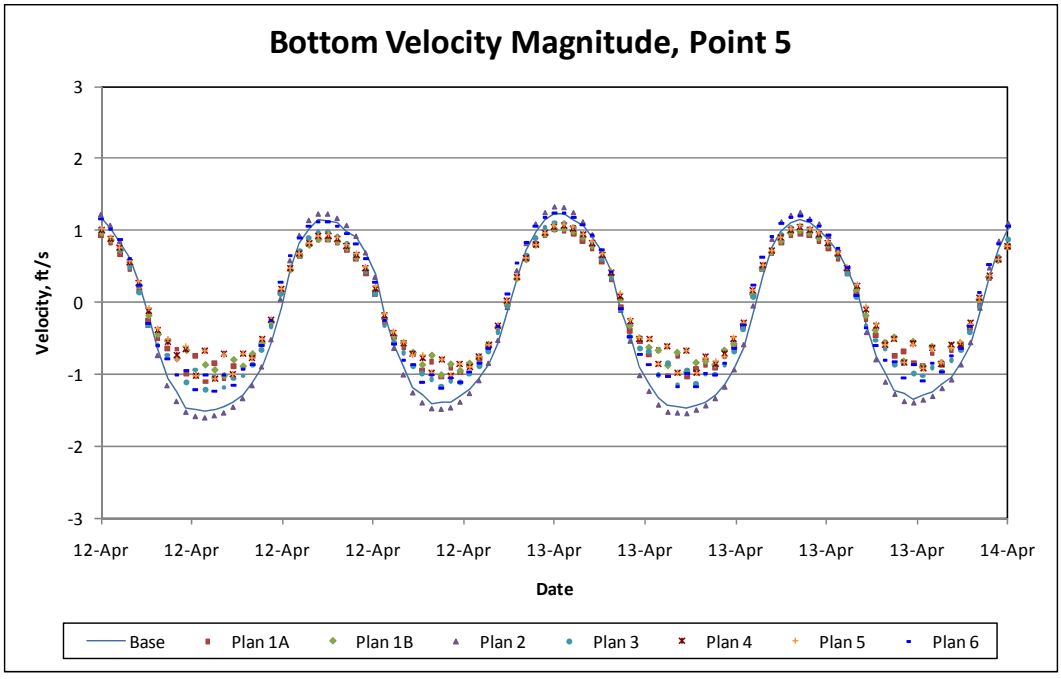

Figure 6-19. Bottom velocity at Point 5.

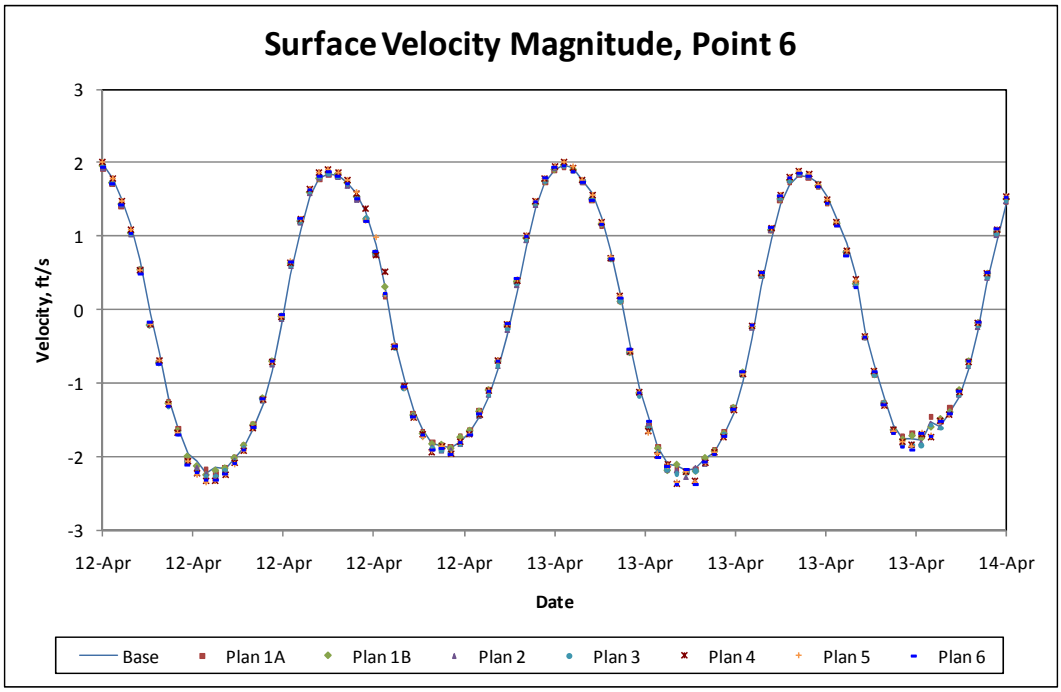

Figure 6-20. Surface velocity at Point 6.

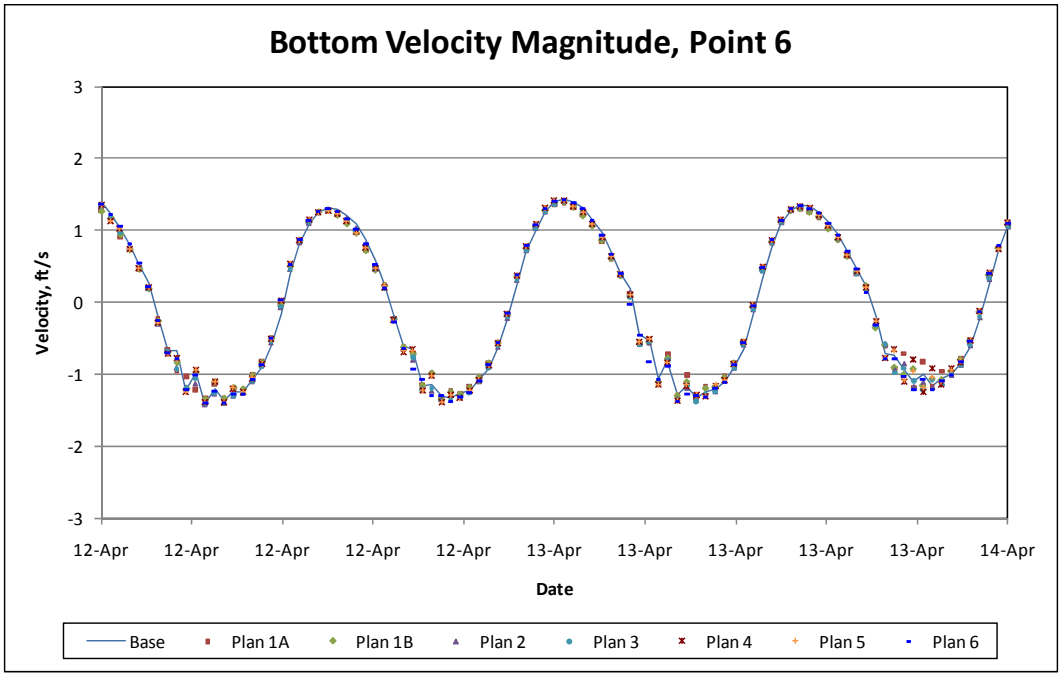

Figure 6-21. Bottom velocity at Point 6.

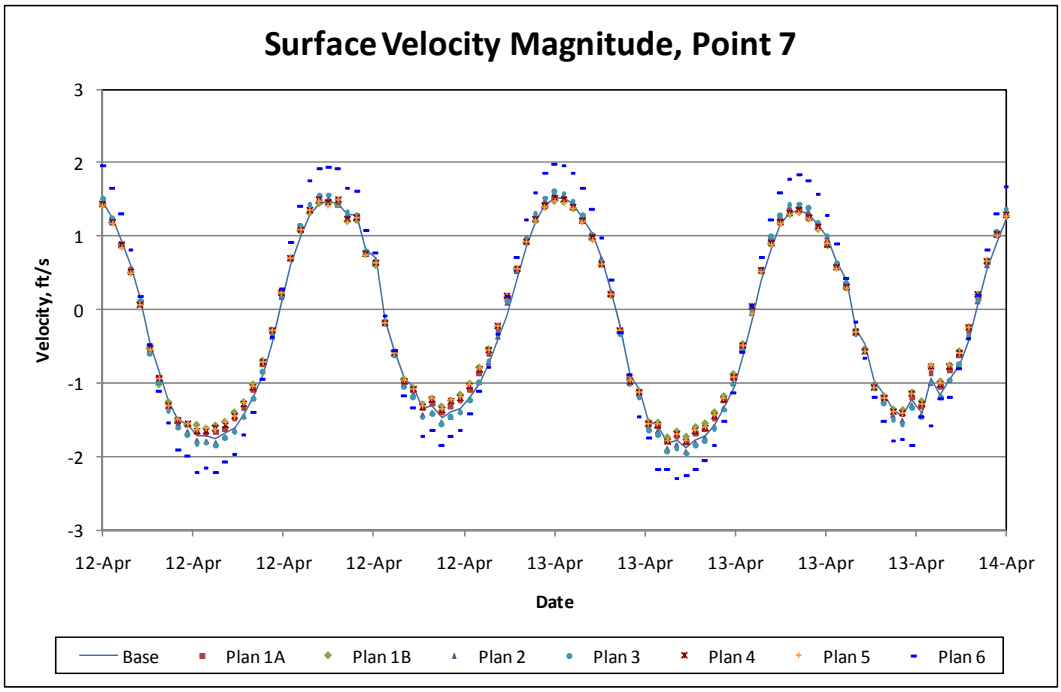

Figure 6-22. Surface velocity at Point 7.

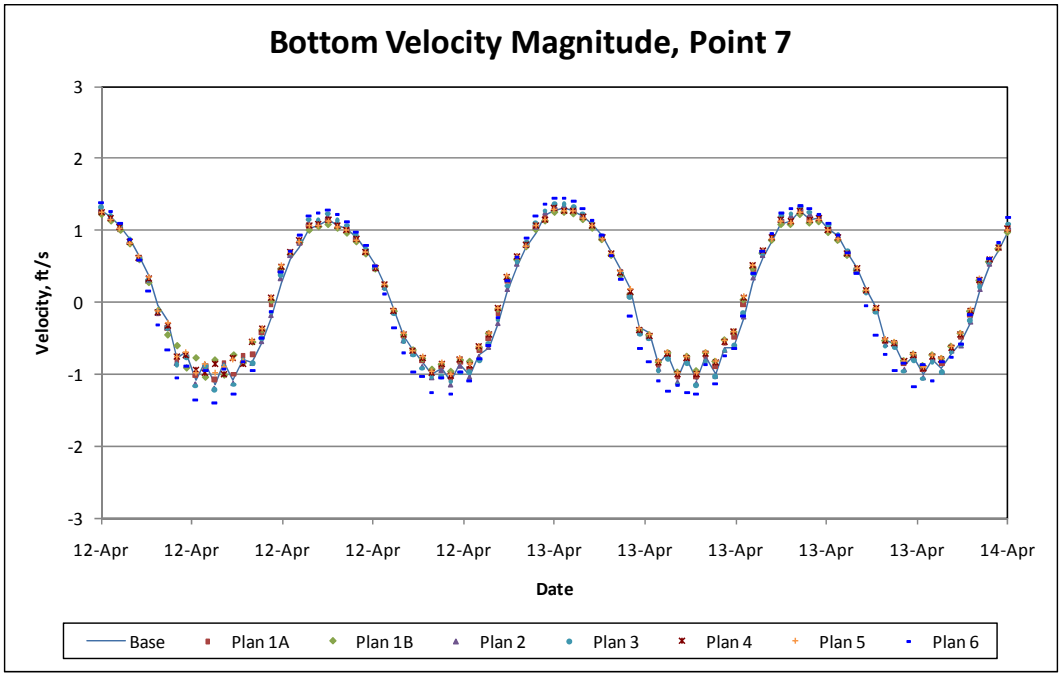

Figure 6-23. Bottom velocity at Point 7.

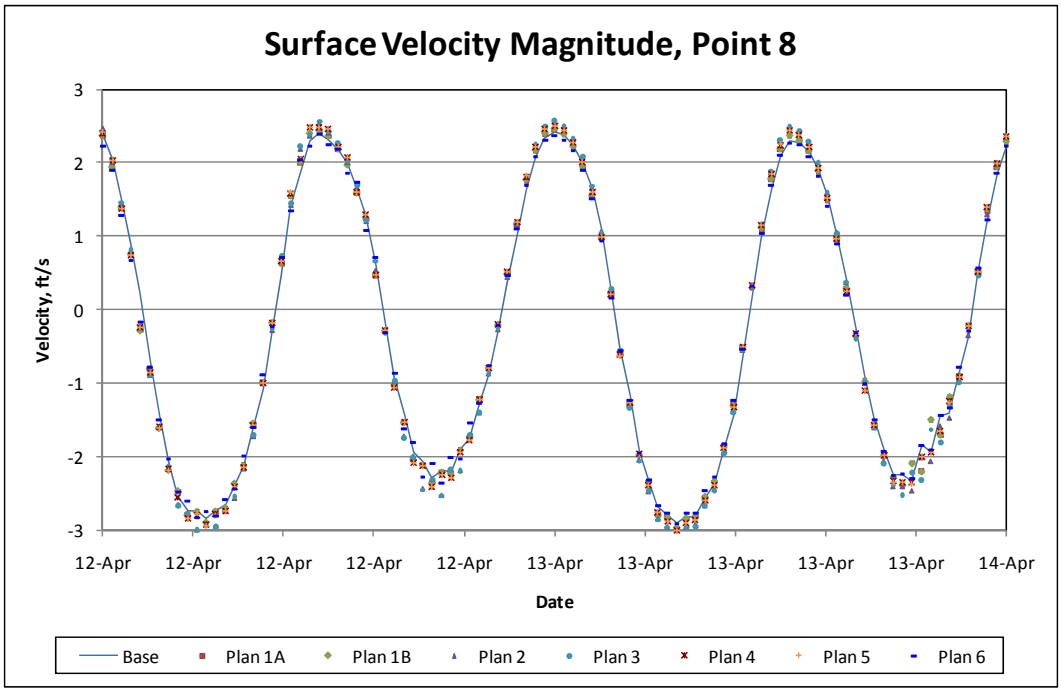

Figure 6-24. Surface velocity at Point 8.

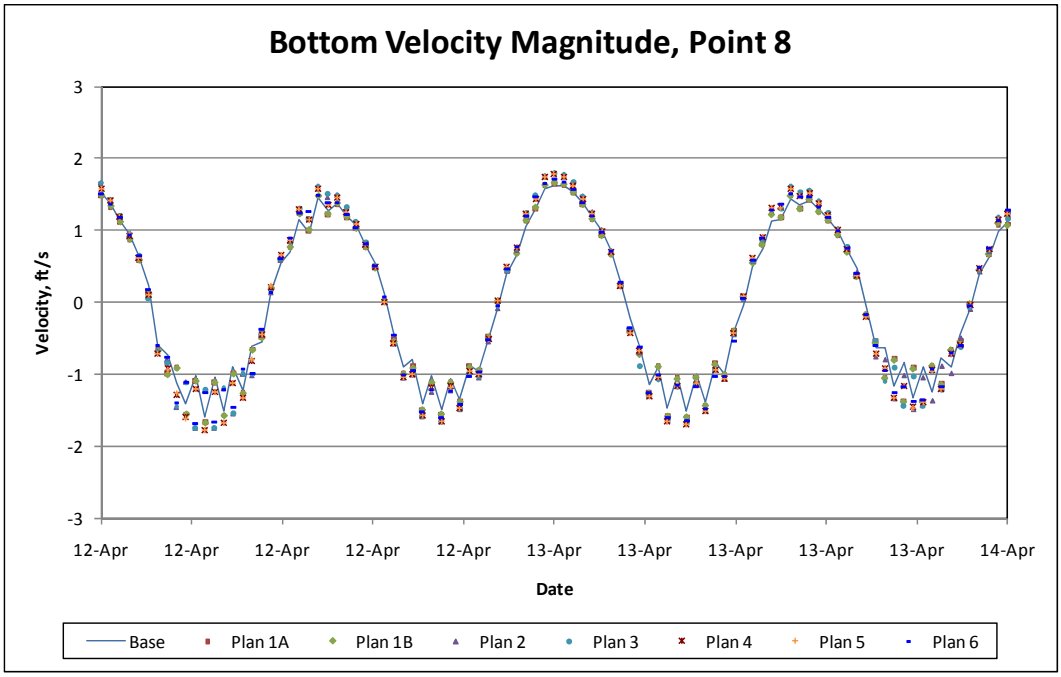

Figure 6-25. Bottom velocity at Point 8.

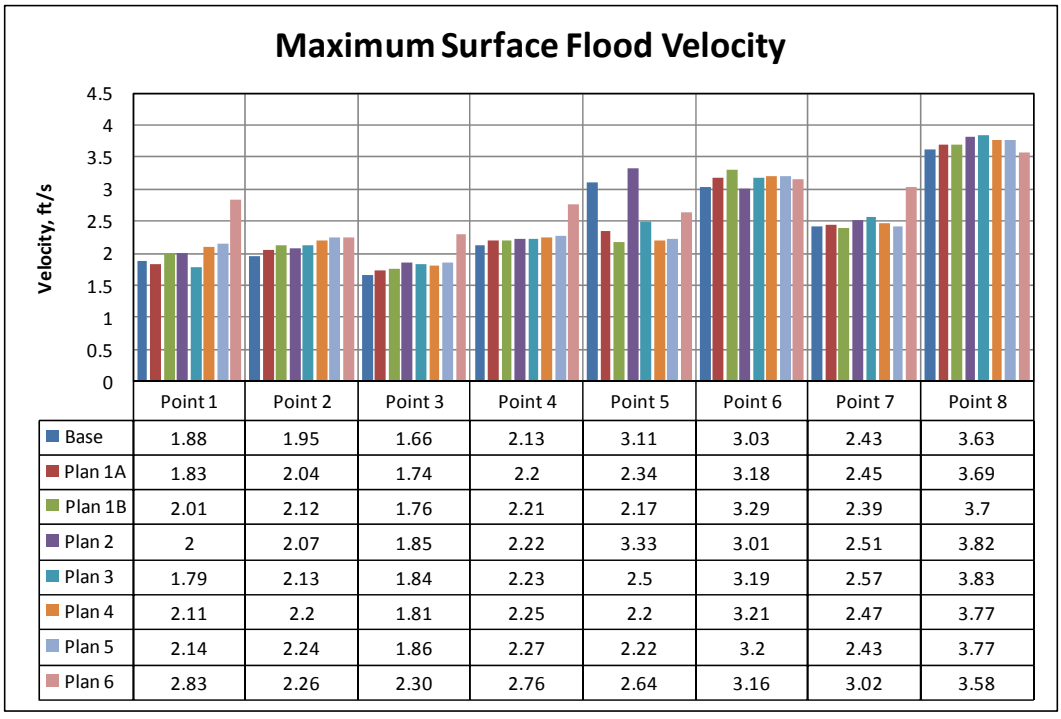

	Point 1	Point 2	Point 3	Point 4	Point 5	Point 6	Point 7	Point 8
Base	1.88	1.95	1.66	2.13	3.11	3.03	2.43	3.63
Plan 1A	1.83	2.04	1.74	2.2	2.34	3.18	2.45	3.69
Plan 1B	2.01	2.12	1.76	2.21	2.17	3.29	2.39	3.7
Plan 2	2	2.07	1.85	2.22	3.33	3.01	2.51	3.82
Plan 3	1.79	2.13	1.84	2.23	2.5	3.19	2.57	3.83
Plan 4	2.11	2.2	1.81	2.25	2.2	3.21	2.47	3.77
Plan 5	2.14	2.24	1.86	2.27	2.22	3.2	2.43	3.77
Plan 6	2.83	2.26	2.30	2.76	2.64	3.16	3.02	3.58

Figure 6-26. Maximum flood velocity at the surface for all locations and plans.

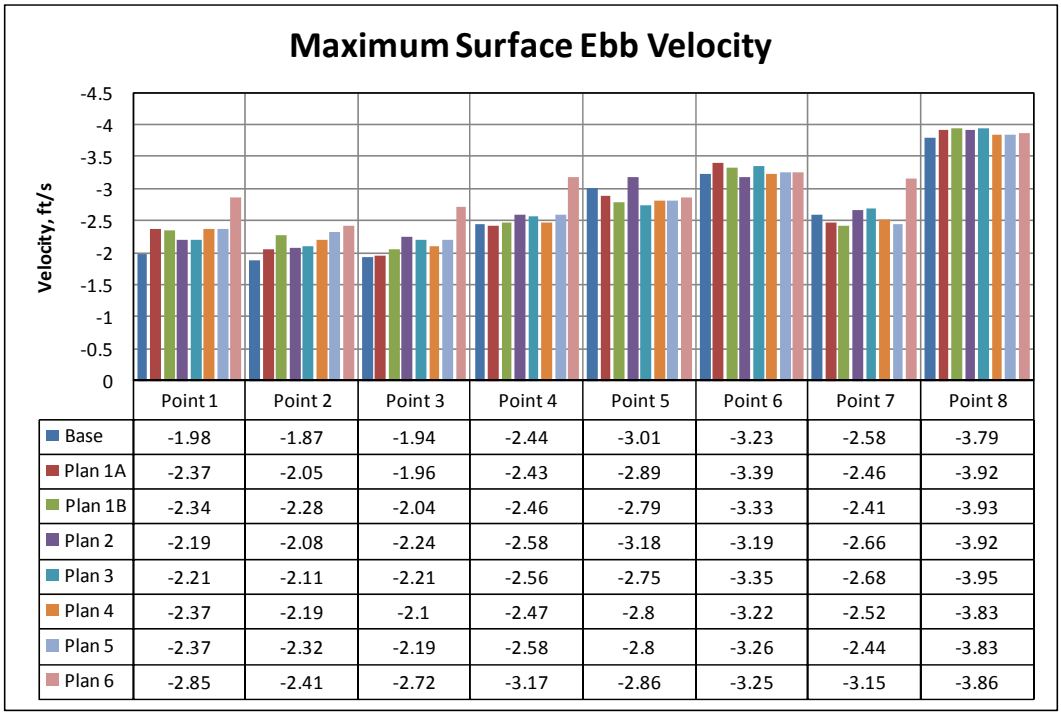

	Point 1	Point 2	Point 3	Point 4	Point 5	Point 6	Point 7	Point 8
Base	-1.98	-1.87	-1.94	-2.44	-3.01	-3.23	-2.58	-3.79
Plan 1A	-2.37	-2.05	-1.96	-2.43	-2.89	-3.39	-2.46	-3.92
Plan 1B	-2.34	-2.28	-2.04	-2.46	-2.79	-3.33	-2.41	-3.93
Plan 2	-2.19	-2.08	-2.24	-2.58	-3.18	-3.19	-2.66	-3.92
Plan 3	-2.21	-2.11	-2.21	-2.56	-2.75	-3.35	-2.68	-3.95
Plan 4	-2.37	-2.19	-2.1	-2.47	-2.8	-3.22	-2.52	-3.83
Plan 5	-2.37	-2.32	-2.19	-2.58	-2.8	-3.26	-2.44	-3.83
Plan 6	-2.85	-2.41	-2.72	-3.17	-2.86	-3.25	-3.15	-3.86

Figure 6-27. Maximum ebb velocity at the surface for all locations and plans.

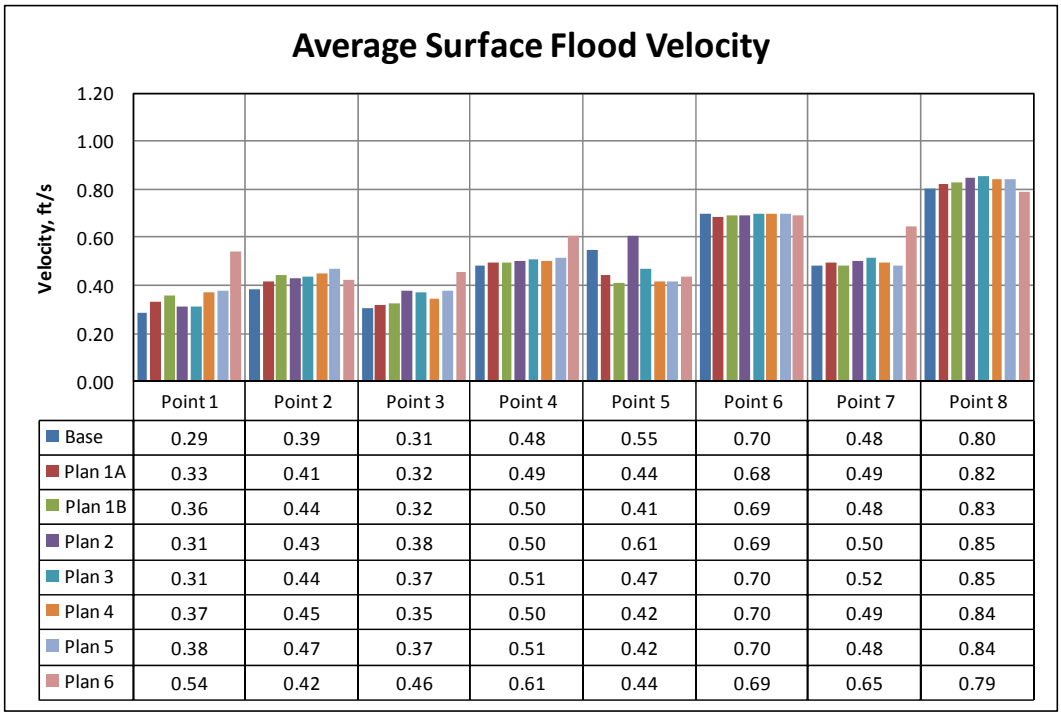

	Point 1	Point 2	Point 3	Point 4	Point 5	Point 6	Point 7	Point 8
Base	0.29	0.39	0.31	0.48	0.55	0.70	0.48	0.80
Plan 1A	0.33	0.41	0.32	0.49	0.44	0.68	0.49	0.82
Plan 1B	0.36	0.44	0.32	0.50	0.41	0.69	0.48	0.83
Plan 2	0.31	0.43	0.38	0.50	0.61	0.69	0.50	0.85
Plan 3	0.31	0.44	0.37	0.51	0.47	0.70	0.52	0.85
Plan 4	0.37	0.45	0.35	0.50	0.42	0.70	0.49	0.84
Plan 5	0.38	0.47	0.37	0.51	0.42	0.70	0.48	0.84
Plan 6	0.54	0.42	0.46	0.61	0.44	0.69	0.65	0.79

Figure 6-28. Average flood velocity at the surface for all locations and plans.

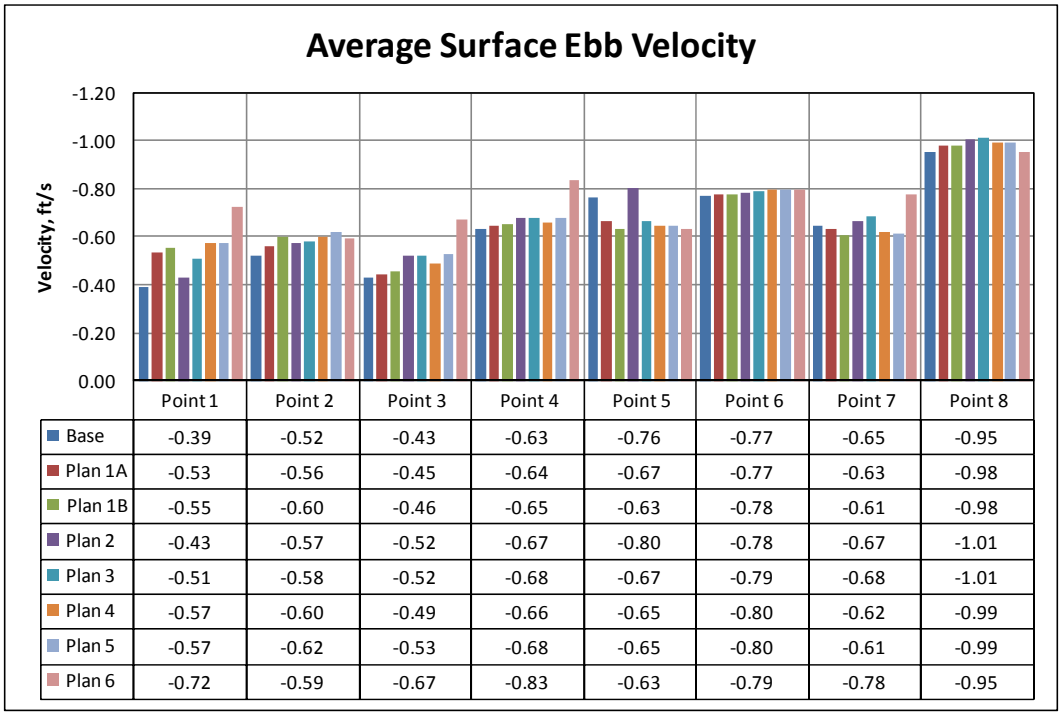

	Point 1	Point 2	Point 3	Point 4	Point 5	Point 6	Point 7	Point 8
Base	-0.39	-0.52	-0.43	-0.63	-0.76	-0.77	-0.65	-0.95
Plan 1A	-0.53	-0.56	-0.45	-0.64	-0.67	-0.77	-0.63	-0.98
Plan 1B	-0.55	-0.60	-0.46	-0.65	-0.63	-0.78	-0.61	-0.98
Plan 2	-0.43	-0.57	-0.52	-0.67	-0.80	-0.78	-0.67	-1.01
Plan 3	-0.51	-0.58	-0.52	-0.68	-0.67	-0.79	-0.68	-1.01
Plan 4	-0.57	-0.60	-0.49	-0.66	-0.65	-0.80	-0.62	-0.99
Plan 5	-0.57	-0.62	-0.53	-0.68	-0.65	-0.80	-0.61	-0.99
Plan 6	-0.72	-0.59	-0.67	-0.83	-0.63	-0.79	-0.78	-0.95

Figure 6-29. Average ebb velocity at the surface for all locations and plans.

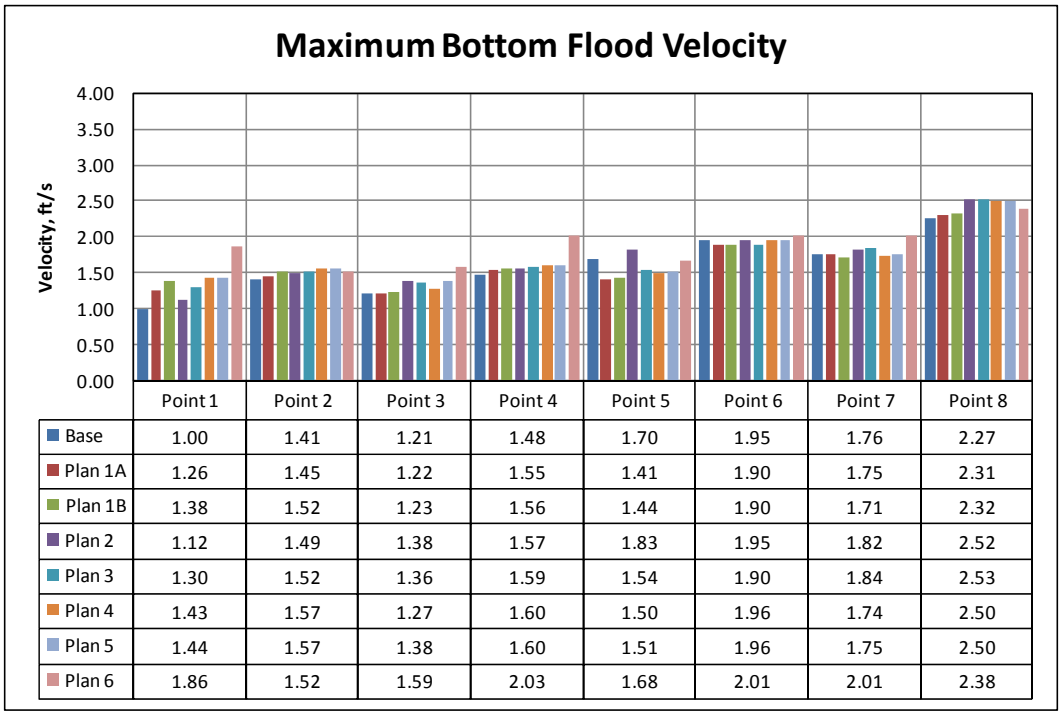

	Point 1	Point 2	Point 3	Point 4	Point 5	Point 6	Point 7	Point 8
Base	1.00	1.41	1.21	1.48	1.70	1.95	1.76	2.27
Plan 1A	1.26	1.45	1.22	1.55	1.41	1.90	1.75	2.31
Plan 1B	1.38	1.52	1.23	1.56	1.44	1.90	1.71	2.32
Plan 2	1.12	1.49	1.38	1.57	1.83	1.95	1.82	2.52
Plan 3	1.30	1.52	1.36	1.59	1.54	1.90	1.84	2.53
Plan 4	1.43	1.57	1.27	1.60	1.50	1.96	1.74	2.50
Plan 5	1.44	1.57	1.38	1.60	1.51	1.96	1.75	2.50
Plan 6	1.86	1.52	1.59	2.03	1.68	2.01	2.01	2.38

Figure 6-30. Maximum flood velocity at the bottom for all locations and plans.

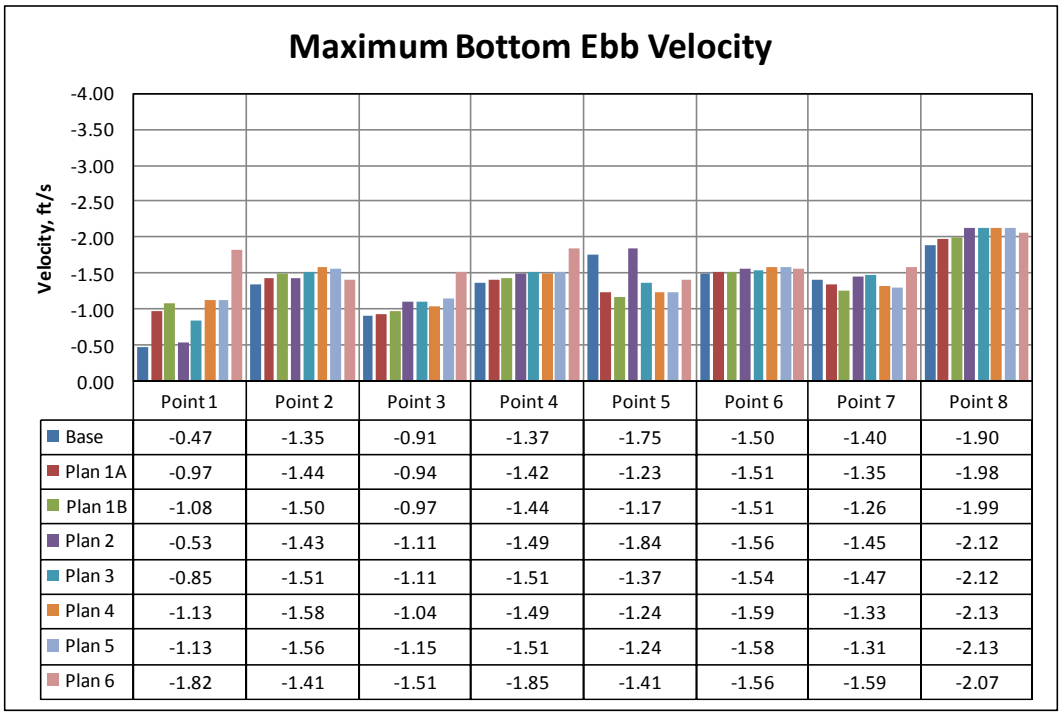

	Point 1	Point 2	Point 3	Point 4	Point 5	Point 6	Point 7	Point 8
Base	-0.47	-1.35	-0.91	-1.37	-1.75	-1.50	-1.40	-1.90
Plan 1A	-0.97	-1.44	-0.94	-1.42	-1.23	-1.51	-1.35	-1.98
Plan 1B	-1.08	-1.50	-0.97	-1.44	-1.17	-1.51	-1.26	-1.99
Plan 2	-0.53	-1.43	-1.11	-1.49	-1.84	-1.56	-1.45	-2.12
Plan 3	-0.85	-1.51	-1.11	-1.51	-1.37	-1.54	-1.47	-2.12
Plan 4	-1.13	-1.58	-1.04	-1.49	-1.24	-1.59	-1.33	-2.13
Plan 5	-1.13	-1.56	-1.15	-1.51	-1.24	-1.58	-1.31	-2.13
Plan 6	-1.82	-1.41	-1.51	-1.85	-1.41	-1.56	-1.59	-2.07

Figure 6-31. Maximum ebb velocity at the bottom for all locations and plans.

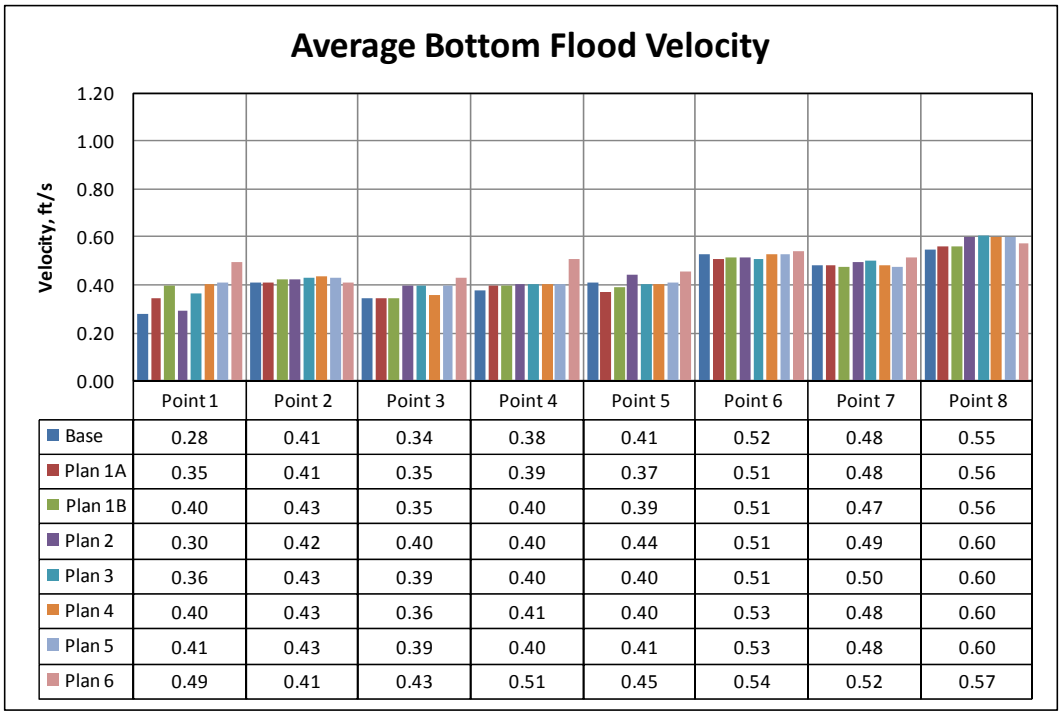

	Point 1	Point 2	Point 3	Point 4	Point 5	Point 6	Point 7	Point 8
Base	0.28	0.41	0.34	0.38	0.41	0.52	0.48	0.55
Plan 1A	0.35	0.41	0.35	0.39	0.37	0.51	0.48	0.56
Plan 1B	0.40	0.43	0.35	0.40	0.39	0.51	0.47	0.56
Plan 2	0.30	0.42	0.40	0.40	0.44	0.51	0.49	0.60
Plan 3	0.36	0.43	0.39	0.40	0.40	0.51	0.50	0.60
Plan 4	0.40	0.43	0.36	0.41	0.40	0.53	0.48	0.60
Plan 5	0.41	0.43	0.39	0.40	0.41	0.53	0.48	0.60
Plan 6	0.49	0.41	0.43	0.51	0.45	0.54	0.52	0.57

Figure 6-32. Average flood velocity at the bottom for all locations and plans.

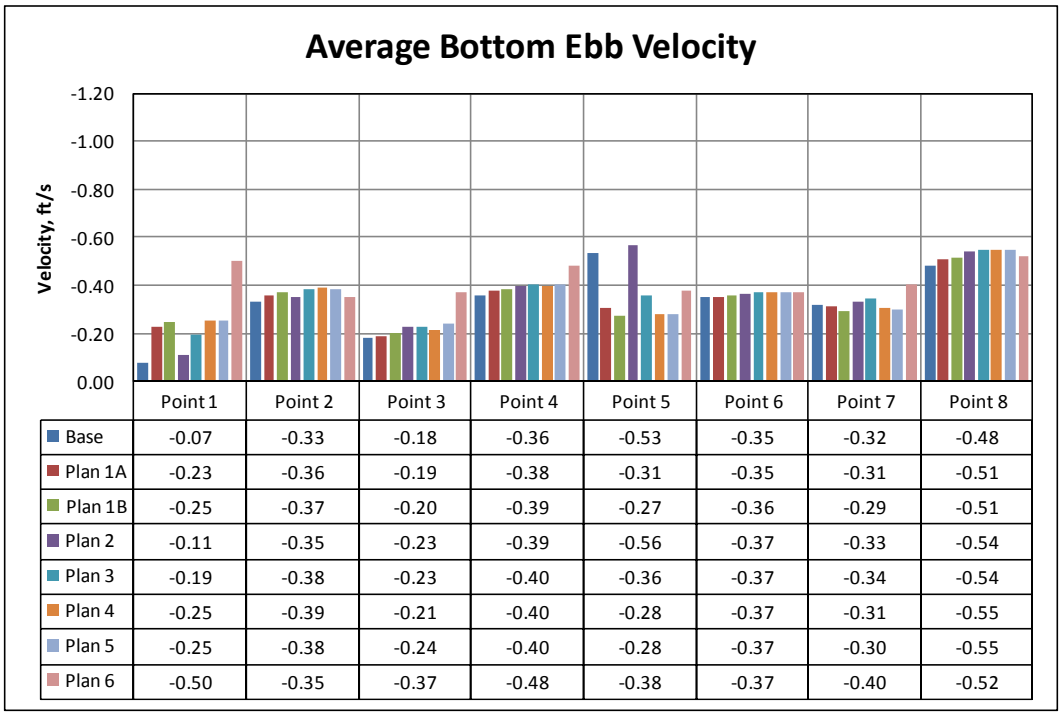

	Point 1	Point 2	Point 3	Point 4	Point 5	Point 6	Point 7	Point 8
Base	-0.07	-0.33	-0.18	-0.36	-0.53	-0.35	-0.32	-0.48
Plan 1A	-0.23	-0.36	-0.19	-0.38	-0.31	-0.35	-0.31	-0.51
Plan 1B	-0.25	-0.37	-0.20	-0.39	-0.27	-0.36	-0.29	-0.51
Plan 2	-0.11	-0.35	-0.23	-0.39	-0.56	-0.37	-0.33	-0.54
Plan 3	-0.19	-0.38	-0.23	-0.40	-0.36	-0.37	-0.34	-0.54
Plan 4	-0.25	-0.39	-0.21	-0.40	-0.28	-0.37	-0.31	-0.55
Plan 5	-0.25	-0.38	-0.24	-0.40	-0.28	-0.37	-0.30	-0.55
Plan 6	-0.50	-0.35	-0.37	-0.48	-0.38	-0.37	-0.40	-0.52

Figure 6-33. Average ebb velocity at the bottom for all locations and plans.

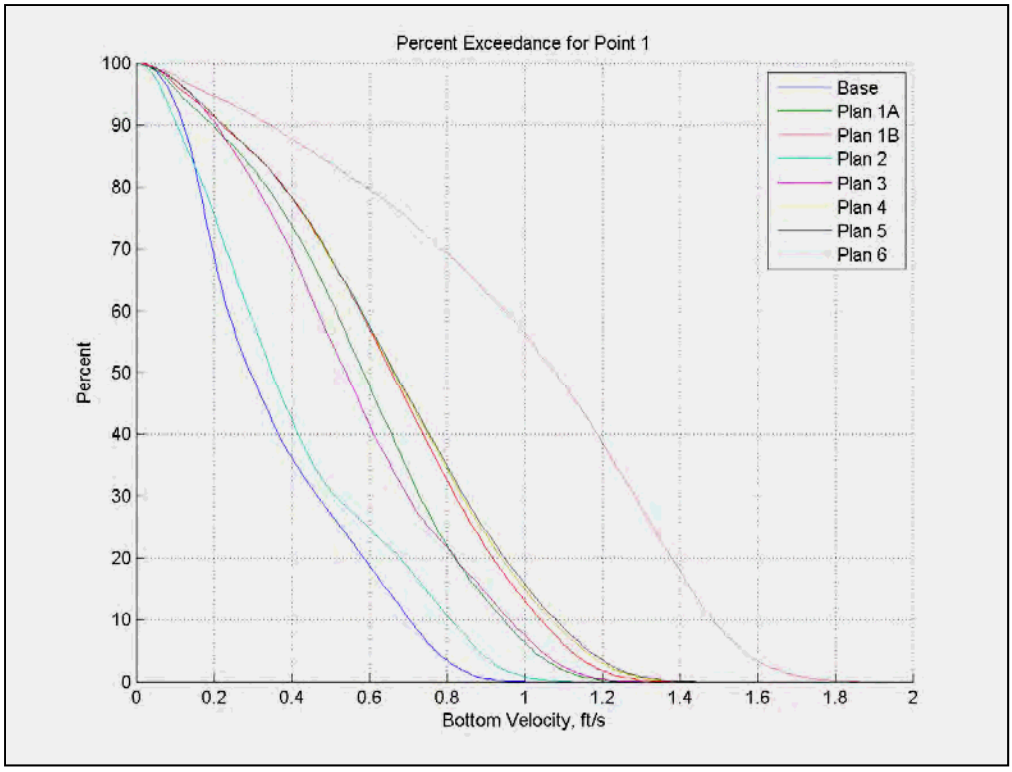

Figure 6-34. CDF curves for all plans at Point 1.

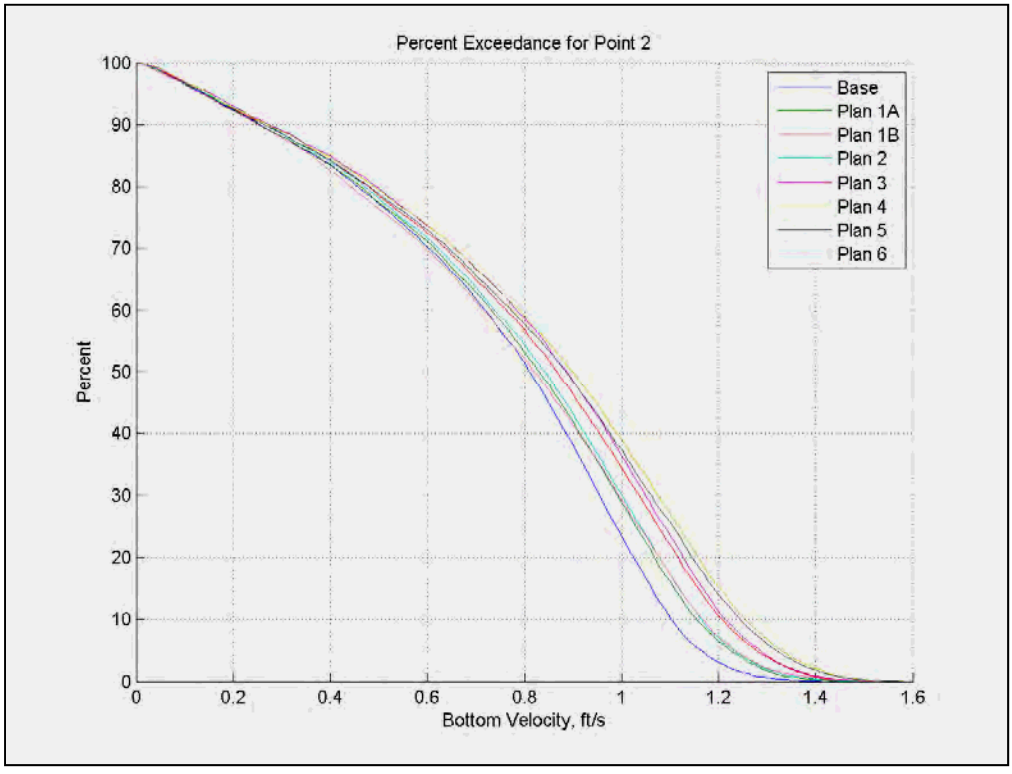

Figure 6-35. CDF curves for all plans at Point 2.

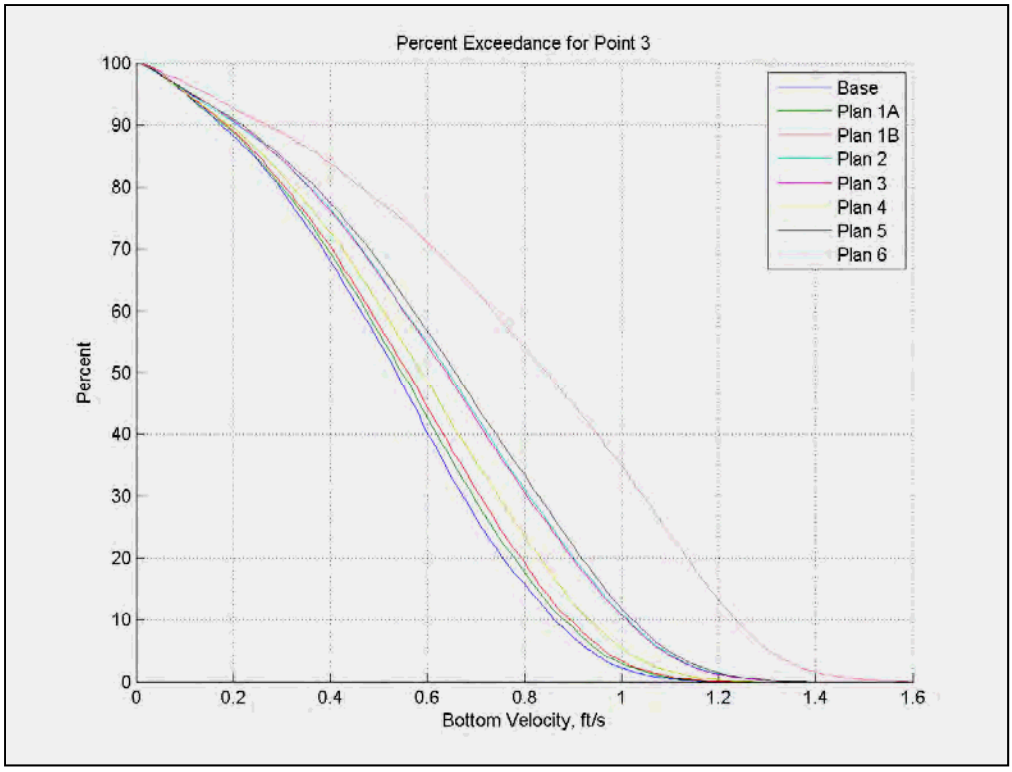

Figure 6-36. CDF curves for all plans at Point 3.

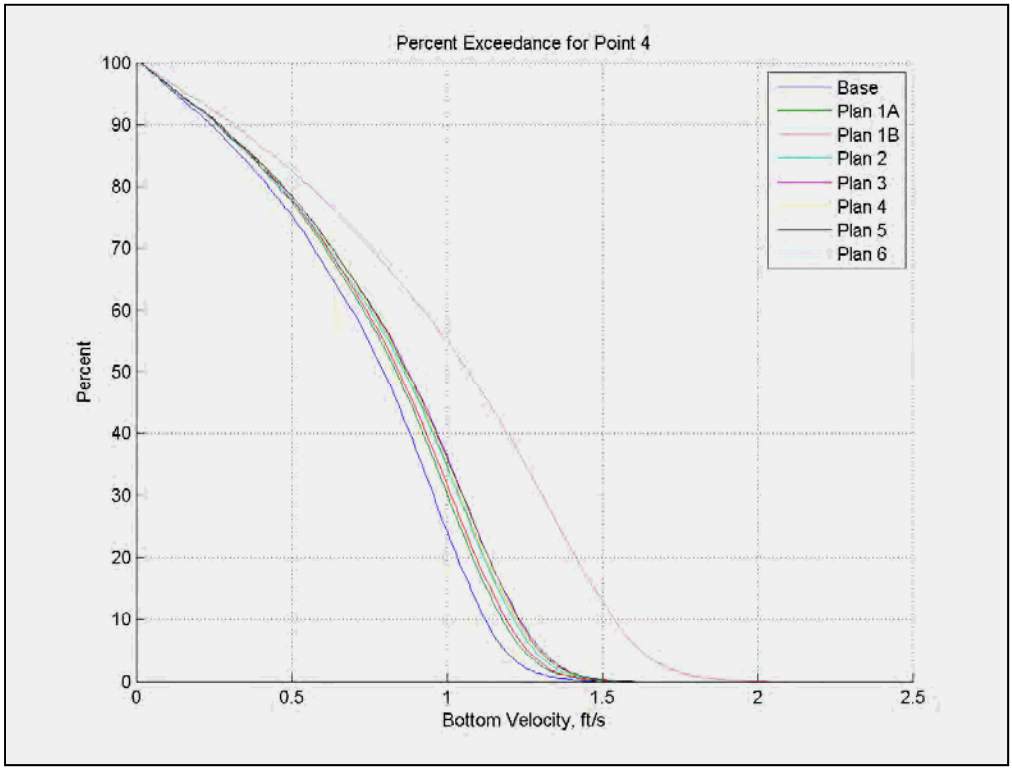

Figure 6-37. CDF curves for all plans at Point 4.

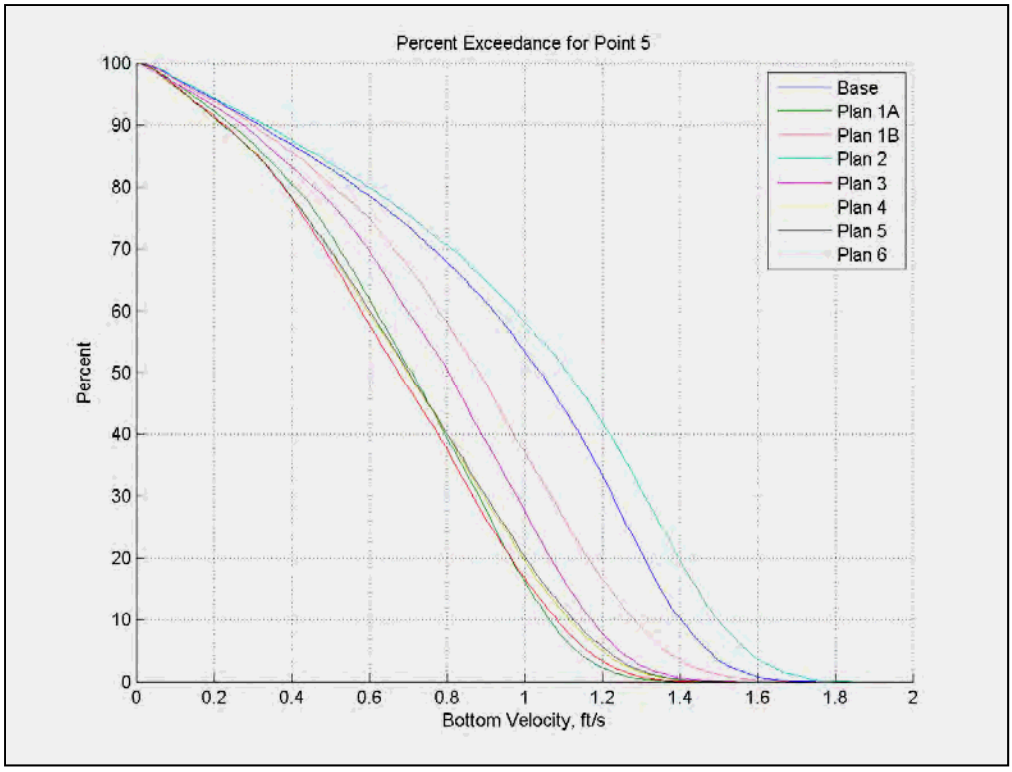

Figure 6-38. CDF curves for all plans at Point 5.

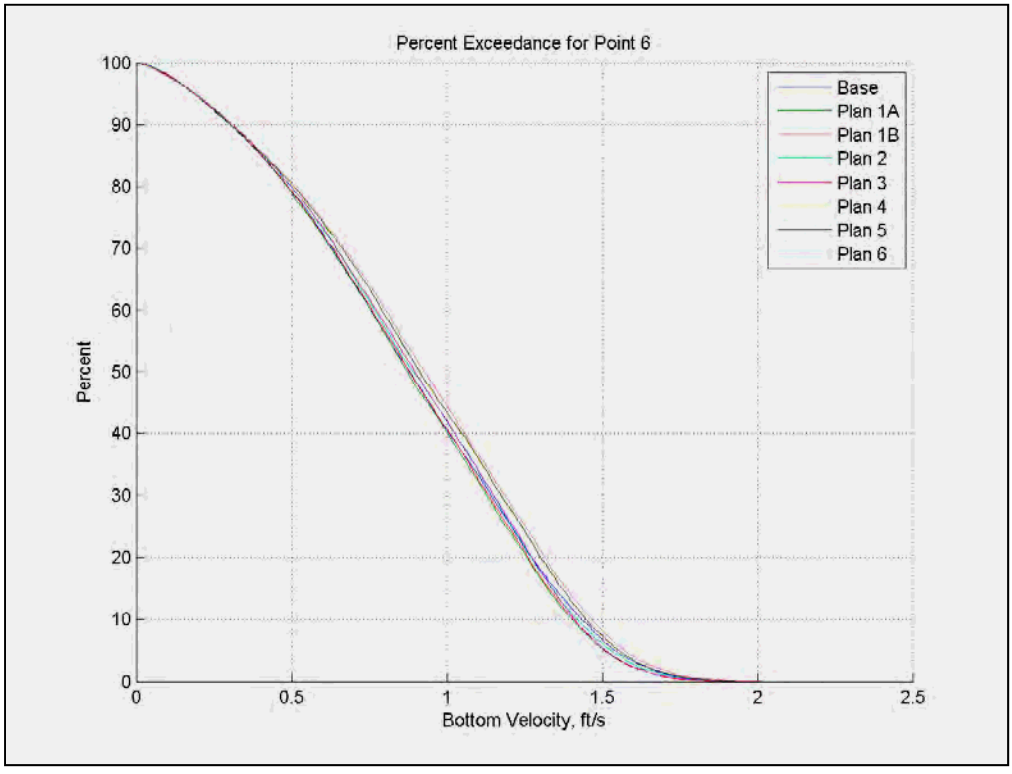

Figure 6-39. CDF curves for all plans at Point 6.

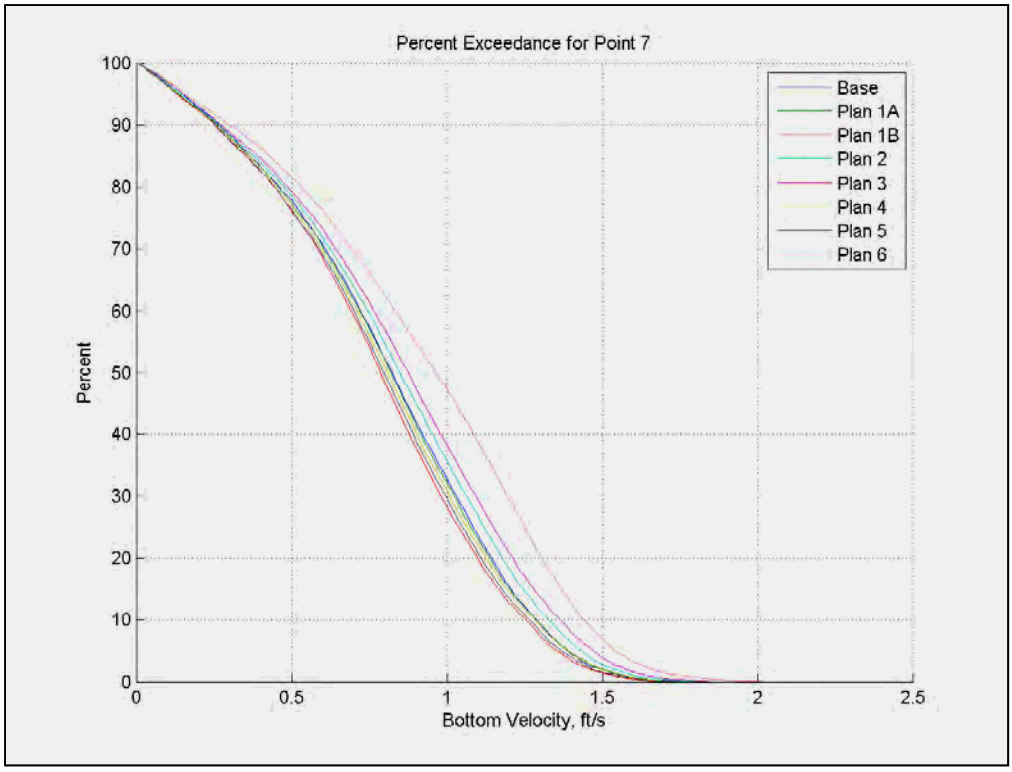

Figure 6-40. CDF curves for all plans at Point 7.

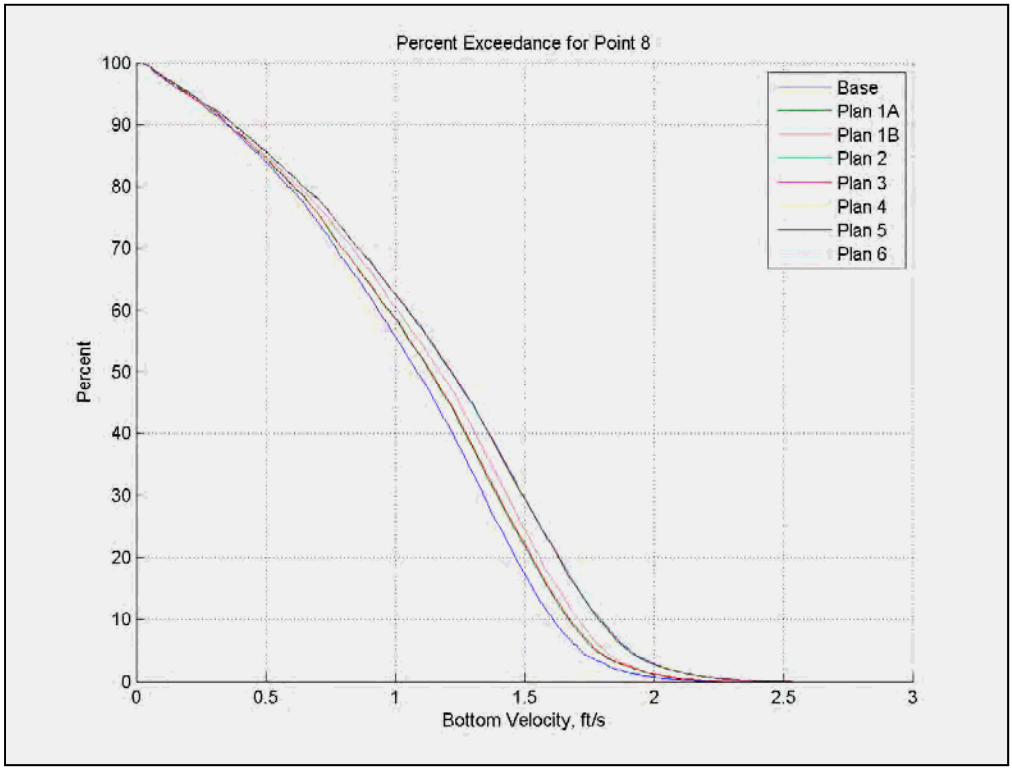

Figure 6-41. CDF curves for all plans at Point 8.

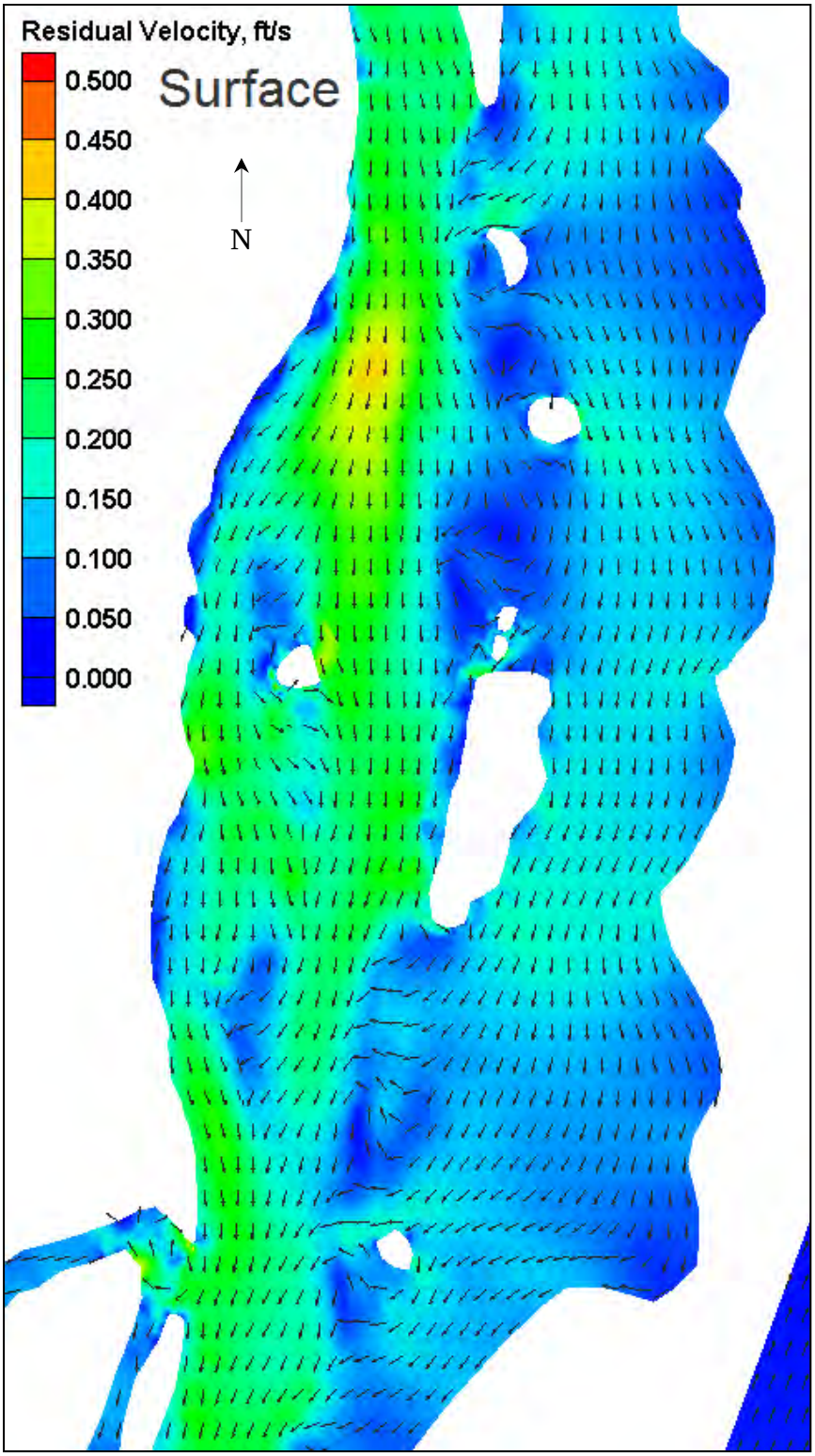

Figure 6-42. Six-month surface velocity residual.

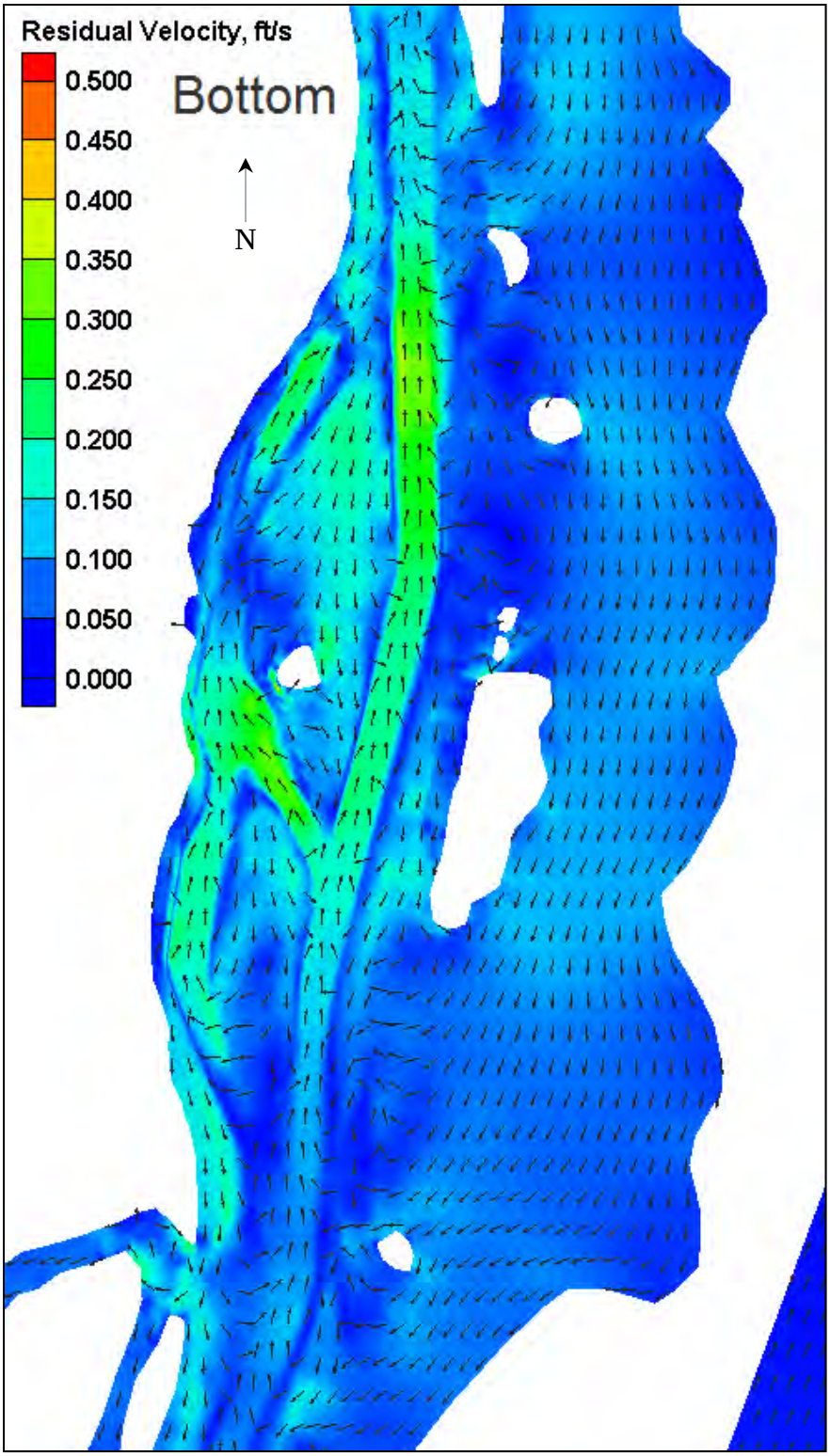

Figure 6-43. Six-month bottom velocity residual.

6.3 Sediment results

The same analysis locations shown in Figure 6-9 were used for the sediment time history analyses. For each analysis location, four plots are provided: the suspended sediment concentrations for the surface and the bed over a two-day period, the bed shear stress over the same two-day period; and the cumulative bed displacement over the entire six-month simulation. Positive values indicate shoaling and negative values indicate erosion. These results are provided in Figure 6-44 through Figure 6-75 and grouped for each analysis location.

The suspended sediment, when compared to the base, is reduced at the surface for most plans at all locations over the two-day period shown. The bottom suspended sediment, however, is not changed much as a result of the plans, although some plans are slightly higher or lower.

The shear stress that the velocity produces on the bed is what drives the erosion and deposition of material. When compared to the base condition, the plans show large changes at some locations, which will be evidenced in the cumulative shoaling, or bed displacement, plots. By opening up the northern alignment as in Plan 1 and Plans 3 through 6, there is increased flow and therefore increased shear stress at Point 1. However, at Point 5 upstream of the northern wharf and in the location of the alignment change, there is actually less shear stress for most plans. This is due to the velocity being higher in the Base condition owing to the lower depth of flow in this area. Once it is deepened, the velocity and resulting shear stress becomes lower than in the Base condition.

Overall, Plan 6 shows the most benefit due to the increased shear stress over most of the domain. This plan forces flow through either the navigation channel or the MOTSU channels by placing an island—an emergent structure designed always to exceed the area's maximum water level—covering 690 acres in the shallow region between the two channels. The design streamlines the flows, maintaining higher velocities to prevent material from reaching and settling on the bed. Plan 6 shows a cumulative bed change less than the Base condition at every location except Point 5, and often less than the other plan alternatives. Based on the model results, material that was settling in this area is now moved elsewhere within the system such that measurable increases in other areas of the model domain are not observed. In other words, all of the material is not simply piling up somewhere else but is being spread throughout the system.

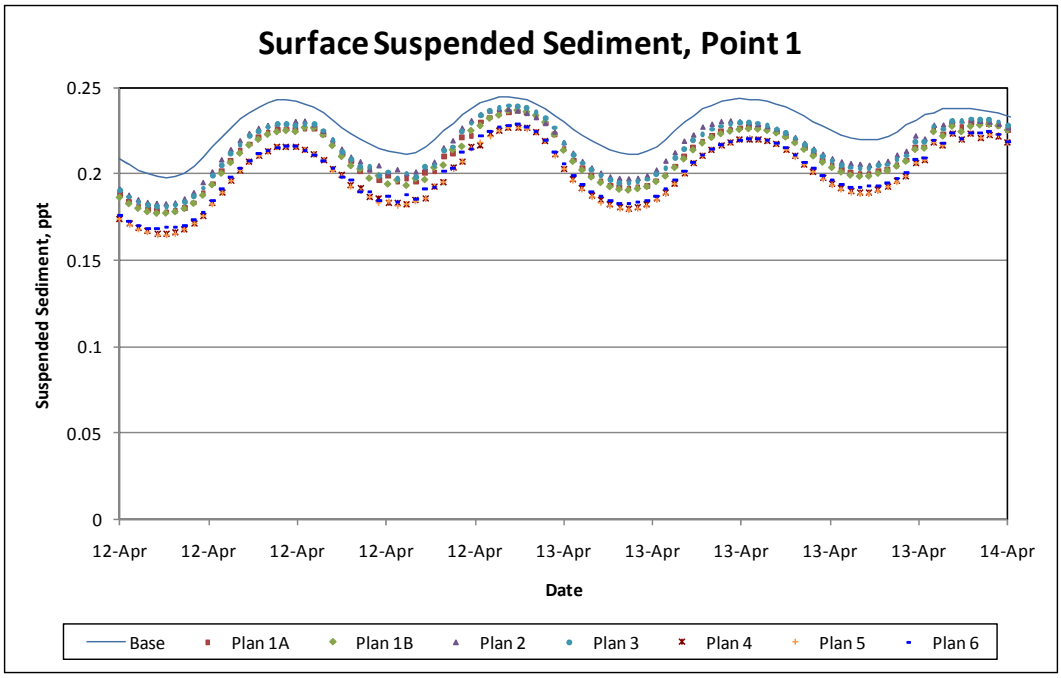

Figure 6-44. Surface suspended sediment concentration for Point 1.

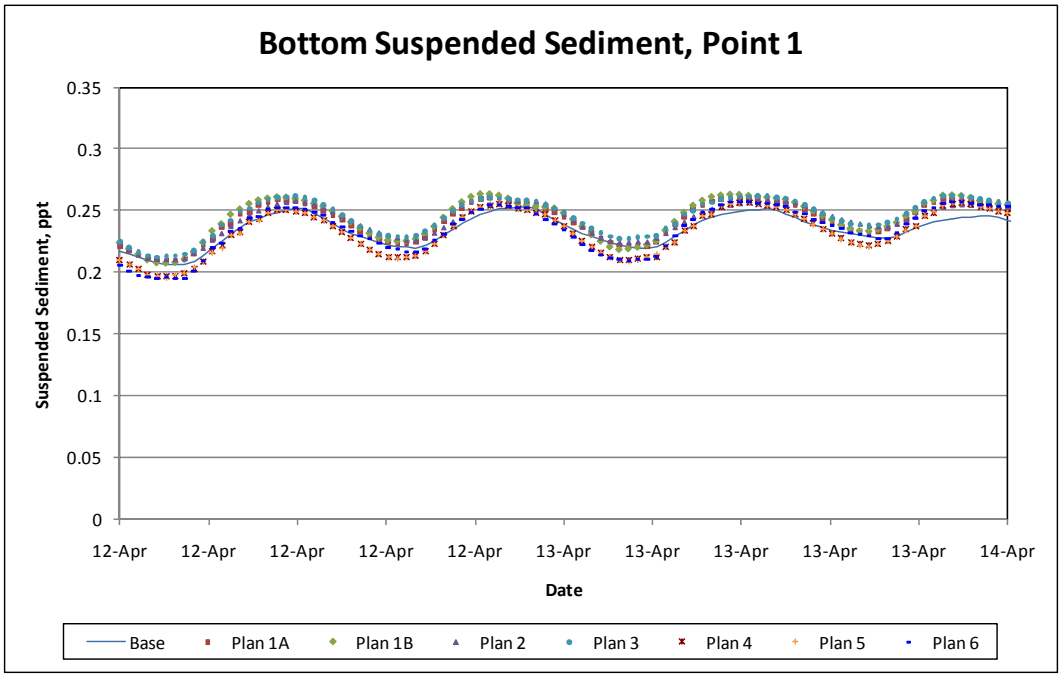

Figure 6-45. Bottom suspended sediment concentration for Point 1.

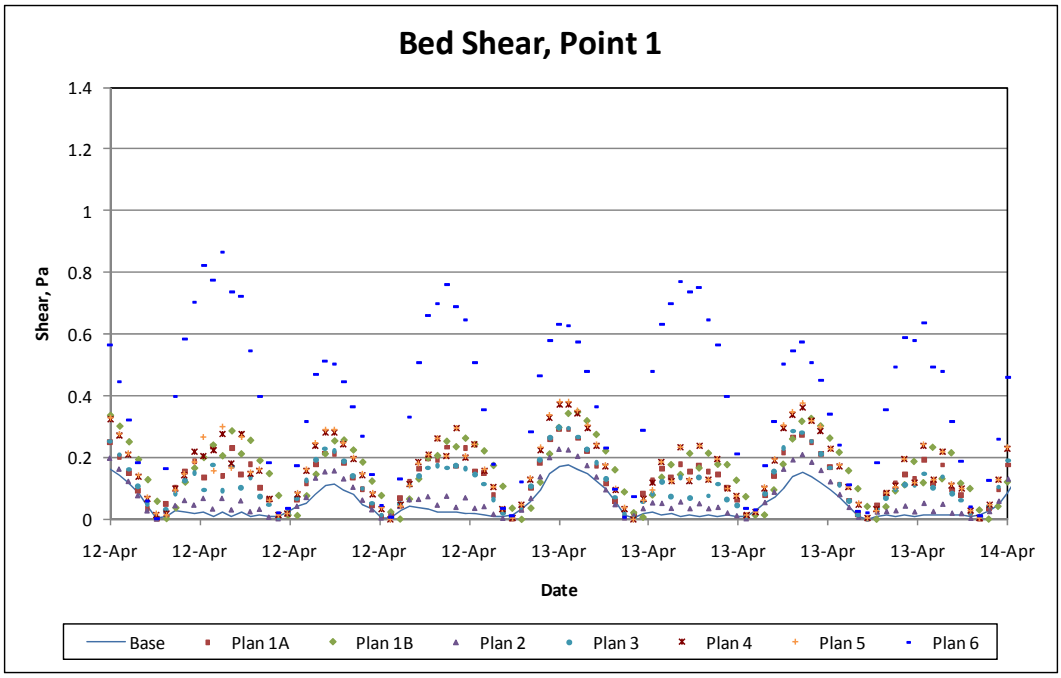

Figure 6-46. Bed shear stress for Point 1.

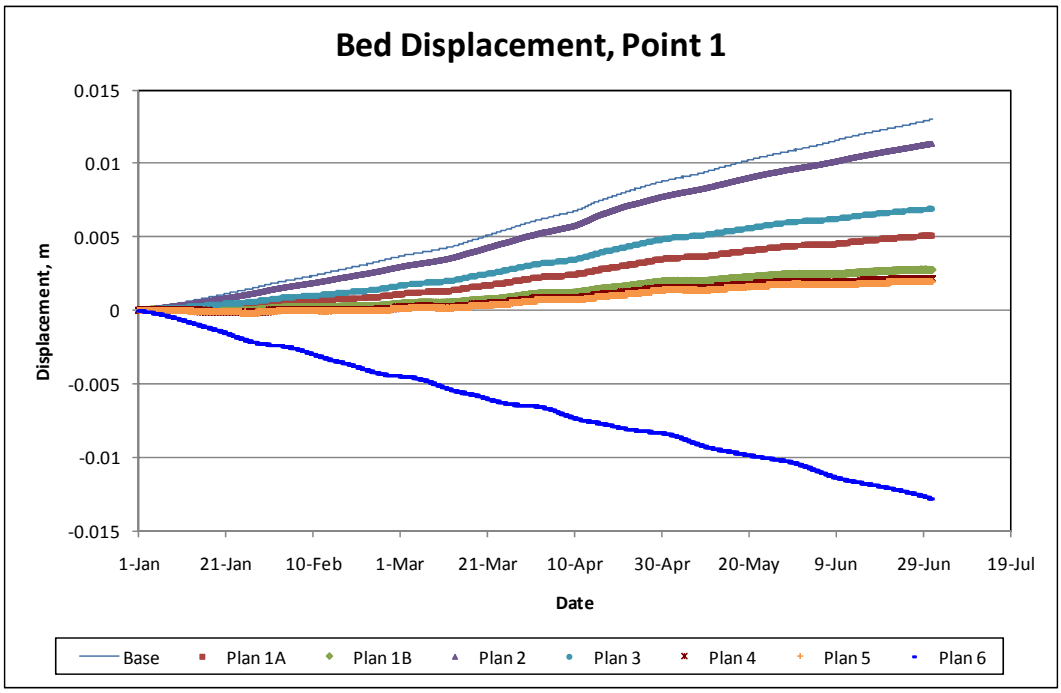

Figure 6-47. Cumulative bed displacement for Point 1.

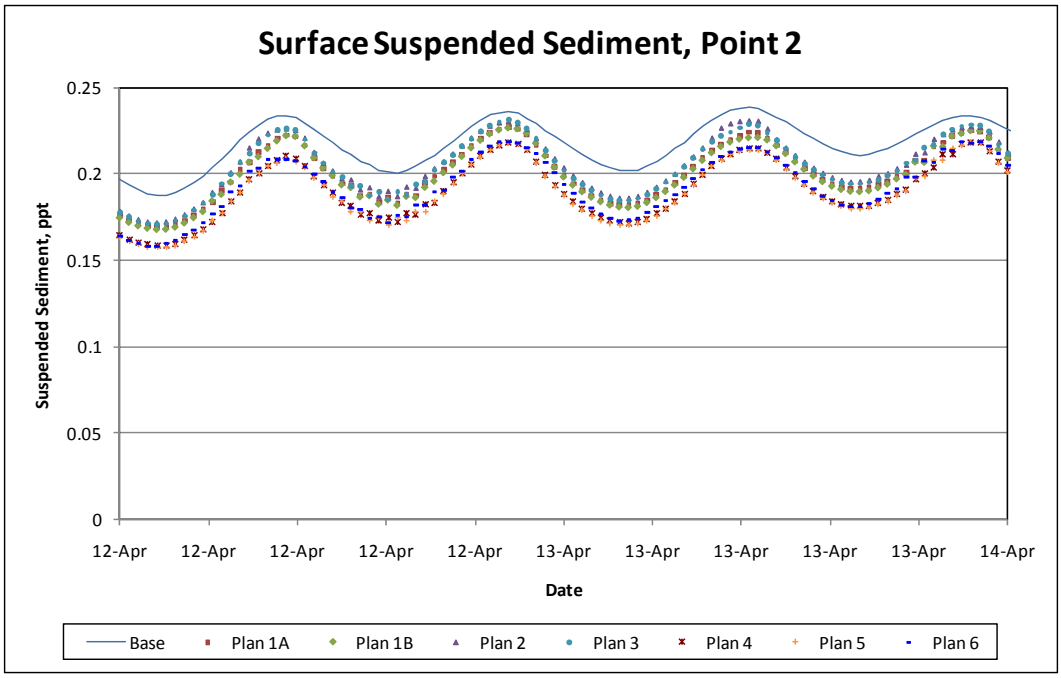

Figure 6-48. Surface suspended sediment concentration for Point 2.

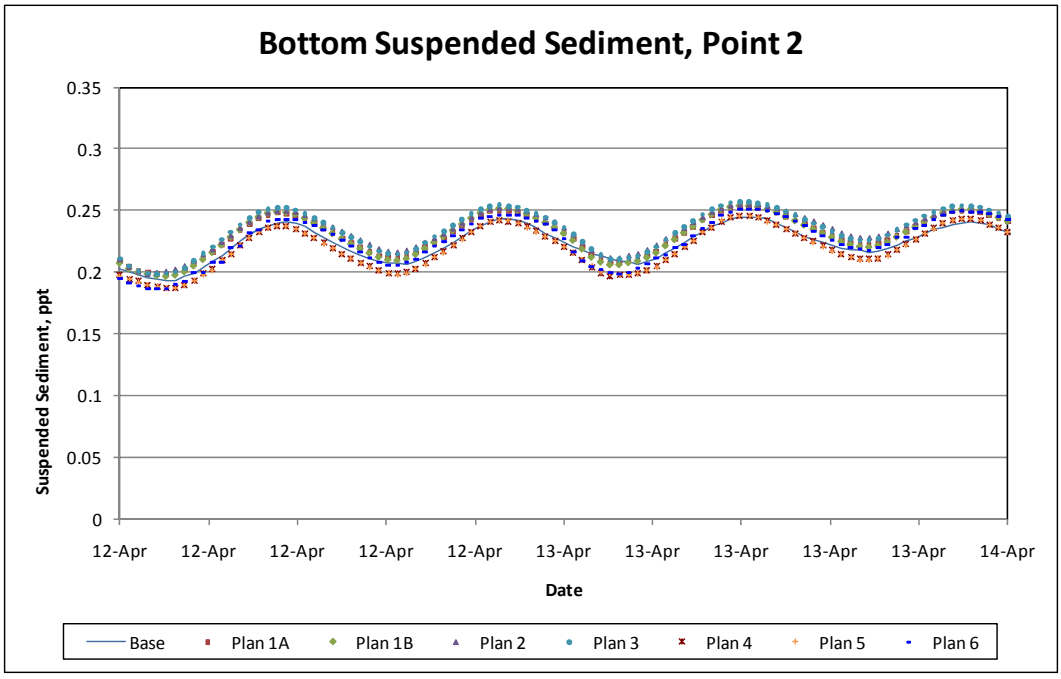

Figure 6-49. Bottom suspended sediment concentration for Point 2.

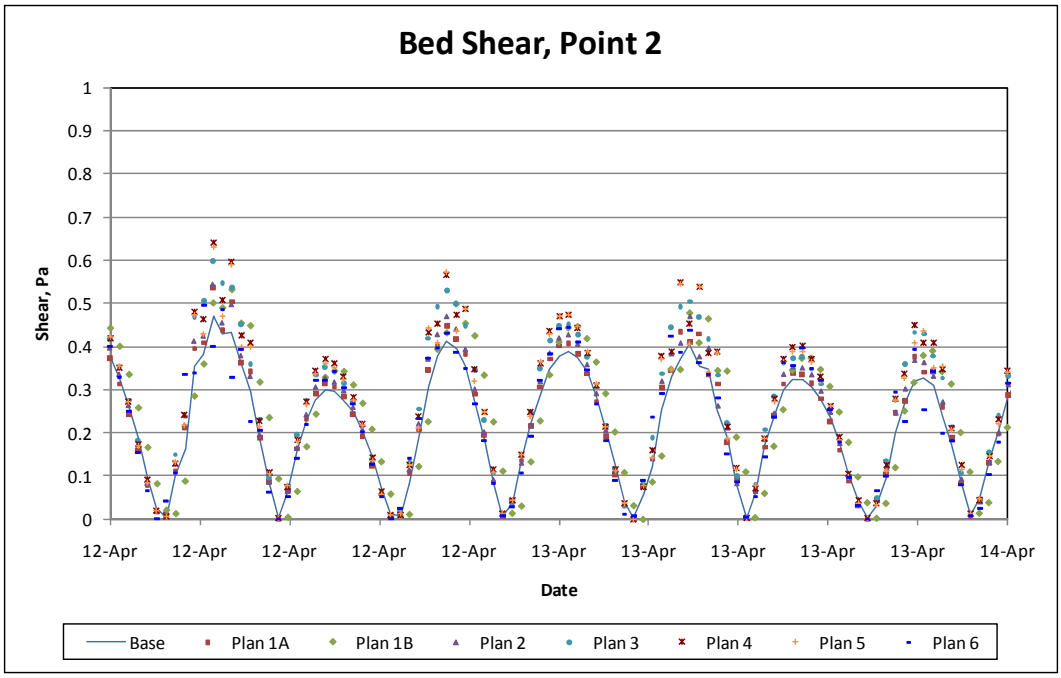

Figure 6-50. Bed shear stress for Point 2.

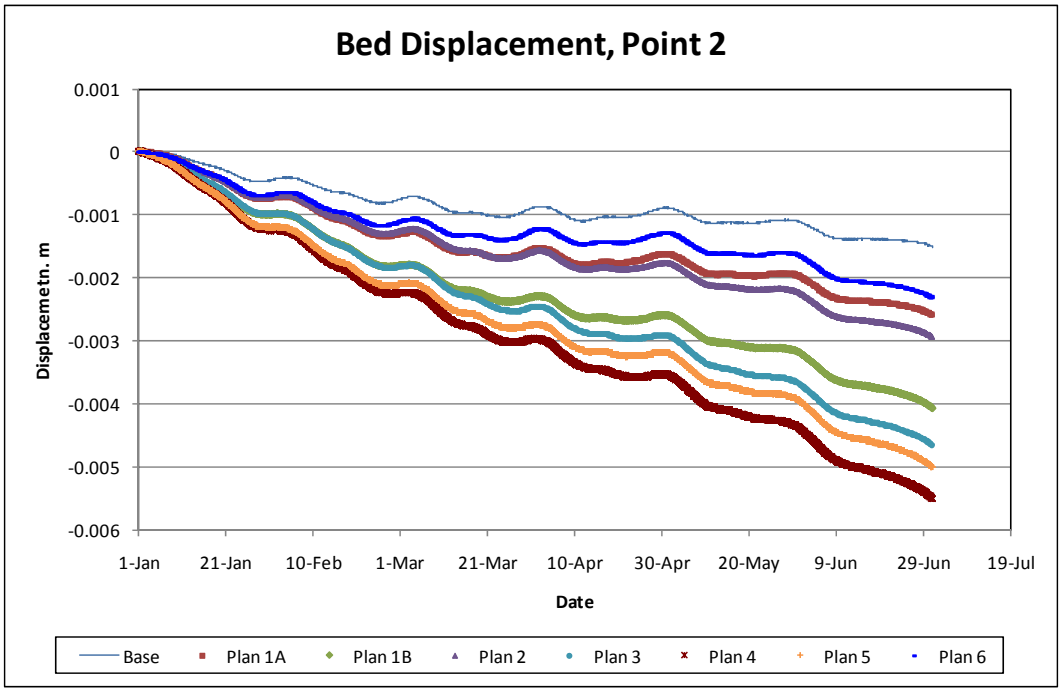

Figure 6-51. Cumulative bed displacement for Point 2.

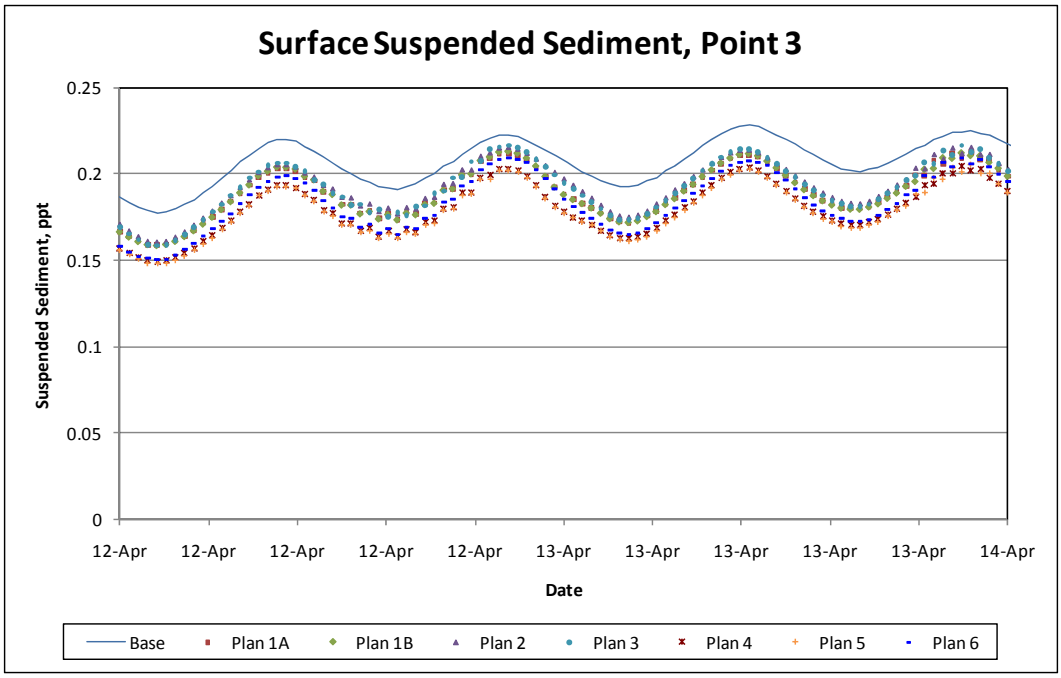

Figure 6-52. Surface suspended sediment concentration for Point 3.

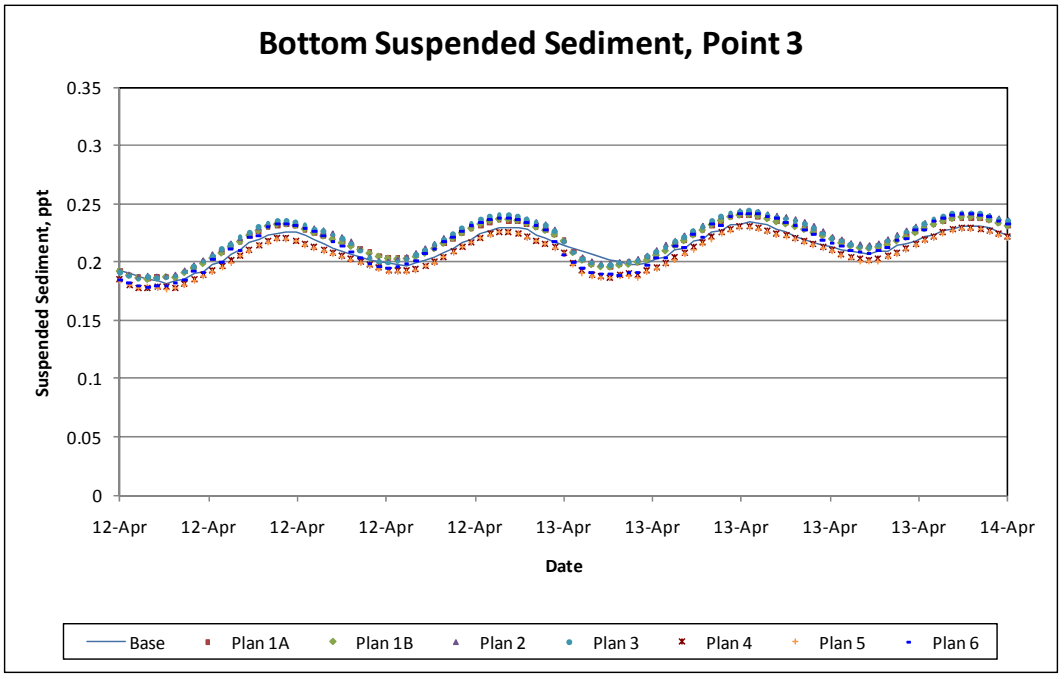

Figure 6-53. Bottom suspended sediment concentration for Point 3.

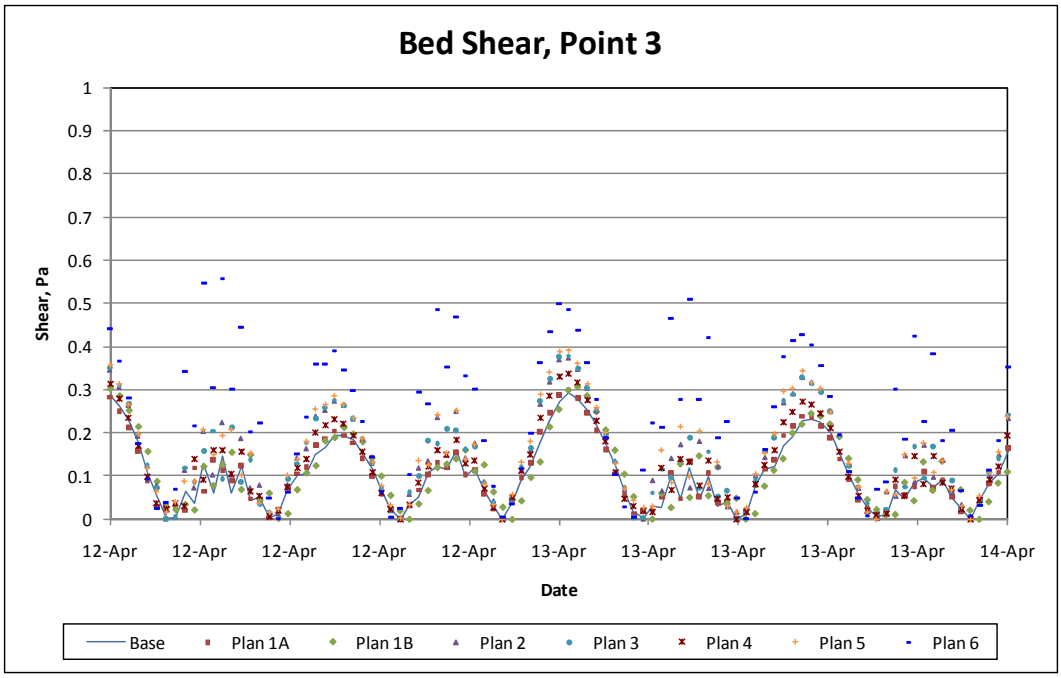

Figure 6-54. Bed shear stress for Point 3.

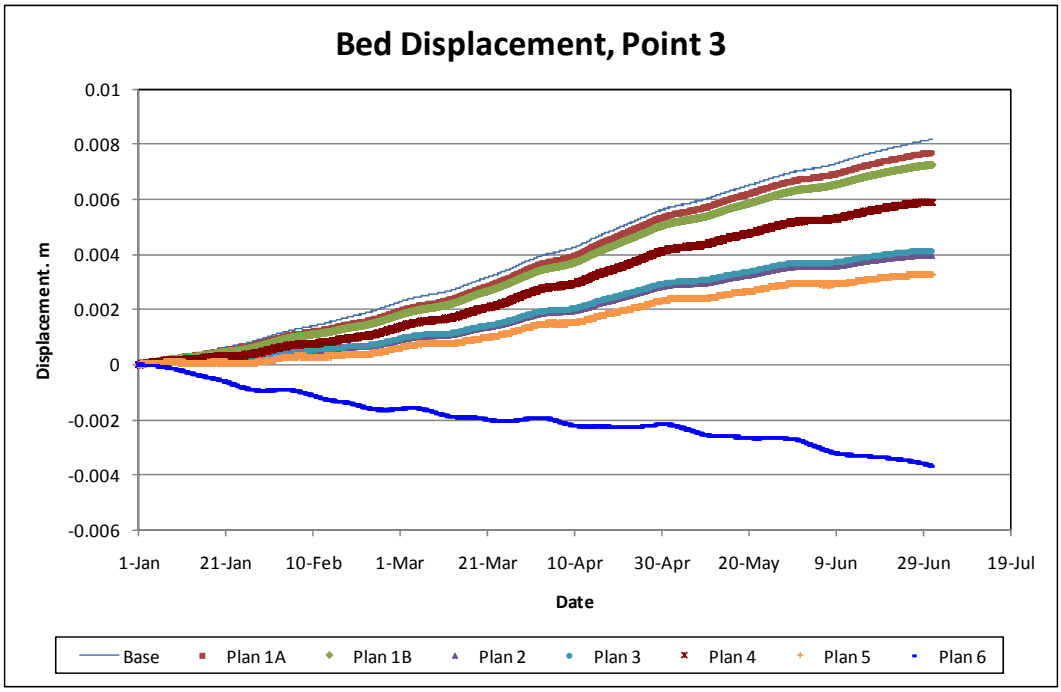

Figure 6-55. Cumulative bed displacement for Point 3.

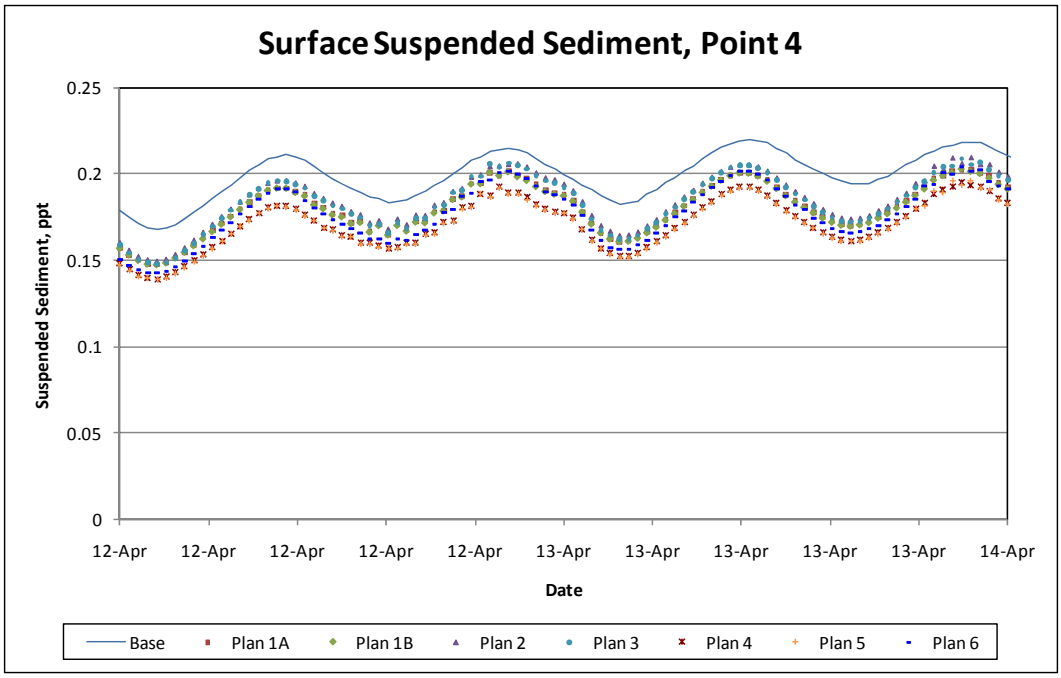

Figure 6-56. Surface suspended sediment concentration for Point 4.

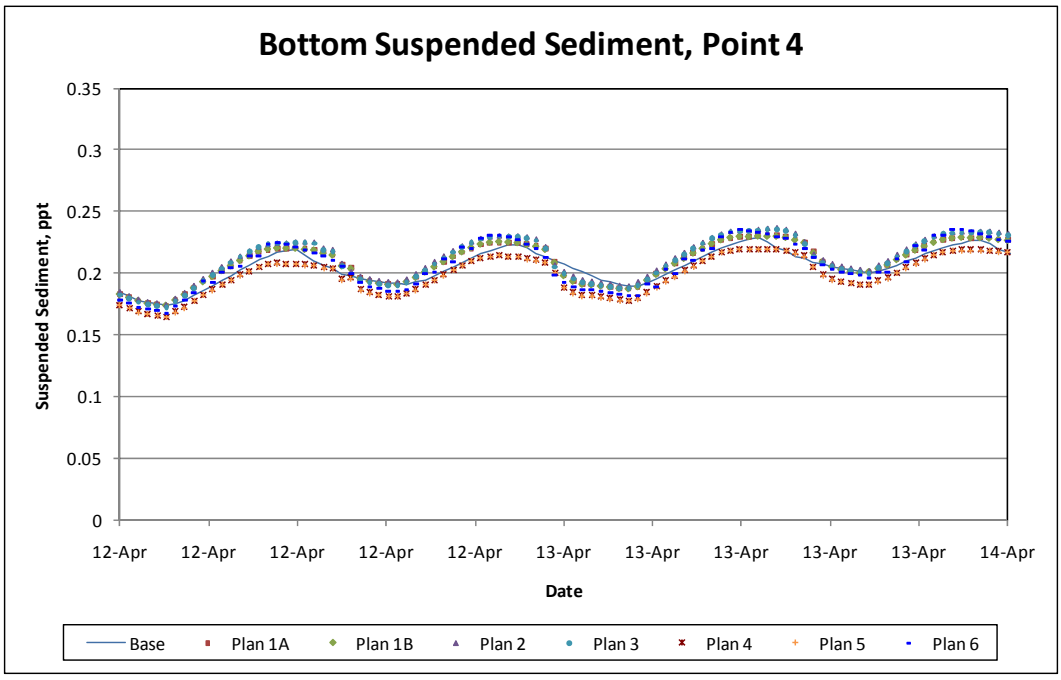

Figure 6-57. Bottom suspended sediment concentration for Point 4.

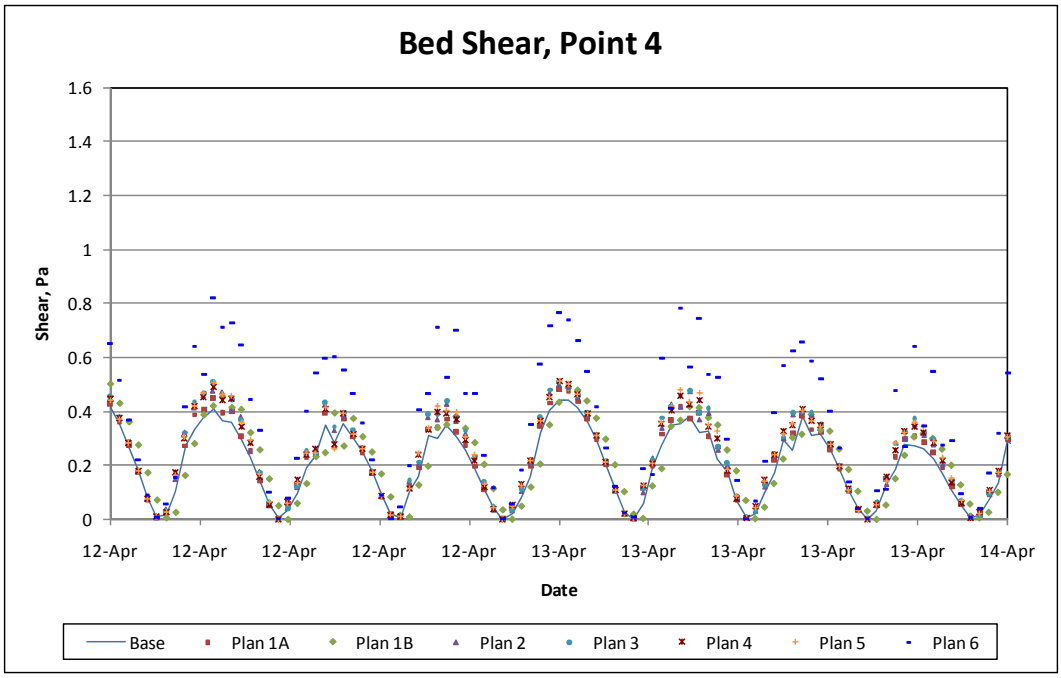

Figure 6-58. Bed shear stress for Point 4.

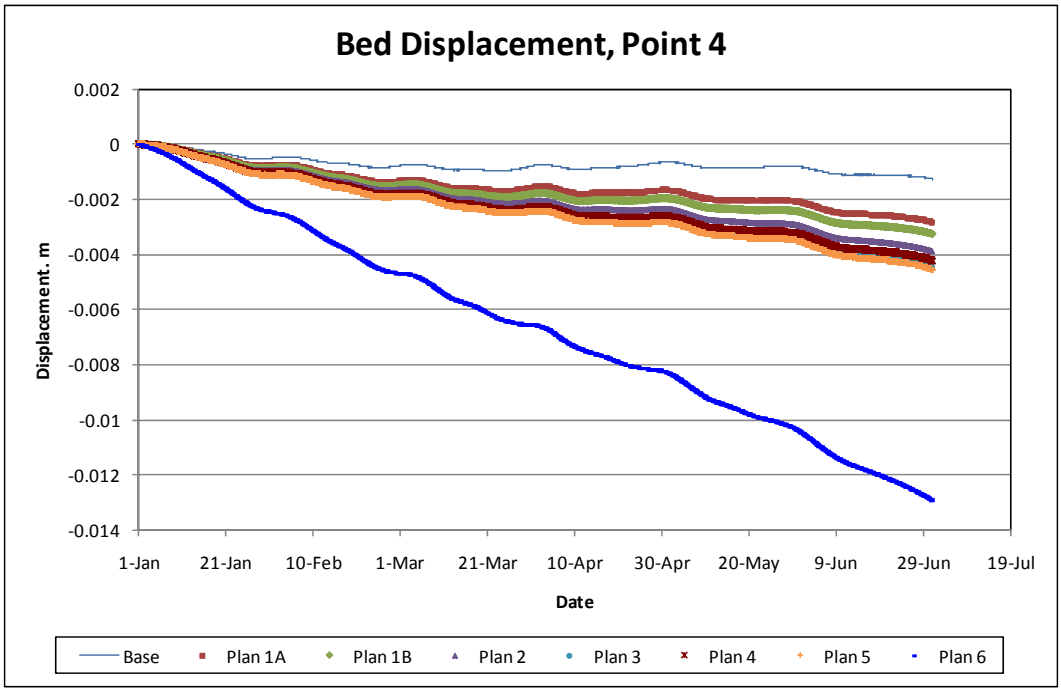

Figure 6-59. Cumulative bed displacement for Point 4.

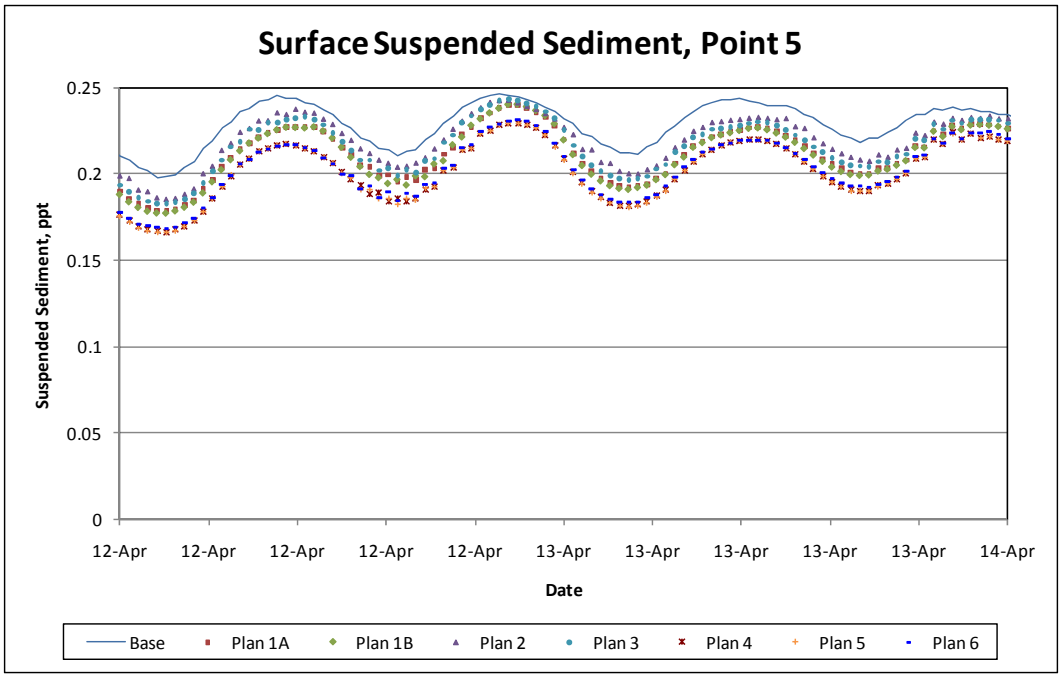

Figure 6-60. Surface suspended sediment concentration for Point 5.

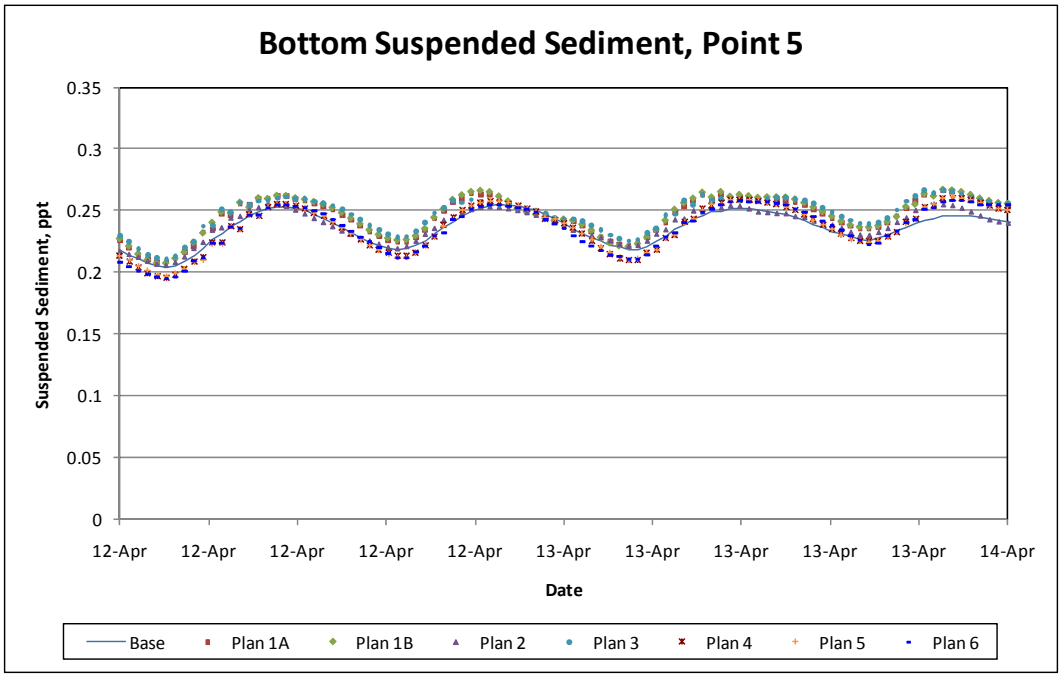

Figure 6-61. Bottom suspended sediment concentration for Point 5.

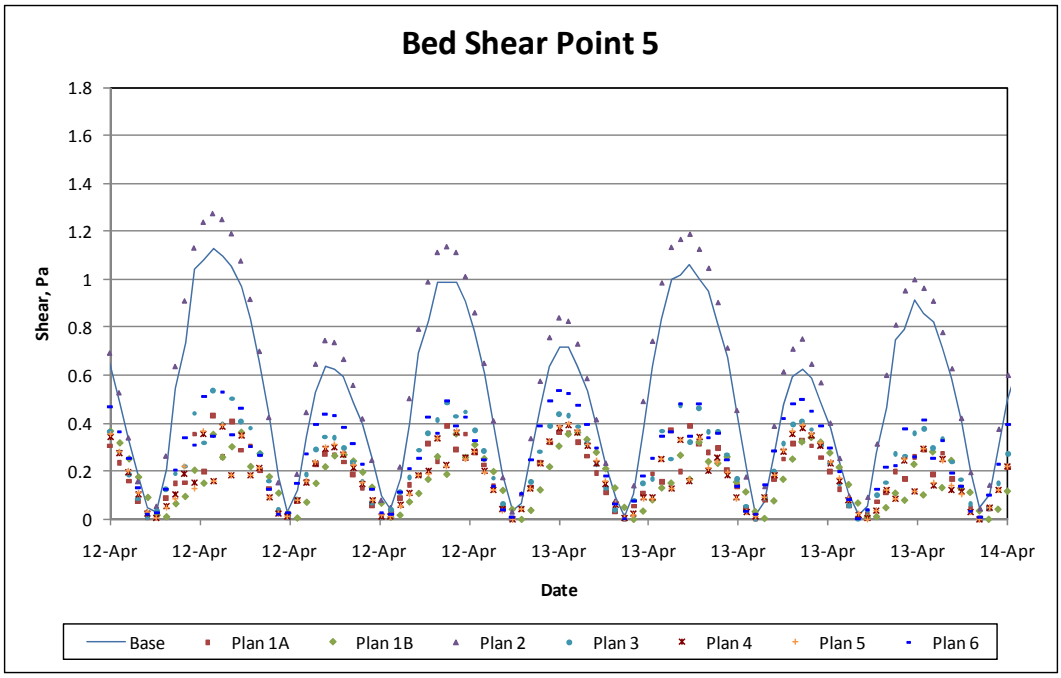

Figure 6-62. Bed shear stress for Point 5.

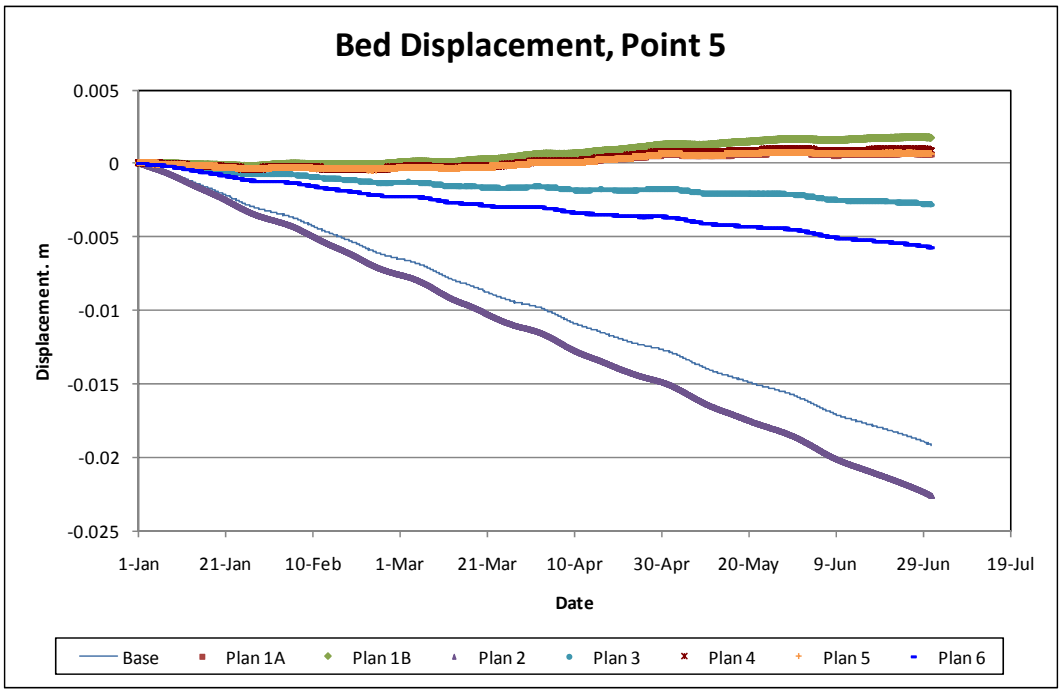

Figure 6-63. Cumulative bed displacement for Point 5.

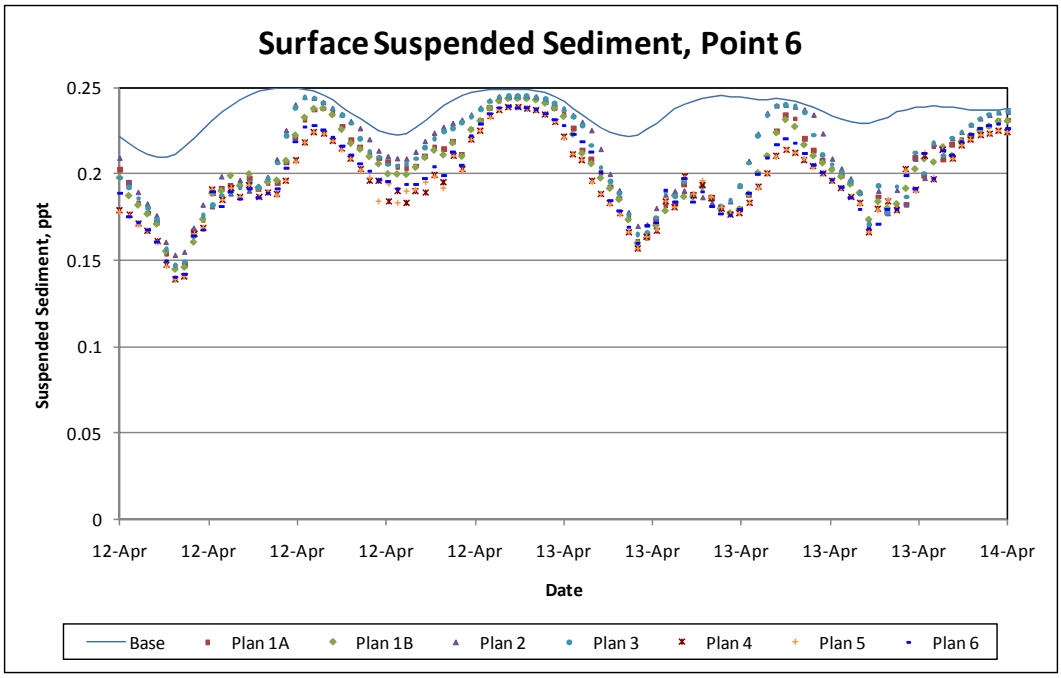

Figure 6-64. Surface suspended sediment concentration for Point 6.

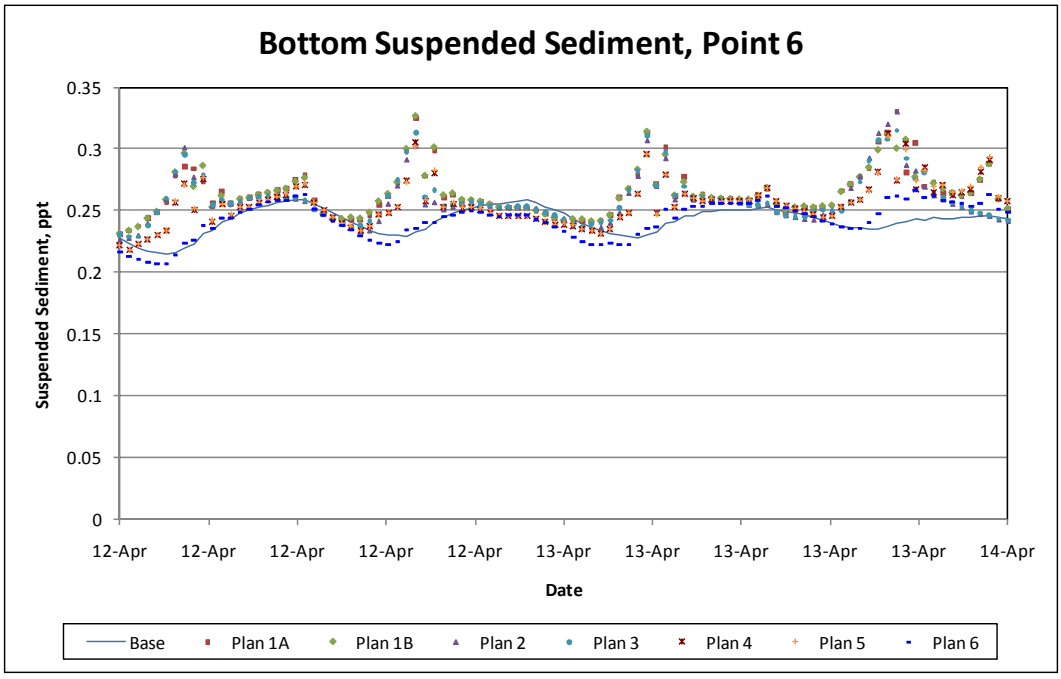

Figure 6-65. Bottom suspended sediment concentration for Point 6.

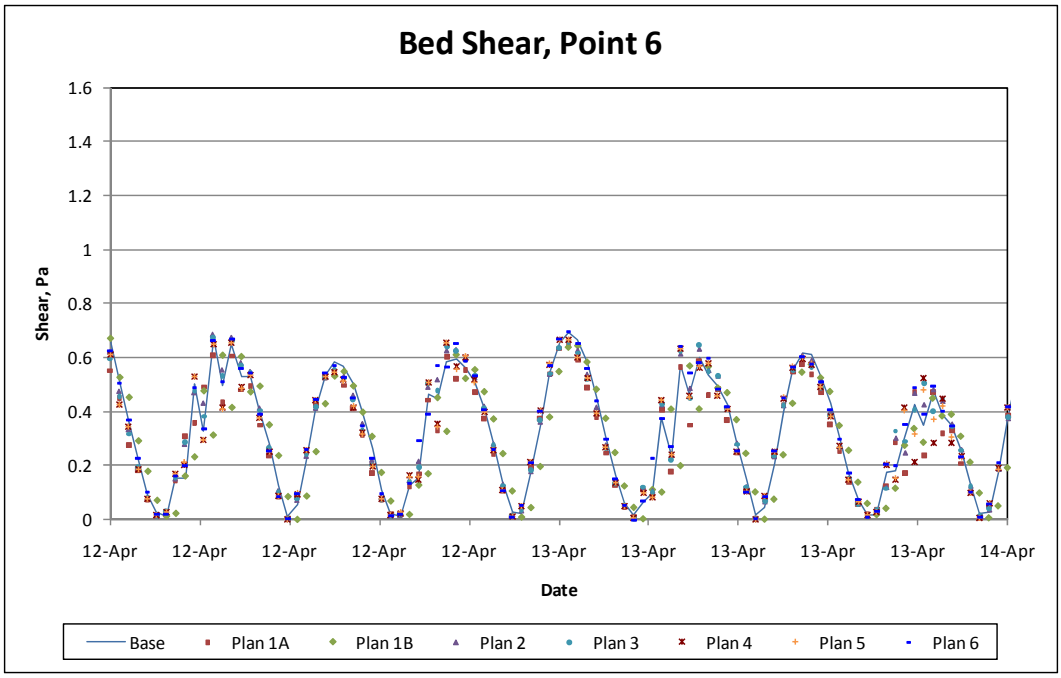

Figure 6-66. Bed shear stress for Point 6.

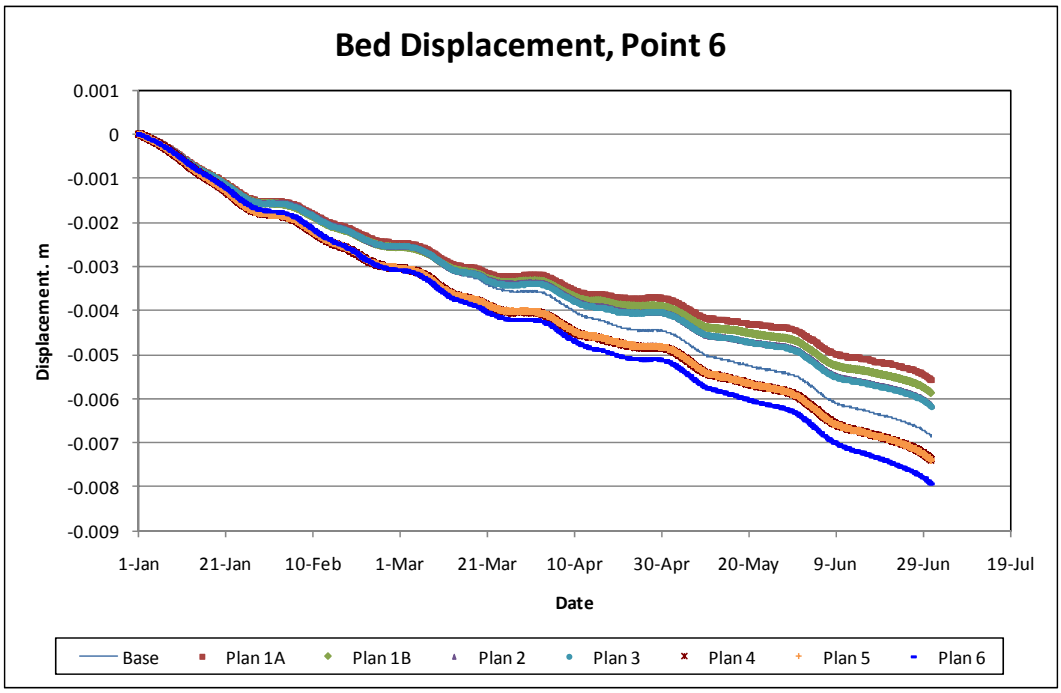

Figure 6-67. Cumulative bed displacement for Point 6.

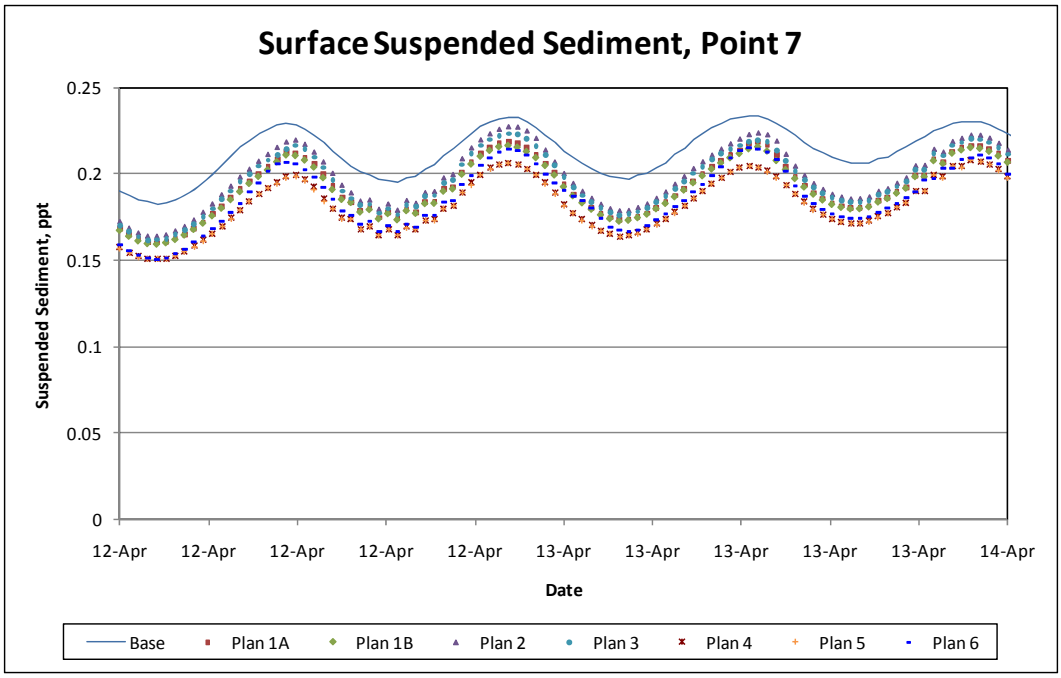

Figure 6-68. Surface suspended sediment concentration for Point 7.

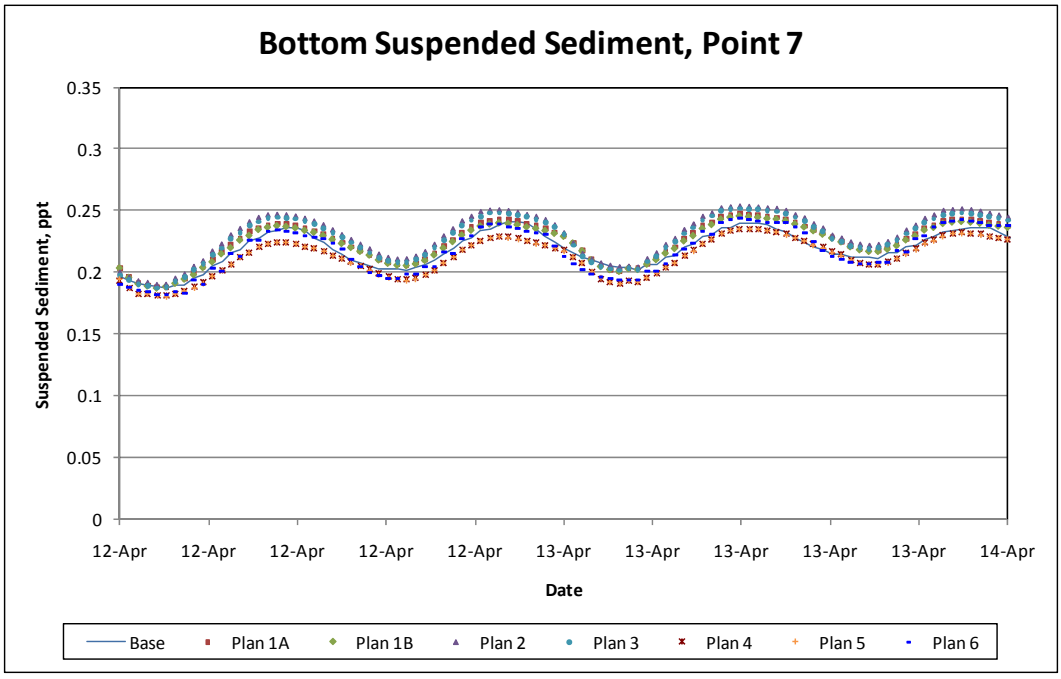

Figure 6-69. Bottom suspended sediment concentration for Point 7.

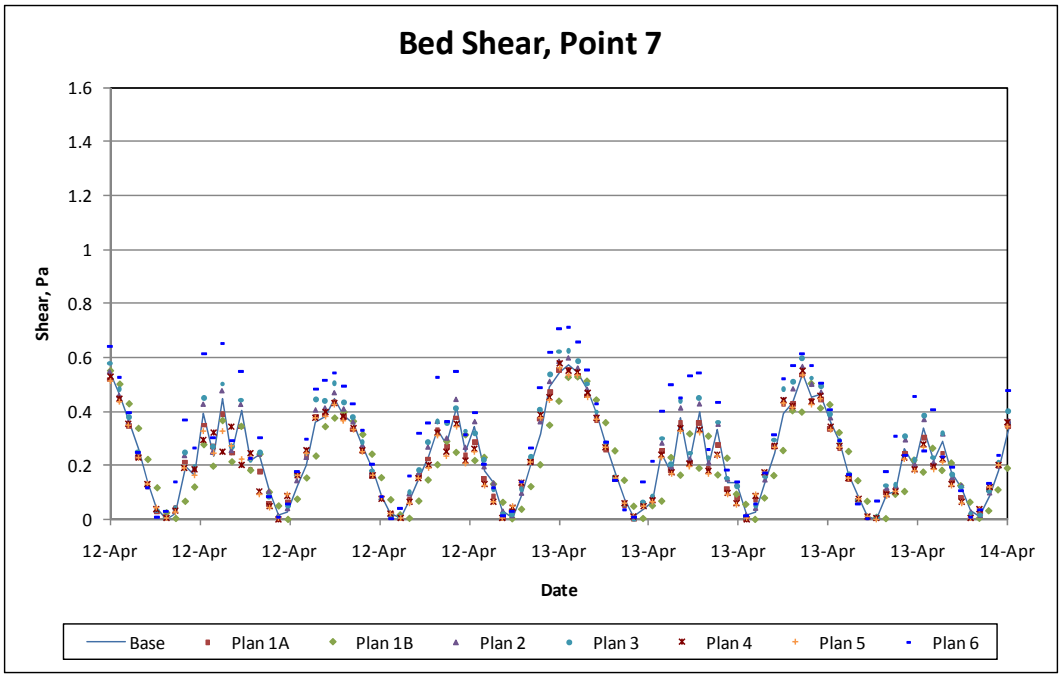

Figure 6-70. Bed shear stress for Point 7.

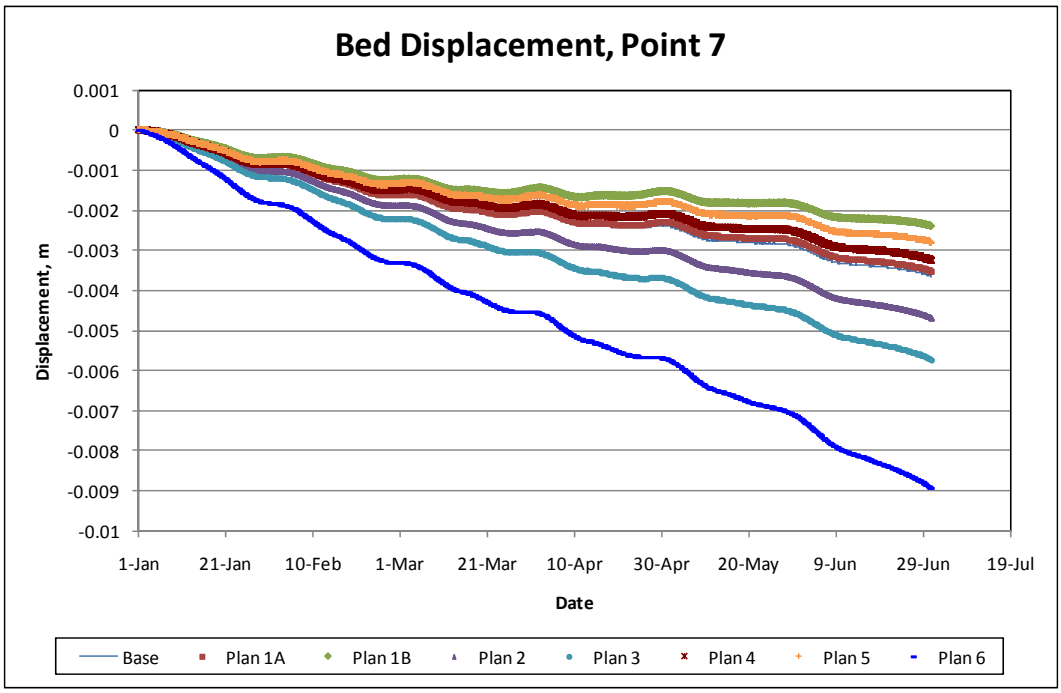

Figure 6-71. Cumulative bed displacement for Point 7.

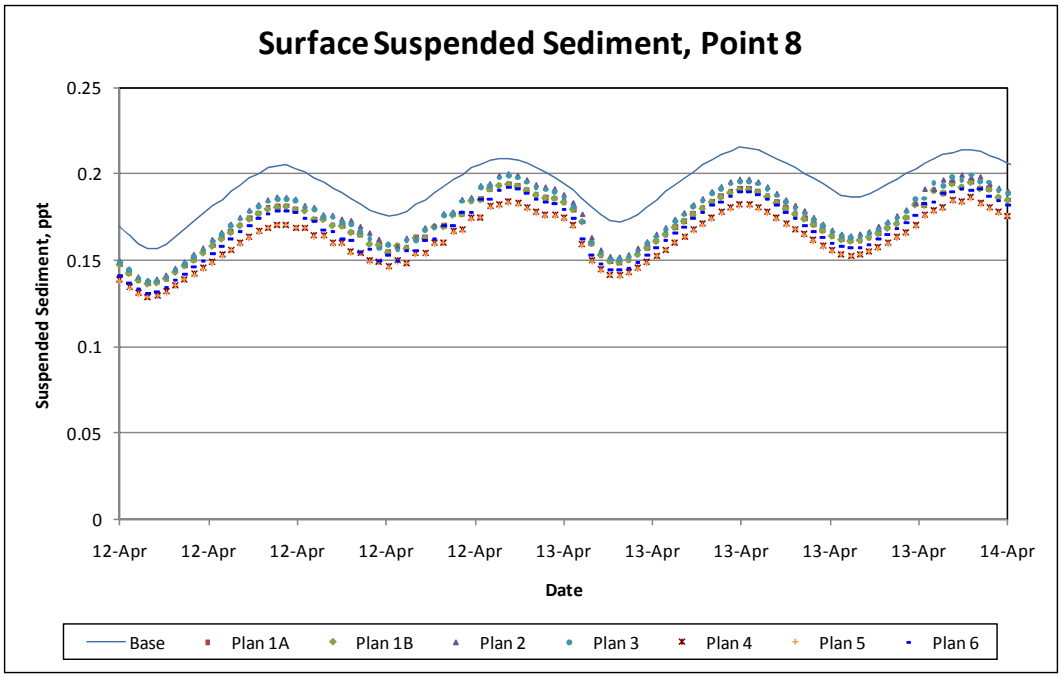

Figure 6-72. Surface suspended sediment concentration for Point 8.

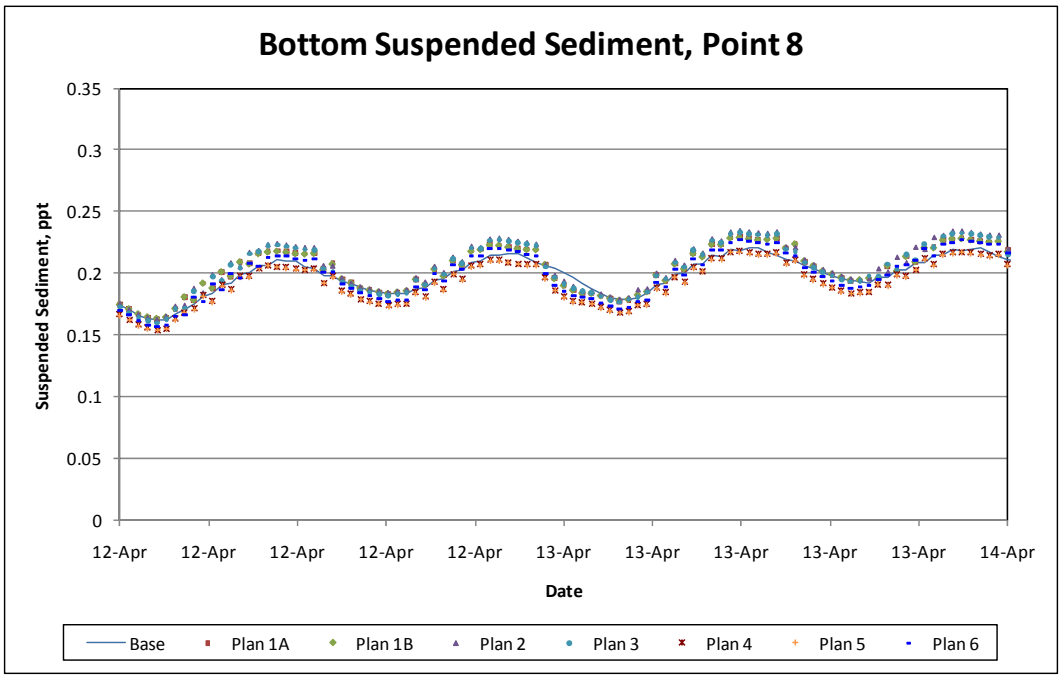

Figure 6-73. Bottom suspended sediment concentration for Point 8.

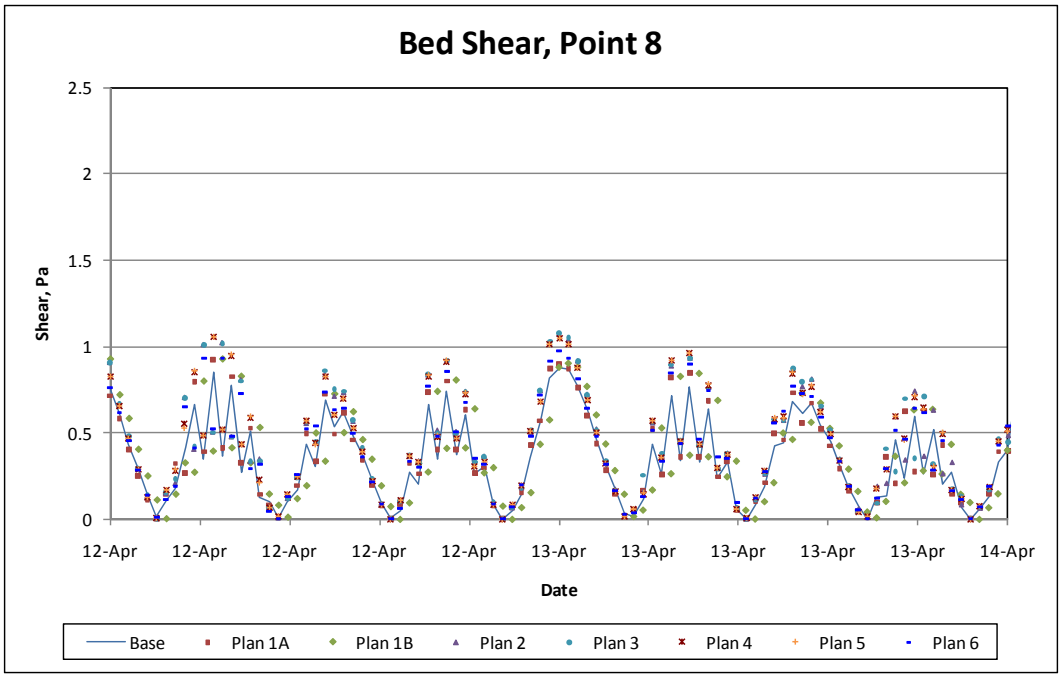

Figure 6-74. Bed shear stress for Point 8.

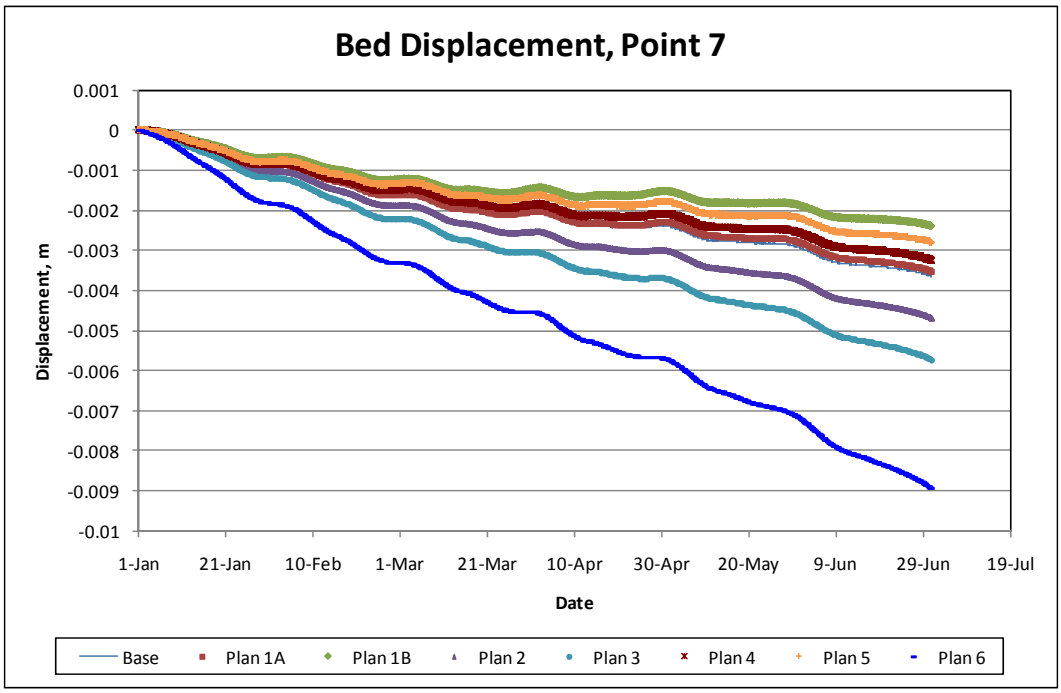

Figure 6-75. Cumulative bed displacement for Point 8.

Additional analyses are performed to better illustrate the shoaling changes each plan generates from the Base condition. Figure 6-76 through Figure 6-82 show the difference between the Base shoaling values and the various plan shoaling values. These computations are only performed on the positive bed displacement changes, i.e., only for values where the bed change is

positive (i.e., shoaled areas) over the six-month simulation period. Therefore, the locations showing a negative cumulative displacement in Figure 6-47 through Figure 6-75 will not indicate changes in the following figures. Areas shaded in blue tints indicate beneficial changes in shoaling due to the plan changes whereas areas shaded in red tints indicate that the plan produces more shoaling and, therefore, produces adverse impacts in that area. The background image provides a reference for the existing channels and wharf geometry of MOTSU.

It is immediately obvious that Plan 1a and 1b, Plan 3, Plan 4, and Plan 5 produce additional shoaling in the navigation channel near its connection with the newly aligned northern entrance channel. Plan 2 does not show this trend since it does not include realigning this entrance. The plans that include straightening out the MOTSU channel between the southern and center wharfs show increased shoaling in this area. However, this is expected for the same reason more shoaling is seen at Point 5 when the northern channel is realigned. By opening up this area, the shear stress is reduced and therefore the tendency for material to settle is increased. The magnitude of this shoaling should be analyzed, though, since more shoaling at this location may not be bad overall, especially if the change produces benefits upstream and downstream of channel realignment.

Plan 6 shows the most improvement from the Base condition. This plan places an island between the MOTSU channel and the main navigation channel such that the flow is streamlined through these pathways. The island area of Plan 6 is not depicted in the figure but the aerial image shows the current configuration. Initially the benefit is seen as the shallows are not available for possible shoaling. However, this plan produces beneficial impacts in the MOTSU channels without generating more shoaling in the navigation channel, unlike several of the other plans. There is additional shoaling in the turning basin, but this is expected and actually occurs outside of the navigation channel where the velocity drops, as is also the case for Plans 4 and 5.

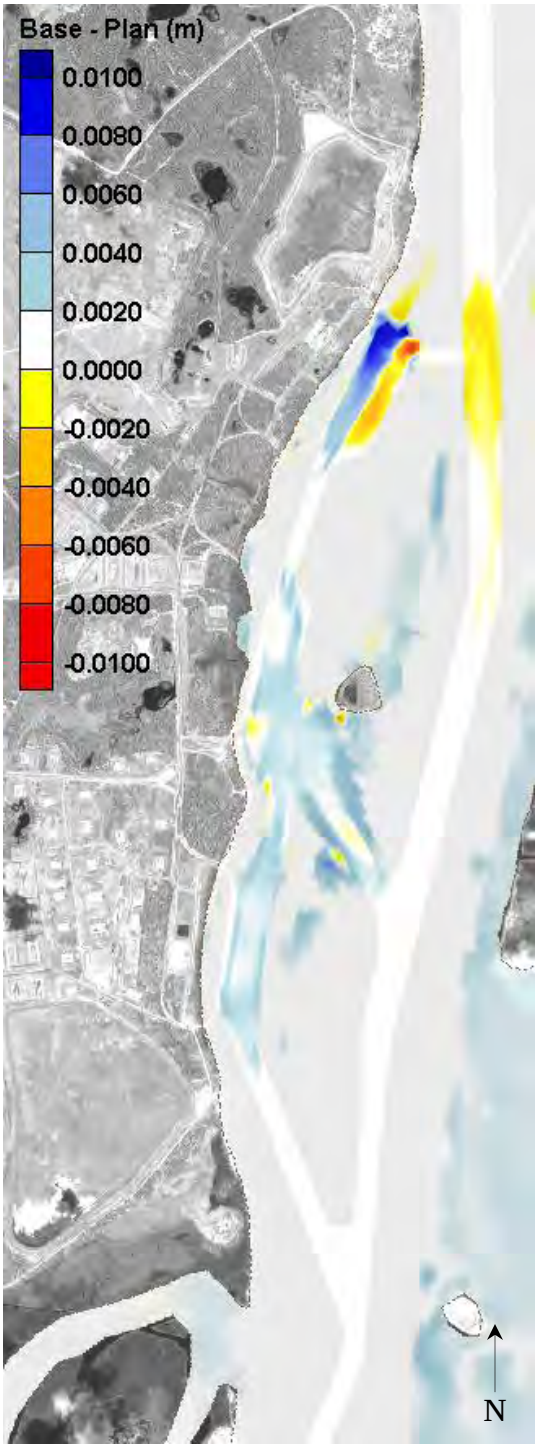

Figure 6-76. Change in shoaling from Base for Plan 1a; positive (blue) means plan generates less shoaling while negative (red) means plan generates more shoaling.

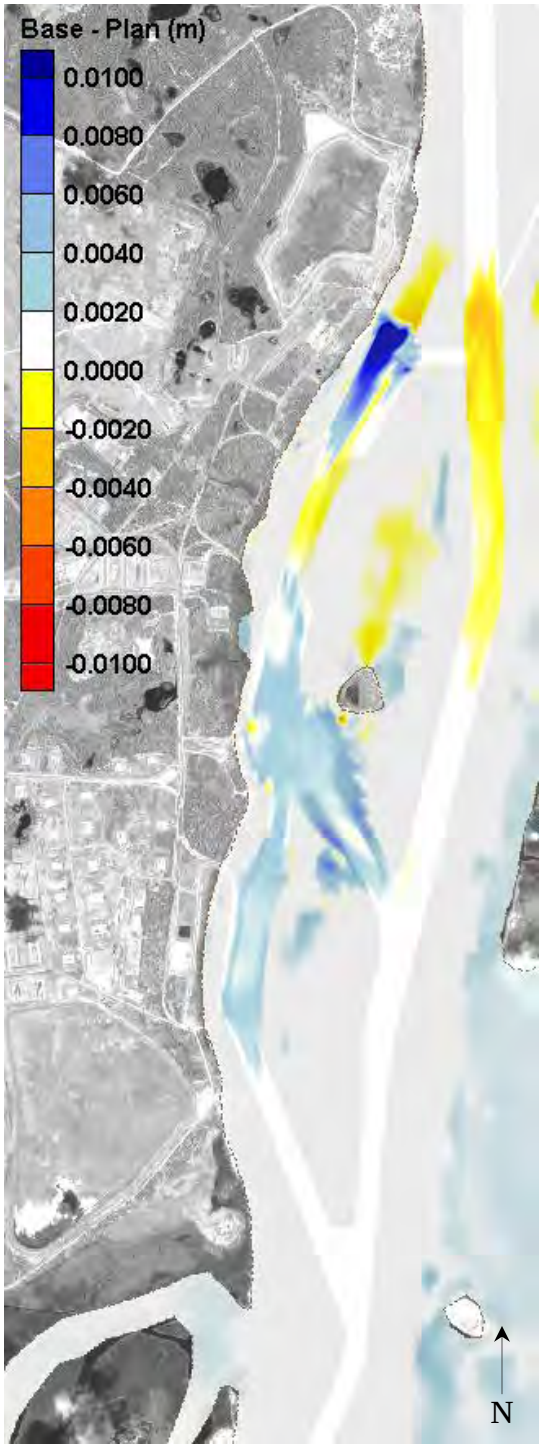

Figure 6-77. Change in shoaling from Base for Plan 1b; positive (blue) means plan generates less shoaling while negative (red) means plan generates more shoaling.

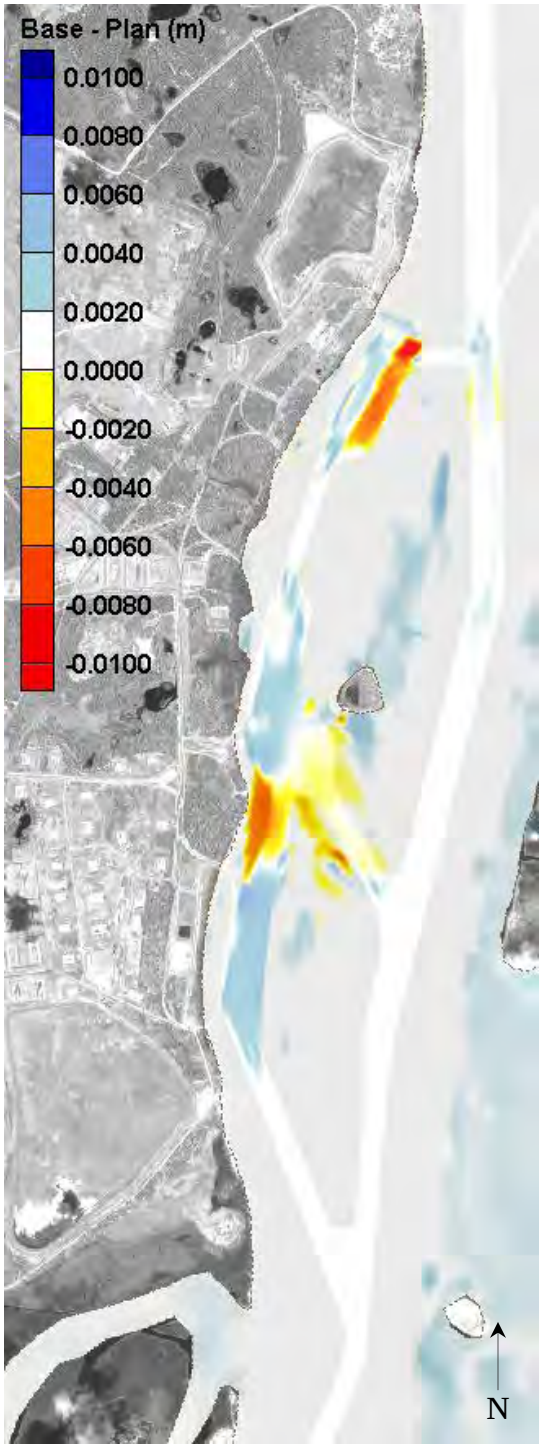

Figure 6-78. Change in shoaling from Base for Plan 2; positive (blue) means plan generates less shoaling while negative (red) means plan generates more shoaling.

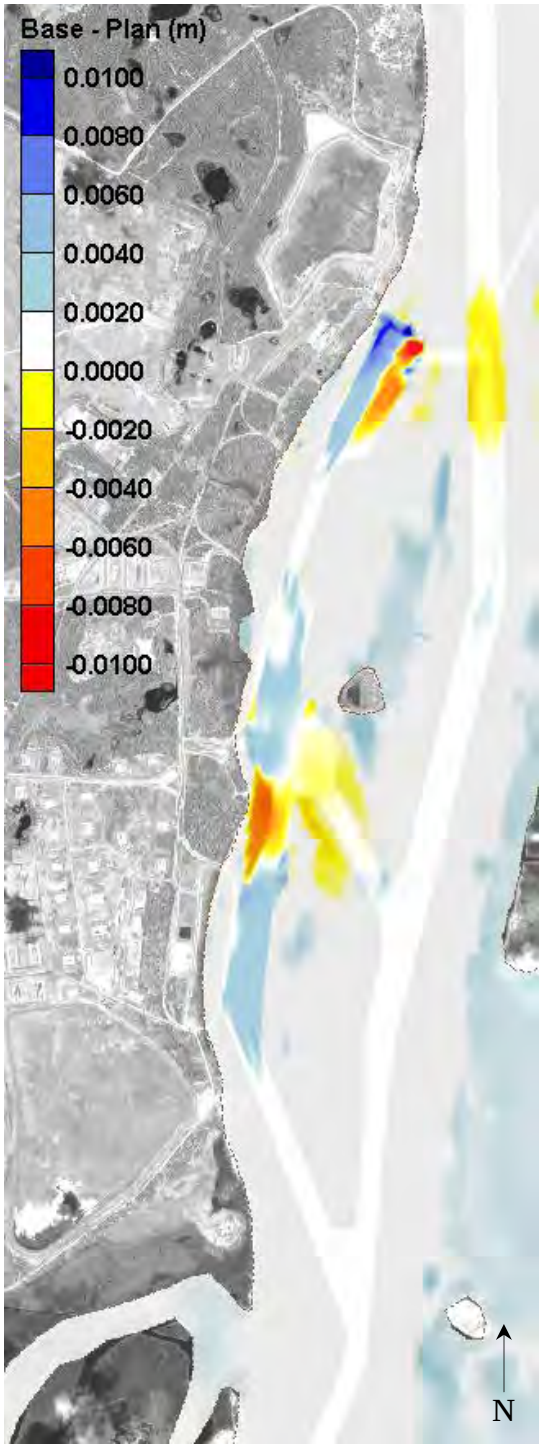

Figure 6-79. Change in shoaling from Base for Plan 3; positive (blue) means plan generates less shoaling while negative (red) means plan generates more shoaling.

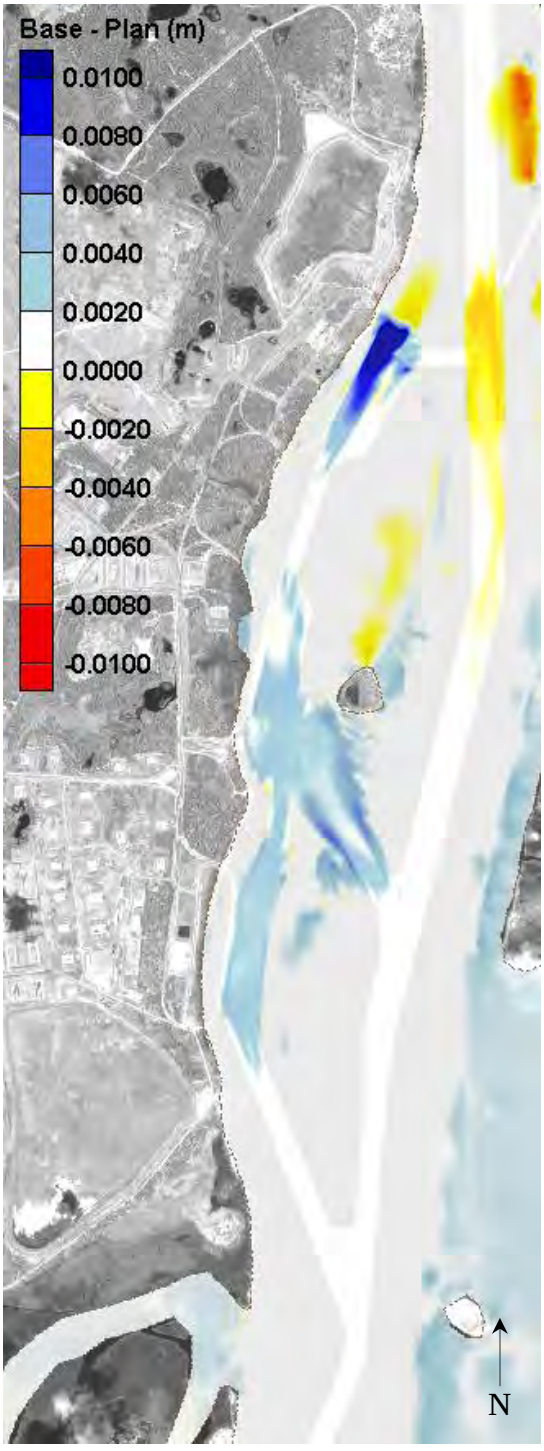

Figure 6-80. Change in shoaling from Base for Plan 4; positive (blue) means plan generates less shoaling while negative (red) means plan generates more shoaling.

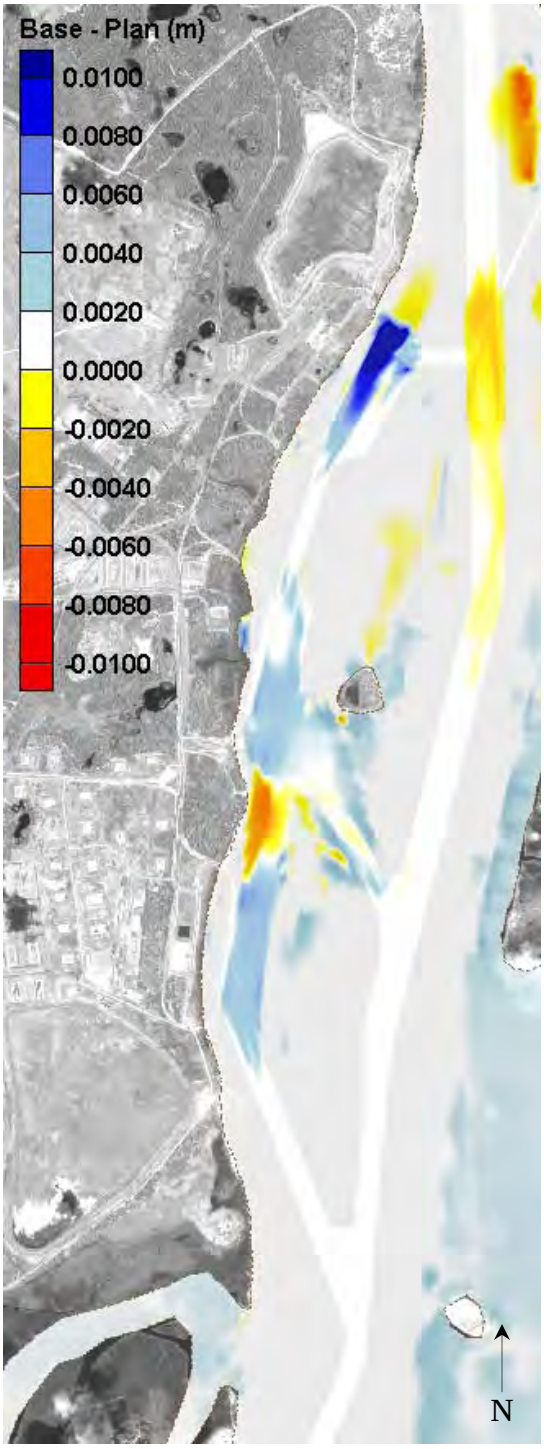

Figure 6-81. Change in shoaling from Base for Plan 5; positive (blue) means plan generates less shoaling while negative (red) means plan generates more shoaling.

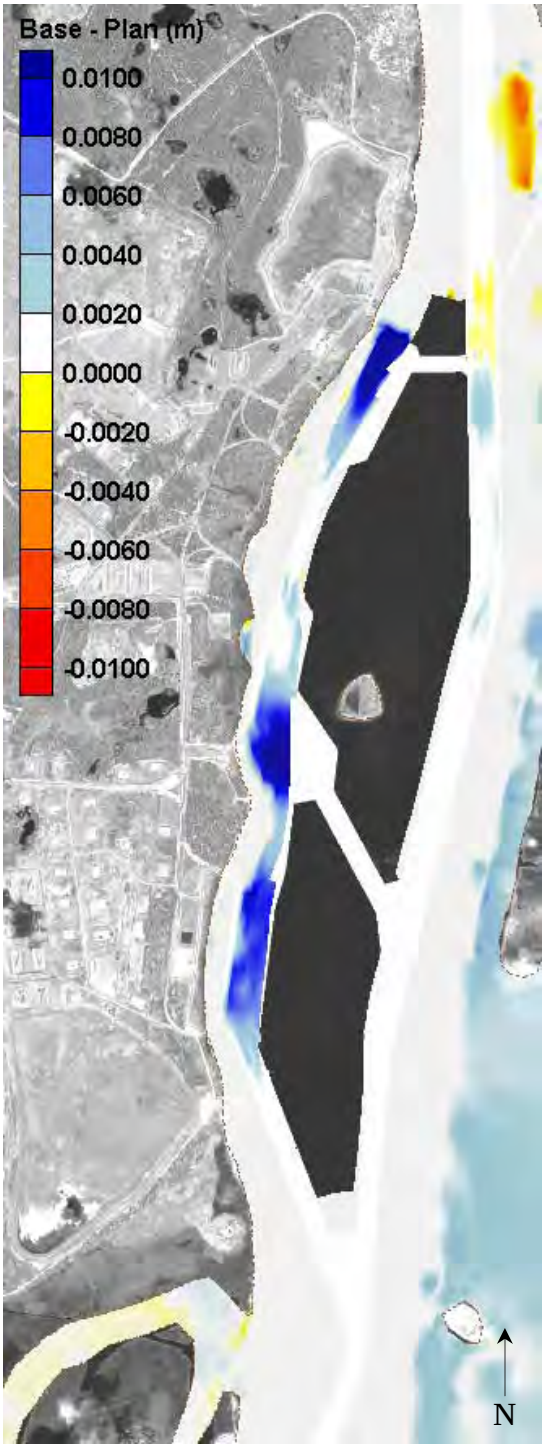

Figure 6-82. Change in shoaling from Base for Plan 6; positive (blue) means plan generates less shoaling, negative (red) means plan generates more shoaling, blacked out area indicates location of the island.

As a means to place a value on the change in shoaling due to the plan alternatives as compared to the Base, a normalized difference computation was determined. This calculation takes the form of:

$$\Delta shoaling = \frac{Base_{shoal} - Plan_{shoal}}{Base_{shoal}}$$

The MOTSU and navigation channels were broken into 19 sub-domains such that these computations could be performed on each area. The breakdown of the analysis regions is shown in Figure 6-83. Figure 6-84 shows the results of this computation for each region, and the values are provided in Table 6-1. Values that are positive indicate that the Base condition produced more shoaling than the plan alternative and, therefore, that the plan alternative is a beneficial change. Negative values indicate that the Base produced less shoaling than the plan alternative and therefore the plan alternative returns negative results. The shoaling comparisons are categorized into *worse* (values less than -0.5), *indiscernible* (values greater than or equal to -0.5 and less than 0.1), *better* (values greater than or equal to 0.1 and less than 1), and *much better* (values greater than or equal to 1.0). These results support the findings presented for the previous velocity and sediment analysis.

Plan 6 provides the best overall results, but there are locations where other plans provide more benefit, such as in the northern sections of the center wharf. Based on these figures, the increase in the depth and width of the northern wharf with the new northern alignment and without the northern turning basin, as in Plan 1b, causes deposition in the MOTSU channel between the northern and center wharfs, whereas all of the other plans generate some erosion. Of the plans evaluated, only Plan 2 and 6 result in less shoaling in the navigation channel than the Base condition. However, Plan 2 generates some measurable increases in shoaling at the northern wharf.

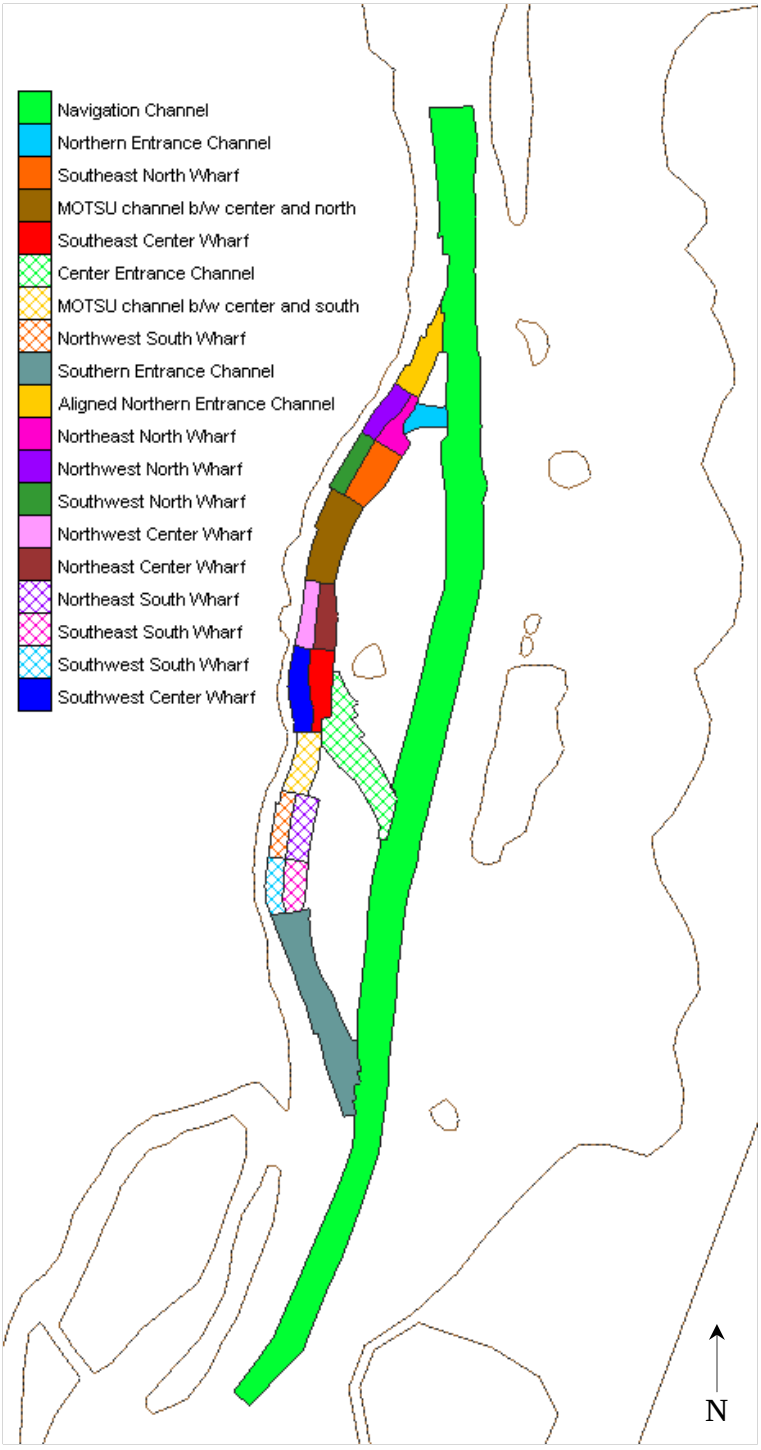

Figure 6-83. Shoaling change analysis regions.

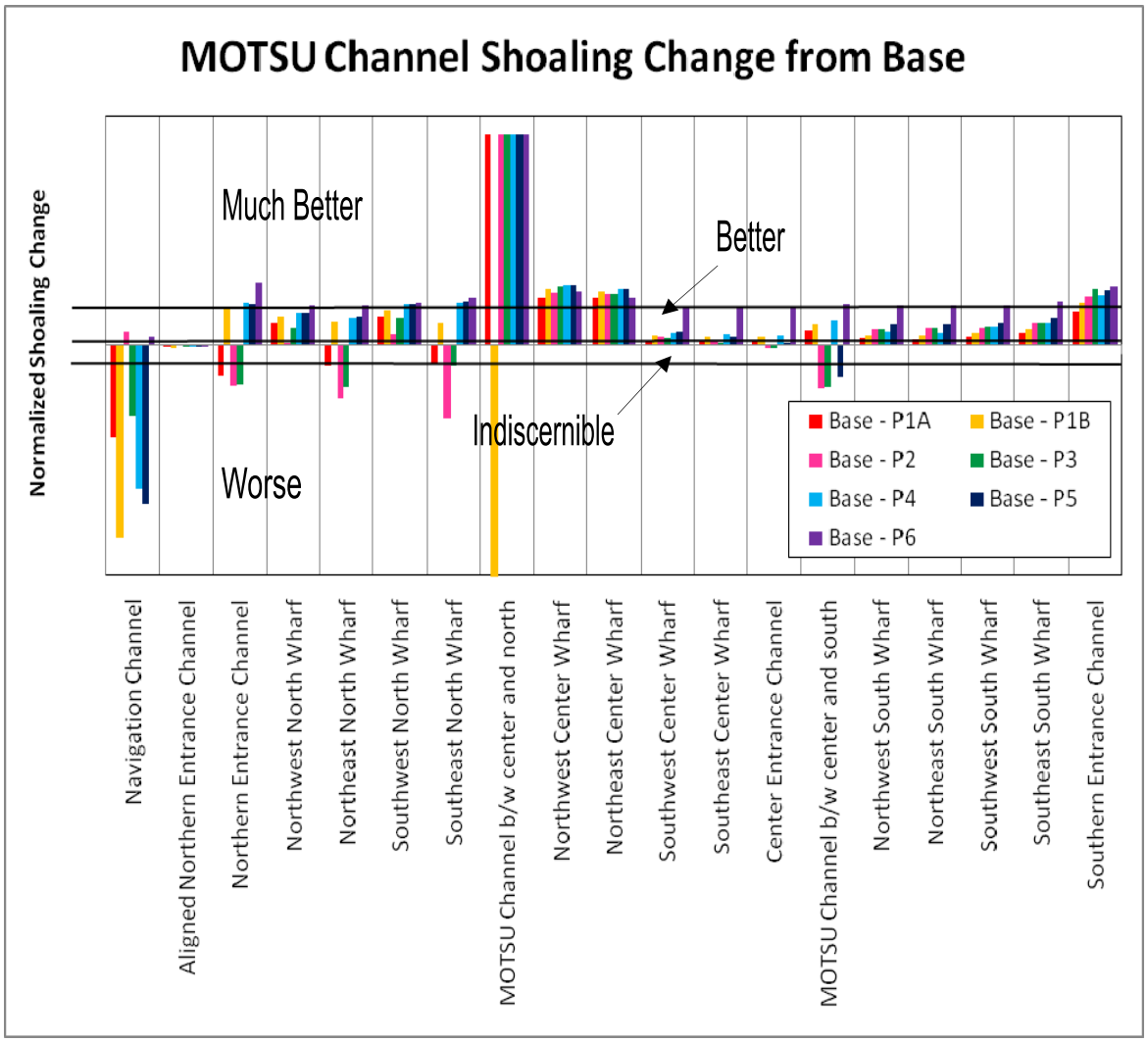

Figure 6-84. Shoaling change comparison for each plan as compared to the Base.

Table 6-1. Normalized shoaling change comparison values for each plan as compared to the Base.

Area	BASE	Base - P1A	Base - P1B	Base - P2	Base - P3	Base - P4	Base - P5	Base - P6
Navigation Channel	162.75	-2.41	-5.04	0.37	-1.86	-3.74	-4.15	0.24
Aligned Northern Entrance Channel	-1967.25	-0.02	-0.06	0.00	0.00	-0.03	-0.03	0.00
Northern Entrance Channel	12.72	-0.78	0.94	-1.06	-1.03	1.10	1.07	1.64
Northwest North Wharf	582.17	0.57	0.75	0.05	0.45	0.84	0.86	1.06
Northeast North Wharf	170.60	-0.53	0.62	-1.39	-1.09	0.71	0.74	1.04
Southwest North Wharf	162.33	0.75	0.91	0.28	0.71	1.07	1.08	1.12
Southeast North Wharf	109.61	-0.45	0.60	-1.92	-0.52	1.12	1.15	1.25
MOTSU Channel b/w center and	3.13	5.51	-34.74	5.51	5.51	5.51	5.51	5.51
Northwest Center Wharf	25.45	1.26	1.48	1.39	1.56	1.59	1.56	1.42
Northeast Center Wharf	50.90	1.23	1.43	1.34	1.33	1.49	1.48	1.24
Southwest Center Wharf	731.62	0.13	0.25	0.21	0.21	0.33	0.35	0.98
Southeast Center Wharf	799.19	0.14	0.24	0.09	0.07	0.29	0.22	0.98
Center Entrance Channel	2163.12	0.13	0.23	-0.07	-0.06	0.26	0.07	1.02
MOTSU Channel b/w center and	241.52	0.38	0.55	-1.12	-1.09	0.66	-0.82	1.08
Northwest South Wharf	289.76	0.20	0.26	0.43	0.42	0.36	0.54	1.05
Northeast South Wharf	407.34	0.17	0.25	0.44	0.45	0.33	0.55	1.05
Southwest South Wharf	219.44	0.24	0.31	0.45	0.48	0.49	0.57	1.05
Southeast South Wharf	210.28	0.31	0.41	0.58	0.58	0.57	0.73	1.14
Southern Entrance Channel	28.03	0.89	1.10	1.27	1.47	1.32	1.44	1.53

- = increase in shoaling from Base;+ = decrease in shoaling from Base.

A facility-wide shoaling comparison was also performed to provide a quick look at how each plan improves shoaling when compared to the Base conditions. Figure 6-85 shows the delineation of the MOTSU area and the navigation channel for this analysis. Table 6-2 provides the percentage increase in shoaling as compared to the Base condition such that positive values indicate an increase in shoaling and negative values indicate a decrease in shoaling. The same overall trends are indicated in this analysis as in the previous shoaling change comparisons. Plans 2 and 6 are the only plans that do not generate an increase in shoaling in the navigation chan-

nel. Plan 6 shows a large improvement in shoaling for both the navigation channel and the MOTSU facility.

Figure 6-85. Facility shoaling change map (MOTSU is yellow, navigation channel is green).

Table 6-2. Total facility shoaling change percentage from Base.

	% increase in Shoaling from Base	
	MOTSU	**Navigation**
Plan1A	-21.56	4.55
Plan1B	-30.43	35.26
Plan2	0.13	-16.23
Plan3	-7.21	7.62
Plan4	-39.24	53.26
Plan5	-29.33	66.04
Plan6	-98.11	-47.87

7 Channel Access Restriction Alternative

7.1 Description

In addition to the main study, Wilmington District requested a modeling investigation involving restriction of access to the MOTSU area. This alternative would erect a wall along the facility's northern and eastern boundaries while maintaining access from the south to accommodate vessel traffic. The Base condition (see Figure 6-1) is used as the starting domain for this plan. The wall extends perpendicular to the flow just north of the northern wharf and then turns parallel to the flow just before reaching the navigation channel. It then extends southward to the southern entrance of the channel as shown by the red line in Figure 7-1.

Figure 7-1. MOTSU closure alternative.

All boundary conditions and model parameters for this plan are the same as used for the other plan alternatives. Likewise, a similar analysis of simulation results is provided for this plan with respect to the Base condition. The locations of all time history results are the same as those in Figure 6-9. This plan is referred to in the plots as "Wall."

7.2 Velocity analysis

Figure 7-2 through Figure 7-17 show the time history of velocity magnitude and direction for the eight points in the study area. These figures show 2 days of the six-month model simulation. Positive values are flood-directed and negative values are ebb-directed.

It is immediately obvious that the points in the MOTSU area that are closed off to through-flow have very little velocity. This includes Points 1, 2, and 3. Not only is the velocity much lower in magnitude than the Base values, but the phasing is much different as well. This area becomes a dead end where the tidal propagation is forced to slow and reflections occur, as seen by the oscillations at Point 3. Point 4 is located to the south of the MOTSU area, so there is more flow here but it is lower than in the Base condition, and the phasing is shifted as well. Points 5 through 8 are back in phase since all are located outside of the structure surrounding MOTSU. Point 5 has lower velocity magnitudes due to the slowing that will occur as the water approaches the blockage just to its south. The velocities at Points 6 and 8 are similar to the Base condition due to their locations upstream and downstream from the modified area. However, Point 7 lies along the wall and shows the plan producing higher velocity magnitudes than the Base due to the flow being streamlined in the navigation channel.

Figure 7-18 through Figure 7-25 show the maximum and average flood and ebb velocity values at each location during the six-month simulation. These results support the findings discussed previously. Closing off the MOTSU area to all through-flow forces the velocities in the area to drop significantly. The residual currents for the Base condition, as shown in Figure 6-34 and Figure 6-35, indicate that material settling to the bed will be pushed upstream, into the MOTSU area, and then settle out at a greater rate due to the drop in velocity magnitude once within the confines of MOTSU and the proposed wall.

Figure 7-26 through Figure 7-33 show the percent exceedance curves for the Base and Wall plans at the eight analysis locations for the bottom ve-

locity magnitude. These figures indicate the percentage of time during the simulation that a velocity magnitude is experienced at each location. Values with a percentage near zero are the maximum velocity values for that plan. The minimum value, zero, is the 100% exceedance value since all velocities are greater than the minimum. As observed in the previous results, the Wall condition causes the velocity magnitude to drop compared to the Base condition. Thus, there is a reduction in flow through the facility, which eliminates all flushing action. This is the case at all locations except Point 7, which shows an increase due to the streamlining of flow in the navigation channel along the wall.

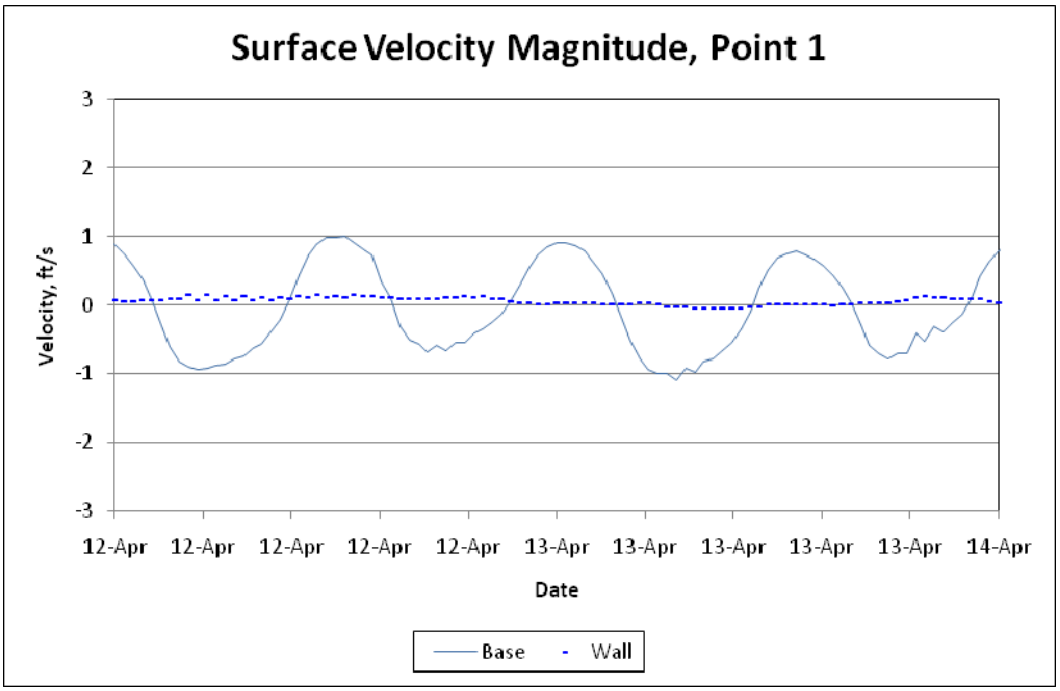

Figure 7-2. Surface velocity at Point 1.

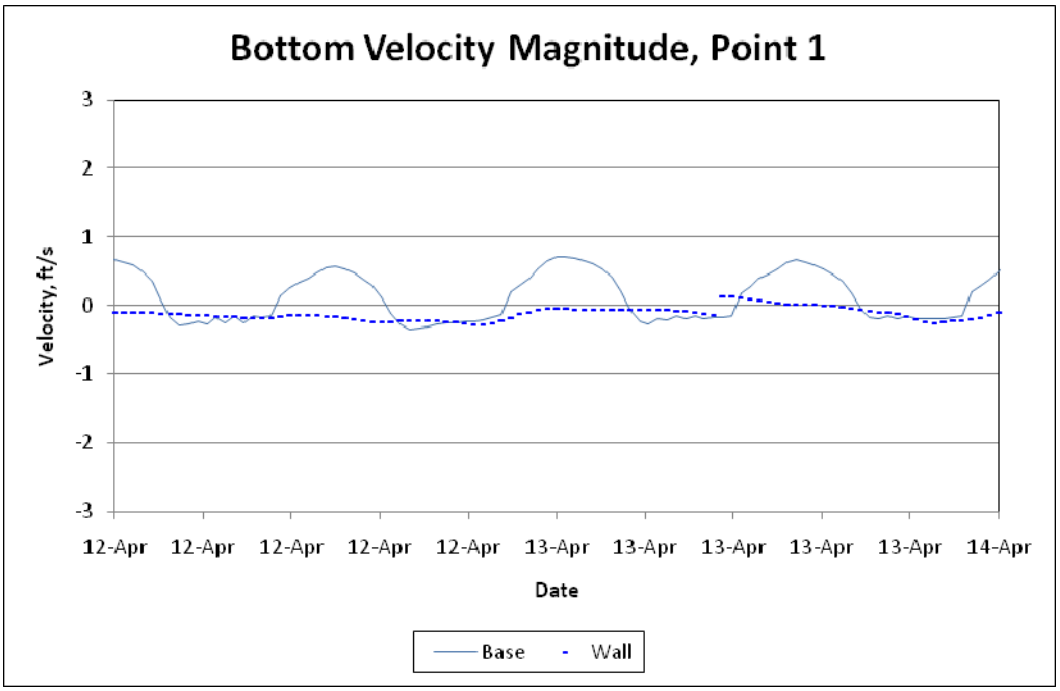

Figure 7-3. Bottom velocity at Point 1.

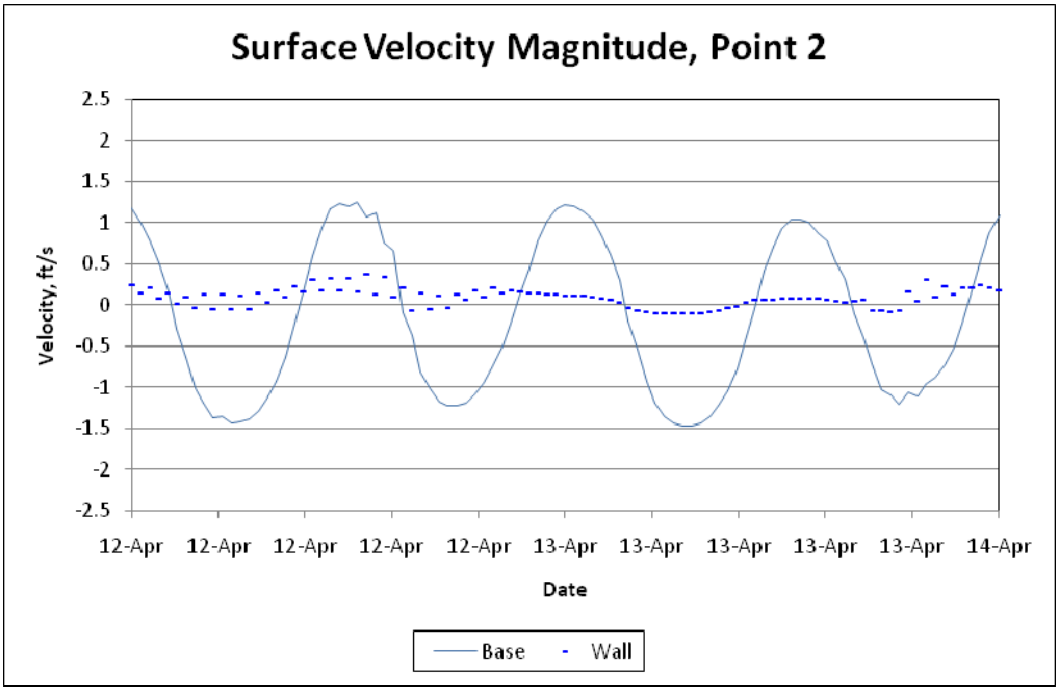

Figure 7-4. Surface velocity at Point 2.

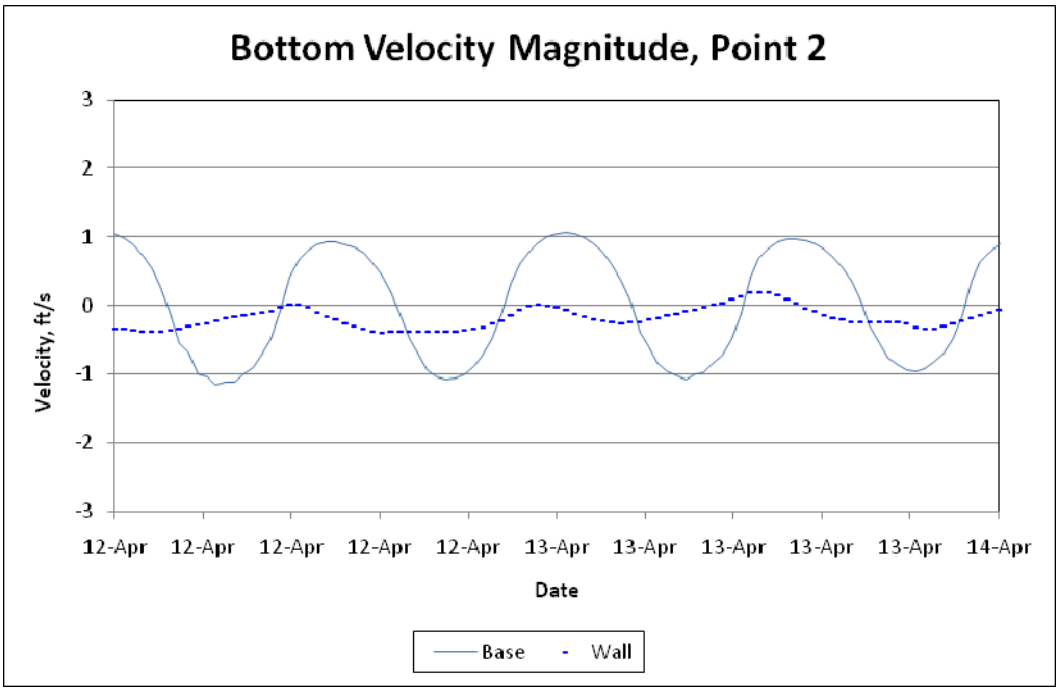

Figure 7-5. Bottom velocity at Point 2.

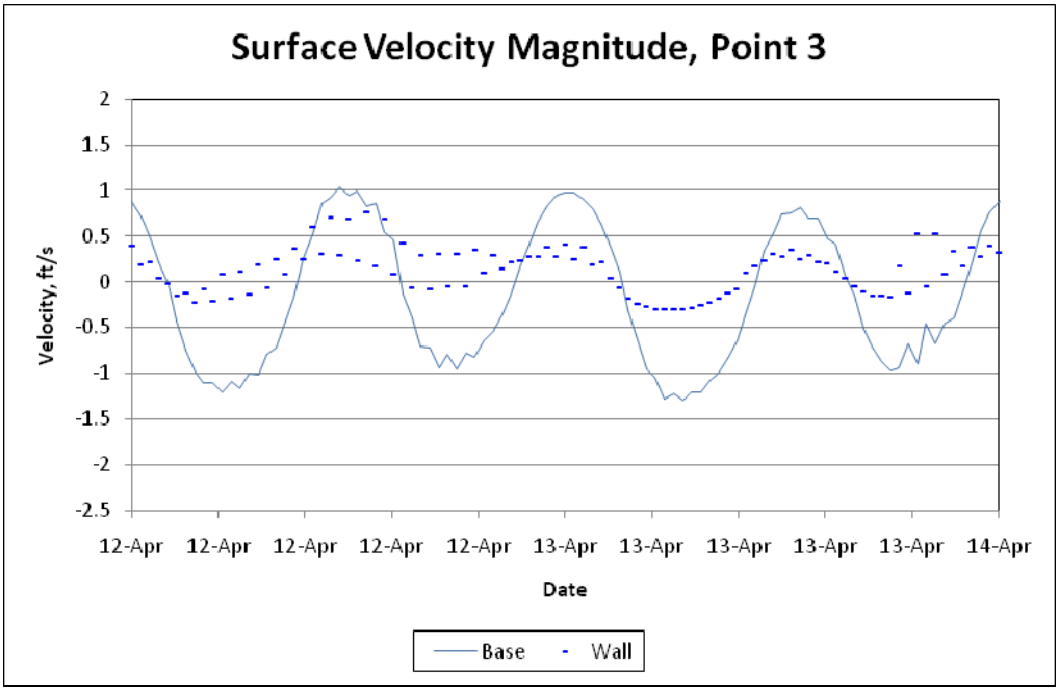

Figure 7-6. Surface velocity at Point 3.

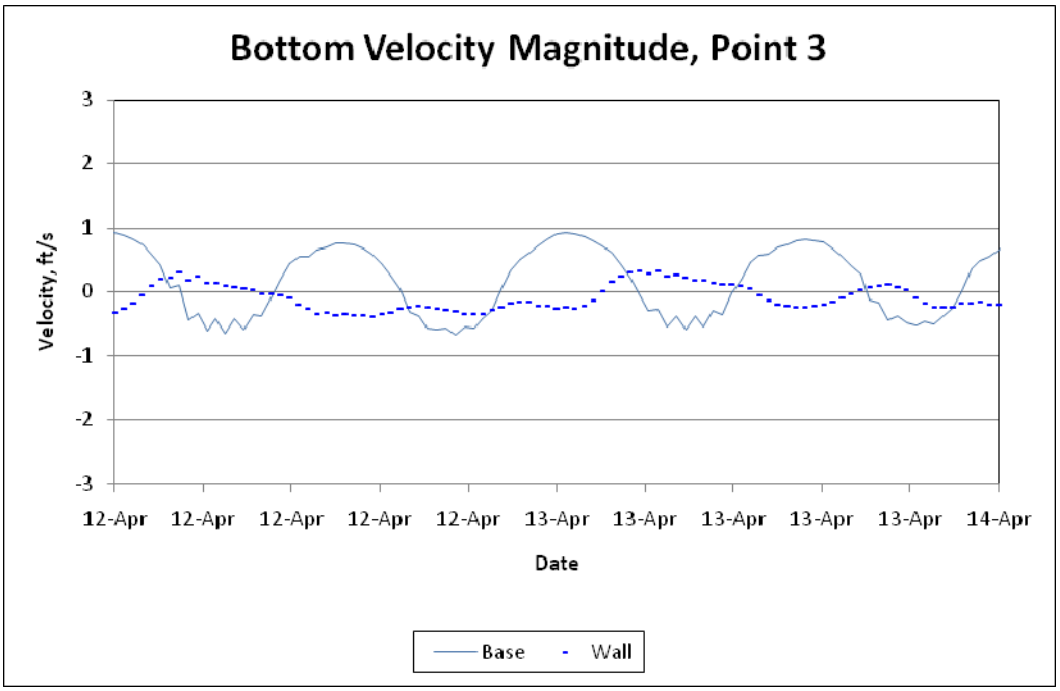

Figure 7-7. Bottom velocity at Point 3.

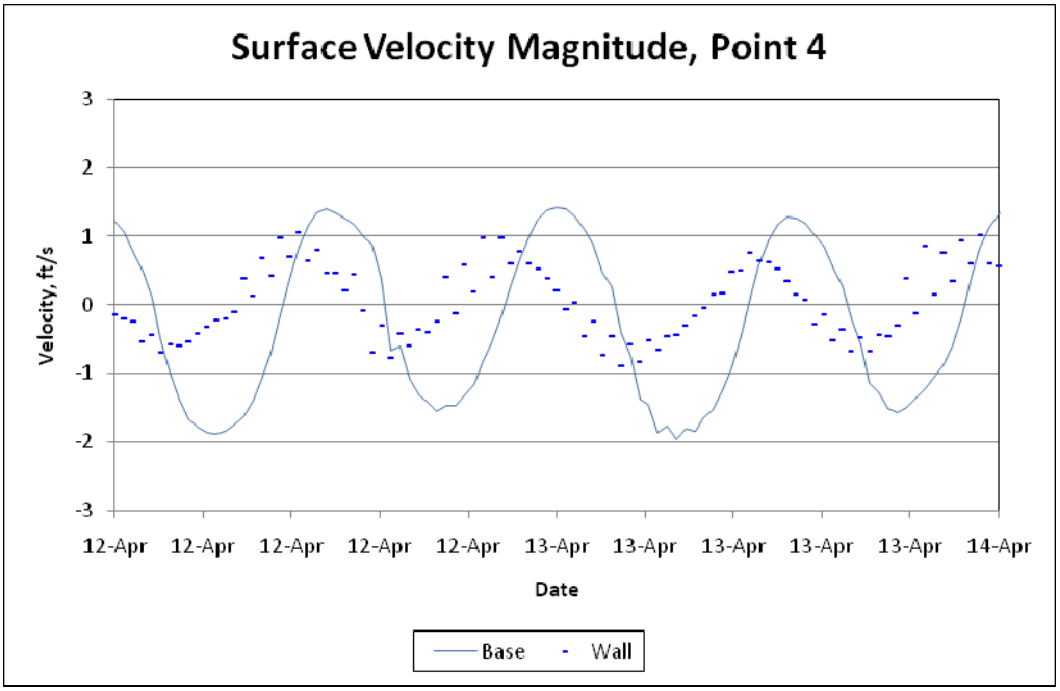

Figure 7-8. Surface velocity at Point 4.

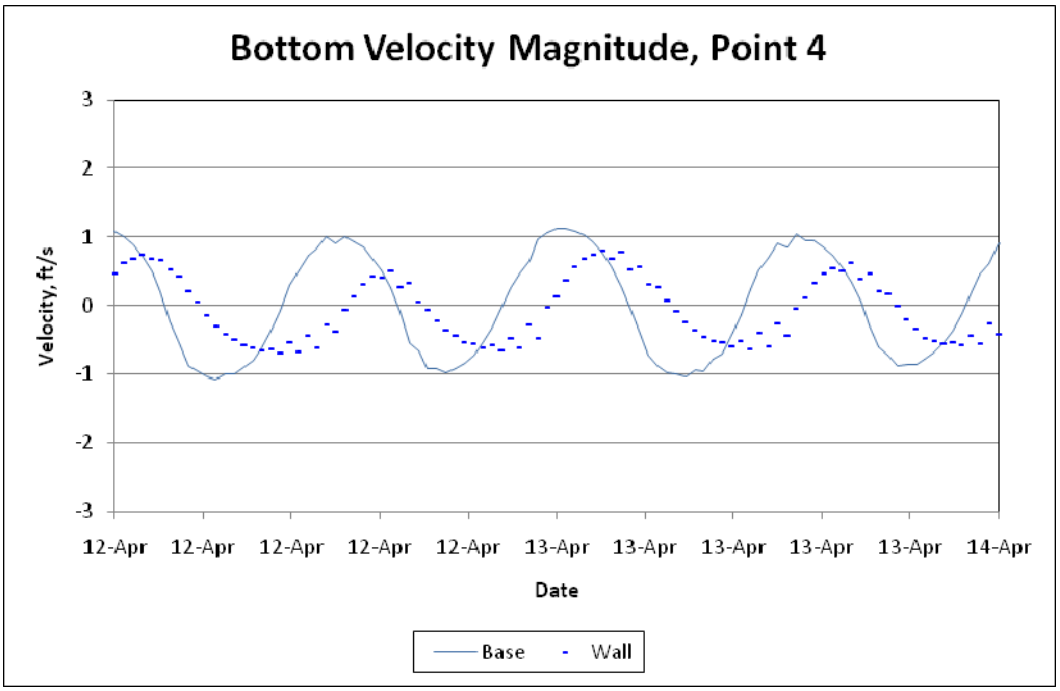

Figure 7-9. Bottom velocity at Point 4.

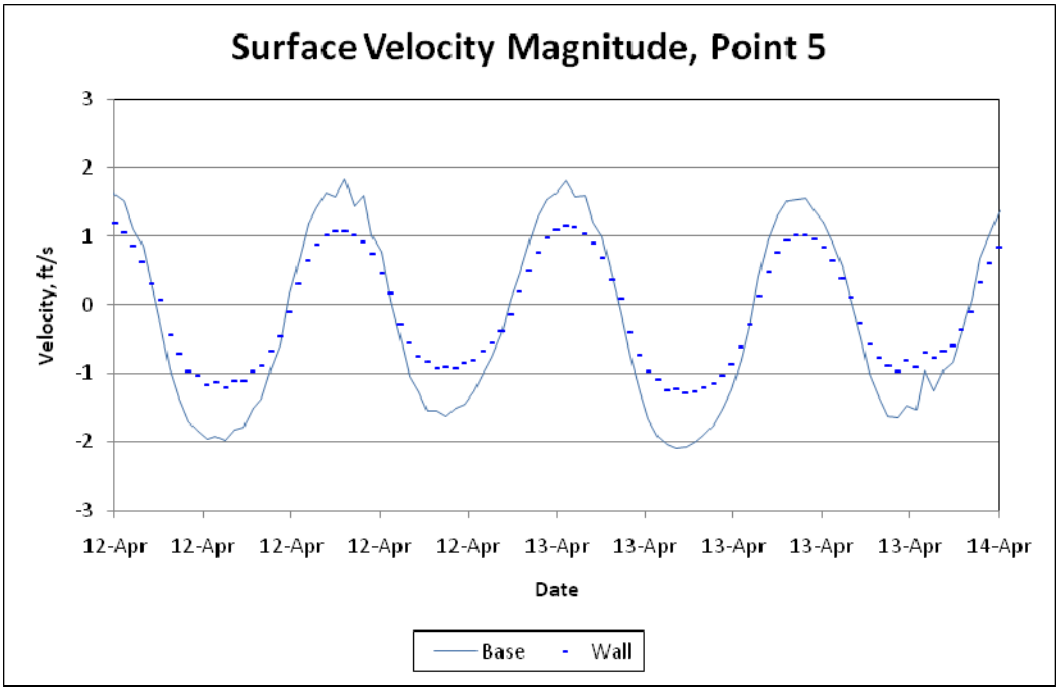

Figure 7-10. Surface velocity at Point 5.

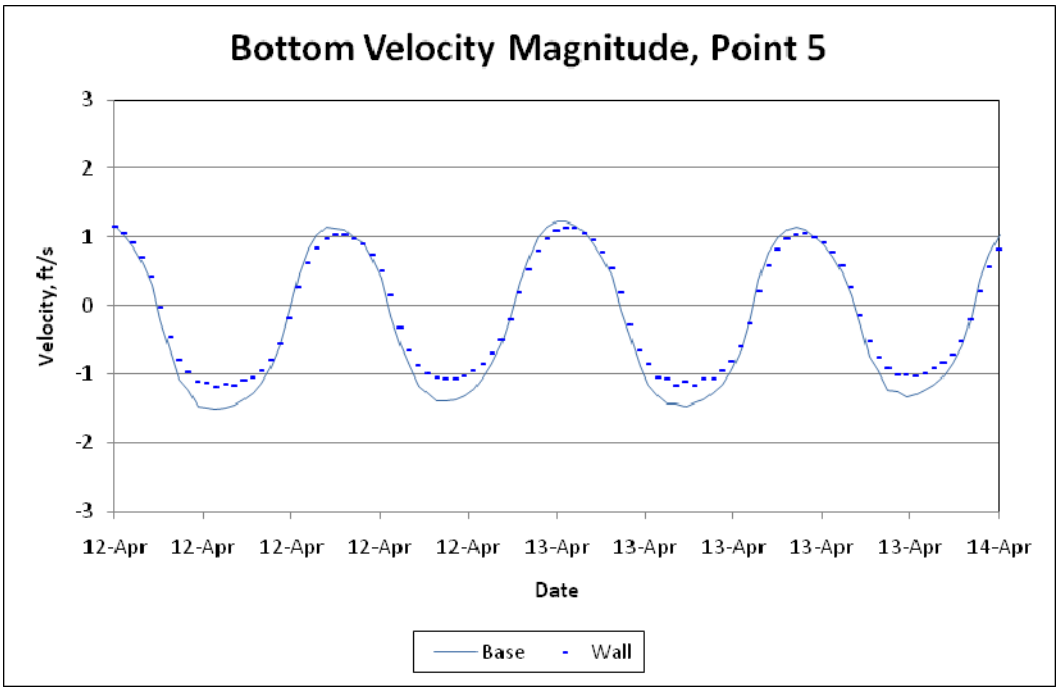

Figure 7-11. Bottom velocity at Point 5.

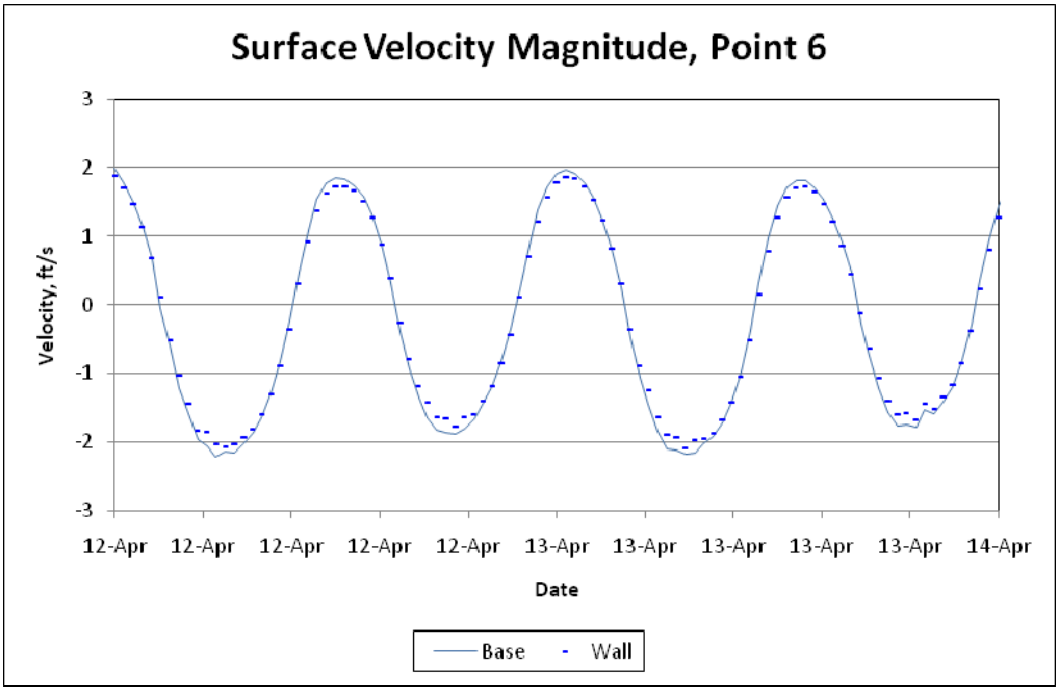

Figure 7-12. Surface velocity at Point 6.

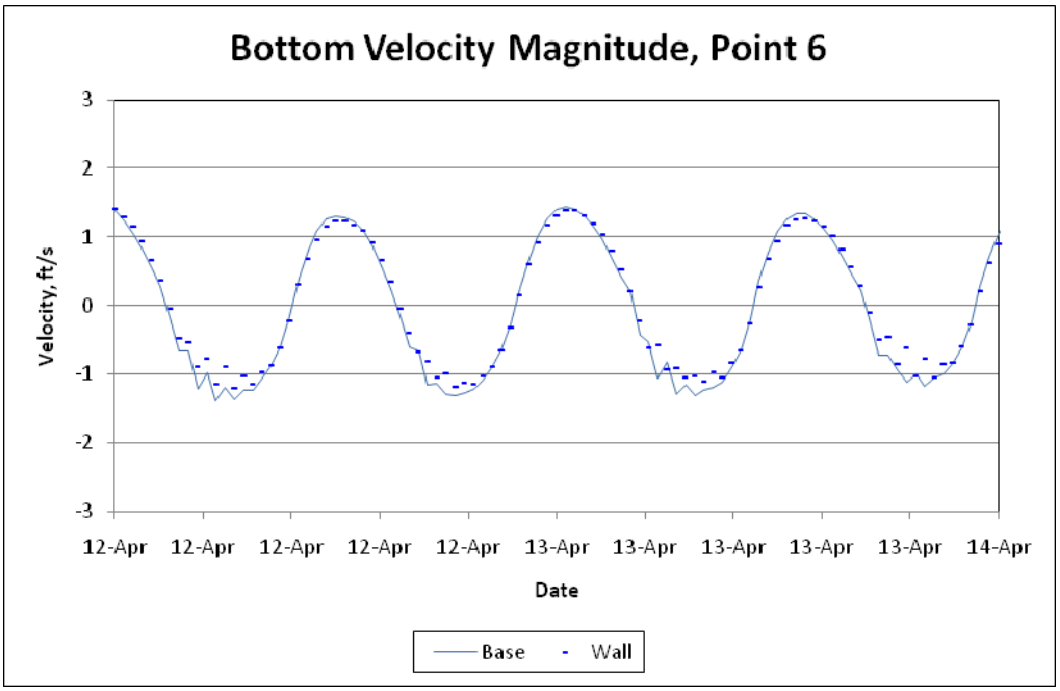

Figure 7-13. Bottom velocity at Point 6.

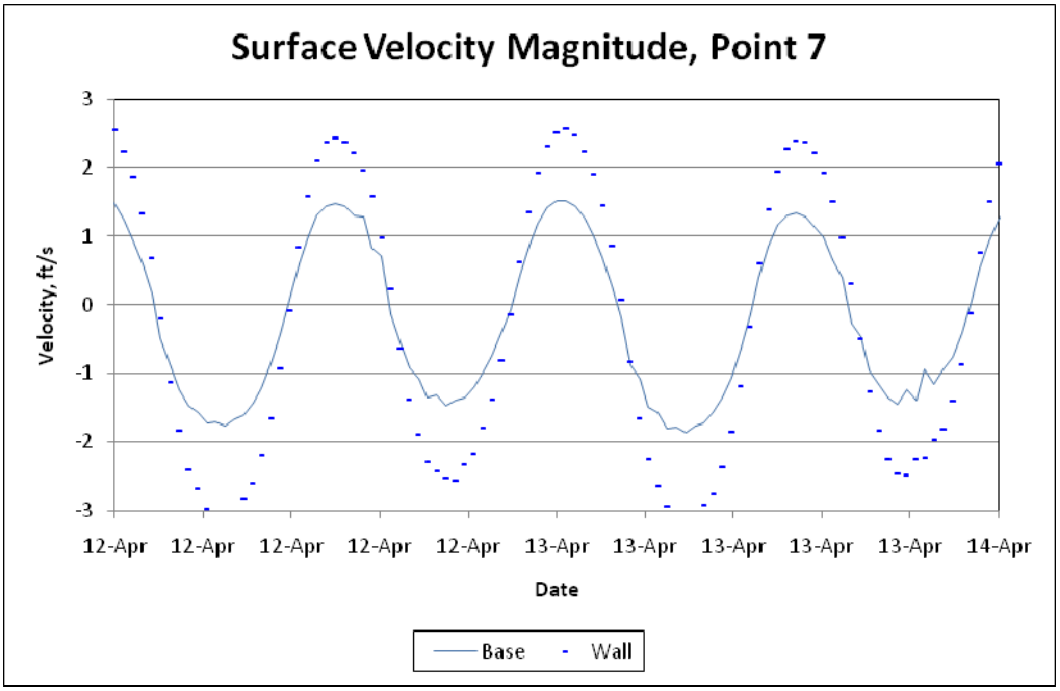

Figure 7-14. Surface velocity at Point 7.

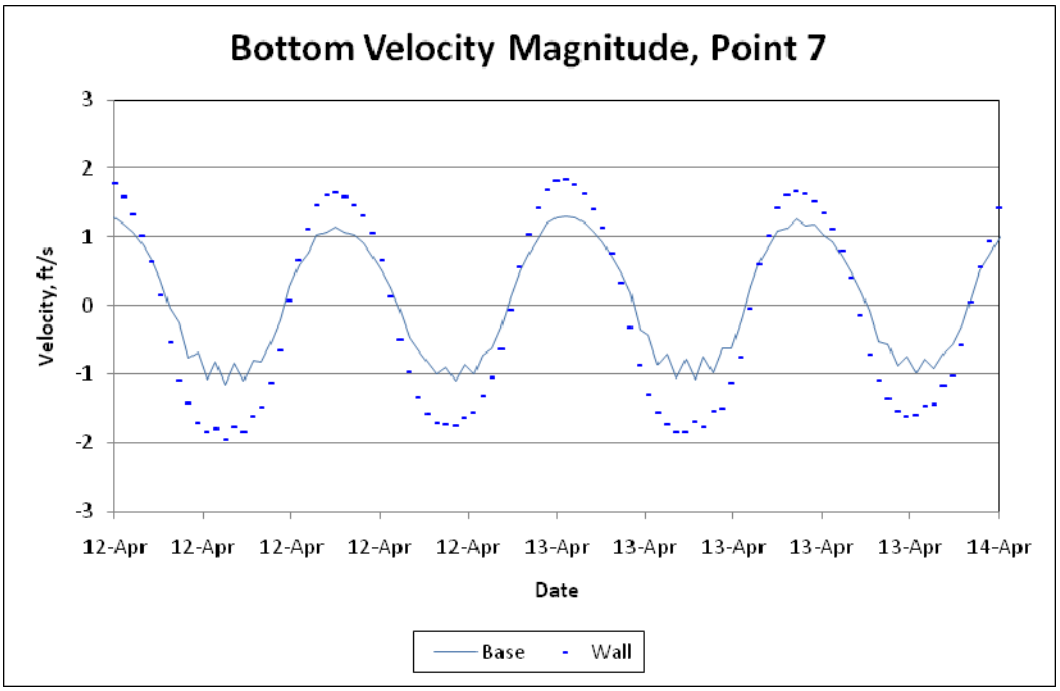

Figure 7-15. Bottom velocity at Point 7.

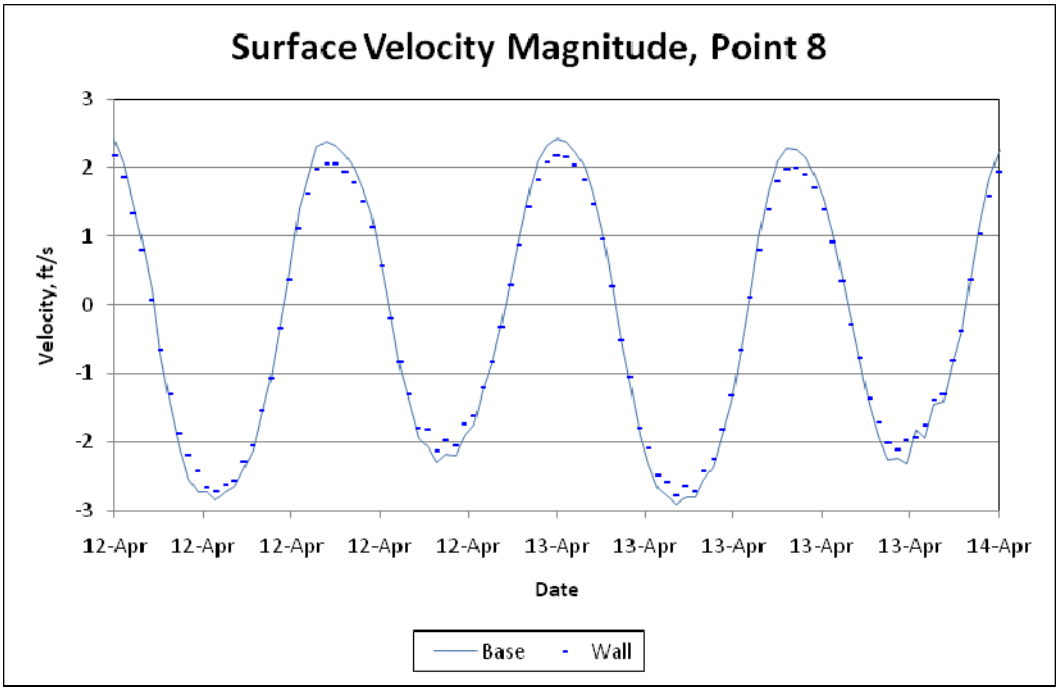

Figure 7-16. Surface velocity at Point 8.

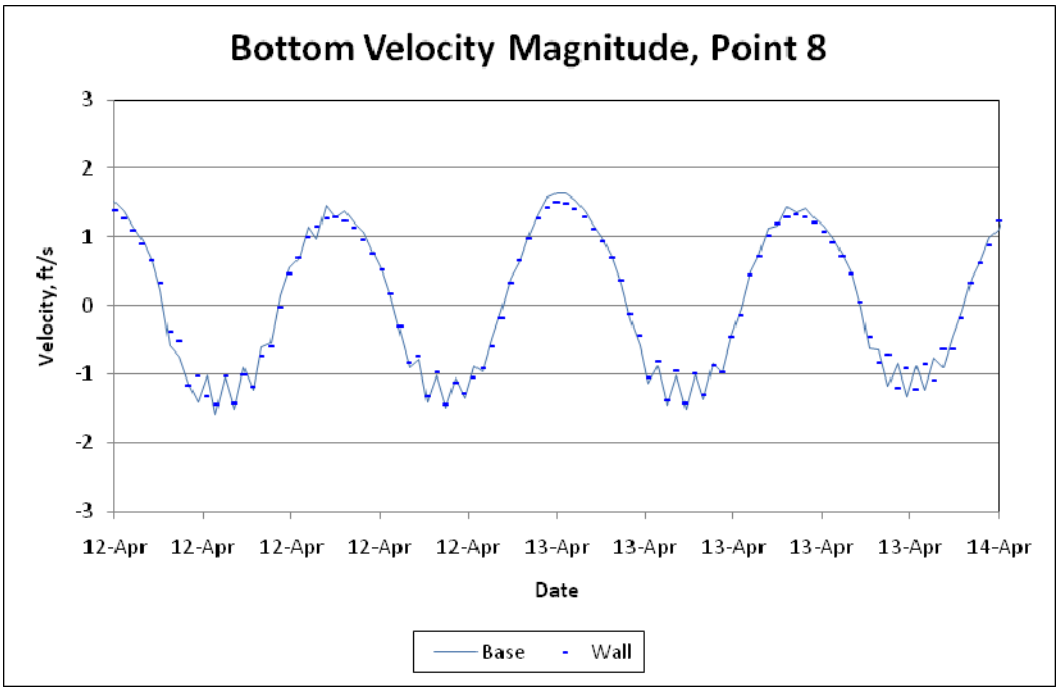

Figure 7-17. Bottom velocity at Point 8.

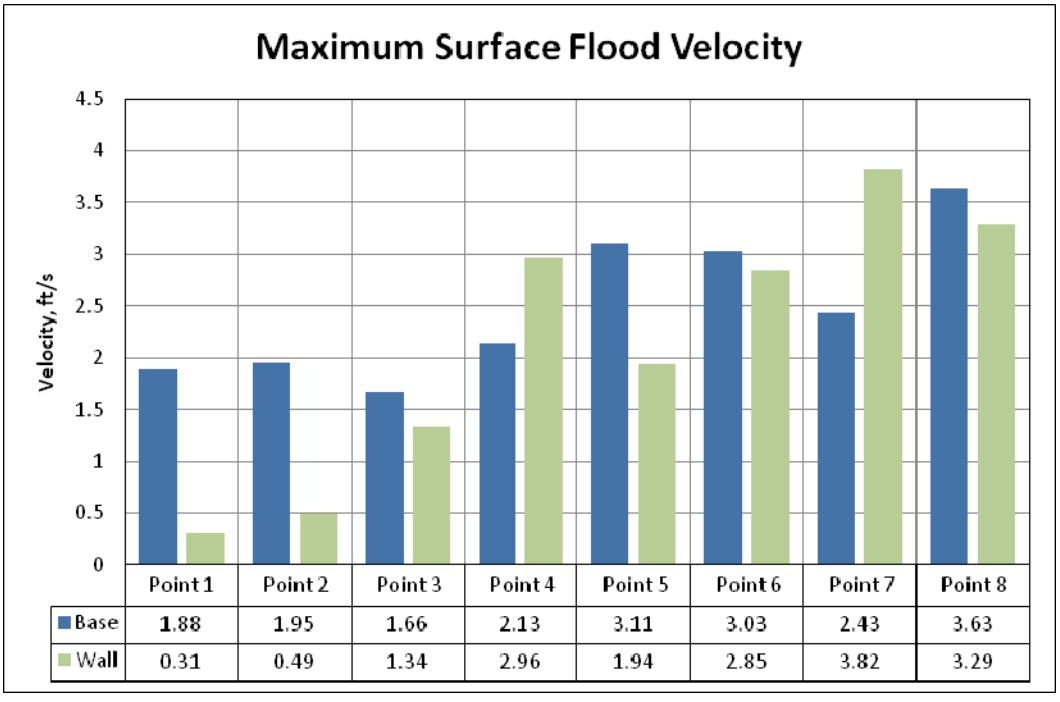

	Point 1	Point 2	Point 3	Point 4	Point 5	Point 6	Point 7	Point 8
Base	1.88	1.95	1.66	2.13	3.11	3.03	2.43	3.63
Wall	0.31	0.49	1.34	2.96	1.94	2.85	3.82	3.29

Figure 7-18. Maximum flood velocity at the surface for all locations and plans.

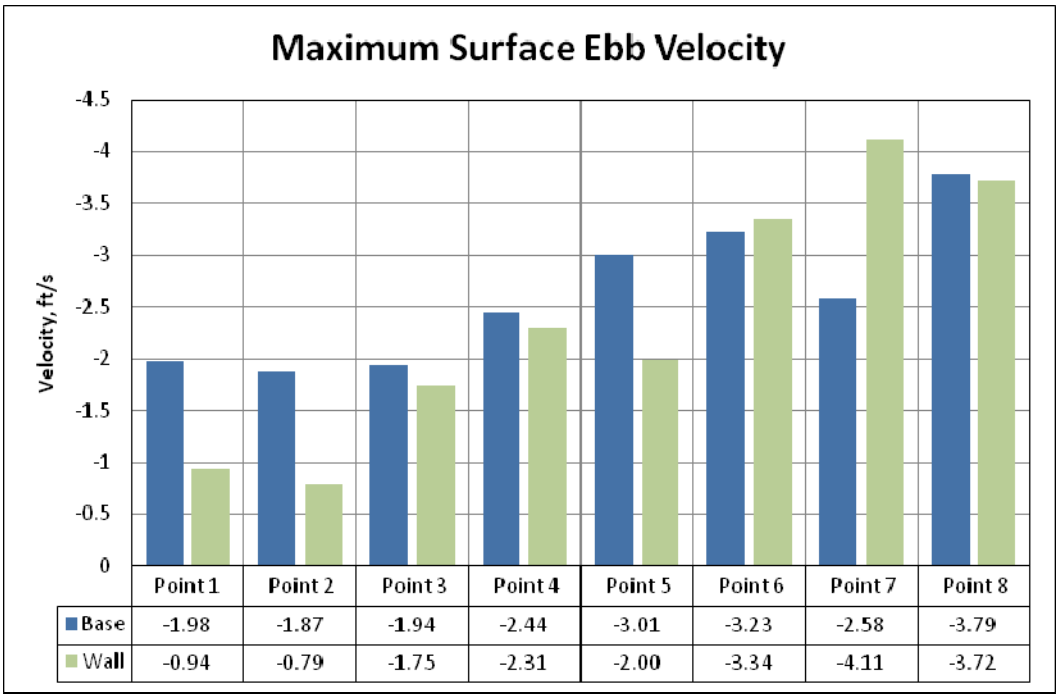

Figure 7-19. Maximum ebb velocity at the surface for all locations and plans.

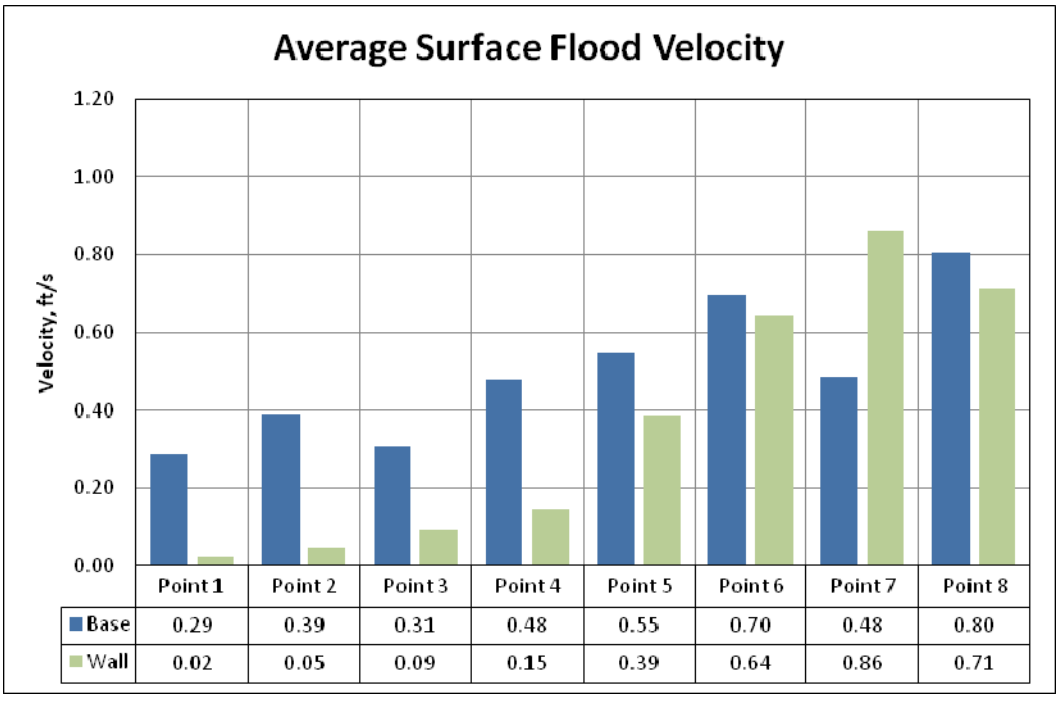

Figure 7-20. Average flood velocity at the surface for all locations and plans.

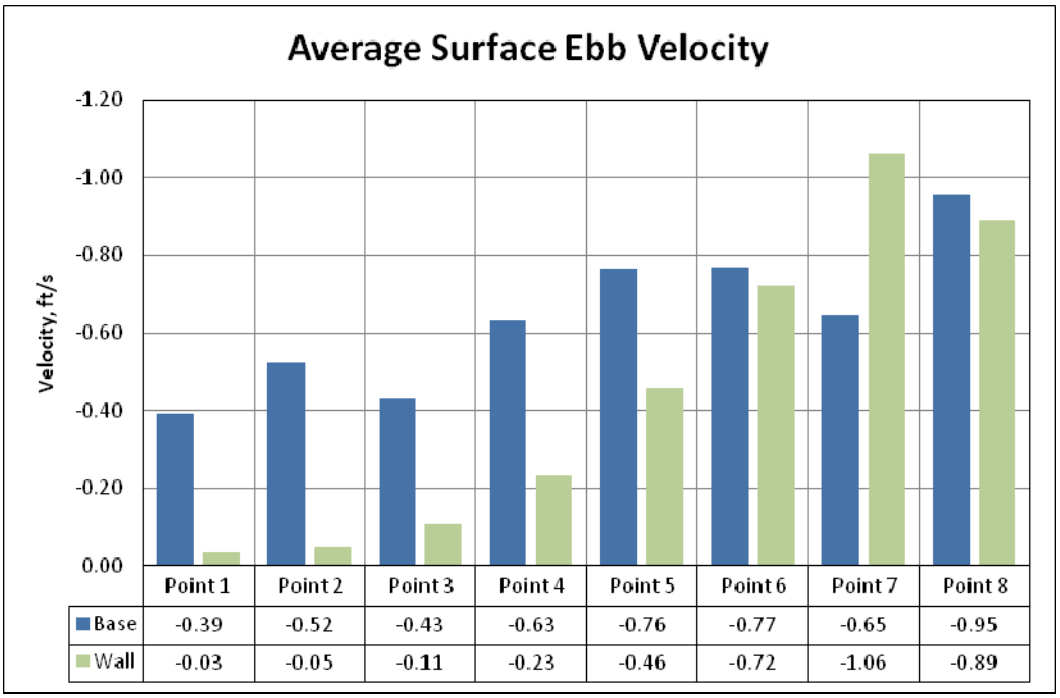

Figure 7-21. Average ebb velocity at the surface for all locations and plans.

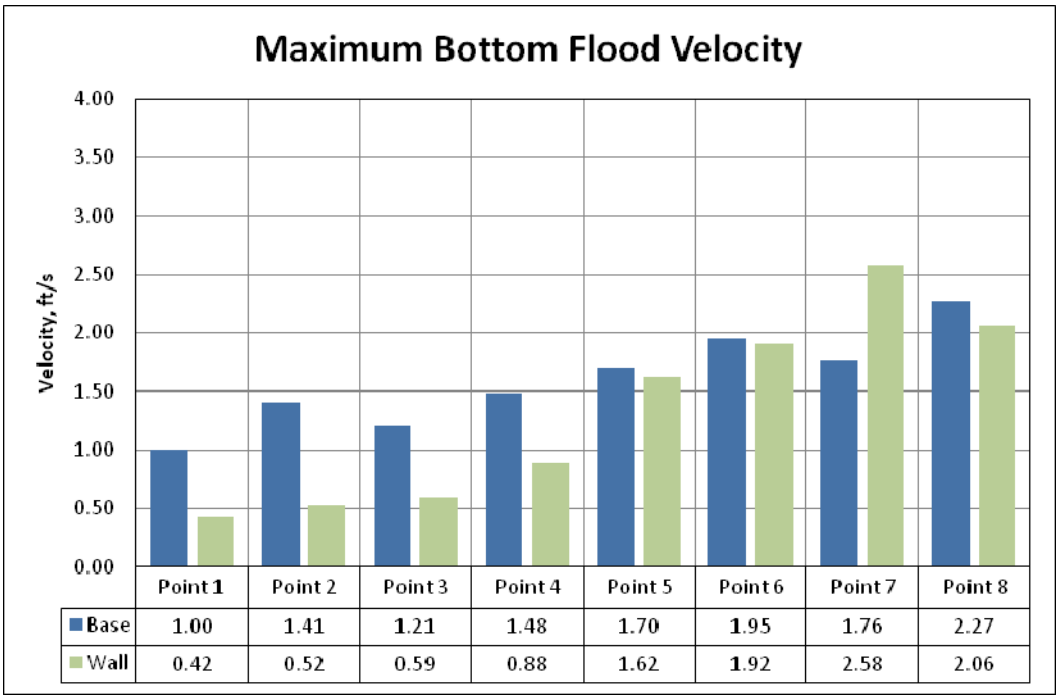

Figure 7-22. Maximum flood velocity at the bottom for all locations and plans.

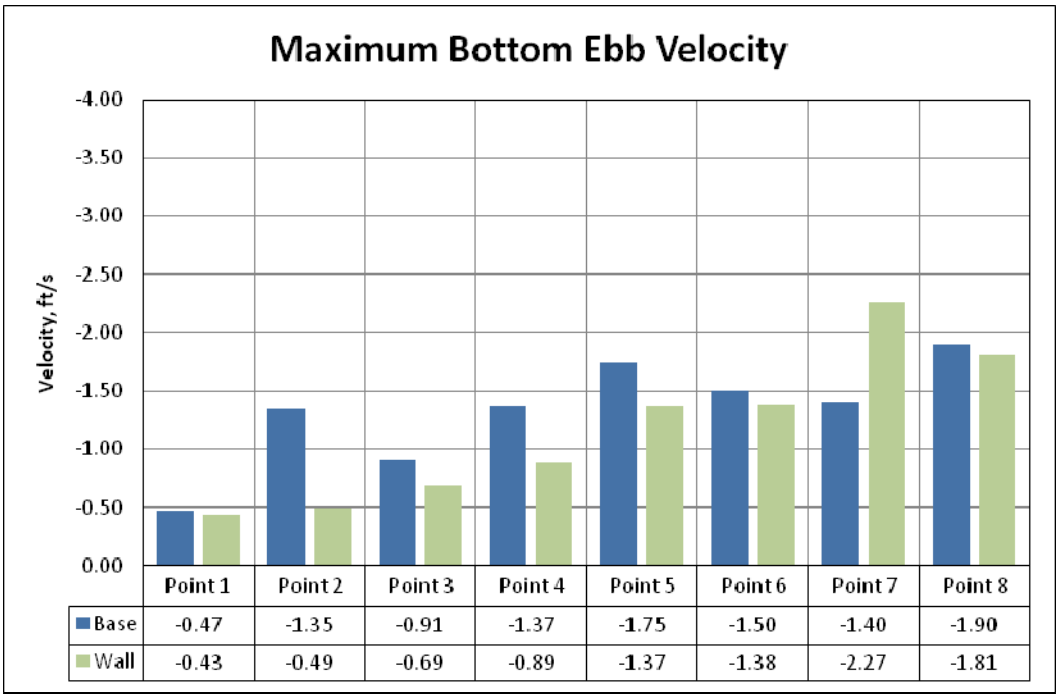

Figure 7-23. Maximum ebb velocity at the bottom for all locations and plans.

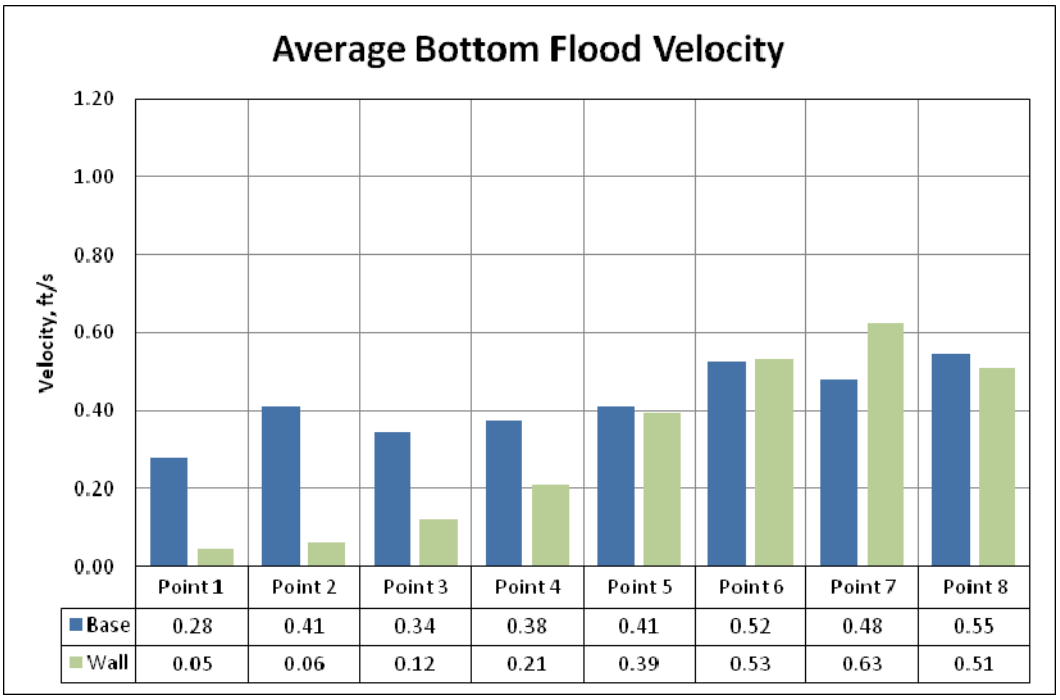

Figure 7-24. Average flood velocity at the bottom for all locations and plans.

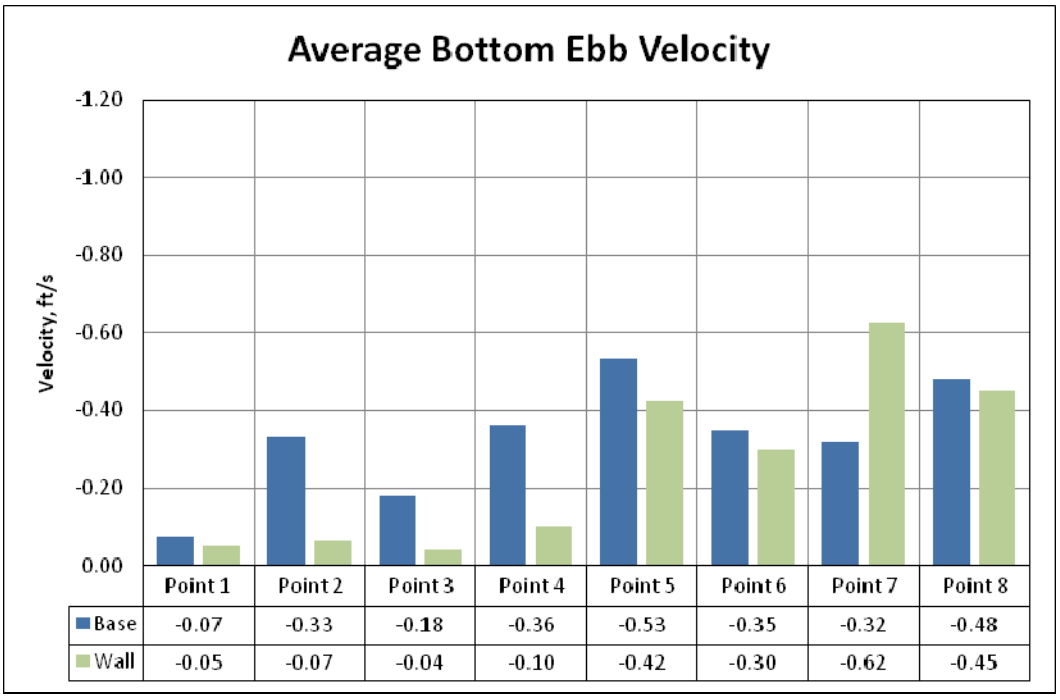

	Point 1	Point 2	Point 3	Point 4	Point 5	Point 6	Point 7	Point 8
Base	-0.07	-0.33	-0.18	-0.36	-0.53	-0.35	-0.32	-0.48
Wall	-0.05	-0.07	-0.04	-0.10	-0.42	-0.30	-0.62	-0.45

Figure 7-25. Average ebb velocity at the bottom for all locations and plans.

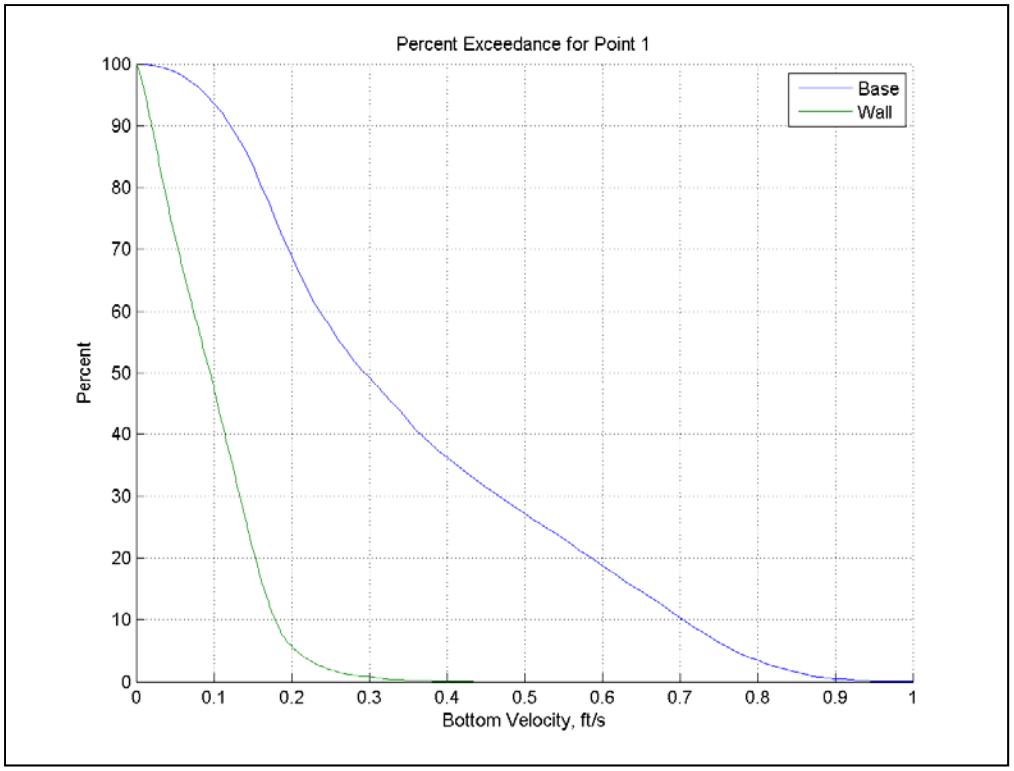

Figure 7-26. CDF curves for the Base and Wall plans at Point 1.

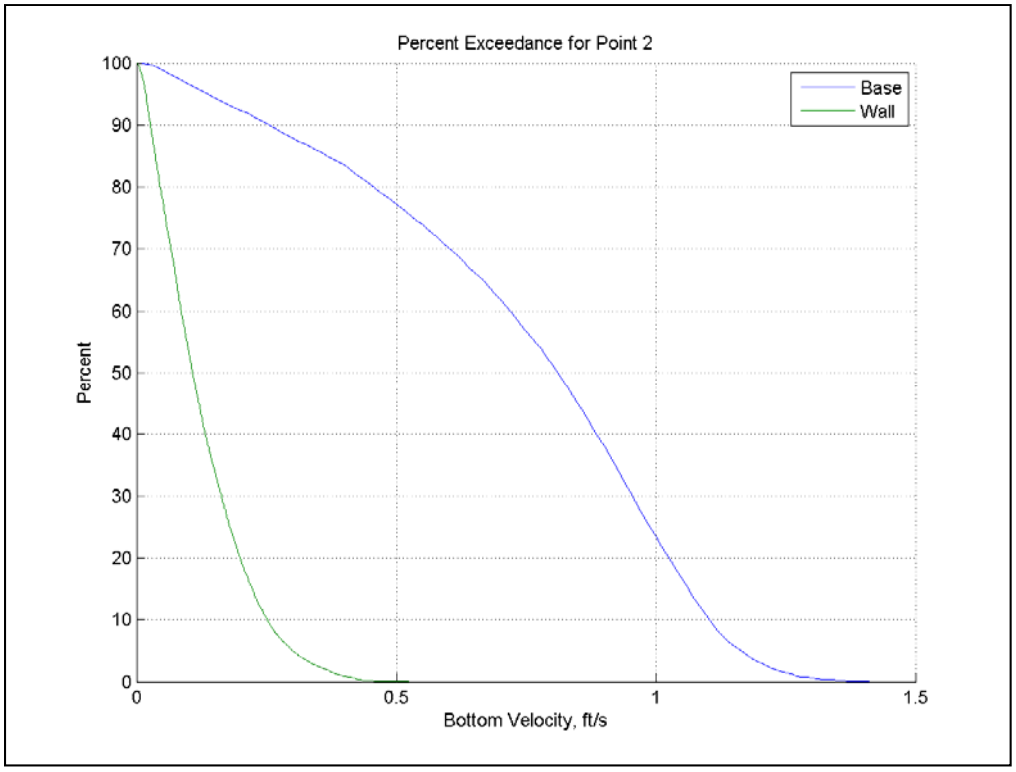

Figure 7-27. CDF curves for the Base and Wall plans at Point 2.

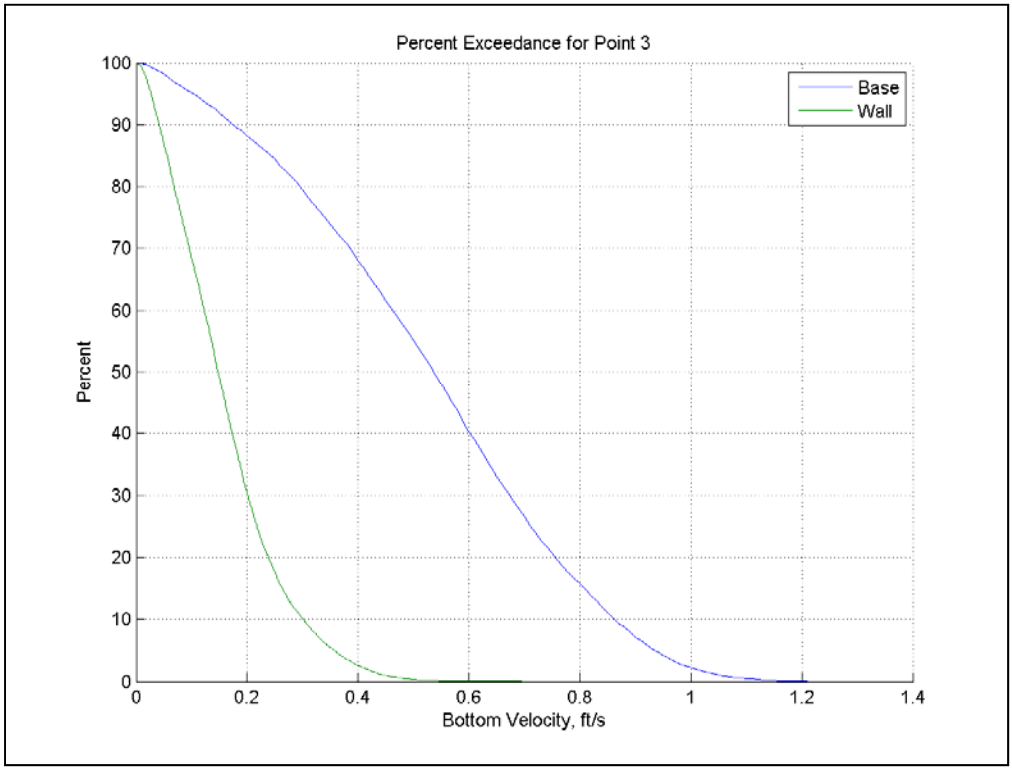

Figure 7-28. CDF curves for the Base and Wall plans at Point 3.

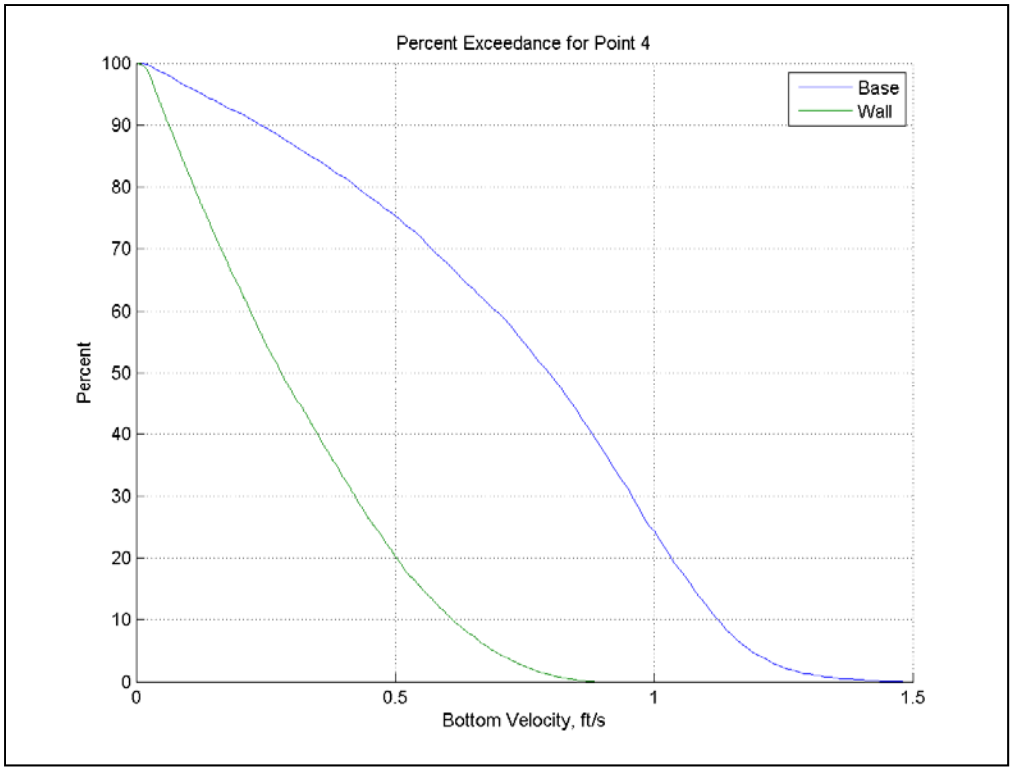

Figure 7-29. CDF curves for the Base and Wall plans at Point 4.

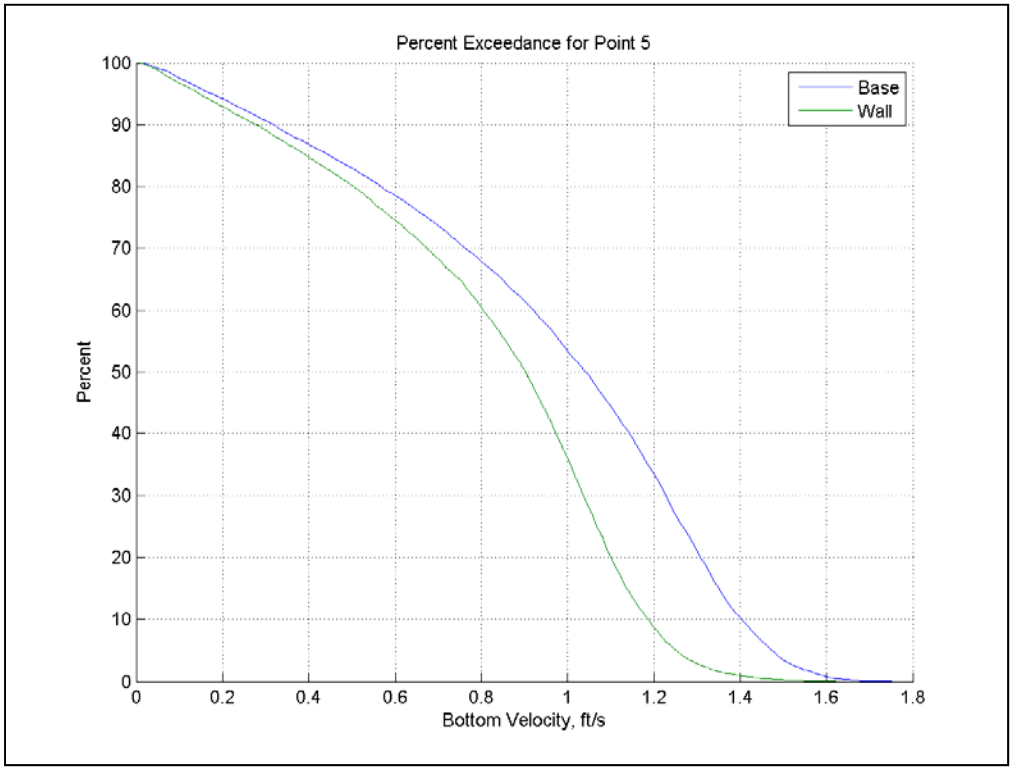

Figure 7-30. CDF curves for the Base and Wall plans at Point 5.

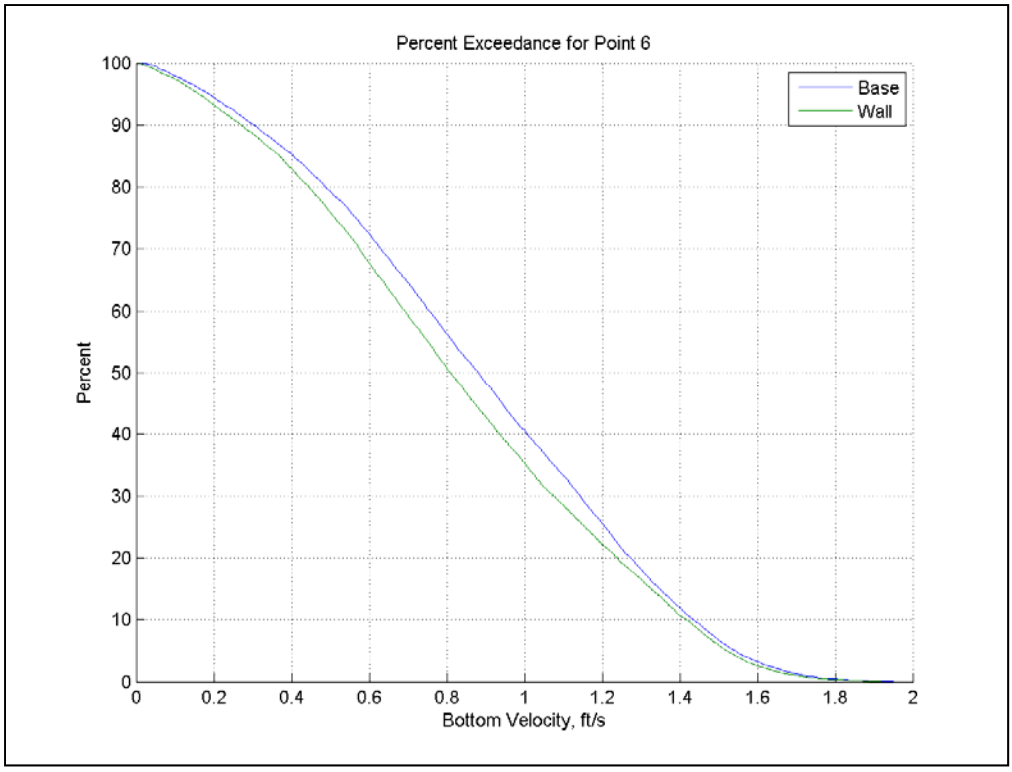

Figure 7-31. CDF curves for the Base and Wall plans at Point 6.

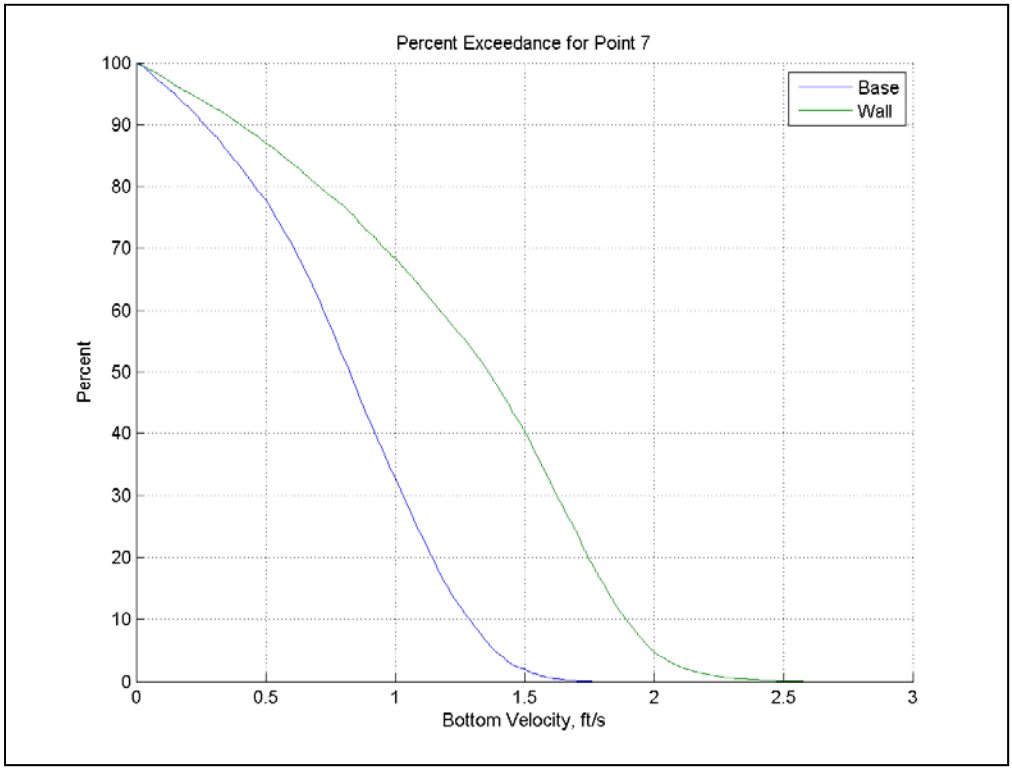

Figure 7-32. CDF curves for the Base and Wall plans at Point 7.

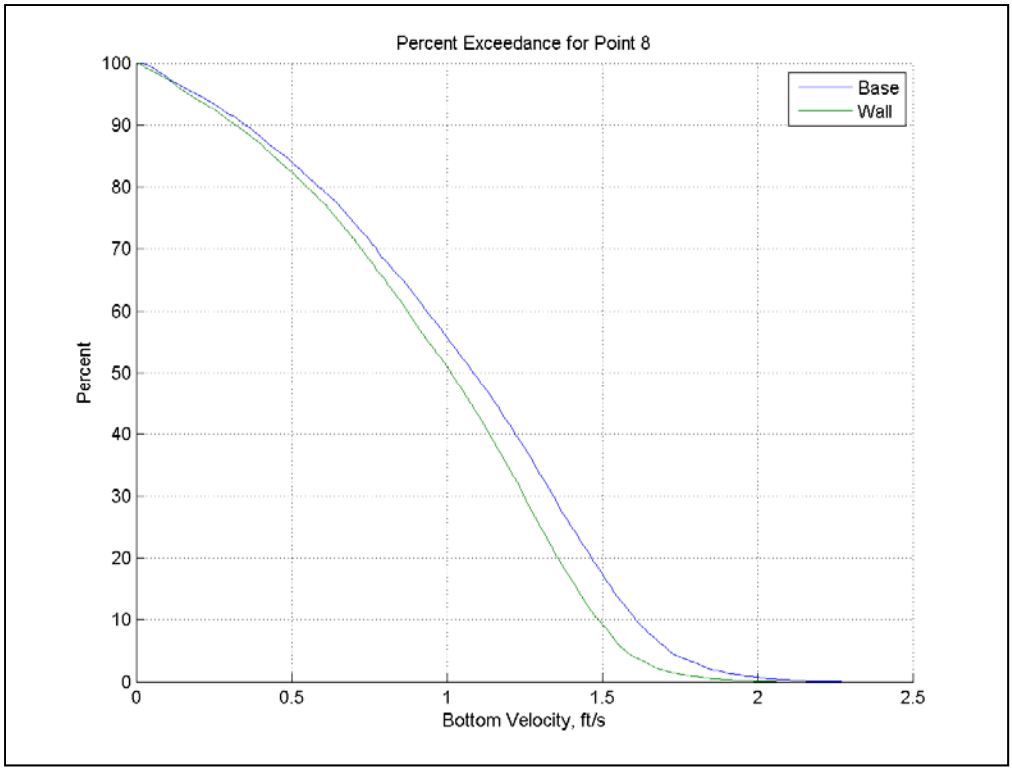

Figure 7-33. CDF curves for the Base and Wall plans at Point 8.

8 Discussion

8.1 Relevant findings from previous studies

Multiple studies have been conducted in an attempt to mitigate the shoaling problem at MOTSU. Below is a discussion of the most valuable mitigating alternatives as well as approaches that should be avoided.

From the beginning of port operations it has been evident there is unacceptable shoaling at MOTSU. Both successful and unsuccessful shoaling mitigation solutions have been recommended and implemented. The most apparently unsuccessful solution was an effort to control shoaling by blocking off and realigning the northern entrance channel in the 1960s. Once believed a viable answer, this alternative has proven to increase the trapping efficiency and cause more shoaling. A solution that proved to be beneficial was the cessation of depositing dredged material in sites on the east bank of the Cape Fear River that are adjacent to MOTSU. This eliminated the problem of dredged material migrating back into the MOTSU channels, which fed an endless source-sink cycle. Before executing any new solution, it is imperative that the historical alternatives be evaluated in light of current knowledge to avoid replicating previous studies.

In an attempt to reduce dredging, the Wilmington District conducted a feasibility study on reducing dredging cost (USACE 1976). This effort determined that the majority of the material was entering the Port from the deeper navigation entrance channels. As part of mitigating this source, it was recommended that movable barriers be used to circumvent the source to create a system that required less maintenance dredging. The District requested a physical and numerical model study to analyze the proposed solution. The hybrid study, a joint numerical and physical model analysis, conducted by the USACE Waterways Experiment Station was completed in 1982. For the study, the District provided 13 plans for evaluation (Trawle 1982). Investigators used the validated physical model for boundary conditions in the numerical model. The numerical model was used to predict the shoaling of the navigation and MOTSU channels. The study simulated various wall/blocking structures that would block some to all flow entering the Port to reduce the amount of material entering. After all 13 plans were considered, it was determined that blocking structures would only increase the trapping efficiency, and therefore would increase the shoaling (Trawle

1982). In conjunction with current knowledge and the report on that investigation, ERDC affirms that blockages inhibiting a streamlined flow through the facility should be avoided.

The hybrid model study showed that the sediment could not be kept out of the facility, so research turned toward keeping the sediment moving. One means to do so is fairway realignment. This concept was first tested in the Cape Fear physical model. Later, the numerical model was used to evaluate the movement of fine-grained material in the new alignment (USACE 1983b). The realignment alone reduced dredging by 6%. Complemented with flow training structures, an 18% reduction was achieved (USACE 1983b). Based on this finding, the fairway realignment was also recommended in the MTMC 1984 and 1986 reports. From pilot specifications, it was suggested a channel width of 530 ft be applied (MTMC 1986). This provides adequate room for passing and maneuvering while also providing enough constriction to move sediment. The fairway realignment has been recommended multiple times (USACE 1983b, USACE 1986, Barry 2008).

Considering the efficacy of fairway realignment as affirmed in these historic studies, ERDC recommends fairway realignment as a viable partial solution to the shoaling problem. Plan 5 alone would not provide a complete solution, but coupling it with other measures could provide the necessary remediation.

8.2 Supplemental application of scour jet technology

In order to enhance the effectiveness of the fairway realignment alternative, the researchers evaluated a candidate technology that could address the portion of shoaling that would not be mitigated by the fairway. The effectiveness of scour jet technology has previously been tested and verified by the Corps of Engineers (USACE 1998b). Analysis of scour jets specifically for MOTSU shoaling has previously been conducted by SedCon, one manufacturer of the technology. The SedCon's investigation deemed MOTSU a viable location for the use of scour jets (SedCon 2005). A supplementary recommendation is for the use of nautical depth (USACE 1998b). Nautical depth would provide a reduction in the required dredged volume at MOTSU. Careful consideration is essential for the application of scour jets since an considerable amount of maintenance is required for upkeep once they are installed.

8.2.1 Technology description

Scour jets reside at the fluid mud layer, or just above "old bed," ejecting energy into the system to remove recently deposited material and inhibit further shoaling. Careful consideration of freshwater flow, tidal impacts, and jet orientation is required in the design of a scour jet system (Bailard 1987). River flow supplies fine, dispersed particulate from upland locations. As the material encounters saline waters of an estuary along with flow reversal from the tides, it begins to flocculate and form larger aggregates that in turn increase deposition rates. Settling typically occurs in quiescent areas such as berthing facilities, which may form a fluid mud layer. The fluid mud can further consolidate to form a new layer of bed where individual flocs become interconnected in a matrix of particles, and compaction/dewatering occurs such that the material remains stationary. In such cases the required shear stress to remove this material is greatly increased. Scour jets inhibit the material from dewatering and allow the tidal currents to continue moving the particles downstream.

In the 1970s the Naval Facilities Engineering Command (NAVFAC) began to see the need for dredging alternatives to contain the rising costs. The Naval Civil Engineering Laboratory (NCEL) was funded to investigate dredging alternatives. Most of the work was done via contract to Scripps Institution of Oceanography, where several alternatives were evaluated, including scour jet technology (Bailard 1983). The turbulent and mixing potential of submerged jets had been studied since the 1960s (e.g., Verhoff 1963). Soon thereafter, use of these jets for the mitigation of sedimentation problems in reservoirs and harbors was explored. Application of a scour jet system for the reduction of berthing sedimentation was first conceived by Van Dorn et al. (1975). Later it was further developed by the Navy and Scripps Institution of Oceanography, NCEL), and Van Dorn in the 1980s. Through experimental work, Van Dorn et al. (1975, 1977, and 1978), and Jenkins et al. (1981) produced an equation as a function of jet diameter, discharge velocity, and jet orientation in relation to the bottom for determining the maximum scour potential. The first test location in a berth was at the Mare Island Naval Shipyard, CA, in 1983 (Bailard 1987).

There are two basic types of configurations tested for scour jets: the linear scour jet array and the spatial scour jet array. Both configurations were tested from 1977 through 1981 (Bailard 1987). In the linear array, jets are located along the wharf; in the spatial array, jets are located on grid pattern on the bottom of the berth. Each was evaluated at the Mare Island

Naval Shipyard. The linear array is best for use in a slip berth configuration where there is an adjacent parallel channel and where sediment can be diverted to and carried out on the ebb tide. A scour jet array is well suited for use in a cul-de-sac. Bailard (1980) went through a design procedure for specifying the number, location, and size of scour jets and estimating the economic benefits of using a scour jet system as opposed to the dredging-only alternative. The economic analysis procedure can be used to optimize the system based on annual cost.

As with the development and application of many new technologies, there is some confusion on the process by which the goal of shoaling reduction is achieved. Two methods have been described as removal of sediment through suspension or through resuspending newly deposited bed (Bryant 2007). Both numerical modeling and practical understanding of the scour jet process requires the application of precise terminology. Keeping sediment in suspension requires continual input that prevents deposition. However, re-erosion only requires intermitted input (i.e., during the ebb tide) to fluidize the new bed for removal by naturally occurring currents. Therefore, the fundamental action that occurs in this process is "resupension of newly deposited flocculated clay sediments, or exclusion of sediment influx to an area" (Bailard 1987, p 141).

Dredging has several inherent disadvantages not shared with scour jet technology. First, increased environmental restrictions have reduced the number of material-disposal sites that are economically affordable. Second, significant negative impacts can result from the intake of sediment-laden water into the cooling system of a vessel, which scour jets can prevent from settling in the berthing areas. Third, loss of berthing availability due to dredging or lack of depth hinders the usability of the facility. Finally, permitting fees and emergency dredging costs can rapidly become cost-prohibitive. A properly applied scour jet system can greatly reduce the need for dredging and the associated costs.

Until the late 1980s, the scour jets tested and used were low-volume/high-velocity systems. In 1990 James A. Bailard was issued a US Patent for high-volume/low-velocity jets. It is this newer type of system that has been investigated for installation at MOTSU (SedCon 2005). Most of the information about the newer system is proprietary, and so not available for inspection. Owing to this lack of technical information, it is unclear how the performance of the new jets compares with the original technology. There-

fore, an independent analysis of SedCon's high-volume/low-velocity jets is highly advisable prior to specifying the use of this technology at MOTSU.

8.2.2 Current implementations

According to the SedCon website (February 2010), there are several locations where these systems have been installed:

- NuStar Asphalt Refinery Company terminal in Savannah, GA, installed in 1998
- CITGO Petroleum Corporation terminal in Linden, NJ, installed in 2002
- Container Berths 6, 7, 8, and 9 at the Georgia Ports Authority Garden City Terminal in Savannah, GA, installed in 2003
- INVISTA terminal in Wilmington, NC, installed in 1997 (Figure 8-1)
- SC State Ports Authority Columbus Street Terminal in Charleston, SC installed in 2006
- US Navy SUBASE in Kings Bay, GA, installed in 2007.

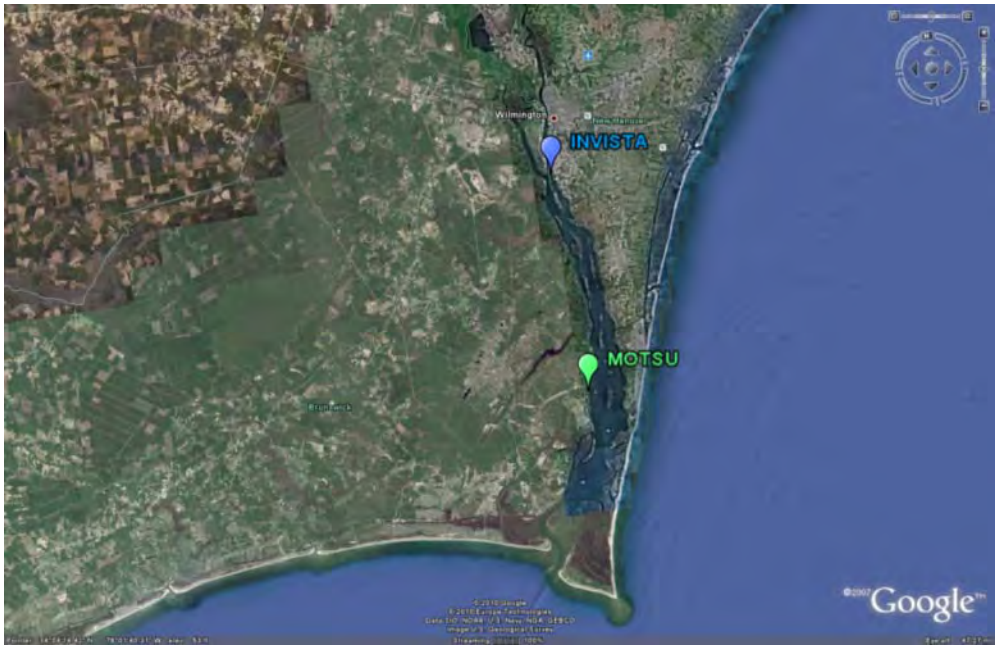

Figure 8-1. SedCon installation at INVISTA in the Cape Fear River.

8.2.3 Implementation considerations

8.2.3.1 Wharf deck clearance issues

To function properly and prevent siltation at MOTSU, scour jets must be located at the draft depth and behind the protection of the fender system. However, careful evaluation of the bathymetry under the wharf is required to determine appropriate clearances for locating the jets. If the bed inhibits the placement of jets then material will require removal and add to the cost of the installation.

8.2.3.2 Area of influence limitations

With an operational reach of approximately 200 ft, the jets would fail to cover the entire channel width of 530 ft and would provide only partial coverage of the port channel. The remaining area might experience increased shoaling due to the relocation of sediment near the wharf to locations in the channel and outside the reach of the jets. This would create the potential for merely shifting the problem and amplifying it by concentrating all the sediment into half of the area originally affected, which could still require the same amount of dredging as previously.

8.2.3.3 Annual operational and maintenance issues

Beyond the initial installation cost, scour jets have an operational and maintenance cost estimated at $260K annually (AH and SedCon 2005). However, this amounts to only about 1 – 5% of the annual dredging cost. Furthermore, pilots and vessel crewmen would need to be aware of the scour jet locations to take precautions when operating against the wharf. Also, in a high-shoaling environment, any breakdowns have the potential to leave the unit vulnerable to being buried in sediment.

8.2.3.4 Future expansion of draft depth

The scour jets are mounted on piles, so any possible future port expansion or increase in draft depth would have to be carefully considered. New mounting piles would have to be driven or planned for to accommodate dropping the piles to a future deeper draft depth.

8.2.3.5 Preliminary modeling requirements

Previous laboratory work has been performed to investigate the shear distribution and scouring capabilities of submerged wall jets as a function of jet diameter and discharge velocity (Bailard 1980, p 4). However, the lack of public domain technical information pertaining to the patented high-flow/low-velocity jets makes it advisable to perform a modeling analysis prior to an installation at MOTSU. Specifically, the individual scour jets should be modeled using the three-dimensional Navier Stokes form of the USACE ERDC Adaptive Hydraulics (AdH) model (https://adh.usace.army.mil/). The Navier Stokes model would calculate the shear stresses induced by the jets as well as the turbulence effects. This information, along with any related physical studies, could then be implemented in a three-dimensional shallow-water AdH model incorporating all sediment loads and proposed jets, providing a full-scale numerical model of the system with the jets. Numerically modeling the system would provide insight into the individual functionality and benefits of the jets from a systems perspective.

9 Recommendations

Recommendations of the most beneficial alternatives are based both on engineering judgment and numerical analyses without cost considerations. Two advantageous approaches for shoaling mitigation are suggested: realignment and dredging alternatives. Each requires specific analyses. Numerical analyses of realignment alternatives are a means to determine their relative effectiveness. Dredging alternatives are based on engineering judgment and success at other locations. Knowledge of dredging alternatives can be gleaned from the numerical analyses of the realignment plans, but prior to implementation, tailored analyses of dredging alternatives is required, and that is beyond the scope of this effort.

Two realignments and two dredging alternatives are recommended for potential selection. Plans 2 and 6 are recommended from the realignment alternatives, and active nautical depth and nautical depth are recommended for dredging alternatives. Both types of shoaling solutions emphasize recommendations that have positive impacts for MOTSU and the navigation channel. Furthermore, these solutions can be combined to achieve an optimum dredging-reduction scheme. By integrating multiple solutions it is possible to create a cost-effective, long-term shoaling-mitigation plan. The following recommendations are provided in priority order of more-promising to less-promising alternatives.

9.1 Rank-ordered recommendations

Plan 6 is the most promising realignment solution for shoaling mitigation. The construction of an island or similar flow-blockage feature would increase velocity and shear stresses in the facility, flushing out excessive material. It would also provide new locations for disposing of dredged material. However, it is the most costly alternative.

Dredging to active nautical depth would be the next-most-beneficial solution. This approach would reduce the dredging requirement. Because of the cost of necessary equipment and pilot education, however, it may be cost-prohibitive and may be resisted professionally by the piloting community.

The third recommendation is to implement the Plan 2 realignment which, like Plan 6, has a positive impact on the navigation channel. It does, however, have some negative impacts in the area of the MOTSU channel realignment. It is considered a beneficial intermediate solution that could be implemented prior to either of the above solutions.

At minimum, nautical-depth dredging could be implemented immediately, but it would require acceptance by and education for the pilots.

All four recommended solutions have the potential to reduce current dredging requirements at MOTSU. Any of these recommendations would require a follow-up study to understand potential impacts in sufficient detail.

9.2 Plan-integration approaches

Plan integration is the best approach for long-term shoaling mitigation. It would reduce shoaling while providing cost-averaging over time. Using a plan-integration approach, the following recommendation is offered.

The first phase would be implementation of Plan 2, which is the least expensive of the four preferred solutions noted above, and it could be accomplished during normal dredging maintenance. During the implementing of Plan 2, measures should be taken to define a nautical depth for MOTSU. Nautical-depth dredging would require a separate investigation entailing a field study. As further dredging is required for MOTSU, dredge material could be used to construct the island structure specified in Plan 6. Opening the old northern entrance channel and construction of the island will dramatically reduce the dredging requirement. If, upon completion of the island, dredging is still an issue, then active-nautical-depth dredging should be implemented. With the execution of all four recommended solutions it is believed that shoaling reduction would be significant and the facility should see improvements in operational readiness.

Because Plan 6 is potentially the most productive shoaling mitigation alternative, special implementation considerations are recommended. A modeling effort, construction forecasting of Plan 6, is recommended to simulate the growth stages of a confined disposal facility island configuration and the corresponding impact to shoaling behavior. If island construction were determined to be cost-prohibitive, the construction could be planned in multiple stages to ultimately produce the island structure

modeled in Plan 6. Here, the smaller disposal facility stages would be constructed in different phases as dictated by dredging requirements. A portion of the future island would be enclosed by levees and filled with dredge material. Material dredged from deepening the port might be usable for disposal facility levee construction. Once the first disposal facility is at capacity, a second would be constructed to advance growth of the island and provide dredge material for placement. Dredging requirements in the port will be reduced as island growth proceeds. Based on a constant dredging rate of 1.1 million cu yd a year, it is estimated that there is the potential for 18 years of dredging placement, not including the material required for the levees. As the island increases in size, however, the dredging rate will decrease. As the island is constructed, nautical-depth and even active-nautical-depth dredging can be practiced for short-term shoaling mitigation.

9.3 MOTSU model refinements

To address uncertainties in the sediment model validation and unknowns in the input data available, additional field data collection and modeling capabilities can be accomplished to improve the study results. A sediment load rating curve in the Cape Fear River as well as just upstream from MOTSU would improve boundary condition data as well as validation data for model comparison in the study area. Full bathymetric surveys of the MOTSU facility, navigation channel, and shallows would help the overall sediment model validation and should be performed just before and after the validation period. Fluid mud should be measured in the area and documented for density ranges and locations to determine its contribution to total shoaling in the field. Additional sediment processes can be included in the model to allow for fluid mud formation and transport to be included in the computations. Currently there is uncertainty about how much of the fluid mud present in the area is accounted for in the bathymetric surveys and how significant this quantity is in the total shoaling measurements.

Regardless of the plan or combination of plans selected, improvements in the model will support continuing efforts to prevent shoaling from interfering with MOTSU operational readiness.

References

Aldridge, D.W., Payne, B.S., and Miller, A.C. (1987). The Effects of Intermittent Exposure to Suspended Solids and Turbulance on three species of freshwater mussels. Environmental Pollution, Vol 45, pp 17-28.

Bailard, J. A. (1980). A Design procedure for a Scour Jet Array. Naval Facilities Engineering Command, Technical Note no. N-1589.

Bailard, J. A. (1987). Controlling Sedimentation in Harbor Berthing Areas Using Scour Jet Array Systems, in Sedimentation Control to Reduce Maintenance Dredging of Navigational Facilities in Estuaries, Marine Board, National Research Council, 141-152

Bryant, Joe T. (2007). A Potential Alternative to Berth Maintenance Dredging. ASCE Ports Conferecnce.

Carpenter, E.J. and W.L. Yonts. (1979). Dye Tracer and Current Meter Studies. Cape Fear Estuary 1976, 1977, 1978. Report to Carolina Power and Light Company, Raleigh, North Carolina.

Giese, G.L., Wilder, H.B., and Parker, Jr, G.G. (1985). Hydrology of major estuaries and sounds of North Carolina, Paper 2221, US Geological Survey, Alexandria, V.A.

Holland, L.E. (1986). Effects of Barge Traffic on Distribution and Survial of Icthyoplankton and small fishes in the Upper Mississippi River. Transactions of the American Fisheries Society, Vol 115, pp 162 – 165.

Jones, Edmunds and Associates, Inc. (1979). Grain Size Analysis, Bioassays, and Bioaccumulation Potential Assessment, Access Channels and Anchorage Basins, Military Ocean Terminal, Sunny Point, North Carolina, prepared for the US Army Engineer District Wilmington, Wilmington, NC.

McAdory, R.T. (2000) Cape Fear-Northeast Cape Fear River, North Carolina: numerical model study. ERDC/CHL TR-00-18. US Army Engineer District, Wilmington.

Mehta, A. J. (2002). “Mudshore dynamics and controls” *Muddy coasts of the World: Processes, deposits and function*, T. Healy, Y. Wang, and J.A Healy, eds. Elsevier, Amsterdam, 19-60.

MTMC (1984). Reconfiguration of the Navigation Basins and Access Channels, Military Ocean Terminal, Sunny Point (MOTSU), N.C.

MTMC (1986). Channel Realignment Project Alternative Study, Military Ocean Terminal, Sunny Point (MOTSU), N.C.

Palermo, Micheal R., Teeter, Allen M., and Homziak, Jurij. (1990). Evaluation of Clamshell Dredging and Barge Overflowing, Military Ocean Terminal, Sunny Point, North Carollina, “ Technical Report D-90-6, US Army Engineer Waterways Experiment Station, Vicksburg, MS.

SedCon Technologies, Inc (2005). Preliminary Study of SedCon Turbo Systems for Military Ocean Terminal Sunny Point Southport, North Carolina. Prepared for: AH Environmental Consultants.

SedCon Technologies, Inc. (2010). http://sedcontech.com/installations.html

Trawle, M.J., A.J. Banchetti, and R.C. Berger (1980). Hydraulic and Salinity Verification of the Cape Fear River Physical Model. USACE. Waterways Experiment Station.

Trawle, M.J. (1982). Hybird Modeling of Military Ocean Terminal, Sunny Point. USACE . Waterways Experiment Station. Letter report

USACE (1971). Reviews of Problems in Tidal Waterways Considered by the Committee on Tidal Hydraulics.

USACE (1976). A Feasibility study on Reducing Maintenance Dredging Costs at the Military Ocean Terminal , Sunny Point. Wilmington District.

USACE (1983). Measurements of Suspended Sediment Concentrations at the Military Ocean Terminal, Sunny Point, North Carolina, During 1978 and 1979. Unpublished data.

USACE (1983b). Sedimentation Prediction for Fairway Alignment. Letter Report to the Military Traffic Management Command.

USACE (1986). Channel Realignment Project Alternative Study, Military Ocean Terminal Sunny Point, North Carolina. Prepared by the Wilmington District for the Military Ocean Terminal at Sunny Point.

USACE (1995). Reviews of Problems in Tidal Waterways Considered by the Committee on Tidal Hydraulics.

USACE (1998). Fluid Mud and Density Measurements at the Military Ocean Terminal Sunny Point (MOTSU) Terminal on the Cape Fear River, NC. Memorandum for Record. Thad Pratt. 11 September.

USACE (1998b). MOTSU; Shoaling and Remediation. Report to provide background to Commander of MOTSU.

USGS (2010). United States NWIS-WI data retrieval. http://nwis.waterdata.usgs.gov/nc/nwis/

Vantorre, M. (1994). Ship behaviour and control in muddy areas: State of the art. Manoeuvering and Control of Marine Craft. 3rd International Conference, MCMC '94, Southampton, UK, 59 – 74 pp.

Verhoff, A. (1963). The two-dimensional turbulent wall jet with and without an external stream. Rep No. 626, Princeton Univ., Princeton, N.J.

Von Dorn, W.G., D.L. Inman, and R.W. Harris (1975). The evaluation of sediment management procedures, Phase I Final Report 1974 – 1975, Scripps Institution of Oceanography Reference No. 77 -10, 80pp.

Von Dorn, W.G., D.L. Inman, R.W. Harris, and S.S McElmery (1977). The evaluation of sediment management procedures, Phase II Final Report 1975 – 1976, Scripps Institution of Oceanography Reference No. 77 – 10, 107 pp.

Wilder, H.B. (1967). Hydrology of Sounds and Estuaries in North Carolina. pp 115-129. In: Proceeding of the Symposium on Hydrology of the Coastal Waters of North Carolina. Report Water Res. Inst. Univ. N.C. Raleigh. 5: 1-154.

REPORT DOCUMENTATION PAGE

Form Approved
OMB No. 0704-0188

1. REPORT DATE *(DD-MM-YYYY)*	2. REPORT TYPE	3. DATES COVERED *(From - To)*
July 2012	Final	

4. TITLE AND SUBTITLE
Sedimentation Solutions for Military Ocean Terminal Sunny Point (MOTSU), North Carolina

5a. CONTRACT NUMBER

5b. GRANT NUMBER

5c. PROGRAM ELEMENT NUMBER

6. AUTHOR(S)
Jeremy A. Sharp, Jennifer N. Tate, and William H. McAnally

5d. PROJECT NUMBER
155479

5e. TASK NUMBER
Customer Order W81LJ802080182

5f. WORK UNIT NUMBER

7. PERFORMING ORGANIZATION NAME(S) AND ADDRESS(ES)
US Army Engineer Research and Development Center
Coastal and Hydraulics Laboratory
3909 Halls Ferry Road
Vicksburg, MS 39180

8. PERFORMING ORGANIZATION REPORT NUMBER
ERDC/CHL TR-12-10

9. SPONSORING / MONITORING AGENCY NAME(S) AND ADDRESS(ES)
US Army Engineer District–Wilmington
69 Darlington Avenue
Wilmington, NC 28403

10. SPONSOR/MONITOR'S ACRONYM(S)
USAED-SAW

11. SPONSOR/MONITOR'S REPORT NUMBER(S)

12. DISTRIBUTION / AVAILABILITY STATEMENT
Approved for public release; distribution is unlimited.

13. SUPPLEMENTARY NOTES

14. ABSTRACT

The US Army's Military Ocean Terminal Sunny Point (MOTSU) went into service in 1955, and serves as a military munitions terminal. The facility is located in Brunswick County, North Carolina, approximately 10 miles upstream of the mouth of the Cape Fear River. Shoaling issues have been a problem since the opening of the port. The objective of this work is three fold: reduce long term dredging costs, achieve operational readiness goals, and maintain or enhance environmental quality at MOTSU at the request of US Army Engineer District–Wilmington (USAED-SAW). The objective was achieved through numerical modeling, literature review, and sediment forecasting. This report documents the results of the numerical modeling study only.

Two advantageous approaches for shoaling mitigation are recommended for further analysis, and those solutions could be combined to achieve an optimum dredging-reduction scheme. It is concluded that by integrating multiple solutions it is possible to create a cost-effective long-term shoaling-mitigation plan.

15. SUBJECT TERMS
numerical modeling, Military Ocean Terminal Sunny Point (MOTSU) ship channel, nautical depth, sediment, dredging

16. SECURITY CLASSIFICATION OF:			17. LIMITATION OF ABSTRACT	18. NUMBER OF PAGES	19a. NAME OF RESPONSIBLE PERSON
a. REPORT	b. ABSTRACT	c. THIS PAGE			19b. TELEPHONE NUMBER *(include area code)*
Unclassified	Unclassified	Unclassified		159	